
Towards underlying Quantum Gravity Constraints on String Inflation

Florian Wolf



München 2018

Towards underlying Quantum Gravity Constraints on String Inflation

Florian Wolf

Dissertation
an der Fakultät für Physik
der Ludwig–Maximilians–Universität
München

vorgelegt von
Florian Wolf
aus Straubing

München, den 6. September 2018

Erstgutachter: Priv.-Doz. Dr. Ralph Blumenhagen

Zweitgutachter: Prof. Dr. Dieter Lüst

Tag der mündlichen Prüfung: 18. Oktober 2018

Zusammenfassung

Inflation ist ein weitgehend anerkanntes Konzept der Kosmologie, das eine beschleunigte Ausdehnung des frühen Universums voraussagt. Für die Klasse der Groß-Feld-Inflationsmodelle stammt die Energie, die die Expansion antreibt, von einem Skalarfeld namens Inflaton, das trans-Plancksche Distanzen in einem bestimmten Potential durchschreitet. Diese Dissertation beabsichtigt zu diskutieren, ob es grundlegende Prinzipien aus der Stringtheorie oder Quantengravitation gibt, die Groß-Feld-Inflation einschränken bzw. verbieten.

Den Rahmen unserer Analyse bilden axionische Inflation und dessen Zusammenspiel mit Modulistabilisierung in der Stringtheorie. Axionische Inflatonfelder treten natürlicherweise in Stringkompaktifizierungen auf und sind durch ihre Verschiebungssymmetrie geschützt vor UV-Korrekturen. Die Dissertation ist im Wesentlichen folgendermaßen gegliedert: Erstens, der Versuch ein vollständiges Modell der Groß-Feld-Inflation innerhalb der Stringtheorie zu konstruieren und zweitens, die Analyse von möglichen grundlegenden Ursachen aus der Quantengravitation, um die allgegenwärtigen Kontrollprobleme zu erklären.

Im Speziellen untersuchen wir ‘aligned’ Inflation in der Nähe einer Konifoldsingularität im Moduliraum der komplexen Struktur, sowie ‘axion monodromy’ Inflation für einen Positionsmodulus einer $D7$ -Brane. Das letztendliche Scheitern aller Szenarien basiert auf der Verletzung einer komplexen Massenhierarchie, welche notwendig ist für die Rechtfertigung der benutzten effektiven Feldtheorien. Diese Probleme können auf die Sumpfland-Vermutungen zurückgeführt werden, die Anspruch auf allgemeine Gültigkeit für effektive Beschreibungen der Quantengravitation erheben. Um mehr Belege für diese Vermutungen zu sammeln, untersuchen wir geodätische Abstände in Moduliräumen von verschiedenen Calabi-Yau-Mannigfaltigkeiten.

Unsere Ergebnisse bekräftigen klar eine der Sumpfland-Vermutungen, die ein Versagen der effektiven Inflationstheorie vorhersagt, sobald man trans-Plancksche Distanzen passiert. Falls sich diese Vermutung bewahrheitet, scheint ein parametrisch kontrolliertes Modell der Groß-Feld-Inflation mit einem einzelnen Inflatonfeld, im Rahmen der Stringtheorie unmöglich zu sein.

Abstract

Inflation is a widely accepted concept in cosmology proposing an accelerated expansion of the very early universe. For the class of large-field inflation models the energy driving the expansion arises from a scalar inflaton field that traverses trans-Planckian distances in a suitable potential. This thesis aims to discuss whether there exist underlying string theory or quantum gravity principles constraining/forbidding large-field inflation.

Our framework is axion inflation and its interplay with moduli stabilization in string theory. Axionic inflaton fields appear naturally in string compactifications and are protected from UV corrections due to their shift symmetry. The thesis is basically organized as follows: first, attempting to engineer a fully-fledged model of large-field inflation within string theory and second, analyzing possible underlying quantum gravity reasons to explain the ubiquitous control issues.

More precisely, we investigate aligned inflation in the vicinity of a conifold in the complex structure moduli space as well as axion monodromy inflation for a $D7$ -brane position modulus. The ultimate failure of all scenarios boils down to the violation of a sophisticated mass hierarchy that is required to justify the employed effective field theories. These obstacles can be traced back to the swampland conjectures which had been claimed to hold generically for effective theories deduced from quantum gravity. In order to gather more evidence for these conjectures we investigate geodesic distances in moduli spaces of various Calabi-Yau manifolds.

Our results strongly support one of the swampland conjectures that predicts a break down of the effective theory of inflation as soon as one moves trans-Planckian distances. If true, parametrically controllable models of large single field inflation seem to be impossible in string theory.

Acknowledgements

Above all I want to express my deep gratitude to my doctoral supervisor Ralph Blumenhagen for giving me the opportunity to work in his research group at the Max Planck Institute. It was a pleasure to join him for an exciting journey into the swampland, to surf the waves of excitement in scientific research and to share his passion for physics. Let me also cordially thank Dieter Lüst for creating an outstanding atmosphere for string theory research in Munich and having at any time a sympathetic ear for students.

The past three years would have been by far less instructive and clearly less fun without the great people in the string theory group of the Max Planck Institute. Accounting for all the amazing stories from in- and outside the institute exceeds the scope of these acknowledgements, so let me just say “thank you very much” to Henk Bart, Max Brinkmann, Pierre Corvilain, Victor Diaz, Iñaki García-Extebarria, Sebastian Greiner, Thomas Grimm, Daniela Herschmann, Michael Fuchs, Daniel Kläwer, Kilian Mayer, David Osten, Diego Regalado, Lorenz Schlechter, Rui Sun, Matthias Traube, Irene Valenzuela and the whole Angnis Schmidt-May group. Two friends from the Improv theater deserve extra appreciation for organizing numerous funny activities to explore Munich and the Bavarian landscape surrounding it. In addition I am grateful for being part of the adventure team that kept me company on my way through the swampland - under the sea and during starry nights in lonely deserts. A big thanks goes also to my office mates Pierre, Rui, Daniel, David and the Dutchman on the couch for the cozy atmosphere, valuable discussions and magic moments.

A huge benefit for doctoral students at the Max Planck Institute is the International Max Planck Research School (IMPRS) managed by Frank Steffen. Events like the yearly workshop at Castle Ringberg not only taught me interesting insights into other research areas, but also provided unforgettable moments as well as friendships throughout the institute. In particular I would like to thank my fellow student representatives Lena Funcke, Miro Gabriel, Tanja Geib, Kazuma Ishio, Nico Köhler and Viktor Papara for intense discussions and excellent team work. In this context, I also have to express my gratitude to the directors of the Max Planck Institute for respecting the needs of the PhD students and helping to permanently improve their working conditions. Equally, one must thank the administration of the Max Planck Institute and especially Monika Goldammer, Sarah

Fischer and Annette Moessinger.

Let me also express my appreciation for Fernando Marchesano for his support and supervision during my three month research visit at the Instituto de Física Teórica in Madrid. Muchas gracias to Federico Carta, Aldo Dector, Michael Fuchs, Eduardo García-Valdecasas, Sebastian Schwieger and Wieland Staessens for discussions and making my time in Spain a memorable experience. I am thankful to the DAAD (German Academic Exchange Service) for financial subsidy.

In the final paragraph I have to thank all my friends for making me laugh and enriching my life outside of physics with so many joyful moments. In particular I am grateful to my girlfriend for her existence and her lovable smile. Last but certainly most, my deepest gratitude belongs to my family. This thesis would have never been possible without their endless support and love.

*“Science is not only a disciple of reason but, also,
one of romance and passion.”*

Stephen Hawking

Contents

I	Introduction	1
1	Motivation and Obstacles of String Inflation	3
II	Conceptual Preliminaries	15
2	Basics of String Compactification	17
2.1	Kähler Geometry and Calabi-Yau Manifolds	18
2.2	Orientifold Projection and D -Branes	23
2.3	Moduli Space	25
2.3.1	Closed String Moduli	26
2.3.2	Open String Moduli	31
3	Periods of Calabi-Yau Manifolds	33
3.1	Hypersurfaces in Weighted Projective Spaces	34
3.2	Mirror Quintic	36
3.2.1	Periods and Metric	38
3.2.2	Mirror Map and Quantum Corrections	43
3.3	Two-Parameter Models	44
4	Fluxes and Moduli Stabilization	47
4.1	Effective $\mathcal{N} = 1$ Supergravity Theory	48
4.1.1	Geometric Flux G_3	49
4.1.2	Superpotential and Scalar Potential	50
4.1.3	Mass Scales and Hierarchy	53
4.2	Non-Geometric Extension	57
4.2.1	Non-Geometric Fluxes	57
4.2.2	Generalized Superpotential	58
4.3	Schemes of Moduli Stabilization	59
4.3.1	KKLT	59
4.3.2	Large Volume Scenario	61
4.3.3	Flux Scaling Scenarios	62

5	Large-Field Inflation in String Theory	65
5.1	Early Universe Cosmology and Inflation	66
5.2	Effective Theory of Large-Field Inflation	68
5.2.1	Different Types of Inflation	72
5.3	UV Sensitivity and Axions	73
5.3.1	Axions in String Theory	76
5.4	Periodic Inflation: Alignment	80
5.5	Polynomial Inflation: Axion Monodromy	82
6	The Swampland Conjectures	87
6.1	The Swampland Idea	88
6.2	Weak Gravity Conjecture	89
6.3	Swampland Distance Conjecture	92
III Developments and Results		95
7	Large-Field Inflation near the Conifold	97
7.1	Flux Induced Exponential Hierarchies	99
7.1.1	Kähler Moduli Stabilization via a Conic LVS	101
7.2	Inflation via Axion Alignment	104
7.2.1	Comment on the Weak Gravity Conjecture	108
7.2.2	Mass Hierarchy	109
8	Axion Monodromy Inflation and the Swampland Distance Conjecture	113
8.1	Moduli Backreaction and Axionic RSDC	114
8.2	Closed String Model	118
8.3	Open String Models	123
8.3.1	Superpotential for Brane Deformations	123
8.3.2	Toy Model O1	128
8.3.3	Model O2 on the Strongly Isotropic Torus	134
8.3.4	Models with Instanton Corrections	137
9	Challenging the Refined Swampland Distance Conjecture	143
9.1	Setup and Objective	144
9.2	RSDC for the Mirror Quintic	148
9.3	RSDC for Calabi-Yau Manifolds with $h^{1,1} = 2$	153
9.3.1	An Illustrative Example: $\mathbb{P}^4_{11222}[8]$	154
9.3.2	$\mathbb{P}^4_{11226}[12]$	167
9.3.3	$\mathbb{P}^4_{11169}[18]$	170

IV	Conclusions	175
10	Summary and Outlook	177
V	Appendices	183
A	Numerical Evaluation of Periods of Calabi-Yau Manifolds	185
A.1	One-Parameter Quintic	185
A.2	Two-Parameter Spaces	187
B	Transformation Matrix m for Periods	193
	<i>Bibliography</i>	207

Part I

Introduction

CHAPTER 1

Motivation and Obstacles of String Inflation

Before introducing cosmic inflation in string theory and outlining the topics to be discussed in this thesis, let us give a brief overview on the contemporary status of physics. In particular, since string inflation is connecting different branches of physics, its importance and location within the big picture shall be highlighted. It will turn out that obstacles of string inflation are tied to a core strategy of physics, that is using effective field theories. Hence, our starting point is a review of how physics approaches nature at varying length scales.

Physics as effective description of nature

Imagine phenomena of nature could only be explained properly by a fully-fledged understanding of the *theory of everything*. On the one hand, this would be extremely unfortunate as such a theory, if it exists, still seems to be far from being discovered. On the other hand, the success of past achievements in science shows that for nature at nearly any length scale there is no need for a theory of everything. As a matter of fact, nature behaves very differently at disparate lengths or equivalently at disparate energies. Recall that in natural units where $c = \hbar = 1$, length l and energy E are inversely related $[l] \sim 1/[E]$, thus small length corresponds to high energy. Physics has to be understood as effective description of nature. That is, given some phenomena at a certain length scale, physics aims to construct a theory effectively quantifying it as accurately as necessary. This strategy works incredibly well. For instance, the physics of an apple falling from a tree is perfectly captured by Newton's classical mechanics, whereas application of quantum mechanics or even string theory would be highly superfluous. To summarize the big picture, our universe at varying length scales may be appreciated as a list of successful physical theories. Crucially, every theory has its range of validity and ultimately becomes insufficient at higher energies.

Effective theory also means that it is entirely incorporated in all theories valid at higher energies. For instance, classical mechanics follows from quantum mechanics in the limit of low energy or a large number of quanta.

In quantum field theory this can be made more precise in terms of *Wilson's renormalization group*. To illustrate the underlying idea, consider a quantum field theory \mathfrak{A} valid up to some energy scale $\Lambda_{\mathfrak{A}}$. One may then ask about a quantum field theory \mathfrak{B} governing the physics up to energy $\Lambda_{\mathfrak{B}} < \Lambda_{\mathfrak{A}}$. The *effective theory* \mathfrak{B} is obtained from \mathfrak{A} by integrating out all degrees of freedom with energies above $\Lambda_{\mathfrak{B}}$. However, these integrated-out modes contribute to loop effects of the quantum field theory \mathfrak{B} . The coupling constants indicating the strength of interactions have to be corrected accordingly. There are two classes of these corrected couplings: renormalizable and non-renormalizable ones, where the latter refers to couplings of the form $1/\Lambda_{\mathfrak{B}}$. If theory \mathfrak{B} contains merely renormalizable couplings, it holds in principle true up to arbitrary high energies. In contrast, non-renormalizable couplings are sub-leading only for energies below $\Lambda_{\mathfrak{B}}$. A standard technique of physics is *perturbation theory* which approximates complicated problems by exact solutions to simplified problems and then adding small perturbations. For interactions, these perturbations are usually expanded in terms of the coupling. If the coupling is not sufficiently small, this approach fails because perturbations are no longer sub-leading. Hence, non-renormalizable theories \mathfrak{B} have a cutoff scale $\Lambda_{\mathfrak{B}}$ where the perturbative treatment breaks down. Note that an additional subtlety arises from the fact that couplings are not fixed, but vary with the energy scale instead. The exact behavior is determined by the renormalization group equation, which shall not be part of the discussion here. Let us comment on the two currently most fundamental (i.e. valid up to highest energies) theories in respect of renormalizability.

First, the standard model of particle physics accounts for the particle content in our universe and agrees with experimental data up to astonishing precision. It is based on the symmetry group $SU(3) \times SU(2) \times U(1)$ explaining the three gauge forces that cause all interactions in the universe except gravitational attraction. The success of the standard model culminated in the detection of the Higgs boson at CERN in 2013 [1], after the particle has been postulated theoretically many years ago. Ongoing, even more accurate measurements keep confirming its predictions and new physics might be hiding at energy scales much above the ones investigate at current accelerators. The standard model has been constructed as a quantum field theory and describes physical processes at microscopic scales. Second, Einstein's general relativity accounts for gravitation. Loosely speaking, mass 'curves' spacetime according to Einstein and consequently affects the dynamics of other massive objects. Assuming further the existence of dark matter and dark energy, one can build a standard model of cosmology known as Λ CDM. This explains not only the present accelerated expansion of the universe, but also its past all the way back to the big bang.

In view of renormalizability and effective field theories it turns out that the standard model of particle physics is renormalizable and may be extrapolated to arbitrary high energies. On the other side, trying to quantize general relativity shows that its coupling constant

scales like $\sqrt{G_N} \sim 1/M_{\text{Pl}}$ with Newton's constant G_N and the Planck mass M_{Pl} . Hence, it is non-renormalizable and gets strongly coupled at energies above M_{Pl} . As a consequence the range of validity of perturbative quantum gravity is limited and one might wonder if it represents simply the low-energy effective description of some ultraviolet (UV) complete theory. In fact, there exist additional issues of the standard model of particle physics as well as cosmology that demand new physics at higher energy scales. The standard model of particle physics constitutes only about 5 % of the energy content in the universe. An appropriate candidate for the 25 % in form of dark matter, which is necessary to explain for instance galaxy rotation curves, is still missing. Moreover, we live in a de Sitter universe since we detect its accelerated expansion. A simple explanation assumes a cosmological constant and assigns to it the obscure name dark energy (the left over 70 %), but a deeper understanding remains challenging. In addition, hierarchy problems such as the comparatively, extremely small cosmological constant or Higgs mass require a very unnatural fine-tuning of parameters.

The most popular way to unify gravity and quantum field theory is string theory, whose basic idea boils down to taking spatially extended strings as fundamental objects instead of point particles. Tension and mass spectrum of the string are entirely fixed by its length l_s which in fact is the only free parameter in string theory. Note that the extended nature of strings can solely be resolved at distances smaller than $l_s \sim 1/M_s$, hence at macroscopic length scales it seems to be point-like. Oscillations of these strings are interpreted as particles or gauge bosons. Remarkably, the massless spectrum of closed strings always includes a spin two mode, which corresponds to the graviton. It is also possible to quantize string theory. In total, string theory is a quantum theory that naturally inherits gravity. One might then ask whether string theory breaks down at some UV cutoff due to non-renormalizable interactions like general relativity. Surprisingly, this is not the case because divergences from probing arbitrary small length scales are absent. Intuitively, strings are not able to access length scales below l_s (note that l_s is larger than the Planck length $l_p \sim 1/M_{\text{Pl}}$), hence strictly localized interactions in spacetime are smeared out by strings. Summarizing, string theory remains valid at arbitrary high energies. However, whether string theory is indeed the theory of everything, i.e. describing properly all phenomena at high energies, stays an open question. Effects above the string scale M_s are highly complicated and maybe more mathematical machinery needs to be developed in order to explore these regimes.

Quantization of string theory leads to another crucial consequence: the superstring must live in $D = 10$ spacetime dimensions. Apparently, this is six dimensions more than the observed three spatial plus one time dimension. In order to solve this mismatch, the superfluous dimensions are compactified. Pictorially speaking, they are curled up small enough such that current experiments are unable to resolve their existence. The geometry of the internal six dimensions (usually) corresponds to a Calabi-Yau manifold. The point is that the precise structure of the compactification manifold substantially determines the physics in the four large dimensions. One implication we want to stress is the appearance of numerous massless scalar fields, known as *moduli*. They basically embody free parameters

of the compactification space, for instance size and shape. Moduli will play a central role in this thesis.

Why string inflation?

In spite of the conceptual beauty and the desired UV properties, string theory will only survive as a physical theory if, in the end of the day, it agrees with observations and produces additional testable predictions. Unfortunately, direct measurement of strings is extremely unlikely as their spatially extended nature becomes visible merely at extremely high energies, that are far beyond reach of any current experiment. At least, string theory ought to result in the standard models of particle physics and cosmology when taking the low-energy limit. The research branch bridging the gap between formal string theory and low-energy physics is called *string phenomenology*.

Obviously, a central question of string phenomenology is to engineer the standard model gauge group including its particle content. There has been indeed much effort devoted to this task and several strategies turned out to come fairly close the standard model. Aside from early attempts via heterotic string theory [2, 3], the standard model can arise in M-theory compactifications on G_2 manifolds [4, 5] or F-theory on Calabi-Yau four-folds [6, 7]. Very fashionable are also D -brane constructions, for instance at singularities [8, 9] or by appropriate intersections of D -brane stacks [10–13]. The latter possibility is particularly intuitive since one can show that a stack of n D -branes gives rise to a $U(n)$ gauge symmetry. Thus the standard model gauge group can simply be achieved by building suitable stacks of branes. Moreover, consider the intersection of two brane stacks. Open strings with legs on both stacks lead to massless chiral matter states charged under the two corresponding gauge groups. Nevertheless, a fully consistent realization of the standard model of particle physics has not been possible so far. One typical issue is the overproduction of particles in conflict with experiments that have not yet detected any new particle.

An additional major topic of string phenomenology goes under the name *moduli stabilization*. As pointed out above, compactification unavoidably leads to a large number of massless scalar moduli fields in the four-dimensional effective theory. However, there are good reasons why moduli ought to be absent: First, new massless scalar fields could be interpreted as fifth forces, which are experimentally excluded. Second, several quantities like coupling of the lower dimensional effective theory depend on moduli. These quantities are fixed and must not vary with the moduli. Third, massless particles would alter big bang nucleosynthesis [14]. All these issues can be resolved if the moduli acquire a mass. In order to achieve this, one can turn on background fluxes, that is, field strengths with non-trivial vacuum expectation values (vev). Fluxes generate a potential for the moduli and stabilize them in its minima. Thereby, moduli obtain a mass term which, if sufficiently large, makes them undetectable for observations and circumvents the phenomenological problems. By now several proposals exist for explicit mechanisms of moduli stabilization in certain well-controlled regimes. One example is the famous *large volume scenario* [15] where a large

overall compactification volume ensures the suppression of dangerous corrections that possibly destabilize the moduli minimum. More complicated setups in other regimes and the (backreaction) effect of fluxes on the geometry are still waiting to be completely conceived. Control issues constitute often faced problems on the road towards a fully-fledged model of moduli stabilization. We shall address these issues in several sections of this thesis.

String phenomenology is apparently a wide field of research. In this thesis we will exclusively focus on cosmic inflation and ask whether it can be embedded in string theory. To that end, let us review the observational motivation for inflation.

Consider the roughly 13.7 billion years history of the universe beginning when it was 10^{-10} seconds old and the average temperature corresponded to an energy of 1 TeV. Note that all physics from there on can be tested by modern experiments, whereas we do not have a direct observational handle on earlier times because the energy has been much higher. Given the presence of standard model particles and a tiny asymmetry of matter-antimatter, at around 3 minutes (0.1 MeV) strong interactions became relevant and *big bang nucleosynthesis* (BBN) started, i.e. protons and neutrons formed nuclei of the atoms H, He and Li. Another milestone happened at 380,000 years after the universe cooled down to 0.1 eV: nuclei captured electrons to make up the first neutral H atoms which is known as *recombination*. As a consequence photons decoupled from the matter-radiation-plasma and suddenly made the universe transparent. This first picture of the universe has been named *cosmic microwave background* (CMB), see figure 1.1, and accidentally discovered by the radio astronomers A. Penzias and R. Wilson [16] in 1964. After some *dark ages*

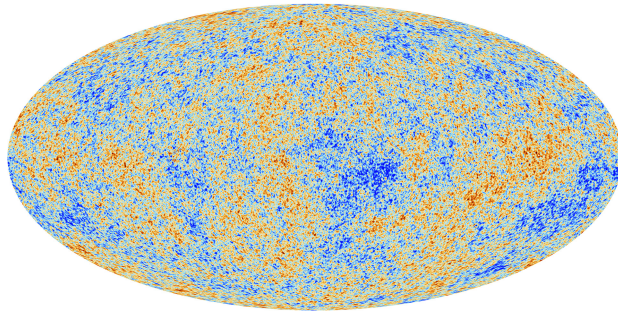


Figure 1.1: Cosmic microwave background (CMB) according to the Planck mission [17].

the first stars were born and illuminated the universe. Slowly also galaxies as well as clusters evolved due to gravity and after one billion years of cosmic time the universe looked basically like nowadays. We summarized the history of our universe in figure 1.2.

Although the universe turns out to be quite homogeneous on large scales, it clearly differs on small scales which can be traced back to fluctuations of the CMB in figure 1.1. These fluctuations of the temperature T are only of order $\delta T/T \sim 10^{-5}$ and the currently most precise chart comes from the Planck collaboration [19]. As one of the most celebrated achievements of inflation, it is able to explain the CMB fluctuations.

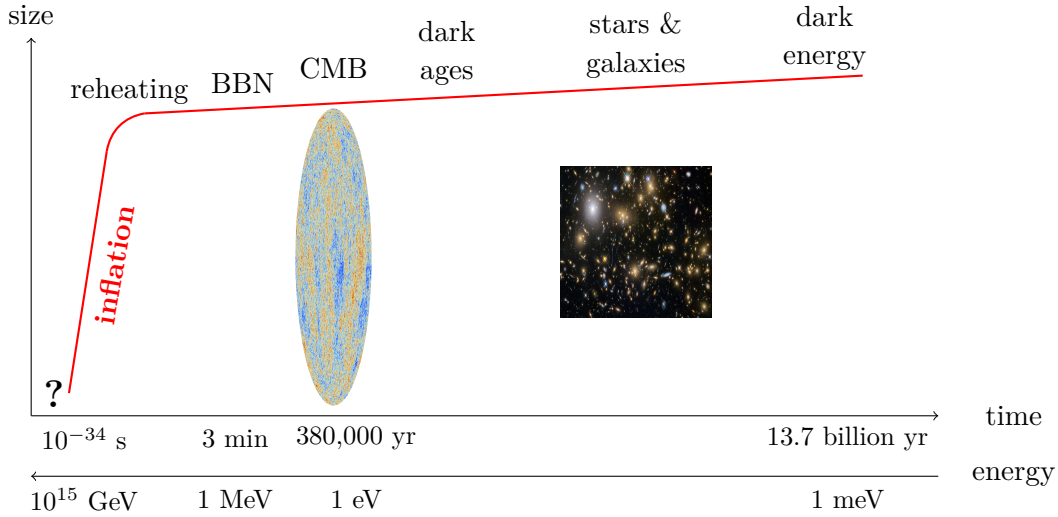


Figure 1.2: Brief history of the universe according to [18]. The axis ‘size’ actually refers to the length scale factor $a(t)$ to be defined in chapter 5.

Inflation stands for an extremely rapid expansion of the universe, where its size (better: scale factor) grew at least by a factor of 10^{26} . It is believed to have occurred in the very early universe at around 10^{-34} seconds and immense high energies of about 10^{15} GeV, see figure 1.2. The energy driving this expansion was in the end of inflation converted into the production of standard model particles. This process is known as *reheating*.

The CMB fluctuations have been arising from microscopic quantum fluctuations in the energy density that were stretched to macroscopic size during inflation. In fact, their size exceeded the physical horizon during inflation and thus they were no longer causally connected. Having reentered the horizon after inflation, they stayed macroscopic and induced the CMB anisotropies. In addition inflation solves a list of other issues of primordial cosmology: The *horizon problem* asks why patches of the CMB separated by more than one degree look astonishingly similar, even though they ought to be never in causal contact. As possible answer, these patches once might have been causally connected, but then left the horizon during inflation and reentered at later times. According to the *flatness problem* tiny deviations from an ultra-flat universe at early stages are expected to grow to large curvature differences in the universe. The observed nearly absolute flatness could therefore be only explained via highly fine-tuned initial conditions. Inflation simply flattens possible primordial curvature deviations. Due to all these novel explanations inflation is a widely accepted concept that triggered much effort in constructing an explicit model.

The energy necessary to drive inflation can be provided by a scalar field, called *inflaton* Θ , moving down some potential $V(\Theta)$. The difference in potential energy $\Delta V(\Theta)$ induces the growth of the universe. Importantly, accelerated expansion requires a slowly rolling inflaton, hence a sufficiently flat potential. As soon as the slow-roll conditions are violated, inflation stops and *reheating* commences. Obviously, the shape of the potential $V(\Theta)$ is

crucial for inflation and in fact a great number of models had been developed. Moreover, one distinguishes between *small-* and *large-field inflation*, where either $\Delta\Theta < 1M_{\text{Pl}}$ or $\Delta\Theta \geq 1M_{\text{Pl}}$, respectively. Here, M_{Pl} denotes the reduced Planck mass given by $M_{\text{Pl}} = 1/\sqrt{8\pi G_N} \sim 2.435 \times 10^{18}$ GeV with Newton's constant G_N . Accordingly, we speak of *sub-* and *trans-Planckian* field distances $\Delta\Theta$. Recent experimental data from the PLANCK 2015 and BICEP2/Keck Array collaboration [20] sets an upper bound on the *tensor-to-scalar ratio* $r < 0.07$. Heuristically, the value r measures the contribution of gravitational waves (more precisely B-modes) to the temperature anisotropy in the CMB. Due to the Lyth bound [21] the value $r < 0.07$ allows for large-field inflation. However, for large excursions $\Delta\Theta$ it is much more involved to ensure corrections to the inflaton potential are suppressed. Since inflation is usually treated using an effective field theory, there are always higher-order corrections that can spoil the trans-Planckian flatness of the potential V and thus stop inflation. For instance, fibre inflation models [22] argue that these unwanted terms are sub-leading in a large volume expansion of $V(\Theta)$. A more popular idea is based on a symmetry protecting the potential. Fields inheriting such a symmetry are *axions*. An axionic inflaton is equipped with a discrete shift symmetry $\Theta \rightarrow \Theta + \text{const.}$ which per se forbids polynomial correction terms. At a first glance $V(\Theta)$ has to be periodic if the inflaton Θ is an axion. Such a simple axionic model with periodic potential is called *natural inflation* [23].

Realizing inflation within string theory is often referred to as *string inflation* and can be based on very distinct mechanisms (see [24] for an overview). In this thesis we shall focus on employing axions as inflaton field. As a matter of fact, axions appear ubiquitously in string theory. To be more concrete, moduli which arise during compactification contain scalars endowed with an axionic shift symmetry. It is therefore natural to consider the interplay between moduli stabilization and axion inflation. Fluxes who stabilize the moduli, can in the same way generate a potential for the axionic inflaton modulus with the crucial feature that the potential is polynomial. Corrections to the potential are certainly suppressed since the simultaneous shift of axion and flux is still a symmetry of the system [25, 26]. Once a particular flux value was chosen, the axion shift symmetry is spontaneously broken and the inflaton can only move along one branch of the potential. Since fluxes are quantized, we obtain a multi-branch potential (see figure 5.4). In other words, the axion experiences a monodromy in its configuration space. This idea is known as *axion monodromy inflation* and relies on the pioneering work of E. Silverstein and A. Westphal [27]. Originally, they considered *D*-branes (spontaneously) breaking the shift symmetry of the axion, but did not connect it directly to moduli stabilization. In [28] the same mechanism was realized using fluxes (inducing F-term scalar potentials) as discussed above.

Recall that we are interested in large-field inflation, i.e. trans-Planckian field ranges. As a consequence periodic inflaton potentials demand for trans-Planckian *axion decay constants* f which corresponds to the periodicity of the axion. However, there is no chance for trans-Planckian f in the controlled perturbative regime [29]. Inflation from periodic potentials seems thus a priori impossible in string theory. A clever way to avoid this issue employs more axions with sub-Planckian decay constants that effectively lead to a trans-Planckian

one. Here, we will focus on *aligned inflation* [30] with two axions, but there exists also *N – fflation* [31] with many more fields. Note that axion monodromy inflation does not suffer from these constraints because polynomial potentials require no trans-Planckian f .

In the last years dozens of string inflation models were constructed and the enthusiastic mood conveyed the impression that a completely consistent scenario is just waiting around the corner. However, looking more precisely into the details nearly every setup revealed some issues. For instance, fluxes constitute an energy source that might warp the compactification manifold. The validity of the effective supergravity description for moduli stabilization can be conscientiously ensured solely in proper limits where the fluxes get dilute. Moreover, string inflation is always based on a tight sequence of effective theories. The supergravity theory for moduli premises heavy string and Kaluza-Klein modes with masses M_{KK} and M_s , respectively, may be safely neglected. For inflation with effectively one axion field there needs to be a mass hierarchy between the inflaton (M_Θ) and all other moduli (M_{mod}). Added together, any viable model of string inflation must satisfy the hierarchy:

$$M_\Theta < M_{\text{mod}} < M_{\text{KK}} < M_s < M_{\text{Pl}}. \quad (1.0.1)$$

The inflaton mass is usually around the Hubble parameter¹ during inflation $M_\Theta \sim H_{\text{inf}} \sim 10^{13}$ GeV. Together with the Planck mass $M_{\text{Pl}} \sim 10^{18}$ GeV the required hierarchy is obviously far from trivial. Many models struggle therefore with controlling all effective theories [32–34]. More concretely, improving the lower part of the hierarchy (ensure single-field inflation) often worsens the control over the upper part drastically (consistent $D = 4$ supergravity theory) and vice versa. The omnipresent problems in string inflation led to a change of paradigm and motivated the central question of this thesis:

*Are there underlying string theory or quantum gravity principles
constraining/forbidding large-field inflation?*

The goal of this thesis is to elaborate on the motivation for that question and test one set of proposals for such quantum gravity constraints known as the *swampland conjectures*. Let us just mention that J. Conlon considered alternative arguments [35, 36] based on entropy of de Sitter space and arrived at the same general conclusion. A further conjecture on the moduli space size is [37]. The swampland idea suggests that effective field theories that arise from quantum gravity are much more restricted than one would expect from the pure low-energy four-dimensional point of view. Effective theories that look consistent but can never be coupled to gravity at high energies have been termed to be in the *swampland* [38]. On the other side, effective theories following from quantum gravity by consistent compactification and in the low-energy limit are named *landscape* theories. Theories in the landscape have to obey certain *swampland conjectures* in contrast to theories in the swampland. Since string theory is UV complete, it suffices as playground for these

¹The Hubble parameter H_{inf} during inflation will be given in section 5.3.1. From the potential slow-roll conditions (5.2.8) one can estimate the inflaton mass $M_\Theta^2 \sim \partial_\Theta^2 V \sim 3\eta H^2$.

conjectures. We will see how the swampland conjectures constrain large-field inflation with periodic as well as polynomial potentials. Periodic potentials are generated by non-perturbative effects and strongly constrained by the weak gravity conjecture [39–42]. Here, particular interest lies on axion monodromy inflation where so far no general reason for the difficulties with the correct mass hierarchy could be determined. The *swampland distance conjecture* [43] claims that any effective theory for moduli has to break down when moving far enough in the moduli space. More concretely, states with mass M_0 get exponentially light $M \sim M_0 \exp(-\Theta/\Theta_c)$ if one moves infinite distances in moduli space $\Theta \rightarrow \infty$. The effective theory becomes invalid after a critical distance $\Theta \sim \Theta_c$, where Θ_c is a priori undetermined. According to the *refined swampland distance conjecture* (RSDC) [44] this happens after traversing distances of $\Theta_c \sim \mathcal{O}(1) M_{\text{Pl}}$. Originally, the conjecture applies to non-periodic moduli (saxions), but taking into account backreaction effects [45] of the inflaton displacement onto the other moduli, it will also affect axions. Eventually, it will have a tremendous impact on trans-Planckian field ranges in axion monodromy inflation. Note that in this thesis it is always the Kaluza-Klein modes whose mass is dropping exponentially according to the swampland distance conjectures (alternatively see [46]). Of course, the impressive power of the swampland story is build purely on conjectures which have not yet been rigorously proven. Hence, in this thesis we will also challenge the RSDC for moduli spaces of specific Calabi-Yau compactifications. Even if the (momentarily very popular) swampland conjectures turn out to be not the final answer to the central question above, they nevertheless emphasize the necessity of control over effective theories which is key to successfully describe nature as discussed in the beginning. Additionally, investigating the swampland might give rise to new insights into fundamental concepts of quantum gravity.

Let us finally point out that this thesis analyzes only (effective) single field inflation, i.e. includes one inflaton field. The mass hierarchy would be much easier satisfied for multi-field models and the inflaton could follow more sophisticated trajectories. However, experiments are not in favor of multi-field inflation due the absence of non-Gaussianities [47].

Objective and outline

To discuss the question whether large-field inflation is constrained or even forbidden within string theory or quantum gravity, the thesis at hand is split into two parts. Part II introduces briefly the theoretical concepts which are well-known and based on a vast literature. New developments and results are collected in part III.

We start off with explaining the origin of moduli from string compactifications in chapter 2. Eventually moduli embody the inflaton and are hence the main objects of this thesis. We consider type IIB string theory compactified on orientifolded Calabi-Yau manifolds [48]. Including D -branes leads to both, closed and open string moduli. The first arise from the massless spectrum of closed string modes as well as geometric properties, i.e. Kähler and complex structure moduli. The latter are interpreted as D -brane moduli such as transverse

position. Chapter 3 studies the complex structure moduli space more precisely in terms of periods. In order to stabilize moduli and generate the inflaton potential we turn on background fluxes [49, 50] in chapter 4. Note that non-geometric fluxes are incorporated as well. Afterwards we summarize the basics of large-field inflation with axions in chapter 5. In particular it is shown why periodic potentials are natural in axion inflation and how fluxes can nevertheless enable polynomial potentials as alternative route towards string inflation. Finally, in the subsequent chapter 6 the swampland idea is motivated and the two relevant conjectures, i.e. the weak gravity [51] and the swampland distance [43] conjectures, are explained.

We begin part III by a new attempt to realize large-field inflation making use of closed string moduli. The main idea of chapter 7 boils down to consider a special point in the complex structure moduli space that is called *conifold singularity*. In contrast to the large complex structure point, there one of the periods exhibits a logarithmic behavior leading to a singularity in the Kähler metric [52]. In agreement with [53] the mass of the cycle shrinking at the conifold is exponentially suppressed. The axionic complex structure modulus related to this particular cycle might represent a good inflaton candidate with respect to the mass hierarchy 1.0.1 (for alternative models in warped throats with red-shifted inflaton mass see [54–56]). Its potential is periodic and we comment on the relation to the weak gravity conjecture. Nevertheless, controlling the warping effects in the vicinity of the conifold requires a large compactification volume which leads to problems with the mass hierarchy. As suggested by [57, 58] employing open string moduli as inflaton might decouple the issues from the closed string moduli. Hence, chapter 8 analyzes different setups including a $D7$ -brane position modulus as inflaton [59–62]. The potentials are then polynomial, i.e. we change to axion monodromy inflation. Note that we stabilize the moduli via tree-level superpotentials [32] as well as with (non-)perturbative corrections (KKLT [63] and LVS [15]). In any case backreaction [44, 45, 64] of the movement of the inflaton modulus θ onto the other moduli will imply a logarithmic growth of the proper distance $\Theta \sim \Theta_c \log \theta$. The constant Θ_c corresponds to the critical distance proposed by the swampland distance conjecture where the effective theory breaks down. The models based on closed string moduli of [32, 34, 45] led all to $\Theta_c \sim \mathcal{O}(1)$, but with open string moduli it will be possible to achieve a flux-dependent Θ_c . Quantization of fluxes and the hierarchy (1.0.1) culminate, however, again in a sub-Planckian Θ_c . These observations reflect just the refined swampland distance conjecture and highly constrain the validity of our axion monodromy inflation models. The drastic consequences follow only from the refined version of the conjecture. Therefore the refined swampland distance conjecture will be challenged in chapter 9. More precisely we calculate geodesic distances in the Kähler moduli spaces of Calabi-Yau manifolds. For that purpose we first determine the periods of the mirror dual manifold to compute distances in the complex structure moduli space and subsequently transform back to Kähler moduli. In addition to (geometric) regions of the moduli spaces with infinite distance points, we analyze also non-geometric phases of stringy nature like the Landau-Ginzburg phase. There one observes only finite distances. According to the refined swampland distance conjecture all finite distances that

do not exhibit the logarithmic behavior must be sub-Planckian. In addition trans-Planckian distances have to grow logarithmically with the moduli and in particular show a critical distance $\Theta_c \leq 1 M_{\text{Pl}}$. Here, we highlight mainly internal manifolds with $h^{1,1} = 2$ and refer to [65] for models with $h^{1,1} = 1$ or $h^{1,1} = 101$. Our results in chapter 9 are strengthening the RSDC and putting pressure on large-field inflation in string theory. We conclude with a summary of our results and give a short outlook taking other recent conjectures into account.

This thesis is based on four publications. Parts of the preliminaries II and in particular of chapters 7, 8, 9 are taken from the following references:

- R. Blumenhagen, D. Herschmann, F. Wolf,
'String Moduli Stabilization at the Conifold',
JHEP 1608 (2016) 110.
- R. Blumenhagen, I. Valenzuela, F. Wolf,
'The Swampland Conjecture and F-term Axion Monodromy Inflation',
JHEP 1707 (2017) 145.
- R. Blumenhagen, D. Herschmann, F. Wolf,
'Challenges for Moduli Stabilization and String Cosmology near the Conifold',
PoS CORFU2016 (2017) 104.
- R. Blumenhagen, D. Kläwer, L. Schlechter, F. Wolf,
'The Refined Swampland Distance Conjecture in Calabi-Yau Moduli Spaces',
JHEP 1806 (2018) 052.

Part II

Conceptual Preliminaries

CHAPTER 2

Basics of String Compactification

The fundamental objects of string theory are tiny open and closed strings. In order to describe the dynamics of strings one can construct an action in analogy with the worldline interval that needs to be integrated for point-like particles. Since strings sweep out a two-dimensional surface, known as *worldsheet*, as they move in spacetime, the *Nambu-Goto action* is simply the integral over the surface of the worldsheet. Equivalently, their dynamics are classically captured by the *Polyakov action*

$$\mathcal{S}_{\text{Polyakov}} = -\frac{\pi}{l_s} \int_{\Sigma} d\tau d\sigma \sqrt{-h} h^{\alpha\beta} \partial_{\alpha} X^{\mu} \partial_{\beta} X^{\nu}. \quad (2.0.1)$$

Here, the coordinates on the worldsheet Σ are given by a “time” coordinate t as well as the extended spatial dimension of the string σ . The functions $X^{\mu}(\tau, \sigma)$ with $\mu, \nu = 0, \dots, D-1$, provide an embedding of the two-dimensional worldsheet Σ into D -dimensional spacetime called *target space*. The metric on the worldsheet is denoted by $h_{\alpha\beta}(\tau, \sigma)$ and the string length by l_s .

The Polyakov action describes the classical bosonic string. The next step is to quantize the classical theory which can be achieved for instance by introducing canonical commutation relations for the coordinates and their canonical conjugate momenta. Thereby one will encounter negative norm states, i.e. ghosts, causing problems with the probabilistic interpretation of quantum mechanics. Astonishingly, it can be proven that these ghosts decouple from the physical Hilbert space in precisely $D = 26$ dimensions. Note that there exist different derivations of the critical dimension $D = 26$. For instance, light-cone quantization leads to a conformal anomaly and the critical dimension arises from restoring Lorentz invariance for physical quantities in the quantum theory.

It is convenient to make the worldsheet supersymmetric by adding fermionic superpartners to $X^{\mu}(\tau, \sigma)$ and a worldsheet gravitino related to the metric $h_{\alpha\beta}(\tau, \sigma)$. A great feature of

the resulting superstring theory is the fact that it leads to spacetime fermions. Although non-trivial, after GSO projections the spectrum enjoys even spacetime supersymmetry. This ensures the absence of tachyonic instabilities that appear naturally in bosonic string theory. The critical dimension for the superstring turns out to be $D = 10$ demanding compactification to lower dimensions.

In this thesis we will mainly focus on type IIB superstring theory, which contains only closed strings. The massless spectrum can be computed by imposing level matching constraints as well as GSO projections for left- and right-movers on the closed string. For completeness, let us list its bosonic field content: a scalar dilaton ϕ , an anti-symmetric 2-form B_2 and a traceless symmetric graviton g in the NS-NS sector plus a 0-form C_0 , a 2-form C_2 and a 4-form C_4 in the R-R sector. Spacetime fermions arise from the NS-R and R-NS sector. For more details about the spectrum and the critical dimension of string theory see the extensive standard literature on string theory, for instance [66–68].

2.1 Kähler Geometry and Calabi-Yau Manifolds

To start off gently with the rather mathematical concepts introduced in this section, let us recall the goals of string compactification. As has been explained already above, superstring theory requires us to live in a critical dimension $D = 10$, whereas the experimentally observed dimension is $D = 4$. So first, compactification has to solve this mismatch of dimensions, which is obviously unavoidable for string theory to be compatible with nature. The second requirement of compactification is in simple words that it preserves some supersymmetry. Motivation for this condition comes mainly from phenomenology and in particular from the fact that the standard model of particle physics is expected to require a supersymmetric extension¹. Independent of phenomenology, supersymmetric compactifications are relatively easy to analyze and do not contain tachyons.

Let us point out that we assume in this chapter geometries clearly larger than the string scale, i.e. we consider the large volume limit. Only then one may rely on the $D = 10$ supergravity approximation and apply tools of classical geometry. Perturbative α' -corrections and non-perturbative string loop corrections (depending on the string coupling g_s) will have a drastic effect on smaller scales. We often refer to the compactifications here as *geometric compactifications*. Other compactifications require a proper treatment within conformal field theory and can only be studied in special cases, such as orbifolds for instance. Later on and in particular in chapter 9 we will come back to these compactifications.

The idea of compactification boils down to simply “curling up” the six extra dimensions of superstring theory on an internal manifold \mathcal{M} of size smaller than what we can probe

¹Popular reasons for the incompleteness of the standard model are the hierarchy problems, such as the light Higgs mass. Supersymmetry can cure the dangerous divergences arising from quantum loop corrections.

experimentally. In other words, the space we live in is believed to consist of a product $\mathbb{R}^{1,3} \times \mathcal{M}$, i.e. $D = 4$ dimensional Minkowski space and a compact $D = 6$ dimensional manifold \mathcal{M} . It is crucial that the physics of the Minkowski space depends on geometrical features of the compact space \mathcal{M} . In chapter 7 we will extend the simple product structure of spacetime by introducing a *warp-factor* of the form e^{2A} that depends only on the internal coordinates of \mathcal{M} . This will still preserve Poincaré invariance in $D = 4$. Warping effects can be caused by branes and fluxes, which we shall define later. However, great care has to be taken with these objects as they might deform the background metric (of \mathcal{M}) in a radical manner.

More precisely, preserving supersymmetry during compactification requires a discussion about holonomy. We refer to the standard literature on string compactification for details, for instance [66,69]. It turns out that string phenomenology focuses mainly² on geometries with $SU(3)$ holonomy. In the end $SU(3)$ holonomy will lead us to Calabi-Yau manifolds which give $\mathcal{N} = 2$ supersymmetry in $D = 4$ after compactifying type II string theory. The supersymmetry may then be further reduced to $\mathcal{N} = 1$ by an inclusion of orientifold projections, which are going to be explained in section 2.2. This leaves just the right amount of supersymmetry for the minimal supersymmetric extension of the standard model (MSSM).

Our goal is now to define Calabi-Yau manifolds. To do so, we begin with geometries that are equipped with less refined mathematical structure and successively build-up to Calabi-Yau manifolds.

One feature of manifolds with $SU(3)$ holonomy is that they belong to *complex manifolds*. In simple terms, complex manifolds look locally like \mathbb{C}^n , just like real manifolds look locally like \mathbb{R}^n . Hence, locally one has coordinate systems that can be consistently patched together globally on the manifold. Transition functions between these coordinate patches have to be smooth for real manifolds and holomorphic for complex manifolds. Moreover, a $2D$ -dimensional real manifold is a D -dimensional complex manifold if it admits a globally well-defined *complex structure*, which we denote by a mixed tensor U_β^α . This tensor has to satisfy the condition $U_\beta^\alpha U_\alpha^\gamma = -\delta_\beta^\gamma$ as well as a vanishing Niejenhuis tensor $N_{mn}^\alpha = \partial_{[n} U_{m]}^\alpha - U_{[m}^\alpha \partial_r U_{n]}^\alpha = 0$ (for holomorphically patching together local complex coordinates). Using complex structures allows to define local complex coordinates. Back to our $2D$ -dimensional real manifold, one may divide the real coordinates in x^α, y^β , with $\alpha, \beta = 1, \dots, d$, and consider the tensor $U = \begin{pmatrix} 0 & \mathbb{1}_d \\ -\mathbb{1}_d & 0 \end{pmatrix}$. Thereby, complex coordinates can be written in terms of the complex structure U_β^α

$$dz^\alpha = dx^\alpha + i U_\beta^\alpha dy^\beta, \quad d\bar{z}^\alpha = dx^\alpha - i U_\beta^\alpha dy^\beta. \quad (2.1.1)$$

The standard example is the $D = 2$ torus, where the complex structure is usually denoted

²Model building from M- and F-theory with different holonomy (for instance M-theory on a $D = 7$ internal space with holonomy G_2) will not be discussed in this thesis.

by a complex parameter τ . Complex coordinates are then given by $dz = dx + i\tau dy$ with x, y being real coordinates.

In the next step we will extend complex manifolds by further mathematical structure: a metric. This leads to Kähler manifolds.

Kähler manifolds

To begin with, we equip our complex manifold with a hermitian metric G . By definition the only non-zero components of G have mixed indices, i.e. $G_{\alpha\beta} = G_{\bar{\alpha}\bar{\beta}} = 0$. More precisely, a hermitian metric is defined as covariant tensor field³ $ds^2 = G_{\alpha\bar{\beta}} dz^\alpha \otimes d\bar{z}^{\bar{\beta}}$ with $G_{\alpha\bar{\beta}}$ being positive definite⁴ and hermitian $G_{\alpha\bar{\beta}} = \overline{G_{\beta\bar{\alpha}}}$. Having a hermitian metric on a complex manifold, one can define a *fundamental (1, 1)-form*

$$J = i G_{\alpha\bar{\beta}} dz^\alpha \wedge d\bar{z}^{\bar{\beta}}. \quad (2.1.2)$$

Note that J^D (linked by wedge products) corresponds to the canonical volume form of the D -dimensional complex manifold. If the fundamental (1, 1)-form⁵ is closed, namely $dJ = 0$, we call $G_{\alpha\bar{\beta}}$ a *Kähler metric*. This gives rise to the following definition:

Definition: *A Kähler manifold is a complex manifold equipped with a Kähler metric.*

Kähler manifolds allow to use powerful mathematical tools, which simplify string compactifications a lot. For instance, from the closed fundamental form $dJ = (\partial + \bar{\partial})i G_{\alpha\bar{\beta}} dz^\alpha \wedge d\bar{z}^{\bar{\beta}} = 0$ one immediately derives

$$\frac{\partial G_{\alpha\bar{\beta}}}{\partial z^\gamma} = \frac{\partial G_{\gamma\bar{\beta}}}{\partial z^\alpha} \quad (2.1.3)$$

and by analogy an expression for \bar{z} . This relation leads to the crucial insight that locally there must exist a *Kähler potential* K which fully determines the metric

$$G_{\alpha\bar{\beta}} = \frac{\partial^2 K}{\partial z^\alpha \partial \bar{z}^{\bar{\beta}}}. \quad (2.1.4)$$

In other words, the fundamental form can be written as $J = i\partial\bar{\partial}K$. Let us stress that the Kähler potential is not unique, in the sense that adding holomorphic $f(z)$ or anti-holomorphic $f(\bar{z})$ functions does not alter the Kähler metric since they vanish when computing the metric.

³Summation over indices is implicit.

⁴Positive definite requires $z^\alpha G_{\alpha\bar{\beta}} \bar{z}^{\bar{\beta}} \geq 0 \forall \{z^\alpha\} \in \mathbb{C}^n$ with equality only if $z^\alpha = 0$.

⁵A (p, q) -form of the space $\mathfrak{W}^{p,q}$ can be written in the form $\frac{1}{p!q!} \mathbf{w}_{i_1, \dots, i_p, \bar{j}_1, \dots, \bar{j}_q} dz^{i_1} \wedge \dots \wedge dz^{i_p} \wedge d\bar{z}^{\bar{j}_1} \wedge \dots \wedge d\bar{z}^{\bar{j}_q}$. The exterior derivative can be split into $d = \partial + \bar{\partial}$ with $\partial : \mathfrak{W}^{p,q} \rightarrow \mathfrak{W}^{p+1,q}$ and $\bar{\partial} : \mathfrak{W}^{p,q} \rightarrow \mathfrak{W}^{p,q+1}$.

Note that large parts of this thesis are concerned with the computation of Kähler potentials. Before heading on to Calabi-Yau manifolds, let us give a prominent example for Kähler manifolds, which we are going to utilize later on in this thesis: the complex projective space.

The D -dimensional *complex projective space* \mathbb{P}^D can be constructed as a complex manifold described by $D + 1$ complex homogeneous coordinates $z = [z^1 : \dots : z^{D+1}]$ that satisfy the equivalence relation

$$(z^1, \dots, z^{D+1}) \sim (\lambda z^1, \dots, \lambda z^{D+1}), \quad (2.1.5)$$

with $\lambda \in \mathbb{C} - \{0\}$. Intuitively, a complex projective space \mathbb{P}^D is given by the set of complex lines through the origin of \mathbb{C}^{D+1} , where two points are on the same line if they can be identified by the equivalence relation (2.1.5).

The point set \mathbb{P}^D can be covered by $D + 1$ coordinate patches $U_i = \{z | z^i \neq 0\}$. Hence U_i describes all lines except the ones in the hyperplane $z^i = 0$. In every patch we can locally introduce D inhomogeneous coordinates $\xi_{(i)}^j = \frac{z^j}{z^i}$ with $j \neq i$. Thereby, one can show that \mathbb{P}^D is actually a Kähler manifold, see e.g. [69]. Note also that \mathbb{P}^D is compact and there is an often used special case $\mathbb{P}^1 \simeq S^2$, i.e. $D = 1$ dimensional complex projective space is equivalent to a sphere.

Besides, we will make use of a slight generalization of projective spaces, where the coordinate identification reads

$$(z^1, \dots, z^{D+1}) \sim (\lambda^{\omega_1} z^1, \dots, \lambda^{\omega_{D+1}} z^{D+1}). \quad (2.1.6)$$

The ω_i are non-zero integers and called weights of the homogeneous coordinates z^i . This defines a *weighted (complex) projective space*, denoted by $\mathbb{P}_{\omega_1, \dots, \omega_{D+1}}^D$.

Calabi-Yau manifolds

Combining the elegant mathematical structure of Kähler manifolds with holonomy brings us finally to the following definition

Definition: *A Calabi-Yau D -fold is a compact Kähler manifold with $SU(D)$ holonomy.*

As mention above, in this thesis we will solely focus on $SU(3)$ holonomy. The Calabi-Yau manifold has then $D = 3$ complex dimensions and we speak of a three-fold. Equivalently to the holonomy constraint, Calabi-Yau manifolds can be defined as compact Kähler manifolds, whose Ricci curvature is zero. This is an interesting feature to keep in mind, also for practical reasons.

The name of these manifolds arose actually from yet another definition stating that Calabi-Yau manifolds are given by compact Kähler manifolds with vanishing first Chern class. For definitions and details about Chern classes we refer to the literature, for instance [70]. From the definition of the first Chern class one can see directly that a Ricci-flat Kähler manifold must have vanishing first Chern class. The other way round, however, is quite subtle. This was first considered by E. Calabi and later proven by S.T. Yau in his famous theorem.

So, which definition is best to determine whether a manifold satisfies the Calabi-Yau conditions? As a matter of fact, it is extremely hard to construct a Ricci-flat metric on manifolds and there is actually no explicitly known Calabi-Yau metric so far in dimension $D = 3$. However, due to Yau's theorem it is sufficient to check the first Chern class of the manifold, which is a much simpler task. Chern classes are related to fundamental topological properties of a manifold. These properties build the basis for subsequent parts of this thesis and shall be analyzed next.

On a complex manifold the notation of p -forms and (de Rham co-)homology can be refined with respect to their holomorphic and anti-holomorphic indices. Considering a complex three-dimensional manifold \mathcal{M} , one has for instance the splitting $H^3(\mathcal{M}, \mathbb{C}) = H^{3,0}(\mathcal{M}) \oplus H^{2,1}(\mathcal{M}) \oplus H^{1,2}(\mathcal{M}) \oplus H^{0,3}(\mathcal{M})$. The refined cohomologies $H^{p,q}$ are called Dolbeault cohomology classes. A basis of $H^{p,q}$ is of the form $dz^{i_1} \wedge \dots \wedge dz^{i_p} \wedge d\bar{z}^{\bar{j}_1} \wedge \dots \wedge d\bar{z}^{\bar{j}_q}$, with p holomorphic and q anti-holomorphic indices. The dimensions of $H^{p,q}$ are topological invariants and of particular interest to us. We call

$$h^{p,q} = \dim_{\mathbb{C}}(H^{p,q}) \quad (2.1.7)$$

the *Hodge numbers* of our manifold. For Calabi-Yau manifolds these Hodge numbers turn out to be quite restricted.

From complex conjugation one can show that $h^{p,q} = h^{q,p}$ and consequently Hodge duality implies $h^{p,q} = h^{D-p, D-q}$. In addition there are two crucial ingredients from the $SU(D)$ holonomy: $h^{D,0} = 1$ and $h^{p,0} = 0$ for $0 < p < D$. Thus for a Calabi-Yau three-fold only $h^{1,1}$ and $h^{2,1}$ remain as independent Hodge numbers. Hodge numbers are usually collected in the Hodge star, which looks for complex $D = 3$ manifolds as follows

$$\begin{array}{ccccccc}
 & & h^{0,0} & & & & 1 \\
 & & h^{1,0} & h^{0,1} & & & 0 & 0 \\
 & h^{2,0} & h^{1,1} & h^{0,2} & & & 0 & h^{1,1} & 0 \\
 h^{3,0} & h^{2,1} & h^{1,2} & h^{0,3} & \xrightarrow{\text{Calabi-Yau}} & 1 & h^{2,1} & h^{2,1} & 1 \\
 & h^{3,1} & h^{2,2} & h^{1,3} & & & 0 & h^{1,1} & 0 \\
 & & h^{3,2} & h^{2,3} & & & 0 & 0 & \\
 & & h^{3,3} & & & & & 1 &
 \end{array}$$

A remarkable discovery within the development of string theory is mirror symmetry. Which states that for a given Calabi-Yau three-fold \mathcal{M} there exists a mirror manifold \mathcal{W} with $h^{p,q}(\mathcal{M}) = h^{3-p,q}(\mathcal{W})$. In particular this implies $h^{1,1}$ and $h^{2,1}$, namely Kähler and complex

structure moduli, being interchanged between \mathcal{M} and \mathcal{W} . This is a fascinating symmetry since the mirror manifold has completely different geometry and even different topology. In chapter 3 we will make extensive use of mirror symmetry.

Let us also point out the existence of a unique nowhere vanishing holomorphic $(3,0)$ -form Ω_3 , recall $h^{3,0} = 1$. That is an important feature of Calabi-Yau three-folds and will be employed several times later on. Furthermore, the reader should keep in mind that there exist a vast number of possible Calabi-Yau three-folds. In fact, it is unclear whether this number is even finite. Furthermore note that a simple method to construct Calabi-Yau manifolds uses hypersurfaces in weighted projective spaces, which have been introduced earlier. Details are presented in chapter 3.

Back to our motivation, compactification of $D = 10$ type II string theory on a Calabi-Yau three-fold leads to a $D = 4$ theory with $\mathcal{N} = 2$ supersymmetry. For usual model building in particle physics the amount of supersymmetry has to be reduced to $\mathcal{N} = 1$. One way to achieve this is introducing orientifold projections and/or D -branes, which shall be discussed in the next section. Notice that background fluxes (see chapter 4) will subsequently break the remaining $\mathcal{N} = 1$ supersymmetry spontaneously.

2.2 Orientifold Projection and D -Branes

As indicated by the name, orientifold projections involve a parity operator Ω_P that reverses the orientation of the string worldsheet. In other words, for closed strings it swaps the left- and right-movers as well as the two ends of open strings. By modding out the worldsheet parity Ω_P we obtain an unoriented theory and one speaks of *orientifold compactifications*. Using these projections the massless $\mathcal{N} = 2$ supersymmetric spectrum is simply truncated⁶ to $\mathcal{N} = 1$ by projecting out certain states. For details we refer to the literature [48,67,71,72].

In type IIB string theory the full orientifold projection includes in fact two operators in addition to Ω_P . At first, there is the operator σ acting as a holomorphic involution (i.e. $\sigma^2 = \text{id}$) of the internal manifold \mathcal{M} without any effect on $D = 4$ Minkowski space. The involution σ leaves the Kähler form of Calabi-Yau three-folds invariant, but has a non-trivial impact on the holomorphic $(3,0)$ -form Ω_3 . Throughout this thesis we consider⁷

$$\sigma : J \rightarrow J, \quad \sigma : \Omega_3 \rightarrow -\Omega_3. \quad (2.2.1)$$

This choice requires another operator $(-1)^{F_L}$ with the left-moving fermion number F_L in order to ensure the orientifold action squares to one. In total the orientifold projection reads

$$\Omega_P (-1)^{F_L} \sigma. \quad (2.2.2)$$

⁶Moreover the couplings are modified appropriately.

⁷We take the pull-back of σ to be implicit.

cohomology group		dimension		basis	
$H_+^{1,1}$	$H_-^{1,1}$	$h_+^{1,1}$	$h_-^{1,1}$	ω_α	ω_a
$H_+^{2,2}$	$H_-^{2,2}$	$h_+^{1,1}$	$h_-^{1,1}$	$\tilde{\omega}^\alpha$	$\tilde{\omega}^a$
$H_+^{2,1}$	$H_-^{2,1}$	$h_+^{2,1}$	$h_-^{2,1}$	$\chi_{\hat{\lambda}}$	χ_λ
H_+^3	H_-^3	$2h_+^{2,1}$	$2h_-^{2,1} + 2$	$\{\alpha_{\hat{\lambda}}, \beta^{\hat{\lambda}}\}$	$\{\alpha_\lambda, \beta^\lambda\}$

Table 2.1: Cohomology groups according to [71] and their dimensions. The basis indices are such that they fill up the dimensions of the corresponding cohomologies.

Let us now introduce *orientifold planes* or Op -planes, where p stands for the number of spatial dimensions. These are defined by points in the full $D = 10$ spacetime that are invariant under the involution σ . Since σ is only acting on the internal space, Op -planes cover the entire Minkowski space. They also wrap a $(p - 3)$ -cycle of the Calabi-Yau manifold. In type IIB, orientifold planes have to be even dimensional (including the time direction), such that solely $O3$ -, $O5$ -, $O7$ - and $O9$ -planes are possible [73]. For further selection assume z^1 , z^2 and z^3 are complex coordinates of the Calabi-Yau manifold \mathcal{M} . One can then always express the holomorphic $(3, 0)$ -form in terms of $\Omega_3 \sim dz^1 \wedge dz^2 \wedge dz^3$. The choice $\sigma\Omega_3 = -\Omega_3$ implies therefore that the internal part of the orientifold plane is either a point or a surface of complex dimension two. As a consequence we are left with $O3$ - and $O7$ -planes. Note that an alternative choice for the involution σ would have led to $O5$ - and $O9$ -planes as extensively studied in [71].

Later in section 2.3.1 we will be more precise about which states survive the orientifold projection, i.e. we will determine the massless (closed string) spectrum of $\mathcal{N} = 1$ Calabi-Yau orientifold compactifications of type IIB string theory with $O3$ - and $O7$ -planes. For now, let us just point out an important consequence of the orientifold projection.

The holomorphic involution σ splits the cohomology groups $H^{p,q}$ into an even eigenspace $H_+^{p,q}$ and an odd eigenspace $H_-^{p,q}$ with dimensions denoted accordingly

$$H^{p,q} = H_+^{p,q} \oplus H_-^{p,q}, \quad h^{p,q} = h_+^{p,q} + h_-^{p,q}. \quad (2.2.3)$$

The action (2.2.1) of σ on Ω_3 implies $h_+^{3,0} = h_+^{0,3} = 0$ and $h_-^{3,0} = h_-^{0,3} = 1$. Table 2.1 lists all non-trivial cohomology groups divided by the involution σ together with their dimensions. There we also defined basis elements for the cohomologies.

The bosonic field content of type IIB string theory can now be expanded in these cohomology bases. Afterwards one can explicitly perform the dimensional reduction with respect to the orientifold projection. The resulting spectrum contains the full list of closed string moduli and is going to be outlined in section 2.3.1. Before introducing moduli fields, let us briefly comment on D -branes and their relation to Op -planes.

D-branes

The presence of orientifold planes requires the introduction of *D*-branes in order to ensure *tadpole cancellation*. More precisely, *O*-planes carry RR-charge inducing tadpole diagrams, i.e. emission of closed string excitations out of the vacuum. Flux lines of RR *p*-forms cannot escape on a compact manifold due to Gauss's law and hence the overall RR-charge must add up to zero. The negative RR tadpoles of the orientifold planes can in fact be canceled by *D*-branes, who are themselves equipped with a positive RR-charge. One can show that the tadpoles of *O3*- and *O7*-planes, which we consider here, are canceled by *D3*- and *D7*-branes. A *Dp*-brane extends into *p* spatial dimensions and has to span Minkowski spacetime because of $D = 4$ Poincaré invariance. Guaranteeing that the *D*-branes do not break supersymmetry (in addition to the *O*-planes), *D7*-branes must wrap a 4-cycle. There exists no such criterion for *D3*-branes as they are point-like on the Calabi-Yau manifold. For more information regarding our setups we refer to [32, 74, 75].

2.3 Moduli Space

Compactification of string theory leads inevitably to numerous free continuous parameters in the lower dimensional theory. For instance, a simple compactification on a circle \mathcal{S}^1 leaves the radius a priori as unfixed parameter. In the one dimension lower theory we obtain a massless scalar field whose vacuum expectation value (vev) corresponds to the radius. This field is called *modulus*. More concretely we define

Definition: *Moduli in string theory are massless scalar fields arising during compactification, whose vevs label different string backgrounds.*

The story becomes much more involved for Calabi-Yau compactifications with orientifolds and *D*-branes as there are different types of moduli.

Note that a Calabi-Yau manifold with certain Hodge numbers is not at all unique since it may still vary in size and shape. Consider for instance a real two-dimensional torus T^2 with radii R_1 and R_2 . Compactification on the torus leads to two moduli fields which we denote by

$$U_{\text{torus}} \sim \frac{R_1}{R_2}, \quad T_{\text{torus}} \sim \frac{1}{\alpha'} R_1 R_2. \quad (2.3.1)$$

The vev of U_{torus} gives information about the “shape” of the torus and will later be referred to as complex structure modulus. On the other hand, T_{torus} governs the “size” of the torus and will be named Kähler modulus. These moduli arise from the geometry or more precisely from the deformations of the metric of the compactification manifold.

In addition there are moduli coming from the bosonic field content of closed strings, which we call *closed string moduli* (together with metric deformations). Deformations of D -branes will give further moduli denoted as *open string moduli*. Moduli fields span a space, known as *moduli space*, which is often equipped with a rich geometrical structure.

2.3.1 Closed String Moduli

Size and shape of a Calabi-Yau manifold are encoded in its Ricci-flat Kähler metric. Hence, a natural question that pops up is whether there exist deformations of the metric G which do not spoil the Calabi-Yau condition

$$R_{\mu\nu}(G + \delta G) = 0 \quad \implies \quad \nabla^\rho \nabla_\rho \delta G_{\mu\nu} + 2R_{\mu}{}^\rho{}_\nu{}^\sigma \delta G_{\rho\sigma} = 0. \quad (2.3.2)$$

The relation on the right was termed Lichnerowicz equation and arises from the left one after eliminating unappealing diffeomorphisms (coordinate transformations). Employing the Riemann tensor for Kähler manifolds, one finds two possible solutions to the Lichnerowicz equation: $\delta G_{\alpha\bar{\beta}}$ and $\delta G_{\alpha\beta}$. These deformations become scalar fields in four-dimensions. In fact, the deformations $\delta G_{\alpha\bar{\beta}}$ with mixed components will correspond to Kähler moduli, whereas $\delta G_{\alpha\beta}$ with pure components to complex structure moduli.

More precisely, $\delta G_{\alpha\bar{\beta}}$ can be understood as deformations of the Kähler form $J = i G_{\alpha\bar{\beta}} dz^\alpha \wedge d\bar{z}^\beta$. Using a basis $\{\omega_A\}$ of $H^{1,1}(\mathcal{M})$ of harmonic $(1,1)$ -forms on a Calabi-Yau manifold \mathcal{M} , we expand

$$J = t^A \omega_A \quad A = 1, \dots, h^{1,1}. \quad (2.3.3)$$

The t^A are real scalar fields which depend only on $D = 4$ spacetime coordinates, i.e. not on the internal coordinates of \mathcal{M} . The other deformations $G_{\alpha\beta}$ can be related to harmonic $(1,2)$ -forms via the holomorphic $(3,0)$ -form Ω_3

$$\delta G_{\alpha\beta} = \frac{i}{\|\Omega\|^2} \bar{U}^B (\bar{\chi}_B)_{\alpha\bar{i}\bar{j}} \bar{\Omega}^{\bar{i}\bar{j}}{}_\beta, \quad B = 1, \dots, h^{2,1}. \quad (2.3.4)$$

Here, $\{\bar{\chi}_B\}$ is a harmonic basis of $H^{1,2}(\mathcal{M})$ and $\|\Omega\|^2 = \frac{1}{3!} \Omega_{ijk} \bar{\Omega}^{ijk}$. The U^B are complex scalar fields in four-dimensions and again do not depend on the internal coordinates.

In order to obtain the full massless spectrum after compactification on the Calabi-Yau manifold \mathcal{M} , one must also take into account the other ten-dimensional fields. In type IIB string theory there are in addition to the metric the dilaton ϕ and the anti-symmetric 2-form B_2 from the NS-NS sector as well as the C_0 , C_2 and C_4 forms from the R-R sector. These fields can be expanded in harmonic forms on \mathcal{M} similarly to the metric deformations. However, the orientifold projection will truncate the $D = 4$ spectrum drastically as we are going to explain next.

Massless spectrum of $\mathcal{N} = 1$ Calabi-Yau orientifolds

The massless spectrum of orientifold compactifications has been well-studied in the literature [73, 76, 77] and our analysis follows in particular [71]. Consider the orientifold projection described in section 2.2 together with $O3$ - and $O7$ -planes. The four-dimensional compactified theory contains only states that are invariant under the projection. Recall that the orientifold projection splits the cohomologies and thus all fields need to be expanded in bases listed in table 2.1.

At first, notice that the holomorphic involution σ does not change the Kähler form J according to (2.2.1). Consequently, only the $h_+^{1,1}$ even deformations t^α survive the orientifold projection

$$e^{-\phi/2} J = t^\alpha \omega_\alpha, \quad \alpha = 1, \dots, h_+^{1,1}. \quad (2.3.5)$$

The dilaton factor $e^{-\phi/2}$ was included for convenience. It is important to keep in mind that the $\{t^\alpha\}$ are therefore expressed in Einstein frame.

On the contrary, due to (2.2.1) only complex structure deformations in $H_-^{2,1}$ are kept in the spectrum with $\{\bar{\chi}_\beta\}$ being now a basis of $H_-^{2,1}$

$$\delta G_{\alpha\beta} = \frac{i}{\|\Omega\|^2} \bar{U}^\lambda (\bar{\chi}_\lambda)_{\alpha\bar{i}\bar{j}} \Omega^{\bar{i}\bar{j}}{}_\beta, \quad \lambda = 1, \dots, h_-^{2,1}. \quad (2.3.6)$$

An expansion of the other fields requires some knowledge about the behavior under the orientifold projection. As stated in [71], ϕ , G and C_2 are even under the worldsheet parity Ω_P and B_2 , C_0 and C_4 are odd. The left-moving fermion operator $(-1)^{F_L}$ leaves all NS-NS fields invariant and produces a minus sign for R-R fields. The states invariant under the full projection (2.2.2) have to transform under the involution σ such that it compensates the effect of $\Omega_P(-1)^{F_L}$. Therefore, the invariant states obey

$$\sigma = \begin{cases} \text{even} & \text{for } G, \phi, C_0, C_4, \\ \text{odd} & \text{for } B_2, C_2. \end{cases} \quad (2.3.7)$$

This implies that the forms B_2 , C_2 and C_4 can be expanded in bases of table 2.1 according to⁸

$$\begin{aligned} B_2 &= b^a \omega_a, \\ C_2 &= c^a \omega_a, & a = 1, \dots, h_-^{1,1}, \\ C_4 &= V^{\hat{\lambda}} \wedge \alpha_{\hat{\lambda}} + \rho_\alpha \tilde{\omega}^\alpha, & \hat{\lambda} = 1, \dots, h_+^{2,1}, \alpha = 1, \dots, h_+^{1,1}. \end{aligned} \quad (2.3.8)$$

The b^a , c^a , ρ_α are scalar fields in $D = 4$ and $V^{\hat{\lambda}}$ are $U(1)$ gauge bosons. The complete massless spectrum of the $\mathcal{N} = 1$ Calabi-Yau orientifold compactification is depicted in table

Multiplet	Number	Fields	Description
gravity multiplet	1	$G_{\mu\nu}$	Minkowski metric
vector multiplets	$h_+^{2,1}$	V^{λ}	gauge bosons
	$h_-^{2,1}$	U^{λ}	complex structure moduli, cf. (2.3.6)
chiral multiplets	1	(ϕ, C_0)	axio-dilaton, cf. (2.3.11)
	$h_-^{1,1}$	(b^a, c^a)	G-moduli, cf. (2.3.11)
	$h_+^{1,1}$	(t^α, ρ_α)	Kähler moduli, cf. (2.3.12)

Table 2.2: $\mathcal{N} = 1$ spectrum of $O3/O7$ -orientifold compactification [71].

2.2, where we arranged everything in multiplets. The scalar fields can be grouped together to form complex-valued moduli fields in $D = 4$. It turns out that the moduli space satisfies all criteria to be a Kähler manifold. Next, we give expressions for the Kähler potentials of the moduli spaces.

Kähler potentials

A useful feature of the moduli space \mathcal{X} is its block-diagonal structure in the sense that complex structure deformations do not mix with the other moduli

$$\mathcal{X} = \mathcal{X}_{cs}^{h^{2,1}} \otimes \mathcal{X}_{\text{rest}}^{h^{1,1}+1}. \quad (2.3.9)$$

Each factor is actually a Kähler manifold and the complex structure moduli space $\mathcal{X}_{cs}^{h^{2,1}}$ is even a *special Kähler manifold*. This refined structure shall be introduced in the next section.

The earlier defined *complex structure moduli* U^λ (see (2.3.6)) turn out to be already good Kähler coordinates on $\mathcal{X}_{cs}^{h^{2,1}}$. We will be more precise about this statement when discussing special geometry. As a matter of fact, there exists a natural metric on the complex structure moduli space known as Weil-Petersson metric that is completely determined by the holomorphic $(3, 0)$ -form Ω_3 . This metric is Kähler and can be locally extracted from the Kähler potential [71]

$$K_{cs} = - \log \left(-i \int_{\mathcal{M}} \Omega_3 \wedge \bar{\Omega}_3 \right). \quad (2.3.10)$$

The other (real) scalar fields have to be combined such that one obtains good Kähler coordinates on the moduli space $\mathcal{X}_{\text{rest}}^{h^{1,1}+1}$. Following the literature [32, 71] we define the

⁸The expansion of C_4 allows actually for more degrees of freedom [71]. However, these can be eliminated by their equations of motion.

axio-dilaton S and the *axionic odd G -moduli* by

$$S = e^{-\phi} - iC_0 := s + ic, \quad G^a = Sb^a + ic^a, \quad (2.3.11)$$

and the *Kähler moduli* to be of the form⁹

$$T_\alpha = \frac{1}{2}\kappa_{\alpha\beta\gamma}t^\beta t^\gamma + i\left(\rho_\alpha - \frac{1}{2}\kappa_{\alpha ab}c^a b^b\right) - \frac{1}{4}e^\phi \kappa_{\alpha ab}G^a(G + \bar{G})^b, \quad (2.3.12)$$

where the parameters $\kappa_{\alpha\beta\gamma}$ are triple intersection numbers. The Kähler metric on the moduli space $\mathcal{X}_{\text{rest}}^{h^{1,1}+1}$ mixes all these moduli. In order to determine its precise form, one would have to calculate the $D = 4$ effective action after dimensional reduction and read off the (supergravity) metric [71]. We skip this derivation here and simply state the result

$$K_{\text{rest}} = -\log(S + \bar{S}) - 2\log\mathcal{V}, \quad (2.3.13)$$

with the overall volume \mathcal{V} of the Calabi-Yau manifold \mathcal{M}

$$\mathcal{V} = \frac{1}{3!} \int_{\mathcal{M}} J \wedge J \wedge J = \frac{1}{3!} \kappa_{\alpha\beta\gamma} t^\alpha t^\beta t^\gamma \quad \text{with} \quad \kappa_{\alpha\beta\gamma} = \int_{\mathcal{M}} \omega_\alpha \wedge \omega_\beta \wedge \omega_\gamma. \quad (2.3.14)$$

The real moduli t^α can therefore be understood as 2-cycle volumes. As a consequence, the real parts τ_α of the Kähler moduli T_α correspond to 4-cycle volumes

$$\tau_\alpha = \frac{1}{2} \int_{\gamma_\alpha} J \wedge J = \frac{1}{2} \kappa_{\alpha\beta\gamma} t^\beta t^\gamma = \frac{\partial\mathcal{V}}{\partial t^\alpha}, \quad (2.3.15)$$

where we integrated over a 4-cycle $\gamma_\alpha \in H_4$. Hence, it is intuitive to imagine Kähler moduli as fluctuations of the size of cycles or the overall Calabi-Yau manifold.

The final list of all closed string moduli is given in table 2.3. Before commenting on the special Kähler structure of the complex structure moduli space $\mathcal{X}_{\text{cs}}^{h^{2,1}}$, let us state the complete Kähler potential

$$K = K_{\text{cs}} + K_{\text{rest}} = -\log\left(-i \int_{\mathcal{M}} \Omega_3 \wedge \bar{\Omega}_3\right) - \log(S + \bar{S}) - 2\log\mathcal{V}. \quad (2.3.16)$$

Special (Kähler) geometry

Special (Kähler) geometry is a powerful mathematical structure that actually goes beyond our applications. One has to distinguish between rigid and local special geometry arising in the construction of $\mathcal{N} = 2$ global and local supersymmetric theories, respectively. Viewing a $\mathcal{N} = 2$ vector multiplet in $D = 4$ dimensions as $\mathcal{N} = 1$ vector multiplet plus $\mathcal{N} = 1$ chiral multiplet, it can be shown that the chiral superfields span a manifold governed by special (Kähler) geometry. In the light of table 2.2 our complex structure moduli space obeys the structure of special geometry. For details we refer to the literature [78–80]. Let us start with the definition of special geometry and then show how it simplifies our setup.

⁹In chapter 9 we are going to work in type IIA string theory and hence need to consider a different definition of Kähler moduli.

Number	Modulus	Name
1	$S = s + ic$	axio-dilaton
$h_-^{2,1}(\mathcal{M})$	$U^i = u^i + iv^i$	complex structure
$h_+^{1,1}(\mathcal{M})$	$T_\alpha = \tau_\alpha + i\rho_\alpha + \dots$	Kähler
$h_-^{1,1}(\mathcal{M})$	$G^a = Sb^a + ic^a$	axionic odd

Table 2.3: Moduli in type IIB orientifold compactifications from [32].

Definition: *The Kähler potential of a manifold equipped with special (Kähler) geometry is completely determined by holomorphic coordinates X^Λ and a prepotential $F(X^\Lambda)$.*

Consider again the cohomology basis of 3-forms $\{\alpha_\kappa, \beta^\lambda\}$ with $\kappa, \lambda = 1, \dots, h_-^{2,1} + 1$ of table 2.1. This basis satisfies the relations

$$\int_{\mathcal{M}} \alpha_\kappa \wedge \beta^\lambda = \delta_\kappa^\lambda, \quad \int_{\mathcal{M}} \alpha_\kappa \wedge \alpha_\lambda = \int_{\mathcal{M}} \beta^\kappa \wedge \beta^\lambda = 0. \quad (2.3.17)$$

Now we define¹⁰ the *periods* of the holomorphic (3, 0)-form Ω_3 by

$$X^\lambda = \int_{\mathcal{M}} \Omega_3 \wedge \beta^\lambda, \quad F_\lambda = \int_{\mathcal{M}} \Omega_3 \wedge \alpha_\lambda. \quad (2.3.18)$$

The periods X^λ are related to the complex structure moduli U^λ via

$$U^\lambda = -i \frac{X^\lambda}{X^0}, \quad \lambda = 1, \dots, h_-^{2,1}. \quad (2.3.19)$$

It is necessary to divide by X^0 since the space of X^λ is $(h_-^{2,1} + 1)$ -dimensional and hence over-complete. From equations (2.3.17) and (2.3.18), one can immediately read off an expression for the holomorphic (3,0)-form¹¹

$$\Omega_3 = X^\lambda \alpha_\lambda - F_\lambda \beta^\lambda, \quad (2.3.20)$$

such that we may rewrite the Kähler potential for the complex structure moduli

$$K_{\text{cs}} = -\log \left(i \int_{\mathcal{M}} \Omega_3 \wedge \bar{\Omega}_3 \right) = -\log \left[-i \left(X^\lambda \bar{F}_\lambda - \bar{X}^\lambda F_\lambda \right) \right]. \quad (2.3.21)$$

Special geometry predicts the existence of a *prepotential* $F(X^\lambda)$, a homogeneous polynomial of degree two, which related the periods as follows

$$F_\lambda = \frac{\partial}{\partial X^\lambda} F. \quad (2.3.22)$$

¹⁰One often introduces also a Poincaré dual basis of 3-cycles to specify the definition of the periods.

¹¹Recall also the basis $\{\alpha_{\tilde{\kappa}}, \beta^{\tilde{\lambda}}\}$ of H_+^3 for which (2.3.17) holds analogously. However, all intersections with $\{\alpha_\kappa, \beta^\lambda\}$ of H_-^3 vanish. Expression (2.3.20) guarantees then that 'other' periods $X^{\tilde{\lambda}} = \int_{\mathcal{M}} \Omega_3 \wedge \beta^{\tilde{\lambda}}$ and $F_{\tilde{\lambda}} = \int_{\mathcal{M}} \Omega_3 \wedge \alpha_{\tilde{\lambda}}$ equal to zero [71].

Number	Modulus	Name
$h_-^{2,0}(C_4)$	Φ^I	D -brane position
$h_-^{0,1}(C_4)$	A_J	Wilson line

Table 2.4: Open string moduli for a single $D7$ -brane wrapping a 4-cycle C_4 .

Apparently the Kähler potential (2.3.21) is then completely fixed by the periods X^λ and the prepotential F . More explanations regarding periods of Calabi-Yau manifolds follow in the next chapter.

2.3.2 Open String Moduli

In section 2.2 it was motivated that orientifold planes require the inclusion of D -branes in order to avoid inconsistencies arising from tadpoles. However, D -branes lead to *open string moduli* in the $D = 4$ effective theory as their fluctuations can be described by massless open string states. Since it is quite sophisticated to write down general expressions (for instance for the Kähler potential) for open string moduli from arbitrary Calabi-Yau compactifications, we will focus on one $D7$ -brane in a toroidal setup. This will also be the case of interest in chapter 8.

Consider a space-time filling $D7$ -brane with gauge group $U(1)$ wrapping a 4-cycle¹² C_4 of the orientifolded Calabi-Yau three-fold \mathcal{M} . One part of the massless bosonic spectrum of this $D7$ -brane comes from the $D = 8$ dimensional world-volume gauge field, that correspond to massless open string modes with Neumann boundary conditions. As a consequence, in $D = 4$ dimensions we get a $U(1)$ gauge boson A_μ as well as Wilson line¹³ moduli A_J . In addition there are moduli Φ^I from deformations transverse to the $D7$ -brane, i.e. $D7$ -brane position moduli, represented by massless open string modes with Dirichlet boundary conditions. The number of open string moduli is governed by the cohomology of the 4-cycle C_4 . In fact, intersecting stacks of Dp -branes might cause further charged matter fields [48]. However, these will not be part of our analysis. The two types of open string moduli are listed in table 2.4. For details about the cohomology groups we refer to the literature, in particular to [76, 81].

As shown in [82], Wilson line moduli are not stabilized by fluxes which makes them unattractive for our setup in chapter 8. Besides, for simplicity we restrict our analysis

¹²More precisely, the 4-cycle C_4 has to be the union of the $D7$ -brane cycle and its image under the orientifold projection.

¹³A Wilson line is a gauge invariant observable $W = \text{Tr} \exp \left(i \int_\gamma A \right)$, where γ denotes a closed path and A a 1-form.

to a single position modulus of a $D7$ -brane

$$\Phi = \varphi + i\theta. \quad (2.3.23)$$

If the transverse space of the $D7$ -brane supports 1-cycles, like in a toroidal compactification, the above real fields φ and θ enjoy a shift symmetry.

In order to determine the Kähler potential describing the dynamics of open string moduli, one has to carry out the dimensional reduction of the Dirac-Born-Infeld and Chern-Simons actions. The total Kähler potential will then mix open and closed string moduli. More precisely, it turns out that open string moduli lead to a redefinition of the holomorphic chiral variables. Whereas Wilson line moduli change the Kähler moduli, the $D7$ -brane position moduli we are employing here, modify the axio-dilaton S [76, 83, 84]. For a $D7$ -brane wrapping a 4-cycle T^4 inside $T^6 = T^2 \otimes T^4$, the redefinition reads

$$S \longrightarrow S - \frac{1}{2} \Phi \frac{\Phi + \bar{\Phi}}{U + \bar{U}}, \quad (2.3.24)$$

with U being the complex structure modulus of the transverse T^2 . This can be used to determine the Kähler potential. In our prototype models we will compactify on an isotropic six-torus, whose closed string Kähler potential reads

$$K_{\text{cl}} = -3 \log(T + \bar{T}) - \log(S + \bar{S}) - 3 \log(U + \bar{U}). \quad (2.3.25)$$

Taking now also the open string modulus of the $D7$ -brane into account, according to the redefinition in eq. (2.3.24), one arrives at the Kähler potential we will use for our prototype models [76]

$$K_{\text{op}} = -3 \log(T + \bar{T}) - 2 \log(U + \bar{U}) - \log \left[(S + \bar{S})(U + \bar{U}) - \frac{(\Phi + \bar{\Phi})^2}{2} \right]. \quad (2.3.26)$$

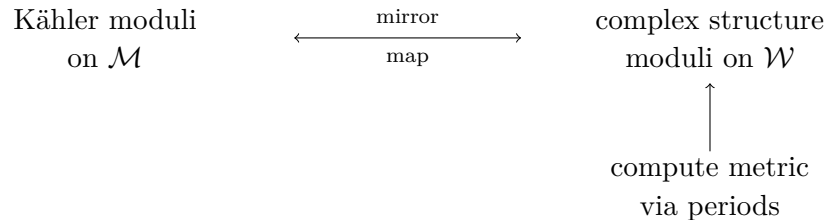
It is known that α' corrections from the Dirac-Born-Infeld action of the brane will appear as higher derivative corrections to the above Kähler potential. However, since we do not have control over all analogous α' corrections in the closed string sector, we will restrict our analysis to leading order in α' for both open and closed string sectors.

CHAPTER 3

Periods of Calabi-Yau Manifolds

This chapter aims to calculate the precise form of the Kähler potential. We will make extensive use of these results to compute distances on the moduli space via its Kähler metric and for moduli stabilization. The Kähler potential of complex structure moduli spaces is found by determining the so-called *periods*. Recall that these were already briefly introduced in the context of special geometry in section 2.3.1. Periods are of quite distinct form at different points in the moduli space. Special points can lead to interesting applications in string phenomenology as demonstrated in chapter 7.

Often periods are also helpful for calculating the metric of the Kähler moduli space of a Calabi-Yau manifold \mathcal{M} due to mirror duality. Instead of computing directly the Kähler moduli metric on \mathcal{M} , we determine the periods of the complex structure moduli on the mirror dual manifold \mathcal{W} and afterwards transform back to \mathcal{M} . Schematically we have



Note that there exist different standard techniques to obtain the periods. In this thesis we focus on the original direct integration method. Nevertheless, let us list the four methods that have been developed up to our knowledge:

1. direct integration of holomorphic $(3, 0)$ -form Ω_3
2. solving the Picard-Fuchs differential equation (see e.g. [85])

3. partition function for gauged linear sigma models (see e.g. [65])
4. metric via a Frobenius algebra [86–88]

After some remarks on hypersurfaces in weighted projective spaces, we obtain a general recipe which will be demonstrated explicitly for a one-parameter example, that is the mirror quintic. The calculation for two-parameter Calabi-Yau's is analogous and briefly summarized subsequently (see also appendices A and B).

3.1 Hypersurfaces in Weighted Projective Spaces

We focus on Calabi-Yau manifolds \mathcal{M} which can be realized as hypersurface¹ embedded in a weighted projective space $\mathbb{P}_{k_1, \dots, k_{N+1}}^N[d]$. More precisely, the hypersurface corresponds to a vanishing polynomial P in the projective space. Following the construction by B. Greene and M. Plesser [89], the mirror dual \mathcal{W} can then be constructed as a quotient \mathcal{M}/G , where G is a product of \mathbb{Z}_n symmetries.

Recall the definition of weighted projective spaces in section 2.1. If the sum over the weights k_i agrees with the degree d of the projective space $\mathbb{P}_{k_1, \dots, k_{N+1}}^N[d]$, i.e. $\sum_{i=1}^{N+1} k_i = d$, the hypersurface is Calabi-Yau. Moreover we take $N = 4$ since we are interested in Calabi-Yau three-folds. The symmetry group G will be specified in each case later on.

The strategy is basically to express P as deformations of a defining polynomial P_0 that are governed by the complex structure moduli Φ_Λ with $\Lambda = 0, \dots, M-1$. See [90] for more details. The periods are then defined in terms of the polynomial and may be computed explicitly as power series expansion in the moduli. For the weighted homogeneous coordinates x_i with $i = 1, \dots, 5$, we define the polynomial P by

$$P(x_i; \Phi_\Lambda) = P_0(x_i) - \Phi_0 \prod_{i=1}^{N+1} x_i + \sum_{\Lambda=1}^{M-1} \Phi_\Lambda M^\Lambda(x_i), \quad (3.1.1)$$

with $M^\Lambda(x_i)$ denoting monomial deformations. We will only work with *Fermat type* polynomials, where the defining polynomial P_0 is given by

$$P_0(x_i) = x_1^{\frac{d}{k_1}} + x_2^{\frac{d}{k_2}} + x_3^{\frac{d}{k_3}} + x_4^{\frac{d}{k_4}} + x_5^{\frac{d}{k_5}}. \quad (3.1.2)$$

The fundamental deformation $\Phi_0 \prod_i x_i$ is always present and has been separated from the others for later convenience. In certain unfavorable circumstances, there exist also non-polynomial deformations [91, 92], which we neglect in the discussion at hand.

Our starting point is the residue formula [93, 94] for the holomorphic $(3, 0)$ -form

$$\Omega_3(\Phi_\Lambda) = \text{Res}_{\mathcal{W}} \left[\frac{\prod_{i=1}^5 dx_i}{P(x_i, \Phi_\Lambda)} \right]. \quad (3.1.3)$$

¹A hypersurface is a $(n-1)$ -dimensional submanifold of an n -dimensional ambient space (here the projective space).

In order to compute the periods, we first determine the fundamental one for sufficiently large Φ_0 and subsequently extend it to the whole parameter space as well as the other periods. For that purpose, it is necessary to define a *fundamental cycle* B_0

$$B_0 = \{x_k \mid x_5 = \text{const.}, |x_1| = |x_2| = |x_3| = \delta, \quad (3.1.4)$$

$$x_4 \text{ given by the solution to } P(x_i) = 0 \text{ that tends to zero as } \Phi_0 \rightarrow \infty \},$$

with a small circle radius $\delta \neq 0$. In the limit $\Phi_0 \rightarrow \infty$ the fundamental cycle approximates to a torus T^3 . According to the standard literature [52, 90] we define the *fundamental period* of Ω_3 to be

$$\omega_0(\Phi_\Lambda) = -\Phi_0 \oint_{B_0} \Omega(\Phi_\Lambda) = -\Phi_0 \frac{C}{(2\pi i)^5} \int_\Gamma \frac{\prod_{i=1}^5 dx_i}{P(x_i, \Phi_\Lambda)}, \quad (3.1.5)$$

where C is a normalization constant and the sign as well as factors of $2\pi i$ can be reabsorbed into it. One must choose $\Gamma \in \mathbb{C}^5$ as suitable auxiliary contour that reproduces the residue (3.1.3). Note that expression (3.1.5) is in line with the former definition (2.3.18).

In [90] the residue integral (3.1.5) has been calculated perturbatively in $1/\Phi_0$ to all orders in the large complex structure limit $\Phi_0 \rightarrow \infty$. We will not repeat every step in this rather elaborate computation and refer to the literature instead. Nevertheless let us present the result, in order to get an impression of the general structure of the fundamental period

$$\omega_0(\Phi_\Lambda) = \sum_{n_i, m_\Lambda} \frac{\Gamma(n+1)}{\prod_{\Lambda=1}^{M-1} \Gamma(m_\Lambda+1) \prod_{i=1}^{N+1} \Gamma(n_i+1)} \frac{\prod_{\Lambda=1}^{M-1} \Phi_\Lambda^{m_\Lambda}}{\Phi_0^n} \quad \text{for} \quad \Phi_0 \gg 1. \quad (3.1.6)$$

where the summation indices n_i and m_Λ are highly constraint [90] (for instance $n = \sum_{i=1}^{N+1} n_i + \sum_{\Lambda=1}^{M-1} m_\Lambda$), such that we have only M (number of moduli) independent summation variables. Notice the characteristic structure with the quotient of gamma functions.

The general solution (3.1.6) simplifies drastically in the case of just one modulus Φ_0 , i.e. $h^{2,1} = 1$,

$$\omega_0(\Phi_0) = \sum_{r=0}^{\infty} \frac{\Gamma(dr+1)}{\prod_{i=1}^5 \Gamma(k_i r+1) \Phi_0^{dr}}. \quad (3.1.7)$$

Recall that d denotes the degree and k_i the weights of the weighted projective space $\mathbb{P}_{k_0, \dots, k_5}^4[d]$. A full basis of the periods for the one-parameter Calabi-Yau hypersurfaces has been determined in [95, 96].

There are two tasks that remain to be carried out:

1. **extend the fundamental period $\omega_0(\Phi_0)$ to small Φ_0**

As a matter of fact, the expansion of ω_0 for large Φ_0 will generically be of the form of a generalized hypergeometric function [52, 90]. The small Φ_0 regime can be approached by analytic continuation using Mellin-Barnes type integrals.

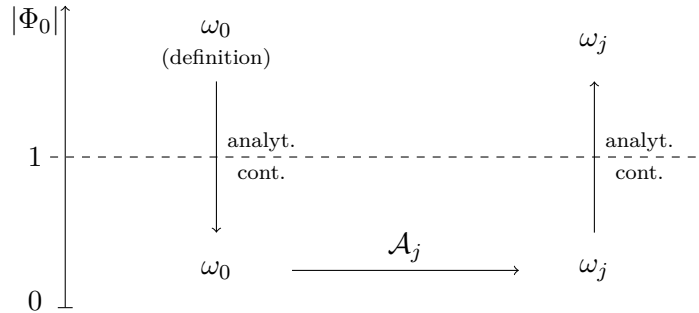
2. compute all other periods

In the regime of small Φ_0 the other periods $\omega_j(\Phi_\Lambda)$ are given by [52]

$$\omega_j(\Phi_\Lambda) = \omega_0(\mathcal{A}^j \Phi_\Lambda), \quad (3.1.8)$$

where \mathcal{A} is an element of the symmetry group of the Fermat type polynomial P_0 . In order to obtain the periods ω_j for large Φ_0 , one has to analytically continue back. Note that the relation 3.1.8 does not lead to new periods in the large Φ_0 regime since there $\omega_0(\mathcal{A}^j \Phi_\Lambda) = \omega_0(\Phi_\Lambda)$. This point will become clear from the mirror quintic periods (3.2.6) and (3.2.10).

These tasks will be demonstrated explicitly for the mirror quintic in the next section. To summarize, one begins with ω_0 for large Φ_0 and follows schematically the procedure:



3.2 Mirror Quintic

Let us apply the direct integration method of the preceding section to the most simple example, the mirror manifold of the quintic $\mathcal{M} = \mathbb{P}_{11111}^4[5]$. The quintic has $h^{2,1} = 101$ complex structure moduli as well as $h^{1,1} = 1$ Kähler modulus. Consequently, the mirror manifold \mathcal{W} is equipped with a single complex structure modulus which we denote by ψ . The space of ψ , i.e. the complex structure moduli space, is denominated by \mathcal{X}_ψ . Following the construction above, \mathcal{W} corresponds to the hypersurfaces $\{P = 0\}/G$ with G being now a $\mathbb{Z}_5 \times \mathbb{Z}_5 \times \mathbb{Z}_5$ symmetry on the coordinates x_i , $i = 1, \dots, 5$. The polynomial P in (3.1.1) and (3.1.2) simplifies drastically since we have only one modulus $M = 1$

$$P(x_i; \psi) = x_1^5 + x_2^5 + x_3^5 + x_4^5 + x_5^5 - 5\psi x_1 x_2 x_3 x_4 x_5. \quad (3.2.1)$$

In agreement with the literature, we have chosen $\Phi_0 = 5\psi$ in (3.1.1). It is crucial to realize that ψ is equipped with a \mathbb{Z}_5 symmetry as it is equivalent to the coordinate transformation $(x_1, x_2, x_3, x_4, x_5) \rightarrow (\alpha^{-1}x_1, x_2, x_3, x_4, x_5)$

$$\psi \rightarrow \alpha \psi, \quad \alpha = e^{\frac{2\pi i}{5}}. \quad (3.2.2)$$

Next, let us be more precise about the geometry of the complex structure moduli space \mathcal{X}_ψ as well as the Calabi-Yau manifold \mathcal{W} itself. In the case of the mirror quintic there exist three special points $\psi = 0, 1, \infty$ obeying characteristic, but quite distinct features.

Obviously, $\psi = 0$ is a special point since it is the minimal value for ψ . The discussion about the mirror map will show that this point corresponds to the one of minimal volume/radius on the quintic \mathcal{M} . According to [97], the expectation values of all x_i are fixed at this point and hence the classical target space is just a point. Nevertheless, there are massless quantum fluctuations which exhibit a residual \mathbb{Z}_5 symmetry $x_i \rightarrow e^{2\pi i/5} x_i$. The fields x_i live therefore effectively in a $\mathbb{C}^5/\mathbb{Z}_5$ and we have a theory known as *Landau-Ginzburg orbifold* [97]. Let us call the point $\psi = 0$ Landau-Ginzburg (LG) point.

In addition there exist values of ψ where the manifold \mathcal{W} is singular. First, for $\psi = \infty$ the mirror quintic \mathcal{W} is singular and described by the reduced polynomial $x_1 x_2 x_3 x_4 x_5 = 0$. This special point is called *large complex structure point* (LCS). The geometry of \mathcal{W} in the neighborhood of this point can locally be understood as a sophisticated arrangement of projective spaces (see [52]). On the mirror dual side, the LCS limit corresponds to the large volume limit of the quintic \mathcal{M} .

The second point where the \mathcal{W} becomes singular occurs when the quintic (3.2.1) fails to be transverse. That is, when we satisfy simultaneously the five equations (with $x_i \neq 0$ for $i = 1, \dots, 5$.)

$$\frac{\partial P(x_i; \psi)}{\partial x_i} = 0, \quad i = 1, \dots, 5. \quad (3.2.3)$$

It is easy to see [52] that (for finite ψ) the only solution is given by $\psi^5 = 1$. At this point the mirror quintic \mathcal{W} is known as *conifold* [98]. Locally, \mathcal{W} around $\psi^5 = 1$ matches a cone with base $\mathcal{S}^2 \times \mathcal{S}^3$. The \mathcal{S}^3 shrinks to zero for $\psi \rightarrow 1$.

Figure 3.1 illustrates the moduli space \mathcal{X}_ψ of \mathcal{W} respecting the \mathbb{Z}_5 symmetry of ψ and including the three special points above. One has to pay attention to distinguish between the geometric target space \mathcal{W} and its moduli space \mathcal{X}_ψ . The moduli space has in fact only a singularity at the conifold $\psi^5 = 1$. However, it has been proven [99] that the conifold is not really singular in the moduli space, but our effective description fails to include all necessary effects. In particular, there are modes (e.g. in type IIB from D -branes wrapping the shrinking cycle) becoming light at the conifold. To keep track of the different singularities in target as well as moduli space, we summarized the discussion above in table 3.1.

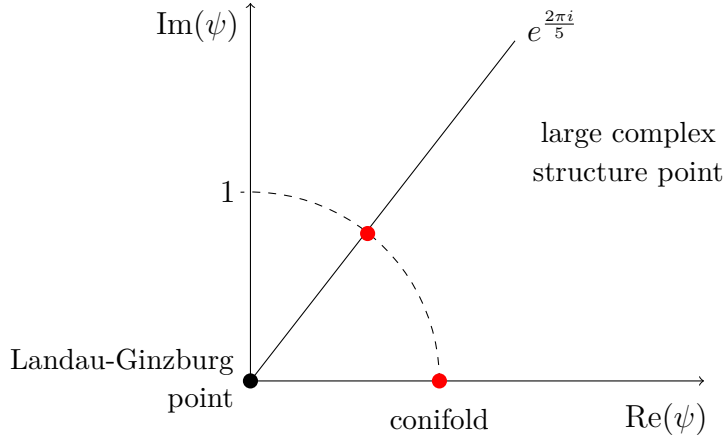


Figure 3.1: Complex structure moduli space \mathcal{X}_ψ of the mirror quintic \mathcal{W} . The Landau-Ginzburg point is marked by a black dot, whereas the conifold including its \mathbb{Z}_5 image by red dots.

Special Point	Singularity of \mathcal{W}	Geometry of \mathcal{W}	Moduli Space \mathcal{X}_ψ
LG	singular orbifold	$\mathbb{C}^5/\mathbb{Z}_5$	smooth
conifold	conic singularity	cone over base $\mathcal{S}^2 \times \mathcal{S}^3$	'singular' due to invalid EFT
LCS	singular	Arrangement of \mathbb{P}_3 's [52]	smooth

Table 3.1: Singularities of the complex structure moduli space and the mirror quintic manifold.

3.2.1 Periods and Metric

The polynomial (3.2.1) of the quintic hypersurface determines the fundamental period $\omega_0(\psi)$ according to (3.1.5)

$$\omega_0(\psi) = -5\psi \frac{1}{(2\pi i)^5} \int_{\gamma_1 \times \dots \times \gamma_5} \frac{dx_1 dx_2 dx_3 dx_4 dx_5}{P(x_i; \psi)}. \quad (3.2.4)$$

We have chosen the constant $C = 1$ and the integration contour $\Gamma = \gamma_1 \times \dots \times \gamma_5$, where γ_i symbolizes the circle $|x_i| = \delta$. The next step is to expand $1/P(x_i; \psi)$ for large ψ using standard tricks² of functional analysis

$$\omega_3(\psi) = \frac{1}{(2\pi i)^5} \sum_{m=0}^{\infty} \frac{1}{(5\psi)^m} \int_{\gamma_1 \times \dots \times \gamma_5} \frac{dx_1 dx_2 dx_3 dx_4 dx_5}{x_1 x_2 x_3 x_4 x_5} \frac{(x_1^5 + x_2^5 + x_3^5 + x_4^5 + x_5^5)^m}{(x_1 x_2 x_3 x_4 x_5)^m}. \quad (3.2.5)$$

The evaluation of this integral follows simply from the residue theorem. However, only terms with $m = 5n$, $n \in \mathbb{N}_0$, contribute since then the numerator contains a term

²Since $1/P(x_i; \psi)$ is vanishing for $\psi \rightarrow \infty$, one may first expand $1/P(x_i; \frac{1}{\psi})$ around $\psi = 0$ and second replace $\psi \rightarrow \frac{1}{\psi}$.

$x_z^{5n} x_2^{5n} x_3^{5n} x_4^{5n} x_5^{5n}$ with coefficient $(5n)!/(n!)^5$. Hence the final solution for the fundamental period for large ψ reads

$$\omega_0(\psi) = \sum_{n=0}^{\infty} \frac{(5n)!}{(n!)^5 (5\psi)^{5n}} = \sum_{r=0}^{\infty} \frac{\Gamma(5r+1)}{\Gamma^5(r+1) (5\psi)^{5r}}, \quad |\psi| > 1. \quad (3.2.6)$$

We rewrote the sum in terms of Γ -functions (recall $\Gamma(n+1) = n!$) to point out that our result agrees with the general expression (3.1.7).

Analytic continuation to small ψ

Obviously, the fundamental period (3.2.6) does not converge for small ψ . In order to obtain an expression for the whole parameter space, we have to analytically continue $\omega_0(\psi)$. Therefore, it is convenient to work with the second sum in (3.2.6), i.e. the one containing Γ -functions. The function $\Gamma(r)$ has poles at $0, -1, -2, \dots$ and its residue is given by the formula

$$\text{Res } \Gamma(-r) = \frac{(-1)^r}{r!}, \quad r \in \mathbb{N}_0. \quad (3.2.7)$$

In the segment $0 < \text{Arg}(\psi) < 2\pi/5$, we may then rewrite the sum (3.2.6) as *Mellin-Barne's integral*

$$\omega_0(\psi) = \frac{1}{2\pi i} \int_C dr \frac{\Gamma(-r) \Gamma(5r+1)}{\Gamma^4(r+1)} e^{i\pi r} (5\psi)^{-5r}. \quad (3.2.8)$$

The contour C is depicted in figure 3.2. For $|\psi| > 1$ the contour can be closed to the right and $\Gamma(-r)$ has poles at $r = 0, 1, 2, \dots$. In this case the fundamental period (3.2.6) is recovered as sum over residues. If, however, $|\psi| < 1$ the contour can be closed to the left and $\Gamma(5r+1)$ exhibits poles. The residues of $\Gamma(5r+1)$ can easily be found by using $\Gamma(5r+1) = 5r \Gamma(5r)$ as well as the formula

$$(2\pi)^2 5^{\frac{1}{2}-5r} \Gamma(5r) = \Gamma(r) \Gamma\left(r + \frac{1}{5}\right) \Gamma\left(r + \frac{2}{5}\right) \Gamma\left(r + \frac{3}{5}\right) \Gamma\left(r + \frac{4}{5}\right). \quad (3.2.9)$$

Eventually, the fundamental period for small ψ is given by the series [52] (with $\alpha = \exp(2\pi i/5)$)

$$\omega_0(\psi) = \frac{1}{5} \sum_{m=1}^{\infty} \frac{\alpha^{2m} \Gamma(\frac{m}{5}) (5\psi)^m}{\Gamma(m) \Gamma^4(1 - \frac{m}{5})}, \quad |\psi| < 1. \quad (3.2.10)$$

As mentioned above, in this regime all other periods $\omega_j(\psi)$ can simply be computed via

$$\omega_j(\psi) = \omega_0(\alpha^j \psi), \quad j = 0, \dots, 4 \quad \text{for } |\psi| < 1. \quad (3.2.11)$$

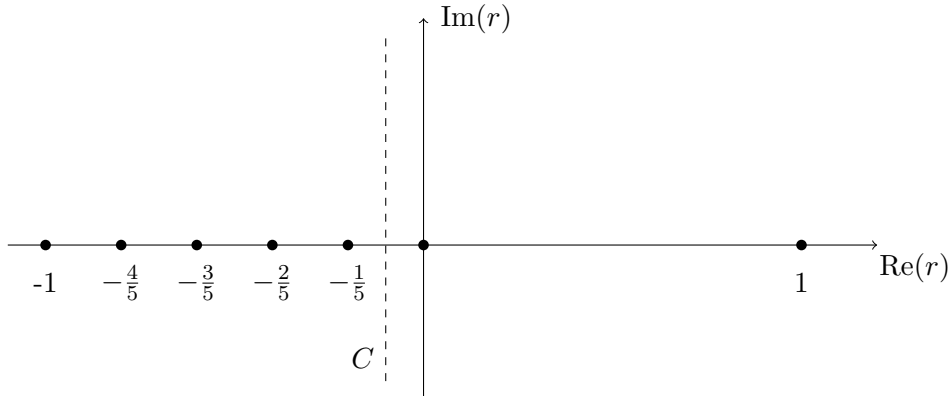


Figure 3.2: Closing the contour C to the right or left leads to the fundamental period for large or small ψ , respectively, as sum of residues [52].

The symmetry transformation $\mathcal{A}^j \psi$ reduces in the one-parameter quintic example to $\alpha^j \psi = \exp(2\pi i j/5) \psi$ in agreement with (3.2.2). Obviously, expression (3.2.11) does not lead to the other periods in the regime $|\psi| > 1$ since the replacement $\psi \rightarrow \alpha^j \psi$ leaves $\omega_0(\psi)$ in (3.2.6) unaffected.

It remains to compute the periods $\omega_j(\psi)$ for large ψ , i.e. analytically continue the results of (3.2.11). A rather sketchy calculation can be found in appendix B of [52]. It is wise to use the periodicity of $\alpha = \exp(2\pi i/5)$ and split the sum in (3.2.11) via $m = 5n + k$

$$\omega_j(\psi) = -\frac{1}{5} \sum_{k=1}^4 \alpha^{k(2+j)} \sum_{n=0}^{\infty} \frac{\Gamma\left(n + \frac{k}{5}\right) (5\psi)^{5n+k}}{\Gamma(5n+k) \Gamma^4\left[1 - \left(n + \frac{5}{k}\right)\right]}. \quad (3.2.12)$$

Together with the Γ -function identity

$$\Gamma\left[1 - \left(n + \frac{5}{k}\right)\right] = \frac{\pi}{\Gamma\left(n + \frac{5}{k}\right) \sin\left[\pi\left(n + \frac{5}{k}\right)\right]}, \quad (3.2.13)$$

one arrives at a convenient expression, still for small $|\psi|$,

$$\omega_j(\psi) = -\frac{1}{80\pi^4} \sum_{k=1}^4 \alpha^{jk} (\alpha^k - 1)^4 \sum_{n=0}^{\infty} \frac{\Gamma\left(n + \frac{k}{5}\right) (5\psi)^{5n+k}}{\Gamma(5n+k)}, \quad |\psi| < 1. \quad (3.2.14)$$

Now the sum over n can be rewritten again as Mellin-Barne's integral in such a way, that (3.2.14) matches the sum of residues for $|\psi| > 1$ when closing the contour to the right. For small $|\psi| < 1$ we may again close the contour to the left to find the desired $\omega_j(\psi)$. Although not obvious, we then face fourth-order poles which ultimately lead to logarithmic terms $\log \psi$, $\log^2 \psi$ and $\log^3 \psi$ as expected in the large complex structure phase. The result is quite lengthy and we just refer to the list in appendix B of [52].

Metric

To compute the Kähler metric on the moduli space we first need to choose a linearly independent set of periods, which can in fact be any four out of the five $\omega_j(\psi)$. The reason is that (3.2.10), (3.2.11) together with the identity $\sum_{j=0}^4 \exp\left(\frac{2\pi i}{5} j\right) = 0$ imply

$$\sum_{j=0}^4 \omega_j(\psi) = 0. \quad (3.2.15)$$

The second step is to transform the periods $\omega_j(\psi)$ (we choose the vector $\vec{\omega}(\psi) = -(2\pi i/5)^3 (\omega_2, \omega_1, \omega_0, \omega_4)$) into a symplectic basis

$$\Pi(\psi) = m \vec{\omega}(\psi). \quad (3.2.16)$$

$\Pi(\psi)$ denotes a vector as well (we dropped the arrow $\vec{\Pi}$ for brevity). Note that we can split the periods in X^λ and F_λ with $\lambda = 0, \dots, h^{2,1}$ via $\Pi = (F_\lambda, X^\lambda)$, such that we obtain the periods defined in (2.3.1). In the end, the Kähler potential is given by

$$K = -\log\left(-i(X^\lambda \bar{F}_\lambda - \bar{X}^\lambda F_\lambda)\right) = -\log\left(-i \bar{\Pi} \Sigma \Pi\right), \quad (3.2.17)$$

with the symplectic scalar product

$$\Sigma = \begin{pmatrix} 0 & \mathbf{1} \\ -\mathbf{1} & 0 \end{pmatrix}. \quad (3.2.18)$$

The basis transformation m can be found case by case by a monodromy calculation [100, 101] or by the algorithmic procedure of [88]. The transformation matrices m are listed in appendix B for all cases discussed in this thesis.

For instance we can use m of the quintic in (B.0.1) to compute the periods of the Landau-Ginzburg phase $|\psi| < 1$ explicitly using (3.2.10) and (3.2.16). Equivalently, one can use the formulas (different ω_0 and m) in [65] to obtain the periods but with different numerical prefactors³

$$\begin{aligned} F^0 &= 2.937558i \psi - 4.289394i \psi^2 + 1.462601i \psi^3 + O(\psi^4) \\ F^1 &= (7.314220 - 11.691003i) \psi - (0.963029 - 6.520577i) \psi^2 \\ &\quad - (0.328374 + 2.223391i) \psi^3 + O(\psi^4) \\ X_0 &= (2.021600 - 1.468779i) \psi - (0.696854 - 2.144697i) \psi^2 \\ &\quad - (0.237613 + 0.731300i) \psi^3 + O(\psi^4) \\ X_1 &= 2.125637i \psi - 1.185559i \psi^2 + 0.404253i \psi^3 + O(\psi^4) \end{aligned} \quad (3.2.19)$$

³If the periods are computed via the Picard-Fuchs equations, one puts a polynomial ansatz (where applicable with logarithm) into the equations and solves iteratively for the numerical prefactors.

where we have actually expanded them up to order 100. In the large complex structure phase $|\psi| > 1$ the periods are given in the appendix of [52]. Altogether we have obtained a metric to cover the entire moduli space of ψ . The result is plotted in figure 3.3. The metric $G_{\psi\bar{\psi}}(\psi)$ is smooth except from the conifold $\psi^5 = 1$, where our effective description is insufficient.

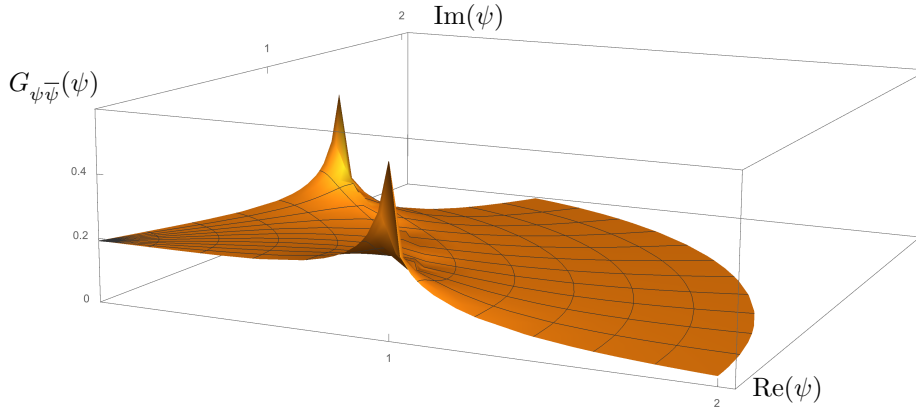


Figure 3.3: The metric on the Kähler moduli space of the quintic [65].

Due to the convergence of the period expansions around the LG and LCS points, the whole moduli space of the mirror quintic can be covered by those two charts. One might also be interested in a chart that is well behaved in the vicinity of the conifold. In fact, a period expansion near $\psi = 1$ is achieved via *monodromy* considerations. Simply speaking, monodromy stands for a non-trivial effect on objects when being transported around singularities. For the quintic, there is a monodromy around $\psi = 1$ as well as $\psi = \infty$. Let us comment briefly on the monodromy around the conifold.

The periods $\Pi(\psi) = (F_\lambda, X^\lambda)$, with $\lambda = 0, 1$ for the quintic, are defined⁴ as integrals of the holomorphic $(3, 0)$ -form Ω_3 over Poincaré dual cycles. The definition of these cycles implies a monodromy for the period X^1 (with some integer n) [52]

$$X^1 \rightarrow X^1 + n F_1. \quad (3.2.20)$$

As a consequence the periods $\omega_j(\psi)$ exhibit a monodromy as well, such that their structure has to be of the form

$$\omega_j(\psi) \sim \frac{c_j}{2\pi i} F_1 \log(\psi - 1) + f_j(\psi), \quad |\psi - 1| < 1, \quad (3.2.21)$$

with coefficients c_j and some analytic functions $f_j(\psi)$. After transforming to the symplectic basis also X^1 contains a logarithm which is characteristic in the vicinity of the conifold and crucial for applications in chapter 7. The coefficients can be found by differentiating the periods computed near the LG point.

⁴This becomes more obvious if one rewrites (2.3.18) introducing a homology basis.

3.2.2 Mirror Map and Quantum Corrections

In chapter 9 we will eventually be interested in the Kähler moduli of \mathcal{M} , instead of the complex structure moduli on \mathcal{W} . The transformation between them is known as *mirror map*. Since the mirror quintic has only one complex structure modulus ψ , it is mapped to a single Kähler modulus $t(\psi)$, the overall volume modulus of the quintic.

In terms of the period vector $\Pi(\psi) = (F_0, F_1, X^0, X^1)$, which is related to the periods $\omega_j(\psi)$ via the matrix m according to (3.2.16) and (B.0.1), the mirror map is defined by [52]

$$t = \frac{X^1}{X^0} = \frac{2(\omega_1 - \omega_0) + \omega_2 - \omega_4}{5\omega_0}. \quad (3.2.22)$$

This expression holds in any regime of ψ . Near the LCS point the mirror map can be determined by its monodromy properties [52]. Alternatively, for one-parameter models the mirror map may be computed without employing the periods, but instead starting with the well-know asymptotic form in the LCS regime and analytically continuing it towards small ψ . This is an algorithmic procedure and step by step explained in [65, 102].

The monodromy considerations also fix the mirror maps for two-parameter models. We will not review this analysis here, but simple refer to the literature [65, 100] when necessary in chapter 9.

In section 9.2 we will explicitly calculate the mirror map t in the vicinity of LCS (large volume) and LG point. Now, let us focus on the large complex structure regime. There, the mirror map (3.2.22) turns out to be [52]

$$-\frac{2\pi i}{5} t = \log(5\psi) - \frac{1}{\omega_0(\psi)} \sum_{m=1}^{\infty} \frac{(5m)!}{(m!)^5 (5\psi)^{5m}} [\Psi(1+5m) - \Psi(1+m)], \quad (3.2.23)$$

with Ψ denoting the polygamma function (defined as derivatives of $\log \Gamma(x)$). For large enough ψ we find the characteristic mapping $t \sim \log \psi$.

It has already been mentioned in section 2.3.1 in the context of special geometry that the period vector can also be expressed in terms of a holomorphic prepotential \mathcal{F} . Let us rewrite this using the mirror map. Just by recalling $F_a = \partial \mathcal{F} / \partial X^a$, it is easy to see that the period vector takes the form

$$\Pi(t) = \begin{pmatrix} F_0 \\ F_1 \\ X^0 \\ X^1 \end{pmatrix} = X^0 \begin{pmatrix} 2\mathcal{F} - t \partial_t \mathcal{F} \\ \partial_t \mathcal{F} \\ 1 \\ t \end{pmatrix}. \quad (3.2.24)$$

In the large complex structure phase the prepotential \mathcal{F} has a very particular form. The leading term is cubic since the highest logarithm in the periods is $\log^3 \psi$ and the mirror map roughly connects $t \sim \log \psi$. The cubic term t^3 leads to the typical large volume

Kähler potential $K = -3 \log(t + \bar{t})$. Together with quadratic and linear corrections in t , we obtain the bare prepotential. In addition there are quantum corrections. Considering the quintic, the loop correction adds an imaginary constant depending on its Euler characteristic $\xi = -200$ as well as $\zeta(3) \approx 1.202$. Lastly, we have non-perturbative corrections, that is instantons, whose contribution $\exp(2\pi i t)$ is exponentially suppressed for large $\text{Im}(t)$. This structure appears also for models with $h^{1,1} > 1$, such as the two-parameter models discussed below. The prepotential of the quintic is given by [52]

$$\mathcal{F} = (X^0)^2 \left(\underbrace{-\frac{5}{6}t^3 - \frac{11}{4}t^2 + \frac{25}{12}t}_{\text{bare prepotential}} - \underbrace{i \frac{25\zeta(3)}{2\pi^3}}_{\text{loop correction}} + \underbrace{\text{expon. small}}_{\text{instanton contributions}} \right). \quad (3.2.25)$$

3.3 Two-Parameter Models

Let us now turn to two-parameter models which show a much richer structure than the quintic and will be our main focus in chapter 9. There exist five two-parameter ($h^{1,1} = 2$) Fermat hypersurfaces in $W\mathbb{C}\mathbb{P}^4$, for which the full set of periods in the Landau-Ginzburg phase was calculated in [90]. These are the Calabi-Yau manifolds

$$\begin{aligned} \mathbb{P}_{(1,1,2,2,2)}^4[8]_{-168}^{86,2}, \quad \mathbb{P}_{(1,1,2,2,6)}^4[12]_{-252}^{128,2}, \quad \mathbb{P}_{(1,1,1,6,9)}^4[18]_{-540}^{272,2}, \\ \mathbb{P}_{(1,4,2,2,3)}^4[12]_{-144}^{74,2}, \quad \mathbb{P}_{(1,7,2,2,2)}^4[14]_{-240}^{122,2}. \end{aligned} \quad (3.3.1)$$

Their mirror dual manifolds are given by the vanishing set of the polynomials

$$P = \sum_{j=1}^5 x_j^{d/k_j} - \psi x_1 x_2 x_3 x_4 x_5 - \frac{d}{q_1} \phi x_1^{q_1} x_2^{q_2} x_3^{q_3} x_4^{q_4} x_5^{q_5}, \quad (3.3.2)$$

after modding out an appropriate discrete symmetry group. Here d denotes the degree of the polynomial, the k_i are the projective weights, $D = d/q_1$ is always an integer and the q_i ($i \neq 1$) can be computed from the projective weights and D through

$$\frac{q_i k_i}{q_1} = \begin{cases} 0, & i \geq D \\ 1, & i < D \end{cases}. \quad (3.3.3)$$

For the computation of the periods it suffices to know that $D = 2$ for all of the above models, except for the case⁵ of $\mathbb{P}_{(1,1,1,6,9)}^4$, where $D = 3$. The fundamental period ω_0 in the large complex structure/large volume regime has been computed in [90]

$$\omega_0(\psi, \phi) = \sum_{l=0}^{\infty} \frac{(q_1 l)! (d\psi)^{-q_1 l} (-1)^l}{l! \prod_{i=2}^5 \binom{k_i}{d} (q_1 - q_i) l!} U_l(\phi), \quad (3.3.4)$$

⁵Due to the differing value of D , the periods for this model behave in a slightly different way. The subsequent formulae are valid for the case $D = 2$ but the method can be easily carried over to $D = 3$, see the appendix of [65].

where the function $U_\nu(\phi)$ can be written in terms of hypergeometric functions as

$$U_\nu(\phi) = \frac{e^{\frac{i\pi\nu}{2}} \Gamma\left(1 + \frac{\nu}{2}(k_2 - 1)\right)}{2\Gamma(-\nu)} \left[2i\phi \frac{\Gamma(1 - \nu/2)}{\Gamma\left(\frac{1+\nu k_2}{2}\right)} {}_2F_1\left(\frac{1 - \nu}{2}, \frac{1 - k_2\nu}{2}; \frac{3}{2}; \phi^2\right) + \frac{\Gamma(-\frac{\nu}{2})}{\Gamma\left(\frac{2+\nu k_2}{2}\right)} {}_2F_1\left(-\frac{\nu}{2}, -\frac{k_2\nu}{2}; \frac{1}{2}; \phi^2\right) \right]. \quad (3.3.5)$$

For fixed values of ϕ the series converges for sufficiently large ψ . Note that the actual convergence criterion is model-dependent.

In order to obtain a full set of periods, this expression has to be analytically continued to small ψ similar to the quintic case. The result is [90]

$$\omega_0(\psi, \phi) = -\frac{2}{d} \sum_{n=1}^{\infty} \frac{\Gamma\left(\frac{2n}{d}\right) (-d\psi)^n U_{-\frac{2n}{d}}(\phi)}{\Gamma(n) \Gamma\left(1 - \frac{n}{d}(k_2 - 1)\right) \prod_{i=3}^5 \Gamma\left(1 - \frac{k_i n}{d}\right)}, \quad (3.3.6)$$

which converges for sufficiently small ψ . By acting with the phase symmetry of the polynomial one derives the remaining periods

$$\omega_j(\psi, \phi) = \omega_0(\alpha^j \psi, \alpha^{jq_1} \phi), \quad (3.3.7)$$

where α is a d -th root of unity. As this set of periods is overcomplete, we have to choose a linearly independent subset⁶. This form of the periods is useful for performing the analytic continuation to large ϕ , since it can be done by standard techniques for the hypergeometric function. In order to continue the periods back to the region where ψ is large, it turns out to be convenient to work with an alternative form, where the principal summation runs over powers of ϕ times a certain generalized hypergeometric function in ψ . This a rather lengthy computation which we skip in the discussion at hand and just refer to the results in [65].

As one might guess from the period expansions, the Fermat-type two-parameter models of (3.3.1) have four different phases. Their structure will be discussed in detail in section 9.3. For now, let us only point out that there are two hybrid regions in addition to LG and LCS regions. The hybrid region where $\phi \rightarrow \infty$ and ψ stays small will be called the \mathbb{P}^1 (-fibration)-phase, whereas the region with $\psi \rightarrow \infty$ and ϕ small will be referred to as the orbifold(-hybrid)-phase.

The reduced set of periods $(\omega_0, \dots, \omega_5)$ form a basis. We can calculate these in the LG phase by expanding the hypergeometric function in (3.3.6) around $\phi = 0$. The result is polynomial in both ϕ and ψ . In the \mathbb{P}^1 fibration region we expand the hypergeometric function around $i\infty$. We find that the even periods ω_{2j} now contain simple logarithms in ϕ . In the orbifold hybrid phase all periods (except ω_0) acquire logarithmic terms up

⁶In the cases of interest to us, one can take the first 6 periods.

to third order $\log(\psi)^3$. For the LCS region, standard tools are available to compute the metric and periods such as INSTANTON [102].

In this thesis we will analyze the Calabi-Yau manifolds \mathbb{P}_{11222}^4 [8], \mathbb{P}_{11226}^4 [12] and \mathbb{P}_{11169}^4 [18]. More details about the computation of their periods and the definition for mirror maps of two-parameter moduli spaces can be found in [65]. The results are briefly summarized in appendix A.

CHAPTER 4

Fluxes and Moduli Stabilization

It was shown in chapter 2 that string compactifications inevitably lead to numerous massless moduli fields. As explained in the introduction 1 these massless scalar fields would cause mayor experimental contradictions. One way to resolve this issue are background fluxes generating a scalar potential for the moduli and hence stabilizing them at its minima. Thereby moduli become massive and are able to avoid observational inconsistencies if their mass is sufficiently large.

Background fluxes simply generalize familiar non-trivial field strengths of classical electrodynamics and obey a crucial Dirac quantization condition. The main goal of this chapter boils down to describing the coupling of such fluxes to moduli fields. Note also that compactification including background fluxes are often referred to as *flux compactifications*.

We will demonstrate how dimensional reduction of the $D = 10$ theory gives rise to an effective $\mathcal{N} = 1$ supergravity action in $D = 4$. Here, 'effective ' means at low-energies up to the Kaluza-Klein scale as explained more precisely in this chapter. From the four-dimensional perspective of $\mathcal{N} = 1$ supergravity, moduli and their interplay with fluxes are fully described by three ingredients:

- a *Kähler potential* K describing the geometry of the moduli space as elaborated in the last two chapters.
- a *superpotential* W coupling fluxes and moduli. Deriving the form of the superpotential will be the main task of this chapter.
- a *gauge kinetic function* f_{kin} denoting a complexified gauge coupling for the field strengths of each gauge group.

4.1 Effective $\mathcal{N} = 1$ Supergravity Theory

The bosonic field content of type IIB string theory in $D = 10$ is effectively captured by the low-energy supergravity action [66]

$$\mathcal{S}_{\text{IIB}} = \frac{2\pi}{l_s^8} \int d^{10}x \sqrt{-G} \left[e^{-2\phi} \left(\mathcal{R} + 4(\nabla\phi)^2 - \frac{1}{2}|H_3|^2 \right) - \frac{1}{2}|F_1|^2 - \frac{1}{2}|\tilde{F}_3|^2 - \frac{1}{4}|\tilde{F}_5|^2 \right], \quad (4.1.1)$$

with \mathcal{R} being the ten-dimensional Ricci curvature scalar and ϕ the dilaton. The field strengths $F_{p+1} = dC_p$ were combined with the NS-NS 2-form $H_3 = dB_2$

$$\begin{aligned} F_1 &= dC_0, & \tilde{F}_3 &= dC_2 - C_0 dB_2, \\ \tilde{F}_5 &= dC_4 - \frac{1}{2}C_2 \wedge dB_2 + \frac{1}{2}B_2 \wedge dC_2. \end{aligned} \quad (4.1.2)$$

Obviously, the action is in the string frame. For later convenience it is useful to rewrite the action in Einstein frame by absorbing a dilaton factor in the metric (cf. section 4.1.3). Note that we will not put an extra label on the metric and tensors to indicate the Einstein frame. Employing the combined axio-dilaton $S = e^{-\phi} - iC_0$ as well as the 3-form $G_3 = F_3 - iS H_3$, the action in Einstein frame reads

$$\mathcal{S}_{\text{IIB}} = \frac{2\pi}{l_s^8} \int d^{10}x \sqrt{-G} \left(\mathcal{R} - \frac{\partial_M S \partial^M \bar{S}}{2(\text{Re}(S))^2} - \frac{1}{2} \frac{|G_3|^2}{\text{Re}(S)} - \frac{1}{4} |\tilde{F}_5|^2 \right). \quad (4.1.3)$$

In addition, the action \mathcal{S}_{IIB} above may receive a contribution from a topological Chern-Simons term

$$\mathcal{S}_{\text{CS}} = \frac{2\pi}{l_s^8} \int \frac{1}{4i \text{Re}(S)} C_4 \wedge G_3 \wedge \bar{G}_3. \quad (4.1.4)$$

Moreover, D -branes and O -planes can be understood as localized sources and hence they contribute to the action as well. They are summarized by \mathcal{S}_{loc} . For instance, the leading contribution to the Dirac-Born-Infeld action of a single Dp -brane reads

$$\mathcal{S}_{\text{loc}} \supset -T_p \int_{W_{p+1}} d^{p+1}\xi \sqrt{-G} + \mu_p \int_{W_{p+1}} C_{p+1}, \quad (4.1.5)$$

where ξ denotes the intrinsic $(p+1)$ -dimensional coordinates on the world-volume W_{p+1} of the Dp -brane and T_p the Dp -brane tension. Furthermore, $\mu_p = \pm T_p$ for brane and anti-brane. Note that we have neglected B_2 and the field strength F . Without this convention, the first term above would be the usual Dirac-Born-Infeld action. The latter term describes again a topological Chern-Simons coupling of the Dp -brane to the R-R fields. Similarly, O -planes have opposite tension and R-R charges.

Let us remark that there exists an alternative *democratic* formulation of the type IIB supergravity action (4.1.3) including for every C_p -form a dual C_{8-p} -form [103]. This formulation treats electric as well as magnetic branes on equal footing and is often useful for flux compactifications.

4.1.1 Geometric Flux G_3

The 3-form G_3 will be our first example for a background flux and hence we start with the definition

Definition: *A field strength with non-trivial vev is called background flux.*

Pairing the vevs of the NS-NS 3-form flux $H = \langle dB_2 \rangle$ with the R-R 3-form flux $\mathfrak{F} = \langle dC_2 \rangle$ we obtain the well-known flux

$$G_3 = \mathfrak{F} - iSH. \quad (4.1.6)$$

Hence, the often used expression 'turning on fluxes' stands for choosing non-zero vevs \mathfrak{F} , H . In section 4.2 we will introduce additional 3-form fluxes with different characteristics, but G_3 is the geometrically best understood and in the literature most used flux. Before showing how fluxes generate a potential for the moduli, let us emphasize some important features of them.

Fluxes and localized D -branes backreact on the geometry [53] and can introduce a significant warping in the Calabi-Yau metric. In fact, these backreaction effects might spoil the Ricci flatness of the Calabi-Yau manifold. Working at large compactification volume dilutes flux-induced warping effects and the validity of the effective theory is maintained. In general, however, great care has to be taken to control this backreaction, in particular when non-geometric fluxes are included [32]. We will come back to this issue in chapter 7.

Recall that the $\mathcal{N} = 1$ supersymmetry after compactification might be spontaneously broken by fluxes. In the case of G_3 , supersymmetry is preserved iff it is primitive and its only non-zero component is $(2, 1)$. This constraint follows from the vanishing F -terms for axio-dilaton, complex structure and Kähler moduli. Calabi-Yau manifolds turn out to satisfy the primitivity condition $G_3 \wedge J = 0$ automatically. Equivalently, there is a nice connection with the imaginary self-dual condition $iG_3 = \star_6 G_3$, which only allows for the components $(2, 1)$ and $(0, 3)$. Therefore, $\mathcal{N} = 1$ supersymmetry after a Calabi-Yau compactification survives if the $(0, 3)$ -component of G_3 is zero. For details we refer to [67, 104].

Moreover, one can show that fluxes are quantized and their charges obey a Dirac quantization condition. For a nice and detailed prove we refer to the appendix of [67]. In the case of our 3-form fluxes \mathfrak{F} and H consider the 3-cycles $\{A^\Lambda, B_\Sigma\}$ with $\Lambda, \Sigma = 0, \dots, h^{2,1}$, representing a basis of the homology group H_3 defined by

$$A^\Lambda \cap B_\Sigma = -B_\Sigma \cap A^\Lambda = \delta^\Lambda_\Sigma, \quad A^\Lambda \cap A^\Sigma = B_\Lambda \cap B_\Sigma = 0. \quad (4.1.7)$$

Then, quantization of the fluxes requires

$$\begin{aligned} \int_{A^\Lambda} \mathfrak{F} &= 2\pi \tilde{f}^\Lambda \in 2\pi\mathbb{Z}, & \int_{B_\Lambda} \mathfrak{F} &= 2\pi \mathfrak{f}_\Lambda \in 2\pi\mathbb{Z}, \\ \int_{A^\Lambda} H &= 2\pi \tilde{h}^\Lambda \in 2\pi\mathbb{Z}, & \int_{B_\Lambda} H &= 2\pi h_\Lambda \in 2\pi\mathbb{Z}. \end{aligned} \quad (4.1.8)$$

Using the dual¹ cohomology basis $\{\alpha_\Lambda, \beta^\Lambda\}$, $\Lambda = 0, \dots, h^{2,1}$, set by equations (2.3.17), the fluxes \mathfrak{F} , H can be rewritten as follows

$$\mathfrak{F} = -\tilde{f}^\Lambda \alpha_\Lambda + \mathfrak{f}_\Lambda \beta^\Lambda, \quad H = -\tilde{h}^\Lambda \alpha_\Lambda + h_\Lambda \beta^\Lambda. \quad (4.1.9)$$

Throughout this thesis one should keep in mind that $\tilde{f}^\Lambda, \mathfrak{f}_\Lambda, \tilde{h}^\Lambda, h_\Lambda \in \mathbb{Z}$. It will turn out that geometric and non-geometric fluxes are quantized analogously.

4.1.2 Superpotential and Scalar Potential

Eventually all models investigated in chapters 7, 8 are entirely described by the standard $\mathcal{N} = 1$ supergravity formalism in $D = 4$. The original $D = 10$ action (4.1.1) carries way to much information and is not necessary for our purposes. We will now connect the ten-dimensional theory to the four-dimensional effective one by introducing a proper superpotential W .

Consider again the $D = 10$ type IIB supergravity action (4.1.3). For now we dismiss contributions from $\mathcal{S}_{\text{CS}} + \mathcal{S}_{\text{loc}}$ and come back to this point in section 8.3.1. Assume a constant axio-dilaton S , such that $\partial_M S = 0$. Furthermore we neglect warping effects because they are subleading at large volume, implying² $\tilde{F}_5 = 0$. We also drop the curvature term \mathcal{R} in (4.1.3), which will lead to the familiar Einstein-Hilbert action $\mathcal{S}_{\text{EH}} \sim \int d^4x \sqrt{-g_E} \mathcal{R}_E$ as explained in subsection 4.1.3. Then the $D = 10$ type IIB action reduces to

$$\frac{2\pi}{l_s^8} \int d^{10}x \sqrt{-G} \frac{1}{2} \frac{|G_3|^2}{\text{Re}(S)}. \quad (4.1.11)$$

Note that we have employed the notation³ $|F_p|^2 = \frac{1}{p!} F_{M_1 \dots M_p} F^{M_1 \dots M_p}$.

¹The Poincaré dual space of the homology group H_3 is just the cohomology group H^3 due to the fact that our Calabi-Yau three-fold \mathcal{M} has real dimension $D = 6$.

²The warp factor $\alpha = e^{2A(y)}$ expresses also the size of the 5-form flux [67]:

$$\tilde{F}_5 = (1 + *_{10}) [d\alpha \wedge dx^0 \wedge dx^1 \wedge dx^2 \wedge dx^3]. \quad (4.1.10)$$

³ $*_{10}$ denotes the 10d Hodge-star operator. It is useful to know the symmetric inner product

$$\int_{\mathcal{M}} F_p \wedge *_{10} F_p = \frac{1}{p!} \int_{\mathcal{M}} d^{10}x \sqrt{-g} F_{\mu_1 \dots \mu_p} F^{\mu_1 \dots \mu_p} \equiv \int_{\mathcal{M}} d^{10}x \sqrt{-g} |F_p|^2. \quad (4.1.12)$$

In order to perform the dimensional reduction one decomposes the ten-dimensional metric into a $D = 4$ part $G^{(4)}$ as well as a part $G^{(6)}$ of the $D = 6$ Calabi-Yau manifold \mathcal{M} . As a result we obtain the simple splitting [105]

$$\int d^4x \sqrt{-G^{(4)}} \left(\int_{\mathcal{M}} d^6x \sqrt{G^{(6)}} \frac{|G_3|^2}{2\text{Re}(S)} \right) \equiv \int d^4x \sqrt{-G^{(4)}} V_{\text{flux}}. \quad (4.1.13)$$

Remarkably, S. Gukov, C. Vafa, E. Witten [49, 50] proved that the potential V_{flux} is equal to the four-dimensional standard $\mathcal{N} = 1$ supergravity potential V_{F} for choosing a superpotential

$$W = \int_{\mathcal{M}} G_3 \wedge \Omega_3. \quad (4.1.14)$$

with the holomorphic $(3, 0)$ -form Ω_3 given in (2.3.20). Therefore, this is often called the *Gukov-Vafa-Witten superpotential*. Note that the superpotential above is holomorphic. Together with the definition (4.1.6) of the flux G_3 , the superpotential can be spelled out explicitly in terms of fluxes and moduli

$$\begin{aligned} W_{\text{GVW}} &= \int_{\mathcal{M}} G_3 \wedge \Omega_3 = \int_{\mathcal{M}} (\mathfrak{F} - iSH) \wedge (X^\Lambda \alpha_\Lambda - F_\Lambda \beta^\Lambda) = \\ &= - \left(\mathfrak{f}_\Lambda X^\Lambda - \tilde{\mathfrak{f}}^\Lambda F_\Lambda \right) + iS \left(h_\Lambda X^\Lambda - \tilde{h}^\Lambda F_\Lambda \right). \end{aligned} \quad (4.1.15)$$

Recall that the scalar potential V_{F} is of the form

$$V_{\text{F}} = \frac{M_{\text{Pl}}^4}{4\pi} e^K \left(K^{I\bar{J}} D_I W D_{\bar{J}} \bar{W} - 3|W|^2 \right), \quad (4.1.16)$$

where the sum runs over all moduli listed in table 2.3. Apparently, the scalar potential only depends on the superpotential W and the Kähler potential K or the Kähler metric $G_{I\bar{J}} = \partial_I \partial_{\bar{J}} K$, respectively. The Kähler-covariant derivatives are defined by

$$D_I W = \partial_I W + (\partial_I K) W. \quad (4.1.17)$$

The potential (4.1.16) is known as *F-term* scalar potential since it contains F-terms F^I . For the rest of this thesis we will, however, drop the specification F-term and denote $V_{\text{F}} \equiv V$. F-terms are given by the expression

$$F^I = e^{\frac{K}{2}} K^{I\bar{J}} D_{\bar{J}} \bar{W}. \quad (4.1.18)$$

Comments on flux vacua and the string landscape

Moduli are said to be *stabilized* if they take on values for which the flux-induced scalar potential V is minimized, i.e. their vevs. This makes sense as the moduli develop a physical mass term at the minima. Minima of the scalar potential are called *flux vacua* and the

Property	Condition	Description
no-scale	$K^{I\bar{J}}(\partial_I K)(\partial_{\bar{J}} K) = 4$ sum over S, T_α, G^a	important for susy breaking and mediation to the standard model [106]
supersymmetric	$D_I W = 0 \forall \text{moduli}$	general condition of supergravity [107]
tachyonic	\exists negative mass eigenstates	Vacua without tachyons often called <i>stable</i> ; tachyonic AdS minima are only stable if above Breitenlohner-Freedman bound [108]
AdS	$V _{\text{Minimum}} < 0$	AdS has negative cosmological constant proportional to vacuum energy density [109, 110]; Minkowski or dS for $V _{\text{Minimum}} = / > 0$

Table 4.1: Properties of flux vacua of the F-term scalar potential (4.1.16).

collection of flux vacua is famously known as *string landscape*. Characteristic features of flux vacua are summarized in table 4.1. According to this table, supersymmetric flux vacua are always AdS since their scalar potential reduces to $V = -e^K |W|^2 \leq 0$. It is widely believed that the number of flux vacua is gigantic. As a rough estimate, a flux configuration is determined by the number of flux quanta along the independent 3-cycles, which are 100 – 300 for a typical Calabi-Yau manifold. Assuming only 10 different flux values, we already obtain the huge number of $10^{100} - 10^{300}$ flux vacua. Of course, there are several constraints like tadpole cancellation that need to be satisfied for a physical vacuum. Nevertheless, more accurate estimates from the literature lead to even larger multiplicities of flux vacua. The huge flux landscape narrows the predictive power of string theory and is thus quite unpopular. Thereto let us point out:

"I would be happy personally if the multiverse [i.e. string landscape] interpretation is not correct, in part because it potentially limits our ability to understand the laws of physics. But none of us were consulted when the universe was created." - E. Witten [111] -

In view of later applications to string inflation, let us mention a powerful no-go theorem by J. Conlon [112]. In many models of string inflaton a single axionic modulus is employed as unconstrained inflaton field, whereas all other moduli are stabilized. However, the no-go theorem of Conlon states that there is no tachyon-free supersymmetric flux vacuum consistent with stabilized moduli and unfixed axions. This is an important restriction on constructing inflationary models within string theory. Conlon also points out several loopholes to the theorem, such as D-term contributions or corrections to the Kähler potential. Due to this theorem, the authors of [32] analyzed non-supersymmetric vacua.

4.1.3 Mass Scales and Hierarchy

It is very convenient to work purely in the four-dimensional effective theory as it is much simpler to handle than the full ten-dimensional equations. For inflation we will yet build another effective theory by fixing all moduli except one (axion) and constructing an effective model of single-field inflation at a scale below the moduli mass scale. Therefore, all models discussed in this thesis and also other typical models of string inflation rely heavily on the validity of effective field theories (EFT). In EFTs one integrates out all physics above a certain energy scale because it would give only sub-leading corrections. So, we may safely trust into an EFT as long as we are working at energy scales sufficiently below the mass scales of integrated-out modes.

In fact, here we face a whole ensemble of EFTs each with a characteristic mass scale. In particular, there is of course the string scale M_s describing physics where the strings need to be treated as spatially extended objects. Below M_s strings behave approximately as point-like objects. Next, there is the Kaluza-Klein scale M_{KK} summarizing effects due to a non-trivial geometry, for instance compactifying on a manifold with cycles. An EFT below M_{KK} basically cannot resolve the fine-grained structures of the geometry. Further below in this subsection we will be more precise about M_s as well as M_{KK} .

In order to justify the pure effective $D = 4$ description of moduli stabilization, the moduli masses ought to be below these scales. For now we denote the moduli space collectively by M_{mod} . In other words, the effective supergravity theory for moduli stabilization developed in the last sections is only valid if we satisfy the mass hierarchy

$$M_{\text{mod}} < M_{\text{KK}} < M_s < M_{\text{Pl}}. \quad (4.1.19)$$

All of these scales are in relative dependence to the Planck mass M_{Pl} . It is absolutely crucial to notice that all scales (except M_{Pl}) depend on the moduli vevs, i.e. are different at each point in the string landscape. Thus, the mass hierarchy (4.1.19) condition rules out many flux vacua, which might be possible at a first glance. This needs to be checked carefully after stabilizing the moduli and will not only constitute a tough constraint on our models, but support the main result of this thesis. Let us now explain how to properly determine the moduli masses M_{mod} .

Canonically normalized mass eigenstates

The moduli introduced so far do not necessarily correspond to the physical states, that one can (in principle) measure. Physical states have to be canonically normalized which will have a drastic implication for the field range as discussed in chapter 8. In addition these states should better be mass eigenstates in order to compare them to other scales listed in the hierarchy (4.1.19). Following closely [113], we shall now show a method guaranteeing both features.

Consider the real moduli x_i and assume they acquire a vev $\langle x_i \rangle$ at the minimum of the scalar potential. Small perturbations around the minimum $x_i \simeq \langle x_i \rangle + \delta x_i$ are then described by the Lagrangian

$$\mathcal{L} \simeq G_{i\bar{j}} \partial_\mu(\delta x_i) \partial^\mu(\delta x_j) - V_0 - \frac{1}{2} \partial_i \partial_j V|_{x_i=\langle x_i \rangle} (\delta x_i) (\delta x_j) + \dots, \quad (4.1.20)$$

For simplicity we specialize in the following on two moduli⁴, although the generalization to arbitrary moduli is obvious. Next, we introduce the canonically normalized fields θ and σ , which we define by

$$\begin{pmatrix} x_1 \\ x_2 \end{pmatrix} \equiv \vec{v}_\theta \frac{\theta}{\sqrt{2}} + \vec{v}_\sigma \frac{\sigma}{\sqrt{2}} \quad (4.1.21)$$

where the vectors \vec{v}_θ and \vec{v}_σ are eigenstates of the matrix (G^{ik} is the inverse Kähler metric)

$$(M^2)_j^i \equiv \frac{1}{2} G^{ik} \partial_k \partial_j V|_{x_i=\langle x_i \rangle} \quad (4.1.22)$$

together with the eigenvalues m_θ^2 and m_σ^2 . The reason for this definition will become clear shortly.

It is easy to check that the kinetic term is of canonical form without any mixed terms $\partial_\mu \theta \partial^\mu \sigma$ if we satisfy the condition

$$\vec{v}_I^T G \vec{v}_J = \delta_{IJ}, \quad \vec{v}_{I,J} \in \{\vec{v}_\theta, \vec{v}_\sigma\}. \quad (4.1.23)$$

By means of the eigenvectors $\vec{v}_\theta, \vec{v}_\sigma$ also the mass term of the Lagrangian takes on a convenient form

$$\begin{pmatrix} x_1 \\ x_2 \end{pmatrix}^T \left[G \cdot \underbrace{G^{-1} \cdot \left(\frac{1}{2} \partial^2 V|_{x_i=\langle x_i \rangle} \right)}_{M^2} \right] \begin{pmatrix} x_1 \\ x_2 \end{pmatrix} = \frac{1}{2} (\vec{v}_\theta \theta + \vec{v}_\sigma \sigma)^T G (m_\theta^2 \vec{v}_\theta \theta + m_\sigma^2 \vec{v}_\sigma \sigma). \quad (4.1.24)$$

In total, definition (4.1.21) together with the normalization (4.1.23) of the eigenvectors, leads to the desired expression for the Lagrangian

$$\mathcal{L} \simeq \frac{1}{2} \partial_\mu \theta \partial^\mu \theta + \frac{1}{2} \partial_\mu \sigma \partial^\mu \sigma - V_0 - \frac{1}{2} m_\theta^2 \theta^2 - \frac{1}{2} m_\sigma^2 \sigma^2 + \dots \quad (4.1.25)$$

For that reason it is convenient to transform⁵ a given moduli ensemble to eigenstates of the mass matrix (4.1.22).

⁴In typical flux-scaling scenarios [32, 64] one often considers the axions $x_i = \{c, \rho\}$.

⁵Alternatively, one may choose a state e.g. $\theta = hc + q\rho$ with h, q flux quanta, and afterwards compute an orthogonal state σ by demanding a standard canonical kinetic term. This method is of course possible for any state and was for instance used in the toy model presented in [64]. In spite of the canonical kinetic Lagrangian, the so constructed states θ and σ do not have to be eigenstates of the mass matrix.

In flux-scaling type models of moduli stabilization [32] all mass eigenstates have usually the same dependence of the fluxes. This has in fact valuable advantages, but is a rather unattractive feature for models of single-field inflation. There one would like to obtain a parametrical hierarchy between the mass eigenstates. More comments on how to realize such a hierarchy are postponed to chapters 7, 8.

String and Kaluza-Klein scales

In order to evaluate the mass hierarchy (4.1.19), it is convenient to express all scales relative to the four-dimensional low-energy (reduced) Planck mass M_{Pl} , which is fixed by $M_{\text{Pl}} \sim 1/\sqrt{8\pi G_N} \approx 2.435 \times 10^{18}$ GeV with Newton's constant G_N . In this section we derive expressions for the string scale M_s as well as the Kaluza-Klein scale M_{KK} in terms of M_{Pl} .

The string scale

$$M_s = \frac{2\pi}{l_s}, \quad (4.1.26)$$

is inverse proportional to the string length l_s . To relate it to the Planck mass we have to carry out a dimensional reduction of the gravitational part of the $D = 10$ string action and compare it to $D = 4$ Einstein-Hilbert gravity. Consider the type IIB action (4.1.1) in string frame

$$\mathcal{S}_{\text{IIB}} = \frac{2\pi}{l_s^8} \int_{\mathbb{R}^{1,3} \times \mathcal{M}} dx^{10} \sqrt{-G} e^{-2\phi} \mathcal{R} + \dots \quad (4.1.27)$$

We assume here that the ten-dimensional metric G decomposes into a $D = 4$ part $G^{(4)}$ of Minkowski space as well as a $D = 6$ part $G^{(6)}$ of the Calabi-Yau manifold \mathcal{M} . At first we transform the action to Einstein frame by introducing the Einstein metric G_E

$$G = e^{\frac{\phi - \phi_0}{2}} G_E. \quad (4.1.28)$$

The identification follows [105] and includes $\phi_0 = \langle \phi \rangle$, which ensures that the metrics are identical in the physical vacuum. As a consequence the determinant produces a dilaton factor and we obtain a Riemann tensor \mathcal{R}_E in Einstein frame (see Appendix E of [114])

$$\sqrt{-G} \rightarrow e^{\frac{5}{2}(\phi - \phi_0)} \sqrt{-G_E}, \quad \mathcal{R} = e^{-\frac{\phi - \phi_0}{2}} \left[\mathcal{R}_E + \frac{9}{2} (\partial\phi)^2 + \frac{9}{2} \nabla^2 \phi \right]. \quad (4.1.29)$$

Hence, the type IIB action in Einstein frame reads

$$\mathcal{S}_{\text{IIB}} = \frac{2\pi e^{-2\phi_0}}{l_s^8} \int_{\mathbb{R}^{1,3} \times \mathcal{M}} dx^{10} \sqrt{-G_E} \mathcal{R}_E + \dots \quad (4.1.30)$$

To carry out the dimensional reduction we simply have to integrate over the six-dimensional internal space [105] (with $e^{\phi_0} = g_s$)

$$\mathcal{S}_{\text{dim. red.}} = \frac{2\pi}{g_s^2 l_s^8} \int_{\mathcal{M}} dx^6 \sqrt{-G_E^{(6)}} \int_{\mathbb{R}^{1,3}} dx^4 \sqrt{-G_E^{(4)}} \mathcal{R}_E. \quad (4.1.31)$$

The prefactor of the resulting integral may be compared to standard Einstein-Hilbert gravity [115]

$$\frac{M_s^2}{2\pi g_s^2} \frac{\text{vol}_6}{l_s^6} = \frac{M_{\text{Pl}}^2}{2}. \quad (4.1.32)$$

The overall Calabi-Yau volume is given by $\mathcal{V} = \text{vol}_6/l_s^6$. However, note that we will later on calculate the volume in terms of the Kähler moduli which rely on the 2-cycle volumes t . Since these have been defined (2.3.5) in Einstein frame, we also express the volume in Einstein frame⁶ $\mathcal{V} \rightarrow e^{\frac{3}{2}\phi_0}\mathcal{V}$. Eventually, the result is in agreement with [32] (using $s = g_s^{-1}$)

$$M_s = \frac{\sqrt{\pi} M_{\text{Pl}}}{\sqrt[4]{s} \sqrt{\mathcal{V}}}. \quad (4.1.33)$$

Next we discuss Kaluza-Klein⁷ states. As they correspond to momentum modes along cycles of the internal space, a typical Calabi-Yau can have many different Kaluza-Klein modes with different masses. For simplicity we restrict ourselves to a toroidal average, hence there might be even lighter Kaluza-Klein states. Assume R is the dimensionful Kaluza-Klein radius of a toroidal compactification. Measured in string lengths l_s from (4.1.26), $R = R_s l_s$ and the Kaluza-Klein mass is given by

$$M_{\text{KK}} = \frac{1}{R} = \frac{M_s}{2\pi R_s}. \quad (4.1.34)$$

Assuming further $R_s^6 \sim \mathcal{V}$ and transforming to Einstein frame via $\mathcal{V} \rightarrow e^{\frac{3}{2}\phi_0}\mathcal{V}$, the string mass (4.1.33) leads to

$$M_{\text{KK}} = \frac{M_{\text{Pl}}}{\sqrt{4\pi} \mathcal{V}^{\frac{2}{3}}}. \quad (4.1.35)$$

⁶To stay in agreement with the literature we drop the index in \mathcal{V}_E .

⁷Let us illustrate the idea of Kaluza-Klein compactifications by considering a theory in $D = 5$ with a free massless scalar $\phi(x^M)$, $M = 0, \dots, 4$ and action $\mathcal{S}_{D=5} \sim \int d^5x \left(-\frac{1}{2} \partial_M \phi \partial^M \phi\right)$. Now we compactify on a circle \mathcal{S}^1 by making the x^4 coordinate periodic $\phi(x^M) = \phi(x^\mu, x^4) = \phi(x^\mu, x^4 + 2\pi R)$ with R being the radius of the circle and $\mu = 0, \dots, 3$. Since any periodic function may be decomposed in Fourier modes, we make the ansatz $\phi(x^\mu, x^4) = \sum_{k \in \mathbb{Z}} \phi_k(x^\mu) \exp(ikx^4/R)$. The resulting action in $D = 4$ reads then $\mathcal{S}_{D=4} \sim -(2\pi R) \sum_{k \geq 0} \int d^4x \left(\partial_\mu \phi_k \partial^\mu \phi_{-k} + \frac{k^2}{R^2} \phi_k \phi_{-k}\right)$, i.e. a massless scalar ϕ_0 and an infinite tower of massive resonances, known as *Kaluza-Klein modes*, with mass $M_{\text{KK}} = k/R$.

4.2 Non-Geometric Extension

A glorified concept of string theory are string dualities, which for instance unify the five different superstring theories as illustrated in almost any modern textbook on string theory, see e.g. [66, 67]. As a natural consequence one may ask whether string dualities affect flux compactifications. Indeed they do have a significant influence as outlined below, although their precise effect on the background geometry remains to be fully understood. Nevertheless, we will briefly summarize how T-duality⁸ leads to new types of fluxes, that will be employed for moduli stabilization in later sections. S-duality⁹ gives rise to even more fluxes for which we only refer to the literature [32, 117] as they will not be part of the analysis in this thesis.

4.2.1 Non-Geometric Fluxes

T-duality transformations ought to be carried out along isometries of the background. On arbitrary backgrounds this procedure is still under investigation. Let us just mention one interesting contribution [118] considering non-Abelian isometries. Starting with a background $G_{\mu\nu}$, $B_{\mu\nu}$, ϕ the *Buscher rules* [119] give explicit formulas for the T-duality transformed background. Note that R-R forms are not affected by the Buscher rules and thus we focus on NS-NS fluxes.

A didactic example to T-dualize is a torus T^3 with H -flux. This is indeed a reasonable model because a Calabi-Yau manifold can in a certain limit be view as a T^3 fibred over some base manifold according to [120]. In this limit mirror symmetry acts like T-duality on the T^3 fibre without changing the base. Here, our presentation of this example will be extremely brief, such that the reader can only get a glimpse of the concept behind non-geometric fluxes and is referred to the literature [121–124] for more information.

Consider the simple metric $ds^2 = dx^2 + dy^2 + dz^2$ on the torus T^3 together with $N \in \mathbb{Z}$ units of H -flux $H_{xyz} = N$. In order to satisfy the quantization condition $\int_{T^3} H = N$, we choose the gauge field $B_{xy} = Nz$. As nothing depends on the x , y -coordinates, they represent isometries we are allowed to T-dualize. Performing a T-duality transformation via the Buscher rules in x -direction changes the background and leads to a new *geometric flux* F_{yz}^x . The metric is still globally well-defined and corresponds to a *twisted torus*. A subsequent T-duality transformation in y -direction produces yet another flux Q_z^{xy} . Since

⁸A simple way to visualize T-duality comes from compactification of bosonic string theory on a circle S^1 with radius R . It turns out that the mass spectrum is equal to the one obtained by compactifying on a different circle with radius $\frac{\alpha'}{R}$ and simultaneous exchange of winding and momentum modes. Frankly speaking, compactification on small or large circles leads to the same physics.

⁹S-Duality, proposed by A. Sen [116] in 1994, is a non-perturbative map between weakly and strongly coupled theories. For instance, $D = 10$ type IIB string theory with string coupling g_s is S-dual to the same string theory but with coupling $\frac{1}{g_s}$.

the new geometry known as *T-fold* is only locally well-defined, but globally no longer a manifold, the new flux is called *non-geometric*. In the literature [125] people also T-dualized the z -direction regardless of the fact that there is no isometry. One then arrives at the purely non-geometric flux R^{xyz} where the metric background lacks even locally of any geometrical description and instead obeys *non-associative* structures [126,127].

Summarizing, T-duality on a 3-torus modifies the background geometry and causes the appearance of new fluxes:

$$\begin{array}{ccccccc}
H_{xyz} & \xleftrightarrow{T_x} & F_{yz}^x & \xleftrightarrow{T_y} & Q_z^{xy} & \xleftrightarrow{T_z} & R^{xyz} \\
\downarrow & & \downarrow & & \downarrow & & \downarrow \\
\text{NS-NS flux} & & \text{geometric flux} & & \text{non-geom. flux} & & \text{non-geom. flux} \\
\downarrow & & \downarrow & & \downarrow & & \downarrow \\
\text{flux background} & & \text{twisted torus} & & \text{T-fold} & & \text{non-associative}
\end{array}$$

4.2.2 Generalized Superpotential

Including these new fluxes, the Gukov-Vafa-Witten superpotential [49] can be extended in the following compact way [122, 128, 129]

$$W = \int_{\mathcal{M}} \left[\mathfrak{F} + \mathcal{D} \Phi_c^{\text{ev}} \right]_3 \wedge \Omega_3, \quad (4.2.1)$$

with the complex multi-form of even degree $\Phi_c^{\text{ev}} = iS - iG^a \omega_a - iT_\alpha \tilde{\omega}^\alpha$ and the moduli, cohomology bases in tables 2.3, 2.1, respectively. The twisted differential \mathcal{D} [123] is defined by

$$\mathcal{D} = d - H \wedge - F \circ - Q \bullet - R \lrcorner, \quad (4.2.2)$$

where the operators appearing in (4.2.2) implement the mapping

$$\begin{array}{ll}
H \wedge : p\text{-form} \rightarrow (p+3)\text{-form}, & F \circ : p\text{-form} \rightarrow (p+1)\text{-form}, \\
Q \bullet : p\text{-form} \rightarrow (p-1)\text{-form}, & R \lrcorner : p\text{-form} \rightarrow (p-3)\text{-form}.
\end{array} \quad (4.2.3)$$

Acting with the extended differential \mathcal{D} from (4.2.2) on the multiform Φ_c^{ev} and keeping solely 3-forms, the total superpotential becomes

$$\begin{aligned}
W &= \int_{\mathcal{M}} \left[\mathfrak{F} + \mathcal{D} \Phi_c^{\text{ev}} \right]_3 \wedge \Omega_3 \\
&= \int_{\mathcal{M}} \left[\mathfrak{F} - iSH + iG^a (F \circ \omega_a) + iT_\alpha (Q \bullet \tilde{\omega}^\alpha) \right]_3 \wedge \Omega_3.
\end{aligned} \quad (4.2.4)$$

Let us point out that there is no R -flux in the superpotential (4.2.4) because $R \lrcorner \Phi_c^{\text{ev}}$ cannot yield a 3-form.

One can be more specific about the action of \mathcal{D} after introducing a symplectic basis for the third cohomology $H^3(\mathcal{M})$ of the Calabi-Yau threefold. Eventually the non-vanishing flux components can be summarized by:

$$\begin{array}{cccc}
 \mathfrak{F} & H & F & Q \\
 \hline
 \{f_\lambda, \tilde{f}^\lambda\} & \{h_\lambda, \tilde{h}^\lambda\} & \{f_{\lambda a}, \tilde{f}_a^\lambda\} & \{q_\lambda^\alpha, \tilde{q}^{\lambda\alpha}\} \\
 \hline
 \end{array} \tag{4.2.5}$$

where $\lambda = 0, \dots, h_-^{2,1}$ and the indices a, α label the moduli G^a, T_α , respectively. Let us stress that all these fluxes, coupling to moduli of the closed string sector, are quantized and may only take integer values.

In terms of the periods X^λ and F_λ of the holomorphic 3-form Ω_3 , the superpotential (4.2.1) simplifies to

$$\begin{aligned}
 W = & - \left(f_\lambda X^\lambda - \tilde{f}^\lambda F_\lambda \right) + iS \left(h_\lambda X^\lambda - \tilde{h}^\lambda F_\lambda \right) \\
 & + iG^a \left(f_{\lambda a} X^\lambda - \tilde{f}_a^\lambda F_\lambda \right) - iT_\alpha \left(q_\lambda^\alpha X^\lambda - \tilde{q}^{\lambda\alpha} F_\lambda \right).
 \end{aligned} \tag{4.2.6}$$

Apparently the superpotential depends only linearly on the moduli S, G^a, T_α and the Kähler moduli couple to non-geometric fluxes at tree-level.

The NS-NS fluxes also give rise to generalized Bianchi identities (from $\mathcal{D}^2 = 0$) and to Freed-Witten anomaly cancellation conditions. Let us remark that for the examples to be discussed in this thesis, these will all be satisfied. Moreover note that most non-geometric type IIB fluxes considered here would correspond to geometric fluxes in the T-dual IIA compactification.

4.3 Schemes of Moduli Stabilization

For later usage we summarize in this section three different types of moduli stabilization. The first two schemes share similar characteristics, whereas the flux-scaling scenario is the only one featuring non-geometric fluxes to fix the Kähler moduli instead of non-perturbative corrections. To compensate the brevity of the explanations here, we refer to the vast literature stated in each subsection. In this section we aim to present only a qualitative overview highlighting the special features of each scheme. Note that there exist more proposals for stabilizing the moduli, but those are not necessary for this thesis.

4.3.1 KKLT

Considering type IIB string theory the main challenge is to stabilize the Kähler moduli in a stable (at best directly dS) vacuum. Complex structure moduli as well as the dilaton may

be fixed via fluxes as demonstrated in the pioneering GKP-paper [53]. The famous work [63] by S. Kachru, R. Kallosh, A. Linde and S. Trivedi consists of two main proposals: first, it gives a simple method to stabilize Kähler moduli by using non-perturbative corrections to the superpotential and second, it suggests an uplift mechanism from an AdS to a dS vacuum.

KKLT assumes complex structure moduli and dilaton have been stabilized at a high scale and been integrated out, such that they only contribute to a constant W_0 in the superpotential. For simplicity they also reduce their setup to a single Kähler modulus $T = \tau + i\rho$. Their starting point is then

$$W_{\text{KKLT}} = W_0 + A e^{-aT}, \quad K = -3 \log(T + \bar{T}). \quad (4.3.1)$$

The Kähler potential K is simply tree-level (no α' -corrections) as introduced in (2.3.16). However, the superpotential receives a non-perturbative correction which KKLT motivated for instance by gaugino condensation¹⁰ on a stack of D7-branes. Note that in string theory the Pfaffian A may depend on other fields and was purely for simplicity assumed to be constant.

For W_0 (exponentially) small (and negative) one immediately finds the KKLT minimum from (4.3.1) (setting the axion in T to zero for simplicity), where the Kähler modulus is stabilized at τ_0 . This minimum is supersymmetric and given by

$$D_T W_{\text{KKLT}} = 0 \quad \implies \quad W_0 = -A e^{-a\tau_0} \left(1 + \frac{2}{3} a \tau_0\right). \quad (4.3.2)$$

The scalar potential $V = -3e^K |W|^2|_{\text{AdS}} = -a^2 A^2 e^{-2a\tau_0} / (6\tau_0)$ at this supersymmetric minimum is negative, i.e. it implies an AdS vacuum. If one adds a positive energy contribution, whose moduli dependence is slowly varying, the original sharply-peaked AdS vacuum can be uplifted without destroying the local minimum. This contribution will break supersymmetry, but only mildly as their impact shall be tuneable. KKLT suggested to include an anti- $D3$ -brane in a warped throat to do the job. The contribution¹¹ to the scalar potential includes a variable α depending on the number of anti-branes as well as the warp factor

$$\delta V_{\overline{D3}} \sim \frac{\alpha}{\tau^3}. \quad (4.3.3)$$

¹⁰We recommend [130] for a nice review of gaugino condensation. To illustrate the idea, consider a $SU(N)$ super-Yang-Mills theory with only one fermion, the gaugino λ^a . The $U(1)_R$ symmetry $\lambda^a \rightarrow e^{i\alpha} \lambda^a$ is broken by instanton effects, which can be understood in terms of the mixed triangle anomaly between one $U(1)_R$ current and two gluons. Since the holomorphic gauge coupling τ corresponds in our case to the Kähler modulus field, one can show (via the instanton effects) that the path integral is invariant under the simultaneous shift of λ^a and $\tau \rightarrow \tau + N\alpha/\pi$, where N is the rank of the gauge group. Assuming the absence of massless particles, holomorphy and the symmetry above fix the superpotential to be $W_{\text{cond}} \sim \exp(2\pi i \tau/N)$. This is the unique form since the superpotential has R -charge 2, i.e. $W_{\text{cond}} \rightarrow e^{2i\alpha} W_{\text{cond}}$.

¹¹In general the $\overline{D3}$ -brane contribution to the scalar potential is $V_{\overline{D3}} \sim \alpha/\mathcal{V}^\beta$ (\mathcal{V} is the overall volume) with $\beta = 2$ if the anti-brane is in the bulk and $\beta = 4/3$ if it is located in a warped throat [32].

The potential of the KKLT scenario for the supersymmetric AdS and the uplifted (non-supersymmetric) dS vacuum is plotted in figure 4.1.

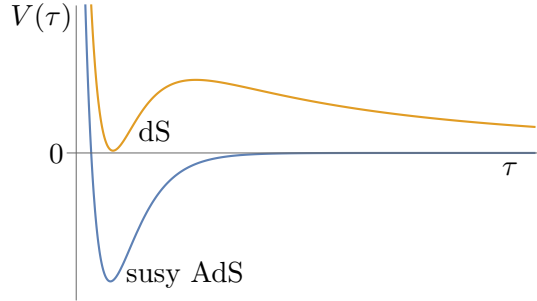


Figure 4.1: Schematic plot of the KKLT scalar potential for the saxionic Kähler modulus τ . In contrast to the blue curve, the orange curve includes an $\overline{D}3$ -brane uplift leading to a Minkowski/dS vacuum.

4.3.2 Large Volume Scenario

The large volume scenario (LVS) [15] by V. Balasubramanian, P. Berglund, J. Conlon and F. Quevedo extends the KKLT idea by including perturbative α' -corrections to the Kähler potential. Let us briefly review their ideas following closely [131]. More precisely, consider a Calabi-Yau manifold with two Kähler moduli T_b and T_s that is of *swiss-cheese type*, i.e. its overall volume reads $\mathcal{V} = \tau_b^{\frac{3}{2}} - \tau_s^{\frac{3}{2}}$. The name swiss-cheese becomes plausible as we take the limit $\tau_b \gg \tau_s$. Altogether, LVS starts with the following super- and Kähler potential

$$W_{\text{LVS}}(T) = W_0 + A_s e^{-a_s T_s}, \quad K = -2 \log \left(\tau_b^{\frac{3}{2}} - \tau_s^{\frac{3}{2}} + \frac{\xi}{2} \text{Re}(S)^{\frac{3}{2}} \right), \quad (4.3.4)$$

with $\xi = -\frac{\chi(\mathcal{M})\zeta(3)}{2(2\pi)^3}$, where $\chi(\mathcal{M})$ is the Euler number of the Calabi-Yau \mathcal{M} and $\zeta(3) \approx 1.202$ Apéry's constant. W_0 is again the value of the GVW-superpotential, after integrating out the axio-dilaton and the complex structure moduli.

For the LVS minimum to exist one needs $\chi(M) < 0$, i.e. $h^{2,1}(M) > h^{1,1}(M)$. Up to Calabi-Yau-geometry dependent coefficients of order one, after freezing the axion ρ_s , the relevant terms in the scalar potential read

$$V_{\text{LVS}}(T) = e^{K_{cs}} \frac{g_s}{2} \left(\frac{|a_s A_s|^2 \sqrt{\tau_s} e^{-2a_s \tau_s}}{\mathcal{V}} - \frac{W_0 |a_s A_s| \tau_s e^{-a_s \tau_s}}{\mathcal{V}^2} + \frac{\xi W_0^2}{g_s^{\frac{3}{2}} \mathcal{V}^3} \right), \quad (4.3.5)$$

where K_{cs} denotes the Kähler potential for the complex structure moduli. The scalar potential (4.3.5) exhibits a non-supersymmetric AdS minimum that stabilizes the Kähler

moduli

$$\tau_s = \frac{(4\xi)^{\frac{2}{3}}}{g_s}, \quad \mathcal{V} = \frac{W_0 \xi^{\frac{1}{3}}}{2^{\frac{1}{3}} g_s^{\frac{1}{2}} |a_s A_s|} e^{a_s \tau_s}. \quad (4.3.6)$$

Note that the scalar potential V_{LVS} close to the LVS-minimum is $1/\mathcal{V}$ suppressed relative to the former no-scale potential for the complex structure and the axio-dilaton moduli.

The canonically normalized Kähler moduli masses can be computed as the eigenvalues of the matrix $(M^2)^i_j = \frac{1}{2} K^{ik} \partial_k \partial_j V$, where the inverse of the Kähler metric is given at leading order in $1/\mathcal{V}$ as

$$\begin{aligned} K^{\tau_b \bar{\tau}_b} &= \frac{4}{3} \mathcal{V}^{\frac{4}{3}}, & K^{\tau_s \bar{\tau}_s} &= \frac{8}{3} \sqrt{\tau_s} \mathcal{V} \\ K^{\tau_b \bar{\tau}_s} &= K^{\tau_s \bar{\tau}_b} = 4\tau_s \mathcal{V}^{\frac{2}{3}}. \end{aligned} \quad (4.3.7)$$

At leading order, the masses of the Kähler moduli are

$$\begin{aligned} M_{\tau_b}^2 &\sim O(1) \frac{W_0^2 \xi}{g_s^{\frac{1}{2}} \mathcal{V}^3} M_{\text{Pl}}^2, & M_{\rho_b}^2 &\sim 0, \\ M_{\tau_s}^2 &\sim M_{\rho_s}^2 \sim O(1) \frac{a_s^2 W_0^2 \xi^{\frac{4}{3}}}{g_s \mathcal{V}^2} M_{\text{Pl}}^2. \end{aligned} \quad (4.3.8)$$

Most important, the modulus τ_b is exponentially lighter than all other massive moduli. For later purposes in chapter 7, note that the masses do not depend on the parameter A_s . In order to uplift the LVS to dS vacua, one can add $\overline{D}3$ -branes similar to KKLT.

4.3.3 Flux Scaling Scenarios

An alternative idea for moduli stabilization that is totally distinct from KKLT and LVS was suggested in [32] and named *flux scaling scenarios*. Instead of employing non-perturbative corrections to the superpotential (KKLT and LVS) and perturbative corrections to the Kähler potential (LVS), one uses non-geometric fluxes (see section 4.2) to fix the Kähler moduli. Axio-Dilaton, complex structure and Kähler moduli are all stabilized at tree-level and hence treated on equal footing. Let us summarize the core principles of flux-scaling models in a simple example.

An illustrative example in [32] is the *STU*-model where one considers an isotropic 6-torus T^6 with $h_+^{1,1} = h_-^{2,1} = 1$ and $h_-^{1,1} = 0$. For a particular choice of background fluxes, the Kähler potential (2.3.16) and generalized superpotential (4.2.6) are given by

$$\begin{aligned} W_{STU} &= -f_0 - 3\tilde{f}^1 U^2 - h_1 U S - q_1 U T, \\ K &= -3 \log(T + \bar{T}) - \log(S + \bar{S}) - 3 \log(U + \bar{U}). \end{aligned} \quad (4.3.9)$$

Computing the scalar potential (4.1.16) from these ingredients, one finds supersymmetric as well as non-supersymmetric minima. All of the analyzed vacua turned out to be AdS and some of them are stable, i.e. tachyon-free. The non-supersymmetric minima are of particular interest as they keep one axionic flat direction unstabilized¹², which is often employed as inflaton field. Consider the non-supersymmetric stable vacuum discussed in [32]

$$\begin{aligned} \tau &= -15v \frac{\tilde{f}^1}{q_1}, & s &= -12v \frac{\tilde{f}^1}{h_1}, & v^2 &= \frac{1}{3 \cdot 10^{\frac{1}{2}}} \frac{f_0}{\tilde{f}^1}, \\ 0 &= h_1 c + q_1 \rho, & u &= 0. \end{aligned} \tag{4.3.10}$$

Since the values of the moduli in the minimum show a simple scaling with the fluxes, one is able to control many properties of the vacuum, for instance $\text{Re}(s) = g_s^{-1}$, $\text{Re}(T)$ in the perturbative regime. All physical masses for the canonically normalized states of this vacuum show the flux dependence

$$M_{\text{mod}}^2 \sim \frac{h_1 q_1^3}{(f_0)^{\frac{3}{2}} (\tilde{f}^1)^{\frac{1}{2}}} M_{\text{Pl}}^2. \tag{4.3.11}$$

Only the numerical prefactors differ for axio-dilaton, complex structure and Kähler moduli. Note that there is one axion remaining unstabilized, so zero mass. As an important characteristic of flux scaling models, the gravitino scale $M_{\frac{3}{2}}^2 \sim e^K |W|^2$ turns out to scale with the fluxes exactly as the moduli. Therefore, we speak of high-scale supersymmetry breaking. The supersymmetry breaking source are now the fluxes. Note that attempts to realize low-scale supersymmetry breaking via sequestering [132] have not succeeded due to high sfermion masses.

¹²Recall the no-go theorem by J. Conlon in section 4.1.2.

CHAPTER 5

Large-Field Inflation in String Theory

Let us now change from string theory and rather mathematical concepts to cosmology. More precisely, we are going to illustrate the principles of cosmic inflation, which has already been motivated in the introduction 1. In spite of the beauty of the underlying idea, a concrete stringy realization of an inflationary model is still missing and highly controversial. Recall that the ultimate goal of this thesis is to shed more light on obstacles for embedding inflation in string theory or generally in quantum gravity.

After the essential idea of inflation has been invented, plenty of explicit models were constructed that relied on quite different mechanisms. Consequently also the numerical outcomes differed substantially. Eventually, one might see reason to believe:

“The inflationary paradigm is so flexible that no test or combination of tests can disprove it.” - P. Steinhardt, Strings Conference 2014 -

However, recent developments in string inflation may disagree with this statement. In 2014 BICEP2 [133] claimed¹ to measure data highly in favor of large-field inflation. This particular class of inflation will be introduced below. Large-field inflation is quite sensitive to physics near the Planck scale and hence model building in pure field theory seems to be insufficient. For that reason the construction of large-field inflation models within string theory became very popular.

In this chapter we will briefly summarize how inflation is realized in field theory and string theory. In particular, two models for axion inflation are explained and well connected with moduli stabilization of the previous chapter. Those two models are aligned and axion monodromy inflation, which will both be critically revisited in part 3 of this thesis.

¹The results of BICEP2 had to be corrected and eventually were much less supporting large-field inflation. Nevertheless, their corrected results combined with the Planck collaboration [20] still agree with this class of inflation.

Since large-field inflation calls for an embedding in a UV complete theory, it constitutes an excellent chance to demonstrate the phenomenological power of string theory. To come back to P. Steinhardt's quote, the next chapter will, however, give rise to the hypothesis that large-field inflation might not be possible within string theory. If this turns out to be true, either large-field inflation or string theory as a theory of our universe would be falsified. In any case, inflation is a fascinating topic that needs to be explored and one can look forward to new insights from future experiments.

5.1 Early Universe Cosmology and Inflation

Cosmic inflation was a short time period that lasted roughly from 10^{-36} to 10^{-34} seconds after the initial big bang singularity where the universe expanded extremely rapidly. This 'bang' of the big bang is able to solve several problems in cosmology, such as the horizon problem or the origin of CMB fluctuations, as discussed in the introduction 1. It was first proposed by A. Guth in 1979 [134] and further developed by several research groups in the subsequent years. In this section we shall see how the inflationary expansion of the universe is described in terms of early universe cosmology. For more details and concrete solutions e.g. to the horizon problem the reader may have a look at the extensive literature [18, 24, 135]. Note also that despite the existence of a vast number of inflationary models, there is still no fully-fledged scenario and many open questions remain to be answered.

A surprising observational fact about our universe is its homogeneous and isotropic structure at large scales. This is encoded in the spatially flat *Friedmann-Robertson-Walker metric* (FRW)

$$ds^2 = -dt^2 + \mathbf{a}^2(t) d\vec{x}^2, \quad (5.1.1)$$

where $\mathbf{a}(t)$ denotes a universal *scale factor* and t cosmic time. The scale factor accounts for the distance between comoving points, i.e. points moving simultaneously with the expansion of the universe. Tracing back the expansion ($\mathbf{a}(t) \rightarrow 0$) culminates in a spacetime singularity which we call the big bang singularity. We choose this to happen at cosmic time $t = 0$. The maximal comoving distance a particle may have traversed since the initial singularity is known as *particle horizon* and given by

$$\Delta\tau = \int_0^t \frac{d\tilde{t}}{\mathbf{a}(\tilde{t})} = \int_0^{\mathbf{a}} \frac{d \log \mathbf{a}}{\mathbf{a} H}, \quad (5.1.2)$$

where we defined the well-known *Hubble parameter*

$$H \equiv \frac{\dot{\mathbf{a}}(t)}{\mathbf{a}(t)}. \quad (5.1.3)$$

As usual $\dot{\mathbf{a}} \equiv d\mathbf{a}/dt$. The Hubble parameter describes the expansion rate of the universe and is positive for an increasing universe. According to the Planck mission its current value

is $67.4 \pm 0.5 \frac{\text{km}}{\text{s Mpc}}$ [19]. Since the Hubble parameter has dimension inverse time, one defines the *Hubble time* $t_H = H^{-1} \sim 14.4$ billion years. At the moment the universe is expanding exponentially due to the dominance of the cosmological constant (i.e. the vacuum energy). The Hubble parameter is therefore constant and the universe grows one e-fold each Hubble time

$$H = \frac{\dot{\mathbf{a}}}{\mathbf{a}} = \text{constant} \quad \Rightarrow \quad \mathbf{a}(t) \sim e^{Ht} = e^{\frac{t}{t_H}}. \quad (5.1.4)$$

In order to find the evolution of the scale factor $\mathbf{a}(t)$, one must solve the Einstein equations $R_{\mu\nu} - \frac{1}{2} G_{\mu\nu} \mathcal{R} = 8\pi G_N T_{\mu\nu}$ with metric $G_{\mu\nu}$. Remarkably it is possible to proceed without detailed knowledge about the field contributions to the energy-momentum tensor $T_{\mu\nu}$. The symmetries of the metric force $T_{\mu\nu}$ to be diagonal and due to isotropy its spatial components have to be equal. These properties are most simply realized by a perfect fluid whose energy-momentum tensor reads

$$T_{\nu}^{\mu} = \begin{pmatrix} \rho & 0 & 0 & 0 \\ 0 & -p & 0 & 0 \\ 0 & 0 & -p & 0 \\ 0 & 0 & 0 & -p \end{pmatrix}, \quad (5.1.5)$$

with p and ρ are the pressure and energy density in the fluid rest frame, respectively. Consequently, the Einstein equations simplify to two coupled, non-linear ordinary differential equations² that are known as *Friedmann equations* (neglecting factors of M_{Pl})

$$H^2 = \left(\frac{\dot{\mathbf{a}}}{\mathbf{a}}\right)^2 = \frac{1}{3} \rho, \quad \dot{H} + H^2 = \frac{\ddot{\mathbf{a}}}{\mathbf{a}} = -\frac{1}{6} (\rho + 3p). \quad (5.1.6)$$

Let us also introduce the *equation of state parameter*

$$\omega \equiv \frac{p}{\rho}. \quad (5.1.7)$$

Combining the Friedmann equations one can deduce the continuity equation and subsequently an expression for the energy density (for constant ω)

$$\frac{d\rho}{dt} + 3H(\rho + p) = 0 \quad \Rightarrow \quad \rho \sim \mathbf{a}^{-3(1+\omega)}. \quad (5.1.8)$$

The equation of state parameter ω varies if the universe is dominated by non-relativistic matter ($\omega = 0$), radiation and relativistic matter ($\omega = \frac{1}{3}$) or a cosmological constant ($\omega = -1$). The solutions for $\rho(\mathbf{a})$ and $\mathbf{a}(t)$ are summarized in table 5.1. Due to the Friedmann equations inflation, i.e. accelerated expansion of the universe $\ddot{\mathbf{a}} > 0$, occurs for $p < -\frac{1}{3}\rho$. Notice that the *strong energy condition* states $\rho + 3p \geq 0$ and is therefore violated during inflation. A simple energy source that can drive inflation is a positive potential energy density of a scalar field as we will see in the next section.

²In case spacetime is not flat, the first Friedmann equation has an additional term $-\frac{k}{a^2}$ on the right-hand side of the equation. The curvature parameter k is $+1$ for a de Sitter and -1 for an anti-de Sitter universe.

Dominated by	ω	$\rho(\mathbf{a})$	$\mathbf{a}(t)$
non-relat. matter	0	\mathbf{a}^{-3}	$t^{\frac{2}{3}}$
radiation	$\frac{1}{3}$	\mathbf{a}^{-4}	$t^{\frac{1}{2}}$
cosm. constant	-1	1	e^{Ht}

Table 5.1: Solutions to the Friedmann equations for a flat universe dominated by matter, radiation or cosmological constant.

Let us mention an equivalent definition for inflation which also follows from the Friedmann equations (5.1.6): $-\dot{H} < H^2$. This leads to the well-known *Hubble slow-roll parameters*

$$\epsilon_H \equiv -\frac{\dot{H}}{H^2}, \quad \eta_H \equiv \frac{\dot{\epsilon}_H}{H \epsilon_H} = -\frac{1}{2} \frac{\ddot{H}}{\dot{H} H}. \quad (5.1.9)$$

Hence, inflation is a period of the very early universe with $\epsilon_H < 1$. The condition $|\eta_H| < 1$ does not really matter for inflation to happen, but large values for η_H will make ϵ_H grow as well. Furthermore, the Friedmann equations (5.1.6) may be combined to express ϵ_H in terms of the equation of state parameter (5.1.7)

$$\epsilon_H = \frac{3}{2} (1 + \omega). \quad (5.1.10)$$

5.2 Effective Theory of Large-Field Inflation

In practice, the inflationary period of the universe can be described by a scalar field moving along a suitable potential. Now we sketch the effective field theory of inflation and postpone its string theory embedding to later sections. The most simple and also best investigated model of inflation employs a single scalar field in a slow-roll setup. The scalar driving the expansion of the universe has been named *inflaton* field. Note that our analysis relies mainly on the excellent lecture notes [18], for further details we recommend [24, 135].

Let us start by assuming a single scalar field Θ minimally coupled to Einstein gravity in $D = 4$

$$\mathcal{S}_{\text{Inflaton}} = \int d^4x \sqrt{-G} \left[\frac{1}{2} \mathcal{R} - \frac{1}{2} G^{\mu\nu} \partial_\mu \Theta \partial_\nu \Theta - V(\Theta) \right] = \mathcal{S}_{\text{EH}} + \mathcal{S}_\Theta, \quad (5.2.1)$$

where the potential $V(\Theta)$ is a priori arbitrary. We denoted the pure Einstein-Hilbert term by \mathcal{S}_{EH} and the action of the scalar field with canonically normalized kinetic term by \mathcal{S}_Θ . The energy-momentum tensor for Θ follows from the variation [18]

$$T_{\mu\nu}^{(\Theta)} \equiv -\frac{2}{\sqrt{-G}} \frac{\delta \mathcal{S}_\Theta}{\delta G^{\mu\nu}} = \partial_\mu \Theta \partial_\nu \Theta - G_{\mu\nu} \left(-\frac{1}{2} \partial^\gamma \Theta \partial_\gamma \Theta + V(\Theta) \right). \quad (5.2.2)$$

If we further assume a spatially homogeneous field $\Theta(t, \vec{x}) = \Theta(t)$ and a FRW metric (5.1.1), the energy-momentum tensor above agrees with the perfect fluid expression (5.1.5) together with the identifications

$$\rho_{\Theta} = \frac{1}{2}\dot{\Theta}^2 + V(\Theta) \quad p_{\Theta} = \frac{1}{2}\dot{\Theta}^2 - V(\Theta). \quad (5.2.3)$$

Negative pressure ($\omega < 0$) and accelerated expansion of the universe ($\omega < -1/3$) occurs if the potential energy dominates over the kinetic energy $\frac{1}{2}\dot{\Theta}^2$

$$\omega = \frac{p_{\Theta}}{\rho_{\Theta}} = \frac{\frac{1}{2}\dot{\Theta}^2 - V(\Theta)}{\frac{1}{2}\dot{\Theta}^2 + V(\Theta)}. \quad (5.2.4)$$

Spacetime is then approximately dS with $\mathbf{a}(t) \approx \exp(Ht)$. The requirement $\dot{\Theta}^2 \ll V(\Theta)$ can also be derived from the Hubble slow-roll condition (5.1.9). In order to see this, we compute at first the equation of motion for Θ from the action (5.2.1)

$$\frac{\delta \mathcal{S}_{\Theta}}{\delta \Theta} = \frac{1}{\sqrt{-G}} \partial_{\mu} (\sqrt{-G} \partial^{\mu} \Theta) + \frac{dV(\Theta)}{d\Theta} = 0. \quad (5.2.5)$$

Rewriting in addition the Friedmann equations (5.1.6) in terms of the scalar field $\Theta(t)$, we arrive at the important relations

$$\ddot{\Theta} + 3H\dot{\Theta} + V'(\Theta) = 0 \quad \text{and} \quad 3H^2 = \frac{1}{2}\dot{\Theta}^2 + V(\Theta), \quad (5.2.6)$$

where $V'(\Theta) \equiv dV/d\Theta$. Having performed a time derivative of the equation of motion and combining it with the Friedmann equation, the Hubble slow-roll condition (5.1.9) reads

$$\epsilon_H \equiv -\frac{\dot{H}}{H^2} = \frac{\frac{1}{2}\dot{\Theta}^2}{H^2} < 1. \quad (5.2.7)$$

With again a little help from (5.2.6), the slow-roll conditions confirm the requirements for the equation of state to imply accelerated expansion of the universe

$$\dot{\Theta}^2 \ll V(\Theta) \quad \text{and} \quad |\ddot{\Theta}| \ll |3H\dot{\Theta}|, |V'(\Theta)|. \quad (5.2.8)$$

Inflation therefore occurs as long as the potential energy of the field Θ dominates over the kinetic energy [24], hence the name 'slow-roll'. The small acceleration ensures that the slow-roll phase persists sufficiently long.

Slow-roll inflation can be intuitively understood by considering a specific potential, for instance figure 5.1. As the inflaton Θ moves down its potential towards the minimum, it passes a slow-roll phase indicated by the green lines and inflation occurs, i.e. the universe expands exponentially. The kinetic energy for the inflaton increases during this phase until the slow-roll conditions are violated and consequently inflation terminates. Eventually, the inflaton will oscillate around the minimum and steadily loose energy. This energy is

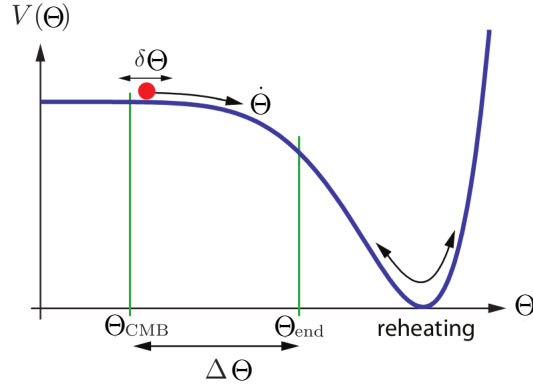


Figure 5.1: Example of an inflaton potential $V(\Theta)$ from [24].

converted into the production of standard model particles as well as radiation. This process is known as *reheating* or *hot big bang*. Quantum fluctuations $\delta\Theta$ at the beginning of inflation are responsible for later fluctuations in the CMB and ultimately for the formation of ‘small’ inhomogeneities in the universe.

Given proper initial values, velocity and acceleration of the inflaton field are also controlled by the shape of the potential $V(\Theta)$. For that purpose, we introduce the *potential slow-roll parameters*

$$\epsilon_V \equiv \frac{1}{2} \left(\frac{V'}{V} \right)^2 \ll 1 \quad \text{and} \quad |\eta_V| \equiv \frac{|V''|}{V} \ll 1, \quad (5.2.9)$$

and require them to be smaller than one for slow-roll. The potential slow-roll parameters are of particular interest since mostly the potential distinguishes between different models of inflation. According to [18] they are related³ to the Hubble slow-roll parameters via

$$\epsilon_V \approx \epsilon_H \quad \text{and} \quad \eta_V \approx \eta_H + \epsilon_H. \quad (5.2.10)$$

The potential slow-roll parameters can be connected to quantities measurable in the CMB spectrum as follows. Curvature perturbations in the CMB are encoded in a scalar and tensor power spectrum. These lead to the spectral index n_s quantifying the scale dependence of the fluctuations, as well as the tensor-to-scalar ratio r which loosely speaking indicates the amount of gravitational waves due to the inflationary expansion. The spectral index n_s and the tensor-to-scalar ratio r obey the following experimental bounds due to the combined results of PLANCK 2015 and BICEP2/Keck Array [20]

$$\begin{aligned} n_s &= 1 + 2\eta_V - 6\epsilon_V = 0.9667 \pm 0.004, \\ r &= 16\epsilon_V < 0.07. \end{aligned} \quad (5.2.11)$$

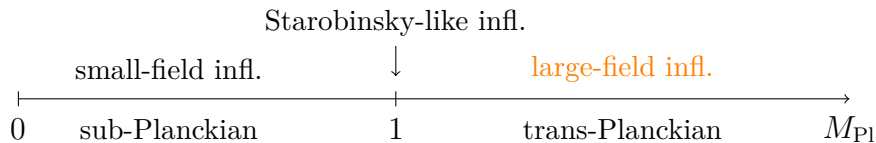
³The relation between Hubble and potential slow-roll parameters holds only in the slow-roll regime.

Let us emphasize again that inflation ends as soon as the slow-roll conditions are violated $\epsilon_H(\Theta_{\text{end}}) = 1$ or $\epsilon_V(\Theta_{\text{end}}) = 1$. For completeness we also express the number N_e of e-folds, which ought to be at least $N_e = 60$ such that inflation lasts long enough to explain the horizon and flatness problems:

$$N_e(\Theta) \equiv \log \frac{\mathbf{a}(t_{\text{end of inflation}})}{\mathbf{a}(t_{\text{begin of inflation}})} = \int_{t_0}^{t_{\text{end}}} dt' H = \int_{\Theta_0}^{\Theta_{\text{end}}} d\Theta \frac{H}{\dot{\Theta}} \approx \int_{\Theta_{\text{end}}}^{\Theta_0} d\Theta \frac{V}{V'}. \quad (5.2.12)$$

The Lyth bound and large-field inflation

It is very useful to distinguish two classes of inflation: *small-field* and *large-field* inflation. This splitting is also reasonable in view of their UV sensitivity as discussed in section 5.3. The difference is the distance $\Delta\Theta = \Theta_{\text{CMB}} - \Theta_{\text{end}}$ that the inflaton Θ traverses during inflation. We call field displacements $\Delta\Theta < 1 M_{\text{Pl}}$ or $\Delta\Theta > 1 M_{\text{Pl}}$ *sub-* or *trans-Planckian*. To summarize, we have



Starobinsky-like (introduced below) inflation can be still counted as model for large-field inflation. However, let us stress that it is on the boundary to small-field scenarios. In the next subsection, there will be more information about this type of models.

This thesis focuses exclusively on large-field inflation (as in string phenomenology in general). One reason for that one-sided investigation will become clear again in the section 5.3 about UV sensitivity. Another reason to motivate our studies arises from experimental input as has been mentioned already above. Recall that the experiments [19, 20] claimed to observe a large tensor-to-scalar ratio r . As we will show now, this is highly in favor of large-field inflation due to the *Lyth bound* [21].

In order to derive this bound, we use the Hubble slow-roll parameter ϵ_H in terms of the inflaton (5.2.7) and combine it with the tensor-to-scalar ratio $r = 16\epsilon_V$ of (5.2.11)

$$r = \frac{8}{M_{\text{Pl}}^2} \left(\frac{d\Theta}{dN_e} \right)^2, \quad (5.2.13)$$

with the number of e-folds $dN_e = H dt$ given in (5.2.12). We are interested in field displacements $\Delta\Theta$ between the time N_e^{CMB} , where observable CMB fluctuations have exited the horizon, until the end of inflation N_e^{end} . Assuming $r(N_e)$ stay approximately constant⁴

⁴Allowing for r to vary with N_e makes the Lyth bound more precise, but only changes it slightly [24].

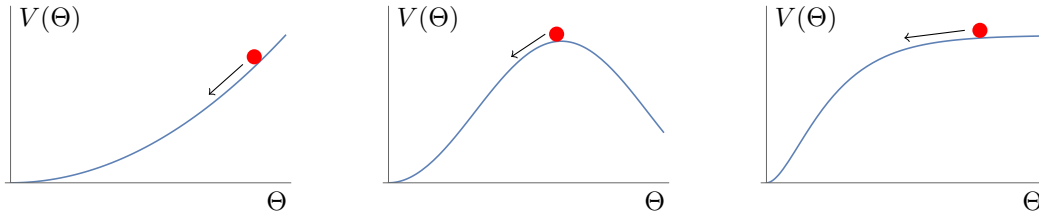


Figure 5.2: Potentials for large-field inflation. The figure on the left displays a polynomial potential corresponding to *chaotic inflation*, the middle one shows a potential for *natural inflation* depending on the periodicity $2\pi f$ and the right plot *Starobinsky inflation*.

during inflation, we find

$$\frac{\Delta\Theta}{M_{\text{Pl}}} \sim \Delta N_e \sqrt{\frac{r}{8}}, \quad (5.2.14)$$

with $\Delta N_e = N_e^{\text{end}} - N_e^{\text{CMB}}$. The r value here is the one measured in the CMB. For $\Delta N_e \approx 60$ we arrive at the famous lower bound

$$\frac{\Delta\Theta}{M_{\text{Pl}}} \geq \mathcal{O}(1) \sqrt{\frac{r}{0.01}}. \quad (5.2.15)$$

Therefore, the experimental value $r < 0.07$ [20] leads to trans-Planckian field ranges $\Delta\Theta$, i.e. large-field inflation.

5.2.1 Different Types of Inflation

There are different kinds of inflationary models that can be classified by the shape of their potential V . In principle, we have to distinguish three categories of slow-roll potentials: *periodic*, *polynomial* and *Starobinsky-like*. The corresponding potentials look typically as plotted⁵ in figure 5.2. Since later parts of this thesis are going to involve models of each of these types, we shall here and in the following sections outline their general features.

In table 5.2 we summarized the typical forms of the potential and the observational parameters n_s as well as r for these three types of inflationary models. Apparently, the potentials V reflect the plots in figure 5.2. In addition table 5.2 states the mechanism that produces each type of inflationary potential in string theory. The next sections 5.4 and 5.5 are devoted to shed more light on this connection.

Let us point out that the cosine potential of periodic inflation in table 5.2 does not yet exhibit the alignment feature, but would rather belong to natural inflation (to be defined in section 5.4). Note that n_s and r of periodic potentials hold only in the limit of large-field

⁵Note that the potential in figure 5.1 is rather an example for small-field inflation and often called *hilltop* inflation. Nevertheless, it is quite illuminating for understanding inflation realized by a scalar field.

Type	Periodic	Polynomial	Starobinsky-like
Stringy Realization	alignment	axion-monodromy	axion-monod. + backreaction
Potential	$V_0 \left[1 - \cos\left(\frac{\Theta}{f}\right)\right]$	$V_0 \Theta^p$	$V_0 \left(1 - e^{-\gamma\Theta}\right)$
n_s	$1 - \frac{2}{N_e}$	$1 - \frac{p+2}{2N_e}$	$1 - \frac{2}{N_e}$
r	$\frac{8}{N_e}$	$\frac{4p}{N_e}$	$\frac{8}{(\gamma N_e)^2}$

Table 5.2: Different types of large-field inflation with their characteristics [24] and realization in string theory as described in the subsequent sections. The parameters V_0 , f , p , γ are model-dependent constants and N_e is the number of e-folds (5.2.12).

inflation. In section 5.4 we will explain that this limit corresponds to $f \gg M_{\text{Pl}}$. Obviously, n_s and r are then equivalent to the formulas for polynomial inflation with $p = 2$, i.e. a quadratic potential which approximates the cosine for large f .

As will be shown later on, the stringy constructions of polynomial and Starobinsky-like inflation differ only by the intensity of backreaction effects. Thus, there is a novel interpolation between these two classes. Since the class of Starobinsky-like models shall not be discussed extensively in an own section, we will briefly demonstrate the original idea here. In the 1980s A. Starobinsky [136] analyzed one-loop corrections to the Einstein-Hilbert action and included an \mathcal{R}^2 -term

$$\mathcal{S}_{\text{Starobinsky}} = \frac{1}{2} \int d^4x \sqrt{-G} \left[\mathcal{R} + \frac{\alpha}{2} \mathcal{R}^2 \right], \quad (5.2.16)$$

with $\alpha = 2.2 \times 10^8$ being a normalization constant. Performing a conformal transformation and defining the inflaton $\Theta := \sqrt{\frac{2}{3}} \log(1 + \alpha\mathcal{R})$, we obtain an action similar to (5.2.1) of a scalar field Θ minimally coupled to gravity and a potential of the form (cf. [24])

$$V(\Theta) = \frac{1}{4\pi} \left[1 - \exp\left(-\sqrt{\frac{2}{3}}\Theta\right) \right]^2. \quad (5.2.17)$$

The potential listed in table 5.2 is very reminiscent of this expression, although more general. That is why we speak of *Starobinsky-like* models. The potential slow-roll parameters (5.2.9) for (5.2.17) are given by [24]:

$$\eta = -\frac{4}{3} \exp\left(-\sqrt{\frac{2}{3}}\Theta\right) \quad \text{and} \quad \epsilon = \frac{3}{4} \eta^2. \quad (5.2.18)$$

5.3 UV Sensitivity and Axions

In this section we emphasize that inflation as a four-dimensional effective theory is eminently sensitive to physics at high energies approaching the Planck scale. In other words,

it strongly depends on the ultraviolet (UV) completion of its underlying quantum field theory and gravity. In particular large-field inflation might be affected by corrections from such UV physics. Therefore it seems natural to embed inflation into an UV complete theory and so far string theory represents the only known consistent candidate satisfying this ambitious constraint. Recapitulating the motivation for realizing large-field inflation within string theory, we find a two-folded answer:

- there is experimental motivation from observations and the Lyth bound.
- large-field string inflation is conceptually interesting since at the moment there is no framework better suited for incorporating UV corrections.

In fact, the list of obstacles to UV complete inflationary models is quite extensive, see for instance [24] where the authors are especially stressing backreaction issues. In addition one might consult [18, 137] as we are going to present only a brief overview. The obstacles are either general for any inflationary model or particularly for large-field scenarios.

One non-trivial constraint for trans-Planckian inflaton excursions in UV complete theories with extra dimensions arises from compactification. Due to compact directions not every field space has trans-Planckian diameter. This is a purely geometrical, hence a kinematic constraint on models of inflation [24].

Another issue of building an effective theory for inflation is known as the *eta problem*. Note that it applies not only to large-field inflation, but any slow-roll model. To cut a long story short, heavy physics above the cutoff scale of the inflationary theory might alter the slow-roll parameter η drastically, such that inflation will not last long enough (e.g. $N_e = 60$ e-folds). Let us be more precise, there exist two different eta problems:

- **radiative instability of the inflaton mass** In the absence of protecting symmetries, the mass of a scalar field is allowed to run up to the cutoff Λ of an effective theory. For inflation this cutoff is at least the Hubble scale $\Lambda \geq H$ and hence the inflaton mass receives quantum correction of order $M_\Theta^2 \sim \Lambda^2 \sim H^2$. Using $M_\Theta^2 = V''$ and $3H^3 \approx V/M_{\text{Pl}}^2$, the eta parameter (5.2.9) gets corrected by

$$\Delta\eta_V \approx \frac{\Delta M_\Theta^2}{3H^2} \gtrsim 1. \quad (5.3.1)$$

This contradicts the slow-roll requirement $\eta_V \ll 1$.

- **higher-dimensional operators** Moreover, integrating out modes above the cutoff gives rise to higher-dimensional operators of the form $\mathcal{O}_\delta/\Lambda^{\delta-4}$, where δ denotes the mass dimension of the operator. Assume a dimension $\delta = 6$ operator, that is even Planck-suppressed $\Lambda \rightarrow M_{\text{Pl}}$. So, as long as not protected by some symmetry, the inflaton Lagrangian might contain the contribution

$$\frac{\mathcal{O}_6}{M_{\text{Pl}}^2} = \frac{\mathcal{O}_4}{M_{\text{Pl}}^2} \Theta^2. \quad (5.3.2)$$

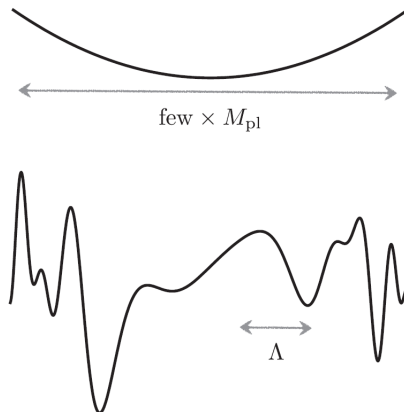


Figure 5.3: Corrections to the inflaton potential cause structures on sub-Planckian scales $\Lambda < M_{\text{Pl}}$ and violate the slow-roll conditions for large-field inflation [24].

If the operator \mathcal{O}_4 has a vev of order the inflationary energy $\langle \mathcal{O}_4 \rangle \sim V$, the definition (5.2.9) of the η parameter leads again to trouble with the slow-roll condition. This problem exists even for small-field inflation $\Theta < M_{\text{Pl}}$, although the corrections to the inflaton potential are small $\Delta V \ll V(\Theta)$.

In the case of large-field inflation the impact of higher-dimensional operators is more dramatic. Again making the optimistic assumption of a Planck-scale cutoff $\Lambda = M_{\text{Pl}}$, integrating out heavy fields can affect the inflaton Lagrangian via non-renormalizable operators

$$\mathcal{L}_{\text{eff}} = \mathcal{L}_{\text{renorm}} + \sum_i c_i \Theta^4 \left(\frac{\Theta}{M_{\text{Pl}}} \right)^i + \dots, \quad (5.3.3)$$

where $\mathcal{L}_{\text{renorm}}$ contains the kinetic term of the inflaton plus renormalizable interactions. The coefficients c_i and \tilde{c}_i are dimensionless. Obviously, these corrections become very important for large-field inflation with trans-Planckian field excursions $\Delta\Theta > 1 M_{\text{Pl}}$.

This is easy to understand intuitively since the higher order terms constitute deformations of the inflaton potential. To be more precise, these corrections deform the potential on *sub-Planckian* scales as indicated in figure 5.3. However, the slow-roll conditions of large-field inflation require a smooth potential over trans-Planckian distances.

The issue of ensuring a trans-Planckian nearly flat inflaton potential is a dynamical one [24], meaning that one also has to take the implication of the inflaton movement onto other fields in the game into account. This effect is called *backreaction* and will be a major task to address when combining inflation with moduli stabilization.

The way to cure the obstacles above is to invoke a global *shift symmetry*

$$\Theta \longrightarrow \Theta + \text{const}. \quad (5.3.4)$$

Thereby, an inflaton mass term and higher-dimensional operators are simply forbidden. Fields equipped with such a shift symmetry are *axions* that arise ubiquitously in string theory as we explain in the next subsection.

5.3.1 Axions in String Theory

A clearly beneficial feature of string theory is the natural generation of axion fields. Axion physics has become more and more popular among particle physics and cosmology. Just to mention the most famous application (i.e. what it originally was invented for): a solution to the strong CP problem [138, 139]. The axion must couple to QCD gauge bosons and have a decay constant in the right window. Here, we are not interested in the QCD axion and instead focus on employing an axion as inflaton field. Due to the definition of axions, they protect inflationary scenarios from the UV corrections explained above:

Definition: *An axion a is a pseudoscalar⁶ equipped with a Peccei-Quinn symmetry $a \rightarrow a + \text{const}$ that is only broken by instanton effects⁷.*

The axion comes together with a characteristic constant known as *axion decay constant* f_a . Its Lagrangian must include a kinetic term as well as a coupling to instantons

$$\mathcal{L}_{\text{axion}} = -\frac{f_a^2}{2} \partial_\mu a \partial^\mu a + \frac{c a}{32\pi^2} \epsilon^{\mu\nu\alpha\beta} \text{tr} F_{\mu\nu} F_{\alpha\beta}, \quad (5.3.5)$$

with some constant c and gauge field $F_{\mu\nu}$. The axion field may be redefined by $\Theta \equiv f_a a$ in order to obtain a canonically normalized kinetic term.

In string theory axions arise from integrating p -form gauge potentials over p -cycles of the compact space. Apart from the NS-NS 2-form B_2 , we get axions from dimensional reduction of the R-R forms C_1, C_3, C_5 in type IIA or C_0, C_2, C_4, C_6 in type IIB. Axions from the geometric moduli (e.g. complex structure) will be discussed below. For instance, integration of B_2 over a 2-cycle Σ_2 defines the axion b

$$b = \int_{\Sigma_2} B_2. \quad (5.3.6)$$

The defining shift symmetry of the axions is inherited from the gauge invariance of the p -forms. Consider for simplicity the case of vanishing fluxes (recall $F_p = \langle F_p \rangle + dC_{p-1}$ with flux $\langle F_p \rangle$), then the supergravity action of type IIB string theory (4.1.3) is invariant under

⁶A pseudoscalar behaves like a normal scalar except that it changes sign under parity inversion.

⁷This does not directly apply to all moduli. For instance, the continuous shift symmetry of complex structure moduli will be broken to a discrete symmetry by higher order terms in the Kähler potential. On the mirror dual side these effects correspond again to instantons.

large gauge transformations of the p -form gauge potentials. These are defined by mappings of the form

$$C_p \longrightarrow C_p + 2\pi \omega_p, \quad \omega_p \in H^p(\mathcal{M}, \mathbb{R}). \quad (5.3.7)$$

Performing a large gauge transformation for an axion c_p given by integrating a C_p gauge potential over a p -cycle Σ_p

$$c_p \equiv \int_{\Sigma_p} C_p \longrightarrow \int_{\Sigma_p} C_p + 2\pi \int_{\Sigma_p} \omega_p = c_p + \text{const}. \quad (5.3.8)$$

Since ω_p is closed but not exact, the second integral does not vanish and manifests the axion shift symmetry instead. So far, we are working at the classical level with the tree-level action (4.1.3) and the axion shift symmetry is continuous. The axion shift symmetry turns out to be perturbatively exact, i.e. holds to all orders in α' and g_s [140, 141].

In the quantum theory the continuous symmetry is broken to a *discrete shift symmetry* due to non-perturbative instanton⁸ effects. Let us stress that the breaking of the axionic shift symmetry can only be spontaneous because it relies on the gauge symmetry of the p -forms, which may never be broken explicitly. To proceed with the large gauge transformation of the C_p forms, remember from (4.1.5) that a $D(p-1)$ -brane wrapping a p -cycle Σ_p contributes to the action via a term $\int_{\Sigma_p} C_p$. Hence, the path integral for quantization is only invariant under large gauge transformations (5.3.7) if they are quantized, i.e. $\omega_p \in H^p(\mathcal{M}, \mathbb{Z})$. Alternatively, focus on a *worldsheet instanton* describing a string worldsheet wrapping a compact 2-cycle Σ_2 . The action of such a process is proportional to

$$e^{-S_{\text{inst}}} \sim \exp\left(-\int_{\Sigma_2} (J + iB_2)\right) = \exp\left(-ib - \int_{\Sigma_2} J\right), \quad (5.3.10)$$

with the axion defined in (5.3.6) and Kähler (1, 1)-form J . To conclude, axions are equipped with a discrete shift symmetry

$$a \longrightarrow a + 2\pi. \quad (5.3.11)$$

⁸Recap: Instantons are classical solutions to the euclidean equations of motion. In a $D = 4$ gauge theory the instanton amplitude is schematically $\mathcal{S}_{\text{inst}} \sim \frac{8\pi^2}{g^2} + i\theta$ with the gauge coupling g and θ angle according to (5.3.5) (there we used a). The instanton couples to the axion θ equipped with decay constant f and the axion potential receives an instanton expansion

$$V_{\text{inst}} = \sum_n c_n e^{-n \text{Re}(\mathcal{S}_{\text{inst}})} \cos\left(\frac{n\theta}{f}\right), \quad (5.3.9)$$

with coefficients c_n . The contribution V_{inst} is suppressed for large instanton actions $\text{Re}(\mathcal{S}_{\text{inst}})$. Back in string theory, let us consider worldsheet instantons as well as D(-1)-brane instantons governed by the action $\mathcal{S}_{\text{inst}} \sim T$ and $\mathcal{S}_{\text{inst}} \sim S$ (T, S are Kähler and complex structure moduli), respectively. They contribute to the superpotential via a term e^{-T} or e^{-S} , which then leads to the instanton expansion (5.3.9) in the scalar potential.

Often people refer to the string theory axions as only *axion-like* fields. In this thesis, however, we will drop this specification. Clearly, all moduli coming from the $D = 10$ dimensional fields (except metric) are equipped with an axionic shift symmetry due to gauge invariance of the higher dimensional fields. This applies also to the imaginary part of a Kähler modulus which arises from the C_4 form. But what about complex structure moduli? First, one might argue that they must have axionic parts as well due to mirror symmetry. Second, on a torus the complex structure does not change when moving around one of the circles. For non-toroidal compactifications this is admittedly not so clear. Often the axionic shift symmetry of complex structure moduli is also motivated by appropriate symmetries of the Kähler potential. In the end we assume all moduli of table 2.3 contain an axion field in any compactification. For convention, the moduli scalars were combined in such a way that we have the identification

$$\text{modulus} = \text{saxion} + i \cdot \text{axion}. \quad (5.3.12)$$

To avoid confusion, note that the term *saxion* corresponds to non-periodic scalars (bosons!), but has nothing to do with fermionic supersymmetry partners of the axions.

Sub-Planckian axion decay constants

In the models discussed later, the axion decay constant f_a can be computed via the Kähler potential. Nevertheless, it is illuminating to derive f_a directly from reducing the p -forms. The low-energy action of an R-R p -form C_p (now adding a field strength F) is given by

$$-\frac{2\pi}{l_s^{8-2p}} \int \frac{1}{2} F_{p+1} \wedge \star F_{p+1} + 2\pi \int C_p. \quad (5.3.13)$$

Recall from (4.1.5) that the second term describes the coupling of the p -form to a $D(p-1)$ -brane wrapping a p -cycle. According to [115], dimensional reduction of this action gives the axion kinetic term

$$\mathcal{L}_{\text{kin}} = -\frac{1}{2} \sum_{\alpha, \beta} \gamma_{\alpha\beta} \partial_\mu a_\alpha \partial^\mu a_\beta \quad \text{with} \quad \gamma_{\alpha\beta} = \frac{1}{2\pi l_s^{8-2p}} \int_{\mathcal{M}} \omega_\alpha \wedge \star \omega_\beta. \quad (5.3.14)$$

where the ω_α correspond to elements of the cohomology basis in which we expand⁹ $C_p = \frac{1}{2\pi} \sum_\alpha a_\alpha \omega_\alpha$. Approximating the overall volume of the six-dimensional compact manifold by $\mathcal{V} \sim R^6$, formulas (4.1.26), (4.1.32) relate the Planck mass as follows

$$M_{\text{Pl}}^2 = \frac{4\pi R^6}{g_s^2 l_s^8}. \quad (5.3.15)$$

By assuming also $\int_{\mathcal{M}} \omega_\alpha \wedge \star \omega_\beta \sim \mathcal{O}(1) R^{6-2p}$ for a generic axion, E. Witten et al. [115] concluded from the kinetic term (5.3.13)

$$f_a = \sqrt{\frac{\mathcal{O}(1) R^{6-2p}}{2\pi l_s^{8-2p}}} = M_{\text{Pl}} \left(\frac{l_s}{R} \right)^p \sqrt{\frac{\mathcal{O}(1) g_s^2}{8\pi^2}}. \quad (5.3.16)$$

⁹The conventional factor 2π follows [115], but disagrees with our previous definition (5.3.6).

As a consequence, trans-Planckian axion decay constants $f_a > M_{\text{Pl}}$ would correspond to either $g_s \gg 1$ or $l_s \gg R$. This is, however, impossible in controlled perturbative string compactifications and thus decay constant of stringy axions are generically expected to be sub-Planckian. As shown by [29, 115] sub-Planckian axion decay constants occur in all computable limits of string compactification [24].

Axion inflation and interplay with moduli stabilization

Let us briefly outline the strategy for constructing models of string inflation in the following two sections. Our goal is to realize large-field inflation within string theory. Since large-field inflation is highly sensitive to UV corrections, it is wise to employ an axion as inflation because its potential will be protected by the axionic shift symmetry. Besides, axions arise numerously in string compactifications. Hence, it is natural to study the interplay of axion inflation and moduli stabilization. We will restrict our investigation to *single-field* inflation, i.e. there should be solely one axionic degree of freedom causing the inflationary expansion of the universe. In this sense, the strategy will be two steps:

1. stabilize all moduli except one axion
2. use this axionic modulus as inflaton and generate an effective potential suitable for large-field inflation

Overall, there is now a whole list of effective theories which have to be clearly separated by their energy scales. It has already been highlighted that the usage of an effective $\mathcal{N} = 1$ supergravity theory for moduli stabilization is only justified as long as we guarantee the mass hierarchy (4.1.19). In order to include an effective theory for inflation, we require the inflaton mass M_Θ to be sufficiently lighter than the mass M_{mod} of the lightest modulus (that is not the inflaton itself, of course). Note also that every field with mass below the Hubble scale H is dynamically active during inflation. Single field inflation requires thus that solely one field has mass $M_\Theta < H$.

Putting everything together, a consistent model for single large-field axion inflation in string theory must satisfy the mass hierarchy

$$M_\Theta < H < M_{\text{mod}} < M_{\text{KK}} < M_s < M_{\text{Pl}}. \quad (5.3.17)$$

These scales are constrained by the amplitude of scalar density perturbations and the value of the tensor-to-scalar ratio. It turns out that the Hubble parameter (in natural units) can be expressed in terms of the tensor-to-scalar ratio r [24]

$$H = 3 \times 10^{-5} \left(\frac{r}{0.1} \right)^{\frac{1}{2}} M_{\text{Pl}}. \quad (5.3.18)$$

For $r < 0.07$ and using the Planck mass $M_{\text{Pl}} = 2.435 \times 10^{18}$ GeV we obtain $H_{\text{inf}} \sim 10^{13}$ GeV. Hence there is not much room left to stabilize the rest of the moduli (M_{mod}) above

the inflaton mass and below the Kaluza-Klein scale (which is also usually of order $M_{\text{KK}} \sim 10^{16} - 10^{17}$ GeV in perturbative string theory). Actually, one would additionally need to include the inflationary energy scale $V_{\text{inf}}^{1/4}$ itself. If this energy is too large it might cause dangerous instabilities.

The energy scale of inflation is defined by

$$V_{\text{inf}}^{1/4} \equiv (3 H^2 M_{\text{Pl}}^2)^{1/4} = 8 \times 10^{-3} \left(\frac{r}{0.1} \right)^{1/4} M_{\text{Pl}}. \quad (5.3.19)$$

and hence $V_{\text{inf}}^{1/4} \sim 10^{16}$ GeV for $r < 0.07$. In this thesis we shall, however, not worry about the energy scale of inflation.

Satisfying the mass hierarchy (5.3.17) is unavoidable to ensure control over all effective theories. This is clearly an extremely difficult challenge for any model of string inflation.

5.4 Periodic Inflation: Alignment

The discrete shift symmetry of axions is on the one hand very convenient as it renders large-field inflation stable against UV corrections, but on the other hand it highly restricts possible inflaton potentials. Apparently, the symmetry $a \rightarrow a + 1$ (for convenience the factor 2π was absorbed into a redefinition of a) implies that axions are periodic fields and hence, their potential should be of the periodic form

$$V(\Theta) = V_0 \left[1 - \cos \left(\frac{\Theta}{f} \right) \right] + \dots, \quad (5.4.1)$$

in agreement with table 5.2. The dots “...” indicate higher harmonics meaning that in principle any periodic function is possible. Here, we have already canonically normalized the axion $\Theta \equiv f a$ with the axion decay constant f . An inflationary model based on the simple cosine potential is known as *natural inflation* [142, 143].

However, large-field inflation with such a simple potential cannot be embedded in controlled string compactifications. The problem is that trans-Planckian field excursions $\Delta\Theta > 1 M_{\text{Pl}}$ require a trans-Planckian axion decay constant $f > 1 M_{\text{Pl}}$. This can be intuitively understood from the argument of the cosine and guaranteeing a relatively flat potential over trans-Planckian distances. Alternatively, the trans-Planckian decay constant follows from the slow-roll conditions¹⁰ (5.2.9) and the spectral index n_s of primordial perturbations (5.2.11). Since inflation occurs close to the maximum of the potential (5.4.1) $V_{\text{max}} = 2V_0$, that is $\Theta \sim \pi f$, we approximate [30, 144]

$$n_s = 1 - 6\epsilon + 2\eta \simeq 1 - \frac{M_{\text{Pl}}^2}{f^2}. \quad (5.4.2)$$

¹⁰Note that we have reintroduced a factor of M_{Pl}^2 in the slow-roll conditions.

The experimental value $n_s \simeq 1$ requires thus a trans-Planckian axion decay constant f .

However, as shown in section 5.3.1, well-controlled string compactifications can only lead to sub-Planckian axion decay constants [29, 115]. Therefore, for realizing large-field inflation in string theory the potential (5.4.1) is not the way to go and one has to come up with clever alternatives instead.

One sophisticated mechanism to avoid this issue has been proposed by J. Kim, H.-P. Nilles and M. Peloso (KNP) [30] and called *aligned inflation*. The basic idea boils down to using two axions each equipped with a sub-Planckian decay constant and aligning them, such that one achieves an effective axionic inflaton with trans-Planckian decay constant.

To illustrate the principles of alignment, consider two axions θ_1 and θ_2 with decay constants f_1 and f_2 , respectively. Having introduced also some constant parameters $V_a, V_b, c_{1a}, \dots, c_{2b}$, it is possible to obtain a scalar potential for the axions of the form

$$V(\theta_1, \theta_2) = V_a \left[1 - \cos \left(c_{1a} \frac{\theta_1}{f_1} + c_{2a} \frac{\theta_2}{f_2} \right) \right] + V_b \left[1 - \cos \left(c_{1b} \frac{\theta_1}{f_1} + c_{2b} \frac{\theta_2}{f_2} \right) \right]. \quad (5.4.3)$$

We refer to the literature how to produce this potential in string theory, e.g. [30, 145]. The key observation of KNP was that the same linear combination, defined as ψ , of the axions appears in the argument of the cosines if

$$\frac{c_{1a}}{c_{2a}} = \frac{c_{1b}}{c_{2b}}. \quad (5.4.4)$$

The orthogonal combination, called ξ , remains a flat direction of the potential. In other words ξ has effectively infinite field range. If the alignment (5.4.4) holds only approximately, we still have an enhancement of this field range and the associated effective decay constant. Thus, ξ is a good candidate for large-field inflation.

In order to give a practical example, assume $V_a \gg V_b$ and for simplicity $c_{1a} = c_{1b} = 1$. With appropriate alignment, the axionic combination ψ will become heavy and may safely be integrated out. For the light combination ξ we get the standard potential [24]

$$V(\xi) = V_b \left[1 - \cos \left(\frac{\xi}{f_\xi} \right) \right] \quad \text{with} \quad \xi = \frac{\theta_2 f_2 - c_{2a} \theta_1 f_1}{c_{2a}^2 f_1^2 + f_2^2}. \quad (5.4.5)$$

Moreover, the effective axion decay constant is given by

$$f_\xi = \frac{\sqrt{c_{2a}^2 f_1^2 + f_2^2}}{|c_{2b} - c_{2a}|}. \quad (5.4.6)$$

Due to alignment f_ξ can be trans-Planckian, although the original decay constants f_1, f_2 were sub-Planckian.

5.5 Polynomial Inflation: Axion Monodromy

As outlined in the introduction, a promising alternative to aligned inflation and periodic potentials in general is *axion monodromy inflation*. In this section its underlying concepts will be summarized as we are going to use it extensively to develop some of the main results of this thesis in chapter 8.

In short, the basic idea is to induce a non-periodic (polynomial) potential for the axion while leaving the discrete shift symmetry unbroken. This leads to the multi-branched structure which allows for a non-compact field range for the axion. A potential with multi-branched structure is plotted in figure 5.4. By rolling down one of the branches a trans-Planckian excursion can be achieved even if the axionic decay constant f (and therefore the underlying periodicity of the system) is sub-Planckian. The discrete shift of the axion if combined with a shift of the integer labeling the different branches, is still a symmetry of the theory. This protects the effective theory from dangerous UV corrections coming from states above the cut-off scale.

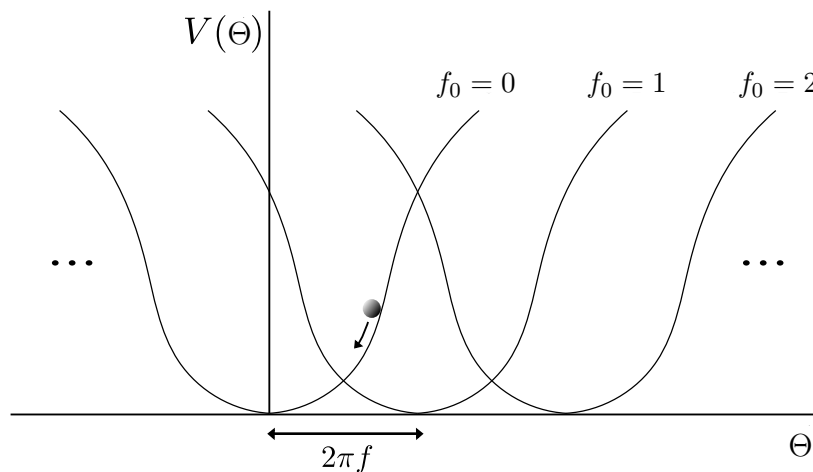


Figure 5.4: Multi-Branched potential for axion monodromy inflation [from I. Valenzuela]. The branches are labeled by n , whereas f denotes the axion decay constant.

Axion monodromy goes back to the pioneering work of E. Silverstein and A. Westphal [27] and was further investigated in the follow-up publication [146]. The starting point were 5-branes wrapping cycles of the compact space (often in a warped geometry). One then derives a $D = 4$ effective potential for the axion from the DBI action. To realize these models together with moduli stabilization and compactification in a consistent manner is quite sophisticated. Details and explanations can be found in the book [24]. Alternatively, F-term scalar potentials generated by background fluxes are able to induce axion monodromy inflation as well [28]. F-term axion monodromy inflation may be understood from the purely four-dimensional point of view by coupling an axion to a 3-form gauge potential, as will be outlined in the following.

The realization in four-dimensional Minkowski space $M = \mathbb{R}^{1,3}$ is given by coupling the axion Θ (again canonically normalized $\Theta = f a$ with decay constant f) to a 3-form gauge field $F_4 = dC_3$ as follows,

$$\mathcal{S}_{\text{KS}} = \int_M -\frac{1}{2} |d\Theta|^2 - \frac{1}{2} F_4 \wedge \star F_4 + m F_4 \Theta + \int_{\partial M} C_3 \wedge (\star F_4 - m\Theta). \quad (5.5.1)$$

This description was first analyzed in detail by G. Dvali [25, 147] and applied to inflation by N. Kaloper and L. Sorbo [26, 148–150].

The second term in the Kaloper-Sorbo action \mathcal{S}_{KS} is a boundary term that does not contribute to the equation of motion, but will have an important impact on the potential. Moreover, the boundary term is necessary to ensure the discrete shift symmetry of the axion $\Theta \rightarrow \Theta + 2\pi f$.

Variation of the integral (5.5.1) with respect to C_3 leads immediately to the equation of motion¹¹

$$\delta \mathcal{S}_{\text{KS}} = \int_M \delta C_3 \wedge d(\star F_4 - m\Theta) = 0 \quad \implies \quad \star F_4 - m\Theta = f_0. \quad (5.5.2)$$

In a pure classical framework the constant f_0 is allowed to take on completely arbitrary values, but in a quantum theory it has to be quantized. There the 3-form C_3 couples to membranes, which may wrap cycles in the compact manifold. Hence, C_3 is promoted to be invariant under large gauge transformations. Since the parameter f_0 symbolizes the value of the field strength $F_4 = dC_3$ in the vacuum, it follows from the large gauge transformations that f_0 must be quantized.

To compute¹² the potential for Θ we only need to plug the constraint (5.5.2) back into action (5.5.1)

$$V = \frac{1}{2} (f_0 + m\Theta)^2. \quad (5.5.3)$$

Since f_0 is quantized, one recovers a scalar potential for the axion with multiple branches. These branches are labeled by f_0 as illustrated in figure 5.4.

Notice that this is not a particular model of F-term axion monodromy, but a dual formulation in four dimensions, since for any massive axion one can always define an effective 3-form field generating the corresponding scalar potential. The 3-form formulation makes the underlying symmetries of the system manifest. In particular, the combined discrete shift

$$f_0 \rightarrow f_0 + c, \quad \Theta \rightarrow \Theta - \frac{c}{m} \quad (5.5.4)$$

¹¹Actually it leads to a constraint which states have to obey in order to be physical.

¹²We remind the reader that we are working in $D = 4$ Minkowski space and thus $\star 1 = dx^4$ and $\star \star F_4 = -F_4$.

is a symmetry of the system. For $c/m = 2\pi f$ the transformation (5.5.4) identifies gauge equivalent branches because the axionic shift symmetry arises from the gauge invariance of the $D = 10$ p -forms (see section 5.3.1). A gauge symmetry cannot be broken as it is simply a mathematical redundancy in the description. So let us stress that the discrete shift symmetry of the axion is still preserved by the system and only spontaneously broken upon choosing a vacuum [57]. Selecting a particular vacuum corresponds to selecting a branch of the potential in figure 5.4.

The axionic shift symmetry and the gauge invariance of the 3-form restrict corrections to the potential enormously. According to [57, 151] corrections to the potential have to be powers n of the gauge invariant combinations (5.5.3)

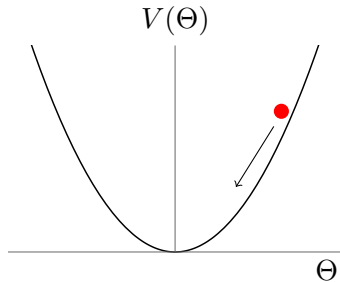
$$\delta V \sim \left(\frac{V}{M_{\text{Pl}}^4} \right)^n. \quad (5.5.5)$$

Consequently, all corrections are under control (even for trans-Planckian $\Delta\Theta$) given that the potential energy is sub-Planckian.

As a comment, let us mention that quantum mechanically there exist in fact transitions between different branches. That is by tunneling effects [152–155] which are mediated by nucleation of membranes electrically charged under the 3-form gauge field. By crossing a membrane, f_0 shifts by an integer times the charge of the membrane. The tunneling rate is exponentially suppressed and inflation will proceed along a single branch. For recent results showing that the tunneling rate is not fast enough to constrain large-field inflation we refer to [156–158]. In terms of the multi-branched potential the difference between slow-roll inflation and tunneling can be illustrated as follows:

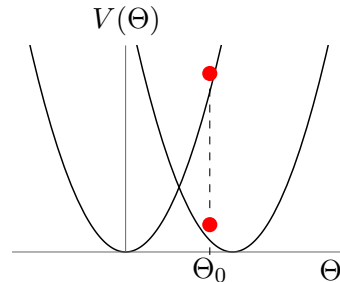
Inflation

- fix flux f_0
- choose single branch
- Θ varies along polynomial pot.



Tunneling

- consider particular value of Θ
- change branch f_0
- potential jumps, no slow-roll



Remarkably, the 3-form mechanism in $D = 4$ introduced here is also underlying flux stabilization of axions in string theory, since the discrete axionic shift symmetry is indeed

a gauge identification and cannot be explicitly broken. As explained, this does not prevent the axions to become massive in a consistent way with the discrete shift symmetry. Thus, all axions arising in string compactifications which are stabilized by internal fluxes are examples of the aforementioned multi-branched structure and candidates for F-term axion monodromy. In those cases, the 3-form fields come from dimensionally reducing higher NS-NS and R-R p -form fields and are dual to the internal fluxes [151, 159].

Lastly, let us mention an important example for inflation with polynomial potential. The monomial $V(\Theta) = \mu^{4-p}\Theta^p$ with $p > 0$ of table 5.2 forms the group of *chaotic inflation*, which is a simple version of the pioneering work of A. Linde [160]. The potential slow-roll parameters (5.2.9) for chaotic inflation are given by

$$\epsilon_V = \frac{p^2}{2} \left(\frac{M_{\text{Pl}}}{\Theta} \right)^2, \quad \eta_V = p(p-1) \left(\frac{M_{\text{Pl}}}{\Theta} \right)^2. \quad (5.5.6)$$

CHAPTER 6



The Swampland Conjectures

In the last couple of years there was much effort in the string phenomenology community to construct a viable model for large-field inflation within string theory. However, taking the details serious, almost all of these models fail to be consistent. Consequently, there might be an underlying principle from quantum gravity constraining or forbidding large-field inflation. The reasons for the breakdown of typical string inflation scenarios seem to be of different nature, though. Hence a common principle was hard to determine.

Independent of these attempts to engineer large-field inflation, C. Vafa [38] postulated the existence of the *swampland*. In short, effective theories have to be distinguished into two classes: ones that can be consistently coupled to quantum gravity and ones that cannot. The latter class of theories is dubbed as swampland and not interesting from the phenomenological point of view since they never arise from full string theory or a consistent quantum gravity. To decide whether an effective theory belongs to the swampland, there exists by now a whole zoo of conjectures. Two of the most prominent ones are the *weak gravity conjecture* and the *swampland distance conjecture* which we are going to summarize in this chapter.

Recently, it was suggested that the underlying issue of string inflation is related to these conjectures. We will see in section 6.2 how the weak gravity conjecture restricts inflationary models with periodic potentials and investigate this further in chapter 7. Inflation using polynomial potentials (axion monodromy) are in fact constrained by the swampland distance conjecture. This is one of the main results of this thesis and will be analyzed in chapter 8. Overall, the swampland conjectures cause severe restrictions¹ on models of string inflation in the sense that

¹Periodic as well as polynomial inflation (actually any moduli potential with positive extremum) would both be highly constrained by the recently proposed *swampland de Sitter conjecture* [161, 162].

Aligend Inflation	Axion Monodromy Inflation
periodic potential	polynomial potential
	
weak gravity conjecture	swampland distance conjecture

6.1 The Swampland Idea

In the early stages of string theory one might have believed that its low-energy effective theory is unique and represents the standard model of particle physics as well as cosmology. Later on, however, it turned out that there exists a landscape of possible effective field theories arising from string compactifications. In fact, the landscape of vacua seems to be not only rich in possibilities, but actually vast. Remember the old, but famous estimate of 10^{500} string vacua [163, 164]. In [165] the number of possible consistent flux compactifications of F-theory to $D = 4$ has been estimated to be 10^{272000} . As a consequence it looks as if every effective theory, that seems to be consistent at low-energies and lower dimensions, can indeed be consistently coupled to UV complete theories such as string theory. If this is true, C. Vafa was wondering “*about the wisdom of trying to construct string vacua using complicated geometries of internal manifolds*” [38]. He furthermore concluded that string theory would become of far less relevance for physics at low-energies and lower dimensions like the standard model of particle physics.

However, this statement is far from being proven. As a potential counter example, it was claimed that any theory of quantum gravity must not allow for global symmetries (discrete and continuous). Although this would be very surprising from the point of view of effective theories in lower dimensions, string theory satisfies this constraint [24, 166]: A global symmetry of the world-sheet induces by Noethers theorem a conserved current, which causes the emission of a massless string excitation. This corresponds to the gauge boson of the symmetry. Hence, in the target space we actually face a gauge symmetry.

In [38] C. Vafa uses arguments about the finiteness of scalar field moduli spaces plus matter fields and restrictions on gauge fields to postulate:

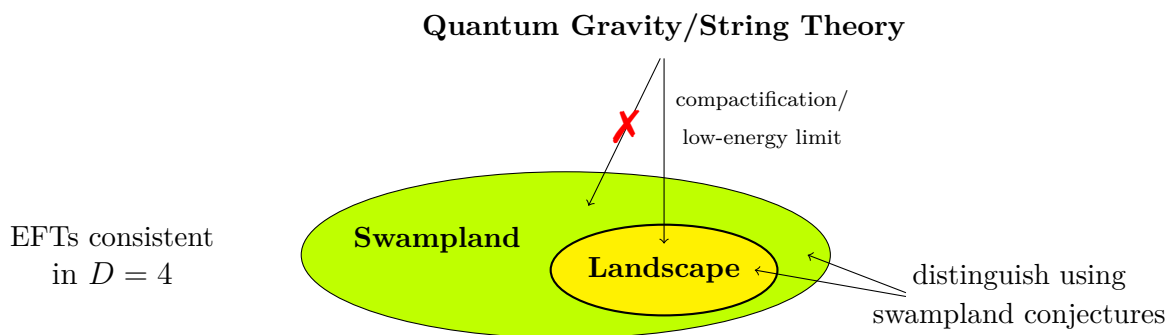
Not every effective theory that looks consistent at low-energies and lower dimensions can arise from quantum gravity.

In other words, not every consistent looking effective theory can be consistently coupled to quantum gravity. This is the core idea of this chapter and the underlying obstruction of string inflation, which we are investigating in this thesis. In the following we are going to employ the subsequent abbreviations:

- **landscape** effective theories that can arise from quantum gravity

- **swampland** effective theories that cannot arise from quantum gravity
- **swampland conjectures** postulated properties that are only satisfied for effective theories in the landscape

It is crucial to note that only theories in the landscape have to exhibit the behavior predicted by the swampland conjectures. Thereby, we can use these conjectures to distinguish between effective theories in the landscape and those in the swampland. The next two sections are devoted to explain solely two of the conjectures. See [43, 161, 167] for additional ones. To get a better understanding of these definitions let us also illustrate the swampland idea graphically:



Let us also stress that most tests of the swampland conjectures are based on string theory examples. In addition there is evidence from semi-classical black hole arguments not relying on string theory. These arguments motivate that the swampland conjectures are not only valid for string theory, but for quantum gravity in general. Hence, in this thesis we will speak of quantum gravity conjectures/constraints.

6.2 Weak Gravity Conjecture

Shortly after Vafa's original paper [38] on the swampland idea, N. Arkani-Hamed, L. Motl, A. Nicolis and C. Vafa [51] published the *weak gravity conjecture* (WGC). Its statement simply reads [51, 167]

In a consistent effective field theory coupled to gravity, gravity must always be the weakest force.

To be more precise, consider a $D = 4$ theory with gravity and a $U(1)$ gauge field with gauge coupling g_{el} . The weak gravity conjecture claims then that there must exist some charged particle with mass m_{el} satisfying

$$m_{\text{el}} \lesssim g_{\text{el}} M_{\text{Pl}}. \quad (6.2.1)$$

Let us emphasize that the conjecture does not require all masses to be less than the gauge coupling. One state satisfying the bound (6.2.1) is sufficient. In words, the conjecture requires the existence of two charged objects whose gauge repulsion is dominating over the gravitational attraction. Schematically, we have

$$\begin{array}{c}
 F_{\text{el}} \sim \frac{g_{\text{el}}^2}{r^2} \qquad \qquad \qquad F_G \sim \frac{m_{\text{el}}^2}{r^2 M_{\text{Pl}}^2} \qquad \qquad \qquad F_{\text{el}} \sim \frac{g_{\text{el}}^2}{r^2} \\
 \leftarrow \text{---} \bullet \text{---} \text{---} \bullet \text{---} \text{---} \rightarrow \\
 m_{\text{el}} \qquad \qquad \qquad m_{\text{el}} \\
 \text{“gravity is the weakest force” [51]}
 \end{array}$$

Evidence for this striking claim comes first of all from our own universe. For instance, the electric repulsion of two electrons exceeds the attractive force induced by gravity. Surprisingly, also all consistent string compactifications seem to be in agreement with the weak gravity conjecture. Before we present more concrete evidence based on black hole arguments, let us introduce the magnetic version of this conjecture.

Consider a magnetic monopole with magnetic coupling g_{mag} . According to P. Dirac’s quantization condition $g_{\text{el}} g_{\text{mag}} \in \mathbb{Z}$, we can use $g_{\text{el}} \sim 1/g_{\text{mag}}$. Moreover, the mass of the magnetic monopole should be of order the energy stored in the magnetic field $\vec{B} \sim \frac{g_{\text{mag}}}{r^2} \vec{e}_r$. If the $U(1)$ theory has a cutoff Λ , the magnetic field energy is roughly given by

$$m_{\text{mag}} \sim \int_{r \leq 1/\Lambda} dV \vec{B}^2 \sim g_{\text{mag}}^2 \int_{1/\Lambda}^{\infty} \frac{dr}{r^2} \sim \frac{\Lambda}{g_{\text{el}}^2}. \quad (6.2.2)$$

As a consequence the weak gravity conjecture for magnetic monopoles constrains the cutoff of the effective theory

$$\Lambda \lesssim g_{\text{el}} M_{\text{Pl}}, \quad (6.2.3)$$

i.e. the effective field theory breaks down at the scale Λ . The result is completely unexpected from the point of view of low-energy. In fact, one might think that smaller coupling g_{el} improves the effective description as it becomes even more weakly coupled. However, at the same time the magnetic WGC reduces the scale of validity Λ . Let us stress three remarks regarding the WGC:

- BPS states have $M \geq Q$ (mass M and charge Q) and can therefore at most saturate the weak gravity bound.
- In addition there exists a *strong form* of the WGC requiring that the conjecture must be satisfied by the lightest particle in the charged spectrum. If some arbitrary particle is sufficient, one often speaks of the *mild form*.
- Since the gauge coupling is a running coupling, one might ask at which scale it should be evaluated. According to [51] for the electric WGC the asymptotic value for the

coupling g_{el} has to be used, i.e. the running coupling evaluated at the mass scale of the lightest charged particle. For the magnetic WGC the running coupling must instead be evaluated near the cutoff scale Λ .

Motivation from Black Holes

One motivation for the weak gravity conjecture comes from the limit where the gauge coupling g vanishes. Then, the gauge symmetry is physically not distinguishable from a global symmetry since covariant derivatives simplify to ordinary derivatives and gauge fields decouple from matter. However, another swampland conjecture [167] postulates that there are no global symmetries in quantum gravity. The WGC rescues this conflict because the cutoff of the effective theory Λ would go to zero as well in the limit $g \rightarrow 0$. Hence, this limit is not allowed within a valid effective theory.

Let us be more precise and summarize the argument of [51]. Suppose we have a black hole with mass M and charge Q under the gauge symmetry. The black hole loses mass due to Hawking radiation and can thereby discharge. In order to completely discharge the black hole can for instance emit Q times the lightest charged particle, whose mass shall be denoted by m . Hence, the black hole mass must be at least

$$M \geq Q m. \quad (6.2.4)$$

Now consider a black hole with very tiny gauge coupling g and mass of order $\mathcal{O}(10)M_{\text{Pl}}$. Consequently, the extremality bound $M \geq Q g M_{\text{Pl}}$ allows the charge Q may be very large. However, if there are no very light particles, none of this charge can be radiated away due to (6.2.4). The black hole can therefore evaporate via Hawking radiation down to Planck scale and still store a high charge. This leads to the remnant problem [168], that is also forbidding global symmetries in quantum gravity.

To solve the issue with stable remnants, let us focus on extremal black holes $M = Q g M_{\text{Pl}}$. Such black holes may only decay if they satisfy (6.2.4), which directly implies the (electric) weak gravity conjecture (6.2.1).

Weak Gravity Conjecture for Axions

In order to deduce an axionic version of the weak gravity conjecture we first generalize it to arbitrary p -form gauge fields in any dimension D . These couple to electrically charged $(p-1)$ -branes and their magnetic dual $(D-p-3)$ -branes. We can assign tensions to the branes [51] given by

$$T_{\text{el}} \lesssim \left(\frac{g^2}{G_N} \right)^{\frac{1}{2}}, \quad T_{\text{mag}} \lesssim \left(\frac{1}{g^2 G_N} \right)^{\frac{1}{2}}, \quad (6.2.5)$$

where the coupling g (charge density) has dimension $[mass]^{p+1-D/2}$ and G_N denotes Newton's constant. This agrees with our conjectures above for $D = 4$, $p = 1$ and the reduced Planck mass $M_{\text{Pl}} = (8\pi G_N)^{-1/2}$.

A 0-form axion couples to a (-1) -brane, i.e. to an instanton. The coupling constant of the axion reads $g \sim 1/f$ with the axion decay constant f . Moreover, in case of an instanton, the “tension” corresponds to the instanton action $\mathcal{S}_{\text{inst}}$. Hence, (6.2.5) in $D = 4$ leads to an (electric) weak gravity conjecture for axions [42, 51]

$$f \cdot \mathcal{S}_{\text{inst}} \lesssim M_{\text{Pl}}. \quad (6.2.6)$$

It is easy to see that the axionic WGC has drastic implications for periodic large-field inflation. In order to ensure a controlled instanton expansion (see (5.3.9)), its action needs to be $\mathcal{S}_{\text{inst}} \gtrsim 1$. The WGC for axions implies then a sub-Planckian decay constant $f \lesssim 1$. For large-field inflation, however, a trans-Planckian axion decay constant f is necessary as elucidated in section 5.4. Using multiple axions and the mild form of the conjecture may be a loophole, see section 7.2. On the other hand, in axion monodromy inflation f remains sub-Planckian and thus it is not affected by (6.2.6). In the next section we will introduce another swampland conjecture which will ultimately constrain polynomial potentials as well.

6.3 Swampland Distance Conjecture

In the original paper by H. Ooguri and C. Vafa [43], what later has been called the *Swampland Distance Conjecture* [44, 46], was just one of the proposed criteria to discriminate effective field theories arising in the string landscape from those that do not admit a UV-completion, i.e. lie in the swampland. Certainly, this criterium was the most quantitative one and, as the name suggests, is about distances in field space. The swampland distance conjecture (SDC) claims:

For any point p_0 in the continuous scalar moduli space of a consistent quantum gravity theory (the landscape), there exist other points p at arbitrarily large distance. As the geodesic distance $\Theta = d(p_0, p)$ diverges, an infinite tower of states exponentially light in the distance appears, meaning that the mass scale of the tower varies as

$$M \sim M_0 e^{-\lambda \Theta}. \quad (6.3.1)$$

Thus, the number of states in the tower which are below any finite mass scale diverges as $\Theta \rightarrow \infty$.

In the initial version of the conjecture, λ is still an undetermined parameter that specifies when the exponential drop-off becomes significant. Infinitely many states becoming exponentially light in field space indicates that the effective quantum gravity theory at the point

p_0 only has a finite range of validity in the scalar moduli space. To determine the exact value of the displacement where the effective theory breaks down, all relevant mass scales have to be taken into account. Therefore, the exact upper bound on the displacement is highly model-dependent, but it is sure that in the presence of the exponential drop-off, any physics that we might derive for larger values $\Theta > \lambda^{-1}$ cannot be trusted.

Example and motivation

The most simple example for the swampland distance conjecture arises from compactification on a circle \mathcal{S}^1 with radius r . The one-dimensional lower effective theory has one modulus, whose vev is equal to the radius of the circle. The moduli space is one-dimensional and equipped with the metric [43]

$$ds^2 \sim \left(\frac{dr}{r}\right)^2. \quad (6.3.2)$$

The geodesic distance Θ from some point r_0 in this moduli space to some other point \tilde{r} is then given by

$$\Theta \sim \int_{r_0}^{\tilde{r}} \frac{dr}{r} = \log(\tilde{r}) - \log(r_0). \quad (6.3.3)$$

Apparently, it is possible to traverse infinite distances in the moduli space². As the radius \tilde{r} becomes large, there will be a Kaluza-Klein mode getting light according to

$$M_{\text{KK}} \sim \frac{1}{\tilde{r}}. \quad (6.3.4)$$

In terms of the geodesic distance Θ , we end up with the prediction of the swampland distance conjecture

$$M_{\text{KK}} \sim e^{-\Theta}. \quad (6.3.5)$$

The Kaluza-Klein mode is becoming exponentially light as we move towards infinite distances in the radius moduli space. Hence, the effective theory (without the Kaluza-Klein state) breaks down at large distances.

Note that this conjecture has been proven for $N > 8$ supercharges in [169]. For more evidence (with $N = 8$ supercharges) we refer to the literature [46, 65, 170] and to chapter 9.

As a side remark, let us investigate what happens to the above example when approaching small radius. For $\tilde{r} \rightarrow 0$ the distance is again infinite and the swampland distance conjecture calls for exponentially light modes. However, this time it cannot be particles because

²The possibility of having infinite directions in any moduli space is itself a swampland conjecture of [43].

all particles would correspond to Kaluza-Klein states which become massive for small radius. Therefore, [167] claims that a consistent theory of quantum gravity must include extended objects, such as strings or membranes. These can wrap around the shrinking circle and produce the tower of light states.

Refined Version of the Conjecture

A natural question is now: how far can one move in the moduli space until the disastrous effects of the swampland distance conjecture become relevant? Giving an exact answer is, of course, model dependent and would require an explicit analysis of each model taking all possible mass scales into account. Remarkably, in [44] D. Kläwer and E. Palti suggested a general length scale where a light tower of states will render the effective theory invalid. Their proposal was termed *refined swampland distance conjecture* (RSDC) and simply states:

The effects of the swampland distance conjecture become relevant after traversing distances $\mathcal{O}(1) M_{\text{Pl}}$, that is at the natural build-in scale of quantum gravity, in the moduli space.

Finding evidence for the refined version of the swampland distance conjecture is more involved than for the original formulation of H. Ooguri and C. Vafa since the refined version is more precisely defined: Is there an infinite tower of states becoming light at finite distances $\mathcal{O}(1) M_{\text{Pl}}$ in the moduli space? What exactly means order $\mathcal{O}(1)$? These questions shall be addressed in chapter 9.

The refined swampland conjecture is clearly in conflict with large-field inflation models, where the inflaton travels trans-Planckian distances along a non-periodic direction. This is the case for *fibre inflation* models [22], which therefore have to be carefully analyzed with respect to the refined conjecture. Periodic moduli, which are used in axion monodromy inflation, look a priori unaffected. However, we will show in chapter 8 that backreaction effects lead to the same tragic fate as for non-periodic moduli.

Finally, let us point out how general the applications of the swampland distance conjecture are. In principle every scalar field in low-energy theories may correspond to a modulus that is arising during compactification of a higher-dimensional theory. In this sense, the conjecture would for example also apply to the Higgs boson (but probably only a mild constraint on the Higgs vev).

Part III

Developments and Results

Large-Field Inflation near the Conifold

We now discuss how to explicitly realize large-field inflation in string theory. An omnipresent challenge for an effective model of inflation within the fully-fledged string description arises from the necessity of satisfying the mass hierarchy (5.3.17). In this chapter we present a novel possibility to generate exponential mass hierarchies by fluxes in the vicinity of conifold singularities. There, the periods over the Calabi-Yau three-fold show logarithmic structures which enable interesting mechanisms for moduli stabilization. In particular, integrating out heavy moduli implies exponential terms in the superpotential very reminiscent of non-perturbative contributions. Ultimately, these terms will lead to an alignment of axions potentially realizing large-field inflation. Our goal is to investigate common issues appearing for moduli stabilization near the conifold and subsequent applications to string inflation. Even though this setup needs to be understood as a toy model, a closer look at the validity of the effective theories reveals characteristic obstacles, which are likely to occur in more serious scenarios as well. This chapter is largely taken from the publications [131, 171], where more details can be found.

Before we dwell into moduli stabilization and aligned inflation, a general issue of working near the conifold shall be stressed: The effective supergravity theory commonly used for stabilizing moduli, does not include Kaluza-Klein states and massive string excitations. However, such modes can become light due to red-shifting of mass scales close to the conifold singularity, which would spoil the validity of the effective theory. Hence, we briefly show that pure warping considerations imply a constraint on the moduli vevs.

It is well known that the backreaction of localized D3-branes on the geometry leads to a warped Calabi-Yau metric [53], i.e.

$$ds^2 = e^{2A(y)} \eta_{\mu\nu} dx^\mu dx^\nu + e^{-2A(y)} \tilde{G}_{mn} dy^m dy^n, \quad (7.0.1)$$

where the warp factor $A(y)$ only depends on the internal coordinates y and \tilde{G}_{mn} denotes

the Ricci-flat metric on the Calabi-Yau three-fold. Locally, the warp factor for a stack of D3-branes reads

$$e^{-4A(y)} = 1 + \frac{4\pi g_s N}{|y|^4}, \quad (7.0.2)$$

i.e. it blows up close to the position of the D3-branes.

However, a warp factor is also induced by fluxes. Locally an H_3 form flux on an A -cycle and an F_3 form flux on its symplectic dual B -cycle leads to the warped metric on the deformed conifold. This can be described as a cone over $T^{1,1}$ cut off in the IR by a finite size S^3 . Close to the tip, the warp factor is related to the value of the complex structure modulus near the conifold [172] via $e^{A_{\text{con}}} \sim |Z|^{\frac{1}{3}}$. However, the moduli dependence is a bit more involved. Scaling the internal metric via $\tilde{G} \rightarrow \lambda^2 \tilde{G}$ describes the breathing mode of the Calabi-Yau, i.e. the Kähler modulus for the overall volume. The relation is $\lambda \sim \mathcal{V}^{\frac{1}{6}}$. In [173] it was shown that the string equations of motion admit an unconstrained deformation λ only if the warp factor scales non-trivially

$$e^{-4A(y)} = 1 + \frac{e^{-4A_{\text{con}}}}{\lambda^4} \sim 1 + \frac{1}{(\mathcal{V}|Z|^2)^{\frac{2}{3}}}. \quad (7.0.3)$$

Therefore, the warp factor can be approximated by a constant in the so-called *dilute flux limit*, which in this case takes the form

$$\mathcal{V}|Z|^2 \gg 1. \quad (7.0.4)$$

Note that in this limit the physical size of the 3-cycle A

$$\text{Vol}(A) = \mathcal{V}^{\frac{1}{2}} |\int_A \Omega_3| = (\mathcal{V}|Z|^2)^{\frac{1}{2}} \quad (7.0.5)$$

remains large, even with $|Z|$ becoming small.

Let us emphasize that, only in this limit, one can use the usual effective low-energy supergravity theory for the massless modes of the Calabi-Yau compactification. It has been argued that in the case of significant warping Kaluza-Klein modes localized in the throat are red-shifted so that their mass is smaller than the mass of some of the stabilized former massless modes. Moreover, the derivation of a full effective theory for the strongly warped case has turned out to be a tough exercise [173–176] with additional subtleties arising from mixing of the modes and the necessity to introduce compensator fields.

Throughout this chapter we will work in the dilute flux limit and investigate to what extent one can achieve moduli stabilization close to the conifold singularity, i.e. for small Z . Special emphasis is dedicated to the question whether new features arise that are not present for the stabilization of the complex structure moduli in the large complex structure regime.

7.1 Flux Induced Exponential Hierarchies

Consider a Calabi-Yau like the mirror of the quintic (with a single complex structure modulus Z) that develops a conifold singularity at $Z = 0$ as discussed in chapter 3. Its four periods in the vicinity of the conifold locus $Z \sim 0$ admit an expansion according to (A.1.7)

$$\begin{aligned} X^0 &= 1, & X^1 &= -\frac{1}{2\pi i} Z \log Z + \tilde{B}_0 + DZ + \dots \\ F_0 &= \tilde{A}_0 - \tilde{B}_0 Z + \dots, & F_1 &= Z. \end{aligned} \quad (7.1.1)$$

The constants can be found in the appendix A as well. For now we restrict our analysis to the stabilization of axio-dilaton S and the complex structure modulus Z and comment on the Kähler moduli later. Inspired by [53], we turn on 3-form fluxes to obtain the following superpotential

$$\begin{aligned} W &= f X^1 + ih S F_1 + ih' S F_0 \\ &= f \left(-\frac{1}{2\pi i} Z \log Z + \tilde{B}_0 + D Z + \dots \right) + ih S Z + ih' S (\tilde{A}_0 - \tilde{B}_0 Z + \dots), \end{aligned} \quad (7.1.2)$$

where $f = -f_1$ and $h = -\tilde{h}^1$, $h' = h_0$ are fluxes as summarized in the GVW superpotential (4.1.15). In the following we take $h \gg h' \tilde{B}_0$.

Since W does not depend on the Kähler moduli, the scalar potential (4.1.16) is of no-scale type

$$V = e^K \left(G^{Z\bar{Z}} D_Z W D_{\bar{Z}} \bar{W} + G^{S\bar{S}} D_S W D_{\bar{S}} \bar{W} \right) \quad (7.1.3)$$

with Minkowski minima at $F_Z = D_Z W = 0$ and $F_S = D_S W = 0$. Let us first freeze the complex structure modulus via $F_Z = 0$, which up to terms that vanish in the $Z \rightarrow 0$ limit leads to

$$\underbrace{\frac{f}{2\pi i} \log Z - ih S}_{\text{order } \log Z} + \underbrace{\frac{f}{2\pi i} - D f + \dots}_{\text{order } O(1)} = 0. \quad (7.1.4)$$

Note that this contribution entirely comes from the $\partial_Z W$ term in F_Z and that the contribution from $(\partial_Z K)W$ in F_Z is subleading. Moreover, we assume that, after all, the axio-dilaton can be stabilized such that $h/(fg_s) \gg 1$ and that $h \gg h'$. Therefore at leading order one finds

$$Z \sim \hat{C} e^{-\frac{2\pi h}{f} S}, \quad \text{with } \hat{C} = \exp(-1 + 2\pi i D) \simeq e^{-1.01 - 1.57 i}, \quad (7.1.5)$$

so that for a sufficiently large exponent one can indeed stabilize the complex structure modulus close to the conifold singularity.

After invoking the relation (7.1.4), the second F -term F_S yields

$$D_S W = \left(i h \hat{C} e^{-\frac{2\pi h}{f} S} + i h' \tilde{A}_0 \right) - \frac{1}{S + \bar{S}} \left(\tilde{B}_0 f + \frac{f}{2\pi i} \hat{C} e^{-\frac{2\pi h}{f} S} + i h' S \tilde{A}_0 \right). \quad (7.1.6)$$

We observe that this F -term is identical to the one that can be derived by inserting the solution (7.1.5) directly into the superpotential (7.1.2) to obtain¹ an effective superpotential for the axio-dilaton modulus

$$W_{\text{eff}} = \tilde{B}_0 f + \frac{f}{2\pi i} \hat{C} e^{-\frac{2\pi h}{f} S} + i h' S \tilde{A}_0 + \dots \quad (7.1.7)$$

This superpotential features the two special properties

- Besides flux induced polynomial terms like $i h' S$ the effective superpotential contains also infinitely many exponentially suppressed terms that, though also flux induced, have the same form as coming from some $D(-1)$ instantons.
- The exponential term suggests that the continuous shift symmetry $S \rightarrow S + i\theta$ is broken to a discrete one by the non-vanishing h -flux. This is evident from the superpotential (7.1.2), as a discrete shift of the universal axion can be compensated by changing the branch of the log Z -term in W .

Therefore, the effective superpotential (7.1.7) offers the possibility to mimic the behavior of non-perturbative effects via flux induced tree-level contributions to W .

Next, we compute the mass of the conic modulus Z . Since the complex structure modulus Z is fixed via $D_Z W = 0$, for determining its mass we can evaluate

$$V_{Z\bar{Z}} = \partial_Z \partial_{\bar{Z}} V = e^K G^{Z\bar{Z}} \partial_Z (D_Z W) \partial_{\bar{Z}} (D_{\bar{Z}} \bar{W}) \Big|_{D_Z W=0}. \quad (7.1.8)$$

In our case $D_Z W$ is holomorphic at leading order and hence the masses of the two real scalars in Z are degenerate. Approximating the metric by the leading-order term $G_{Z\bar{Z}} \sim -\frac{1}{2\pi A} \log(|Z|^2)$ and using the mass formulas $M_Z^2 = \frac{1}{2} G^{Z\bar{Z}} V_{Z\bar{Z}}$ and $M_s^2 \sim \frac{M_{\text{Pl}}^2 \sqrt{g_s}}{\mathcal{V}}$ of section 4.1.3, the mass of the canonically normalized complex structure modulus becomes

$$M_Z^2 \sim \frac{M_{\text{Pl}}^2}{4 \text{Re}(S) \mathcal{V}^2 |Z|^2} \frac{A f^2}{\log^2(|Z|^2)} \sim M_Z^2 \sim \frac{M_s^2}{\mathcal{V} |Z|^2} \frac{A f^4 g_s^{\frac{5}{2}}}{16\pi^2 h^2}. \quad (7.1.9)$$

Due to the $|Z|^2 \sim \exp(-\frac{4\pi h}{f g_s})$ factor in the denominator this mass is exponentially enhanced so that it only makes sense for $\mathcal{V} |Z|^2 \gg 1$, i.e. for exponentially large volume. To summarize:

¹Let us remark that there would be an additional exponential term in the superpotential (à la racetrack [163]) if one considers a point where two conifold singularities collide [177, 178]. However, this did not lead to interesting new features for inflationary models.

- The mass of the conic modulus Z comes out exponentially enlarged so that the volume eventually has to be chosen/frozen at exponentially large values. This makes the large volume scenario the natural candidate for Kähler-moduli stabilization.
- The used effective supergravity theory by itself indicates its limitation, i.e. that it is applicable only in the dilute flux regime $\mathcal{V}|Z|^2 \gg 1$ where warping is negligible.

Before moving on to the Kähler moduli, let us concisely summarize the stabilization of the axio-dilaton and refer to [131] for details. There are two characteristic cases that need to be distinguished: $h' \neq 0$ as well as $h' = 0$. In latter case, the superpotential (7.1.7) is of KKLT-type and one may deduce a periodic potential for the axionic part of S . Since here we generate the exponential not directly via instantons but via moduli stabilization close to the conifold, it is interesting to investigate the appearing value of the axion decay constant. Indeed the decay constant turns out to be sub-Planckian in the regime of control. It was shown in [131], however, that the mass of this axion will not be exponentially suppressed against the complex structure modulus Z (up to Calabi-Yau dependent data). This is inconsistent with the approach of at first integrating out Z and afterwards generating an effective superpotential (7.1.7). For the case $h' \neq 0$, the effective superpotential (7.1.7) is of tree-level form. As a consequence there will be an exponential mass hierarchy $M_S^2/M_Z^2 \sim |Z|^2$. A posteriori, this justifies the use of the effective superpotential for the axio-dilaton modulus. Let us emphasize that this effect is not due to warping, as it remains in the dilute flux limit. In the strongly warped case it is usually the red-shifted modes in the throat that become light, here instead it is actually a bulk closed string mode.

7.1.1 Kähler Moduli Stabilization via a Conic LVS

So far, the scalar potential did not depend on the Kähler moduli, i.e. in particular on the overall volume of the Calabi-Yau manifold. As we have seen, for the mass of the conic modulus Z to remain below the string scale, we need $\mathcal{V}|Z|^2 \gg 1$. Therefore, one needs to dynamically freeze the overall volume modulus at an exponentially large size. This makes it natural to combine our approach² with the large volume scenario, reviewed in section 4.3.2.

Integrating out Z and S , we start with a typical LVS superpotential (4.3.4)

$$W_{\text{inst}}(T_s) = W_0 + A_s Z^N e^{-a_s T_s} \quad (7.1.10)$$

with $W_0 \sim f$ and the complex number $Z \sim \hat{C} \exp\left(-\frac{2\pi h}{f} S\right)$. Note that since we do not explicitly know the one-loop Pfaffian, we allowed it to depend polynomially on Z . Now

²Note that for the LVS minimum to exist one needs $h^{21} > h^{11}$, which is clearly not satisfied for the mirror of the quintic. The minimal setup would therefore be a Calabi-Yau with Hodge numbers $(h^{21}, h^{11}) = (3, 2)$. Close to a conifold singularity with $|Z| \ll 1$ we expect that the two additional complex structure moduli can be stabilized via fluxes at the mass scale of the axio-dilaton (for $h' \neq 0$).

we proceed as in section 4.3.2, where only the value of A_s has been changed according to $A_s \rightarrow A_s Z^N$ and is now an exponentially small number. In the non-supersymmetric AdS-type large-volume minimum the Kähler moduli get now stabilized at

$$\tau_s = \frac{(4\xi)^{\frac{2}{3}}}{g_s}, \quad \mathcal{V} = \frac{W_0 \xi^{\frac{1}{3}}}{2^{\frac{1}{3}} g_s^{\frac{1}{2}} |a_s A_s Z^N|} e^{a_s \tau_s}. \quad (7.1.11)$$

For $N > 0$ the exponentially small value of Z only further enhances the size of \mathcal{V} . For the crucial combination we thus obtain

$$\mathcal{V}|Z|^2 \sim \exp \left[\frac{a_s}{g_s} \left(\frac{h(N-2)}{f} + (4\xi)^{\frac{2}{3}} \right) \right]. \quad (7.1.12)$$

For $N \geq 2$ this is naturally larger than one and for $N \leq 1$ we can choose $f \gg h$ so that the exponent becomes positive. Recall from chapter 4 that there was no direct correlation between the fluxes f and h . For staying in the perturbative regime only $h > h'$ and $f > h'$ was required.

Mass hierarchy

Let us now consider the moduli masses at the minimum. We observe that the masses of the Kähler moduli in (4.3.8) do not depend on the parameter A_s and therefore not on Z . Thus, one still finds

$$\begin{aligned} M_{\tau_b}^2 &\sim \frac{W_0^2 \xi}{A g_s^{\frac{1}{2}} \mathcal{V}^3} M_{\text{Pl}}^2, & M_{\rho_b}^2 &\sim 0, \\ M_{\tau_s}^2 &\sim M_{\rho_s}^2 \sim \frac{a_s^2 W_0^2 \xi^{\frac{4}{3}}}{A g_s \mathcal{V}^2} M_{\text{Pl}}^2. \end{aligned} \quad (7.1.13)$$

The gravitino mass is given by

$$M_{3/2}^2 = e^K |W|^2 \sim \frac{g_s W_0^2}{A \mathcal{V}^2} M_{\text{Pl}}^2. \quad (7.1.14)$$

In Table 7.1 we summarize all relevant mass scales, where we only displayed the dependence on \mathcal{V}, g_s, Z and the large flux f . We choose $h' \neq 0$ to determine the axio-dilaton mass M_S and ordered the mass scales in the perturbative large \mathcal{V} and small $g_s, |Z|$ regime.

Hence, we obtain the mass hierarchy

$$M_{\tau_b} < M_{\tau_s} \sim M_S < M_Z < M_{\text{KK}} < M_s < M_{\text{Pl}}. \quad (7.1.15)$$

Scale	(Mass) ² in M_{Pl}^2
string scale M_s^2	$\frac{g_s^{1/2}}{\mathcal{V}}$
Kaluza-Klein scale M_{KK}^2	$\frac{1}{\mathcal{V}^{4/3}}$
conic modulus M_Z^2	$\frac{f^4 g_s^3}{\mathcal{V}^2 Z ^2}$
small Kähler modulus $M_{\tau_s}^2$	$\frac{f^2}{g_s \mathcal{V}^2}$
gravitino $M_{3/2}^2$	$\frac{f^2 g_s}{\mathcal{V}^2}$
axio-dilaton M_S^2 and c.s. moduli	$\frac{f^2 g_s}{\mathcal{V}^2}$
large Kähler modulus $M_{\tau_b}^2$	$\frac{f^2}{g_s^{1/2} \mathcal{V}^3}$

Table 7.1: Mass scales and moduli masses for the conic LVS from [131].

Since the mass of the modulus τ_s is of the same volume order $1/\mathcal{V}^2$ as the axio-dilaton S , one might worry whether integrating out S and only considering the Kähler moduli is actually justified. However, as shown in [15] the minimum above remains a minimum of the full potential including axio-dilaton and complex structure moduli. The reason is that these moduli are flux-stabilized and enter the scalar potential already at the order $\mathcal{O}(\frac{1}{\mathcal{V}^2})$ that, in the large volume regime, dominate over the terms of order $\mathcal{O}(\frac{1}{\mathcal{V}^3})$ by which the Kähler moduli are stabilized.

We conclude that flux stabilization of the complex structure and the axio-dilaton close to the conifold singularity can be consistently combined with the LVS scenario, thus guaranteeing a reliable effective field theory approach where warping is negligible. The masses of the moduli get split up so that one gains parametric control over their ratios. Any other scheme of moduli stabilization must also freeze the volume at exponentially large values to satisfy $\mathcal{V} |Z|^2 \gg 1$. Stabilizing the Kähler moduli near the conifold with non-geometric fluxes has usually failed due to serious conflicts with the mass hierarchy (basically because the overall volume is not exponentially large).

7.2 Inflation via Axion Alignment

It was shown [131] how the conifold setup introduced above can in principle give rise to aligned inflation realizing a trans-Planckian axion field range. Here, we will critically re-evaluate potential issues of this model with respect to three aspects: validity of the effective theory by checking the mass hierarchies, formal constraints of string theory by taking the full periods into account and the weak gravity conjecture. Our computations are of course model dependent, but nevertheless we intend to stress that a semi-complete scenario for large-field inflation might generically be far from well-controlled. The alignment model at the conifold demonstrates the increased difficulties at one side of the hierarchy if improving the other side, thus a typical lose-lose situation.

Stabilizing axio-dilaton and complex structure moduli

Motivated by the periods of appendix A and the shift-symmetric Kähler potential we analyze the resulting supergravity models for moduli stabilization. Here we proceed analogously to before and first stabilize the Z modulus by the usual combination of R-R and NS-NS fluxes on the two cycles related to the conifold singularity. Integrating out this most heavy complex structure modulus leads to effective Kähler- and superpotentials that we subsequently study in a more phenomenological manner, i.e. without reference to a concrete Calabi-Yau three-fold. Thus, we allow us to be more flexible with independent fluxes and numerical prefactors than an actual threefold example may permit.

For such an effective model with two complex structure moduli (Z, Y) , up to linear order in Y , we make the ansatz

$$K_{\text{eff}} = -2 \log \mathcal{V} - \log(S + \bar{S}) - \log\left(A + \frac{1}{2}(Y + \bar{Y})\right) \quad (7.2.1)$$

and

$$W_{\text{eff}} = f \alpha + h' \beta S + \hat{f}' \gamma Y \quad (7.2.2)$$

with $\alpha, \beta, \gamma \in \mathbb{C}$ and $A \in \mathbb{R}$. However, the minimum conditions $D_S W = D_Y W = 0$ only admit solutions with $\text{Re}(S) = 0$, i.e. in the unphysical domain. Therefore, our ansatz is not yet sufficiently generic.

Adding the second order term to the Kähler potential, we make the ansatz

$$K_{\text{eff}} = -2 \log \mathcal{V} - \log(S + \bar{S}) - \log\left(A + \kappa \text{Re}Y - (\text{Re}Y)^2\right) \quad (7.2.3)$$

$$W_{\text{eff}}^{(0)} = i\alpha\left(f + h' S + \hat{f}' Y\right)$$

for the effective Kähler- and superpotential, with the model dependent order one parameters $A, \alpha, \kappa \in \mathbb{R}$. Just for simplicity, we were choosing $\alpha = \beta = \gamma$. Including just these

single first order terms in W_{eff} implicitly means that we have assumed that possible higher order polynomial terms like Y^n are either not present or are sub-leading. Whether the concrete form of realistic periods admit such a choice remains to be seen.

For the model (7.2.3) we find a Minkowski minimum at

$$\begin{aligned}\Sigma &= \hat{f}' \zeta_0 + h' c_0 = 0 \\ s &= s_0 = \frac{1}{h'} \sqrt{f^2 - A \hat{f}'^2 + \kappa f \hat{f}'} \\ \text{Re}(Y) &= y_0 = \frac{1}{\hat{f}'} \left(-f + \sqrt{f^2 - A \hat{f}'^2 + \kappa f \hat{f}'} \right).\end{aligned}\tag{7.2.4}$$

where $Y = y + i\zeta$. Note that for $f/\hat{f}' \gg 1$ these expressions simplify drastically

$$\Sigma = 0, \quad s_0 = \frac{f}{h'}, \quad y_0 = \frac{\kappa}{2} + O\left(\frac{\hat{f}'}{f}\right).\tag{7.2.5}$$

Therefore, for $f/h' \gg 1$ and $\kappa < 1$ the values of the moduli lie in the perturbative regime of small string coupling and small complex structure modulus Y . In the following, we analyze this model in more detail with special focus on the axion sector. For simplicity we choose $\kappa = 0$ so that

$$\Sigma = 0, \quad s_0 = \frac{f}{h'}, \quad y_0 = -\frac{A\hat{f}'}{2f} + O\left((\hat{f}'/f)^2\right).\tag{7.2.6}$$

Note that the second axion Θ is still massless at this level. It is clear that once additional terms like e.g. $\Delta W = iBY^2$ are present in the superpotential, Θ also gets stabilized with a mass that is governed by the parameter B . For B of order one, all four fields will have the same order of masses, but for a parametrically smaller value of B the axion Θ will be the lightest state of all complex structure and axio-dilaton moduli.

Recall that, after integrating out Z , one also gets an exponential term like $\exp(-\frac{2\pi}{f}hS)$ in W . As its size depends on a different modulus, this term can in principle compete with the higher order polynomial terms Y^n . For illustrative purposes, let us consider in the following section the possible moduli stabilization scheme, once we include only this exponential term in W and assume that polynomial terms are either absent or subleading. We understand that this is a very strong assumption that needs to be tested for concrete Calabi-Yau manifolds (e.g. along the line reported in [85]).

Aligned Inflation

As we have seen, only one linear combination of the two axions is stabilized by terms appearing linearly in W . We now analyse the phenomenological effective supergravity

model (7.2.3)

$$\begin{aligned} W_{\text{eff}} &= W_{\text{eff}}^{(0)} + W_{\text{eff}}^{(1)} \\ &= i\alpha \left(f + h' S + \hat{f}' Y \right) + \frac{f\hat{C}}{2\pi i} \exp\left(-\frac{2\pi}{f} (hS + \hat{f}' Y) \right). \end{aligned} \quad (7.2.7)$$

Here we have included a term $\exp(-\frac{2\pi}{f}\hat{f}'Y)$ which is induced from a coupling $\hat{f}'ZY$ in the original superpotential.

Let us now derive an effective scalar potential V_{eff} for the so far unstabilized axion appearing in the exponent of (7.2.7). If we naively integrate out the already stabilized moduli via

$$\begin{aligned} D_S W_{\text{eff}}|_{S_0, Y_0} &= c_S |Z| \exp\left(-\frac{2\pi i}{f} \Theta \right), \\ D_Y W_{\text{eff}}|_{S_0, Y_0} &= c_Y |Z| \exp\left(-\frac{2\pi i}{f} \Theta \right) \end{aligned} \quad (7.2.8)$$

with $\Theta = (hc + \hat{f}'\zeta)$ and $c_S, c_Y \neq 0$, we realize that $V_{\text{eff}}|_{S_0, Y_0}$ does not depend on the axion Θ and is non-vanishing at order $O(|Z|^2)$. However, this is not what one expects. In the true vacuum (at order $O(|Z|^2)$) the vacuum energy should be vanishing and the remaining axion Θ should be stabilized at $\Theta = 0$.

Indeed to see this, we first have to take the backreaction of the exponential term on the stabilization of the saxions into account. Perturbing around the leading order values y_0, s_0 by $\Delta y_0 \sim O(|Z|)$ and $\Delta s_0 \sim O(|Z|)$, we fix Δy_0 and Δs_0 by requiring $D_S W_{\text{eff}}|_{S_0, Y_0, \Theta=0} = D_Y W_{\text{eff}}|_{S_0, Y_0, \Theta=0} = 0 + O(|Z|^2)$. For $\kappa = 0$, $f/\hat{f}' \gg 1$ and at leading non-vanishing order in $|Z|$ we find

$$\Delta s_0 \sim -\frac{f}{2\pi\alpha h'} \left(1 + \frac{4\pi h}{h'} \right) |Z|, \quad \Delta y_0 \sim -\frac{A\hat{f}'}{2\alpha f} |Z|. \quad (7.2.9)$$

This backreaction induced shift of the vacuum leads to the correct effective scalar potential

$$\begin{aligned} V_1 &= G^{S\bar{S}} D_S W D_{\bar{S}} \bar{W} = \frac{|Z|^2}{2\pi^2} f^2 \left(1 + \frac{4\pi h}{h'} \right)^2 \left(1 - \cos\left(\frac{2\pi}{f} \Theta \right) \right) \\ V_2 &= G^{Y\bar{Y}} D_Y W D_{\bar{Y}} \bar{W} = \frac{|Z|^2 A}{4\pi^2} \hat{f}'^2 \left(1 + \frac{4\pi \hat{f}'}{\hat{f}'} \right)^2 \left(1 - \cos\left(\frac{2\pi}{f} \Theta \right) \right), \end{aligned} \quad (7.2.10)$$

so that in the regime $f/\hat{f}' \gg 1$ and $h/h' \gg 1$ we eventually obtain the effective potential for Θ

$$V_{\text{eff}} = e^{K_{\text{eff}}} (V_1 + V_2) \sim \frac{4|Z|^2}{A\mathcal{V}^2} \frac{fh^2}{h'} \left(1 - \cos\left(\frac{2\pi}{f} \Theta \right) \right). \quad (7.2.11)$$

Note that the potential exhibits the expected Minkowski minimum at $\Theta = 0$.

As a check of our approach, in figure 7.1 we have plotted the axion dependence of the full scalar potential for the saxions fixed at the Minkowski minimum. It nicely shows the periodic form of the potential (7.2.11) and that the height of the potential in Θ direction is hierarchically smaller than in Σ direction.

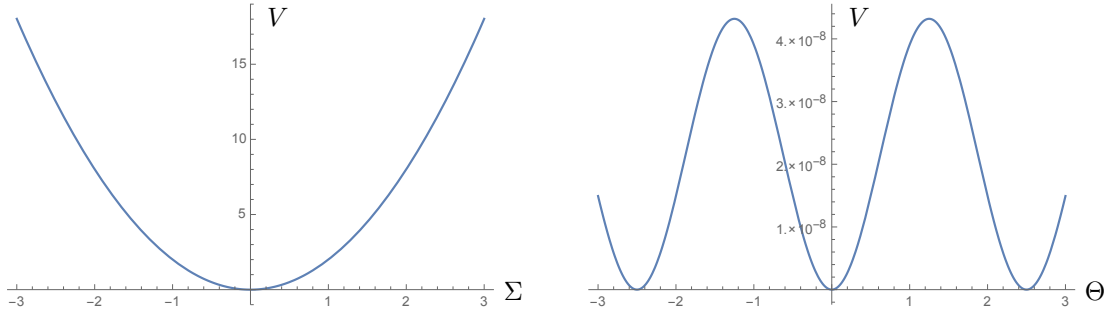


Figure 7.1: Scalar potential for the two axions Σ and Θ for $f = 10$, $h' = \hat{f}' = 1$, $h = -\hat{f} = 2$, $\hat{C} = 1$ and $A = 0.1$.

In order to apply the model at hand to axion inflation, it remains to rewrite the potential in terms of the canonically normalized field $\tilde{\Theta}$ which we then employ as inflaton. Due to the diagonal structure of the Kähler metric, one finds in the regime $f/f' \gg 1$

$$\tilde{\Theta} = \frac{h'}{\sqrt{A\hat{f}'}}\Theta, \quad (7.2.12)$$

such that the canonically normalized inflaton potential is given by

$$V_{\text{eff}} = \frac{4|Z|^2}{AV^2} \frac{fh^2}{h'} \left(1 - \cos \left(\frac{2\pi\sqrt{A}(h\hat{f}' - h'\hat{f})}{fh'} \tilde{\Theta} \right) \right) \equiv V_0 \left(1 - \cos \left(\frac{\tilde{\Theta}}{f_{\tilde{\Theta}}} \right) \right). \quad (7.2.13)$$

The axion decay constant $f_{\tilde{\Theta}}$ signals the appearance of an alignment mechanism as

$$f_{\tilde{\Theta}} = \frac{f}{2\pi\sqrt{A}} \frac{h'}{h\hat{f}' - h'\hat{f}}. \quad (7.2.14)$$

By aligning the fluxes as $(h\hat{f}' - h'\hat{f}) < h'$ we can obtain an axion decay constant larger than one. This is very reminiscent of the KNP-axion alignment mechanism [30], the main difference being that one linear combination of axions is fixed by fluxes at linear order in the fields and only the second combination by instanton-like terms.

Corrections to the superpotential

Let us come back to our assumptions about the suppression of polynomial terms in W . In fact, great care has to be taken of higher order polynomial terms in the periods as they

contribute to the superpotential (7.2.7) and might be dominating over the exponential term. Of course, terms like Z^n with $n \geq 2$ will be subleading since they are exponentially suppressed, but this is not necessarily true for terms like Y^n . It turns out that numerical prefactors governed by the underlying geometry, decide whether large-field inflation can occur.

To be more precise, we include the term iBY^2 in the superpotential (7.2.7)

$$W_{\text{eff}} = i\alpha(f + h'S + \hat{f}'Y) + iBY^2 + \frac{f\hat{C}}{2\pi i} \exp\left(-\frac{2\pi}{f}(hS + \hat{f}Y)\right). \quad (7.2.15)$$

Figure 7.2 displays the new effective potential for Θ (by dashed lines) for two different values of the parameter B .

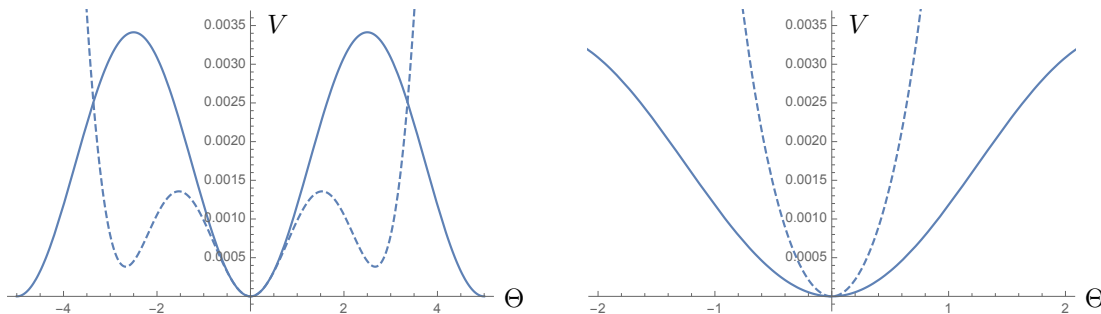


Figure 7.2: Scalar potential (dashed lines) for the axion Θ for $f = 10$, $h' = \hat{f}' = 1$, $h = -\hat{f} = 1$, $\hat{C} = 1$, $A = 0.1$ and $B = 0.01$ in the left-handed plot and $B = 0.1$ in the right-handed plot. For comparison, the solid lines show the potential for $B = 0$.

The left-handed plot shows that here B is sufficiently small so that in the direct neighborhood of $\Theta = 0$ the potential is dominated by the exponential term. Whereas, in the right-handed plot B is so large that the mass of Θ comes from the quadratic term. As said, we are not claiming that higher order terms are really suppressed for a concrete Calabi-Yau, but just want to show which kind of scenarios are in principle possible for moduli stabilization close to the conifold. We would not be surprised if once again a concrete string theoretic proposal for realizing large-field inflation fails as one loses control over certain dangerous terms. In this spirit we proceed with discussing the purely exponential case.

7.2.1 Comment on the Weak Gravity Conjecture

Even though the effective exponential terms in the superpotential do not directly arise from instanton contributions, one can ask whether they satisfy a generalized version of the weak gravity conjecture see chapter 6. For instantons the conjecture says that the product

of the instanton action times the axion decay constant has to be smaller than one

$$S_{\text{inst}} f_{\text{inst}} \leq 1. \quad (7.2.16)$$

If this is to be satisfied for the instanton with the lowest action, one has the strong version of the WGC. Apparently, this is violated for the aligned axion $\tilde{\Theta}$ whose action can be written as

$$S_{\text{inst}} = \frac{2\pi}{f}(hs_0 + \hat{f}y_0) \sim \frac{2\pi}{f}hs_0 \sim \frac{2\pi h}{h'}, \quad (7.2.17)$$

so that in the case of alignment one gets

$$S_{\text{inst}} f_{\tilde{\Theta}} \sim \frac{fh}{\sqrt{A}(h\hat{f}' - h'\hat{f})} > 1. \quad (7.2.18)$$

The *mild* form of the WGC says that for an axion with decay constant $f_{\tilde{\Theta}}$ there is *some* instanton with instanton action $S_{\text{inst}}^{(2)}$ satisfying the WGC condition. Therefore, to satisfy the mild WGC, it is sufficient to have a situation where the contribution of these two instantons reads as

$$V \sim e^{-2S_{\text{inst}}} \left(1 - \cos\left(\frac{\tilde{\Theta}}{f_{\tilde{\Theta}}}\right)\right) + e^{-2S_{\text{inst}}^{(2)}} \left(1 - \cos\left(\frac{k\tilde{\Theta}}{f_{\tilde{\Theta}}}\right)\right), \quad (7.2.19)$$

with $k \in \mathbb{Z}$. For sufficiently large k , the axion decay constant $f_{\tilde{\Theta}}/k$ can be sub-Planckian and for $S_{\text{inst}} < S_{\text{inst}}^{(2)}$ the first term can still be dominant and realize inflation. This loop-hole was pointed out in [39, 42] and has been realized for complex structure aligned inflation in [179].

In our case the situation is similar, where the second exponential contribution could arise from a single $D(-1)$ -instanton. Its action and decay constant are

$$S_{D(-1)} = 2\pi s_0 = \frac{2\pi f}{h'}, \quad f_{D(-1)} = \frac{h'}{2\pi\sqrt{A}\hat{f}'} = \frac{f_{\tilde{\Theta}}}{k} \quad (7.2.20)$$

with $k = (f\hat{f}')/(h\hat{f}' - h'\hat{f})$. With the denominator being equal to one in the case of alignment, k is a large integer. Moreover, for $f/h > 1$ the $D(-1)$ instanton action is sub-leading and inflation can still occur.

7.2.2 Mass Hierarchy

Let us finally compute the different mass scales to confirm our various effective approaches and in particular justify integrating out massive fields at several stages of our computation. We denote by M_{mod} the masses of the moduli Σ , s and $\text{Re}(Y)$ in the minimum (7.2.6). Up

to numerical prefactors of order $\mathcal{O}(1)$, the mass eigenvalues of the canonically normalized mass matrix $(M^2)^i{}_j = \frac{1}{2}G^{ik}\partial_k\partial_j V$ are given by

$$M_{\text{mod}}^2 = \frac{f^2 g_s}{A\mathcal{V}^2}. \quad (7.2.21)$$

In addition one can then read off the mass of the canonically normalized inflaton $\tilde{\Theta}$ from V_{eff} in equation (7.2.13)

$$M_{\tilde{\Theta}}^2 = \frac{V_0}{f_{\tilde{\Theta}}^2} M_{\text{Pl}}^2 \sim \frac{|Z|^2}{f\mathcal{V}^2} M_{\text{Pl}}^2. \quad (7.2.22)$$

Hence the mass of the inflaton is exponentially suppressed relative to the mass of the other moduli stabilized at tree-level. Recall that the latter are also exponentially suppressed relative to the conic complex structure modulus Z , such that we obtain a mass hierarchy of the form

$$M_{\tilde{\Theta}} < M_{\text{mod}} < M_Z. \quad (7.2.23)$$

The mass scale of inflation can be read off from (7.2.13) as

$$M_{\text{inf}}^2 \sim V_0^{\frac{1}{2}} \sim \frac{f^{\frac{1}{2}}|Z|}{\mathcal{V}}. \quad (7.2.24)$$

Therefore, with $g_s \sim 1/f$ we obtain

$$\frac{M_{\text{inf}}^2}{M_{\text{mod}}^2} \sim \frac{(\mathcal{V}|Z|^2)}{f^{\frac{1}{2}}|Z|} \quad \text{and} \quad \frac{M_{\text{inf}}^2}{M_Z^2} \sim (\mathcal{V}|Z|^2) \frac{|Z|}{f^{\frac{1}{2}}} \quad (7.2.25)$$

so that in the regime $\mathcal{V}|Z|^2 \gg 1$ the inflationary scale is larger than the moduli masses, but for sufficiently small $|Z|$ can be lower than the mass of the conic complex structure modulus. Therefore, for correctly describing the dynamics in the slow-rolling phase one can use the effective four-dimensional supergravity theory after integrating out the conic modulus Z . The backreaction of the inflaton on the remaining moduli is expected to lead to a (welcomed) flattening of the quadratic inflaton potential [180]. Note that in this respect this model behaves better than the ones constructed in the framework of the flux scaling scenario [32], where generically the inflationary mass scale was even larger than the Kaluza-Klein scale.

So far we did not stabilize the Kähler moduli for this inflationary model. Let us now assume that we can employ the large volume scenario and estimate the appearing mass scales as in section 7.1.1. We ignore possible subtleties about the order of integrating out for the moment. Since the non-supersymmetric LVS minimum is of AdS type, we also have to assume a proper uplift mechanism. As a first rough estimate, in table 7.2 we list all relevant mass scales.

Scale	(Mass) ² in M_{Pl}^2
string scale M_s^2	$\frac{1}{f^{1/2} \mathcal{V}}$
Kaluza-Klein scale M_{KK}^2	$\frac{1}{\mathcal{V}^{4/3}}$
conic c.s. modulus M_Z^2	$\frac{f}{\mathcal{V}^2 Z ^2}$
inflationary mass scale M_{inf}^2	$\frac{f^{1/2} Z }{\mathcal{V}}$
other moduli M_{mod}^2	$\frac{f}{\mathcal{V}^2}$
gravitino mass $M_{3/2}^2$	$\frac{f}{\mathcal{V}^2}$
large Kähler modulus $M_{\tau_b}^2$	$\frac{f^{5/2}}{\mathcal{V}^3}$
inflaton $M_{\tilde{\Theta}}^2$	$\frac{ Z ^2}{f \mathcal{V}^2}$

Table 7.2: Moduli masses and scales with $g_s \sim 1/f$ from [131].

From the table we extract the relation

$$\frac{M_{\tilde{\Theta}}^2}{M_{\tau_b}^2} \sim \frac{\mathcal{V} |Z|^2}{f^{7/2}} \quad (7.2.26)$$

so that in the reliable supergravity regime with $\mathcal{V} |Z|^2 \gg 1$ we generically find that the large Kähler modulus is lighter than the potential inflaton. Of course this spoils single field inflation and reflects a problem that seems to be very generic for complex structure moduli inflation [33, 34]. One can derive the relation

$$\frac{M_{\tilde{\Theta}}^2}{M_{\tau_b}^2} \sim \frac{M_s^2}{f^2 M_Z^2} \quad (7.2.27)$$

so that in principle for $M_s/M_Z \sim 5 - 8$ one can get that the axion $\tilde{\Theta}$ is the lightest mode for $f \sim 10$. Of course here one is at the boundary of control and numerical factors matter. Thus, the generic hierarchy of scales is of the form

$$M_{\tau_b} < M_{\tilde{\Theta}} < M_{\text{mod}} < M_{\text{inf}} \sim M_Z < M_{\text{KK}} < M_s < M_{\text{Pl}}, \quad (7.2.28)$$

guaranteeing parametric control over the mass scales in our effective supergravity description. It is not excluded that by a certain choice of the flux f one can get that the axion

is in principle the lightest mode. In this case a more detailed analysis is necessary, as one cannot first stabilize the axion $\tilde{\Theta}$ and then integrate out the Kähler moduli.

Summarizing, in this corner of the string theory landscape we managed to design a string motivated effective supergravity model that features an alignment mechanism providing an axion that has an effective decay constant larger than one. The axion sector still satisfies the mild form of the WGC. However, this model will probably fail at the end, as we had to make very strong assumptions about higher order polynomial corrections to W and because it is not yet clear whether one can get the Kähler moduli heavier than the inflaton.

Axion Monodromy Inflation and the Swampland Distance Conjecture

In the last chapter 7 we investigated a model for periodic inflation and attempted to engineer a trans-Planckian flat direction by using multiple axions. As pointed out, a fully-fledged realization of this model is quite sophisticated. In addition, there are tough constraints from the strong form of the weak gravity conjecture (see section 6.2).

Therefore, we will now analyze a promising alternative towards large-field inflation in string theory: axion monodromy inflation. Recall the discussion of section 5.5 for details on this mechanism. Our analysis here is in large parts taken from the publication [181].

Despite all its appealing features, including the apparent robustness against the WGC, we think that there does not exist any completely successful and convincing string realization of F-term axion monodromy inflation, yet. The difficulties are related to moduli stabilization and backreaction effects from the other scalars of the compactification¹. When taking the backreaction into account, the physical field range of the inflaton might be drastically reduced, as we proceed to explain in the next section 8.1. More than a technical issue, these difficulties might again point towards a fundamental obstruction of any consistent theory of quantum gravity. As noticed in [44, 45], in this case these control issues can be related to the swampland distance conjecture.

So, the main result of this chapter is to show that also axion monodromy inflation lacks of a consistent embedding in string theory as it is in conflict with the swampland distance conjecture. To apply the conjecture we at first have to extend it to an axionic version by taking backreaction effects of the moduli into account. Then, we evaluate an illustrative

¹From this perspective, inflationary string model building attempts that did not consider these issues are not yet complete and need to be reevaluated.

closed string as well as more involved open string models to finally draw our conclusion.

Let us emphasize that our focus is on analytically solvable models, where in order to be able to compute also the string and Kaluza-Klein scales, all relevant moduli are included. It is clear that e.g. the string and the Kaluza-Klein scales are only dynamically fixed when we include the axio-dilaton as well as the Kähler moduli as dynamical fields.

For the presented representative examples in this chapter, we focus on the parametric dependence of certain quantities in terms of the background fluxes. Our philosophy is that parametric control is essential to claim that mass hierarchies can be naturally achieved. Just an accidental, model dependent numerical factor of e.g. order $\mathcal{O}(1) - \mathcal{O}(10^2)$ is not sufficient and is surely not related to general arguments from quantum gravity.

8.1 Moduli Backreaction and Axionic RSDC

Any attempt to construct a realistic inflationary model in string theory has to deal with the issue of moduli stabilization as emphasized in section 5.3.1. The strong experimental bounds on non-Gaussianities and isocurvature perturbations favor a scheme of single field inflation or, at most, moderate multi-field inflation involving a few weakly-coupled scalars. To guarantee the consistency of the effective field theory approach as well as to realize a model of single field inflation, one has to stabilize the moduli such that the hierarchy of mass scales (see (5.3.17)) is realized

$$M_{\Theta} < M_{\text{mod}} < M_{\text{KK}} < M_s < M_{\text{Pl}}, \quad (8.1.1)$$

with the inflaton mass M_{Θ} . To achieve this hierarchy of scales at the minimum of the potential is already a challenge for many flux compactifications (see [33, 34] for some no-go theorems for the complex structure moduli space of a Calabi-Yau three-fold). But to guarantee the stabilization of these scales during the whole inflationary trajectory is an even bigger challenge (see also [34, 182–184]).

Let us assume a pseudo-scalar θ parametrizing the inflationary trajectory. When θ is displaced from its minimum, generically the minima of the other scalars will also change,

$$s(\theta) = s_0 + \delta s(\theta) \quad (8.1.2)$$

where s_0 denotes the vacuum expectation value of the scalar s at the minimum of the potential, i.e. when θ is also at its minimum. We will again use the word *saxions* to refer to all non-periodic (non-axionic) scalars. By plugging this back into the effective theory, the scalar potential and the kinetic term for the inflaton can be substantially modified. In other words, the inflationary trajectory is no longer only along θ but corresponds to a combination of θ and s . This backreaction leads to a flattening of the inflaton potential [180].

Note that the above simple procedure of freezing s and plugging (8.1.2) back into the effective theory is an approximation that relies on neglecting the variation of the kinetic energy of the saxion with respect to the potential energy, so it is valid only as long as there is a mass hierarchy between θ and s . Otherwise, a multifield analysis is required to consider simultaneously the dynamics of both fields.

In the Kaloper-Sorbo formulation of the axion coupled to the 3-form gauge field described in section 5.5, these corrections do not appear from higher dimensional operators breaking the shift symmetry. They arise from the fact that the kinetic metric of the 3-form gauge fields is also field dependent (in particular, it depends on the saxions) [57]. When integrating out the 3-form gauge field, the shape of the branches becomes field dependent and can be substantially modified when displacing the inflaton away from the minimum (in a shift invariant way, but potentially dangerous for inflation anyway).

In [45, 64] it was pointed out that the displacement of the saxions will generically backreact on the kinetic metric of the inflaton leading at best to a logarithmic behavior of the proper field distance at large-field. More concretely,

$$\Theta = \int \sqrt{G_{\theta\theta}(s)} d\theta \sim \int \frac{1}{s(\theta)} \sim \frac{1}{\lambda} \log(\theta) \quad (8.1.3)$$

where we have assumed that $K = -\log(s)$ with s being the saxionic partner of the inflaton, and that for large-field excursions $\delta s(\theta) \simeq \lambda\theta$. In (8.1.3), Θ is the canonically normalized inflaton field. This implies that parametrically large displacements are strongly disfavored in string theory, but in principle trans-Planckian field ranges are still possible if $\lambda \ll 1$, so that backreaction effects can be delayed far out in field space. In other words, the field range available before backreaction effects become important and the logarithmic scaling takes place, is given by

$$\Theta_c = \int^{\theta_c} \sqrt{G_{\theta\theta}(s)} d\theta \sim \frac{\theta_c}{s_0} \sim \frac{1}{\lambda} \quad (8.1.4)$$

in Planck units. Here θ_c is the critical value before backreaction effects dominate, which occurs when $\delta s(\theta_c) \simeq s_0$ implying² $\theta_c \simeq s_0/\lambda$. In [44, 45] it was claimed that λ is a flux independent parameter of order one, implying that the backreaction effects are therefore tied to the Planck mass. If this is true in general, it is a very powerful statement which indicates a clear obstruction for having trans-Planckian field ranges.

However, the flux independence of λ was only proved [45] in type IIA flux compactifications where the inflaton belonged to the closed string sector. In [57] a possible loophole involving the open string sector was pointed out (and examined in more detail in [58]). There, the parameter λ is not flux-independent anymore but indeed proportional to the mass hierarchy

²If the Kähler metric for the inflaton depends on more than one saxion, one can extract the value of λ from $G_{\theta\theta}^{-1/2}(s^i) \simeq G_{\theta\theta}^{-1/2}(s_0^i) + \delta G_{\theta\theta}^{-1/2}(s^i(\theta))$ with $\delta G_{\theta\theta}^{-1/2}(s^i(\theta)) \simeq \lambda\theta$ at large-field, and all previous formulae apply.

$M_\Theta/M_{\text{heavy}}$. Therefore a mass hierarchy between the inflaton and the saxions can help to delay the backreaction effects which are not anymore tied to the Planck mass. However, the incorporation of more ingredients to the compactification makes the model more difficult to control, and it is not clear if such a hierarchy can be really achieved in a fully reliable global compactification.

It is the purpose of this chapter to continue the investigation of these models and similar ones, in which λ can depend on the above mass hierarchy. We will see that in some representative models, by setting λ small, we are inevitably also decreasing the Kaluza-Klein scale compared to the moduli mass scale, signaling the breakdown of the effective theory. But before turning to our results, let us discuss in more detail the relation between the logarithmic scaling of the field distance, the breakdown of the effective theory and the swampland distance conjecture.

Refined swampland distance conjecture for axions

Let us remind the reader of the *swampland distance conjecture* [43, 44] which has been extensively reviewed in chapter 6:

For any point p_0 in the continuous scalar moduli space of a consistent quantum gravity theory (the landscape), there exist other points p at arbitrarily large distance. As the distance $d(p_0, p)$ diverges, an infinite tower of states exponentially light in the distance appears, meaning that the mass scale of the tower varies as

$$M \sim M_0 e^{-\alpha d(p_0, p)}. \quad (8.1.5)$$

Thus, the number of states in the tower which are below any finite mass scale diverges as $d \rightarrow \infty$.

Here, the distance is measured with the metric on the moduli space. Moreover, α is a still undetermined parameter that specifies when this behavior sets in, namely beyond $d(p_0, p) \sim \alpha^{-1}$ the exponential drop-off becomes essential. Infinitely many states becoming light beyond a certain distance in field space indicates that the quantum gravity theory valid at the point p_0 only has a finite range d_c of validity in the scalar moduli space. As a consequence any physics that we might derive for larger values $d > d_c$ cannot be trusted.

In this formulation, the flat axion moduli space is assumed to be compact and the logarithmic behavior is expected to hold rather for the saxions. Therefore, it is not immediately clear how this conjecture is related to the question of realizing large-field inflation in string theory. How this proceeds has been suggested in [44, 45] and will also be demonstrated in the very explicit prototype models to be discussed in sections 8.2 and 8.3. Let us already sketch here, how this works.

Say one has managed to stabilize the moduli such that there is only a single light axion Θ with mass M_Θ and a set of heavy other moduli stabilized at M_{heavy} . Then, after integrating

out the heavy moduli one can derive an effective polynomial potential $V_{\text{eff}}(\theta)$ for the light axion, potentially supporting large-field inflation. However, this picture is a bit too naive as we are interested in field excursion of θ that are trans-Planckian. As explained in the previous section, for very large θ one has to take the backreaction of the rolling inflaton onto the other moduli into account. The critical value in proper field space where this behavior becomes essential is $\Theta_c \sim 1/\lambda$ (see eq.(8.1.4)). As discussed above, for field excursions beyond this value, the backreaction causes the following relation between the proper field distance and θ

$$\Theta = \frac{1}{\lambda} \log(\theta) . \quad (8.1.6)$$

Therefore, e.g. Kaluza-Klein modes whose mass scales like $M_{\text{KK}} \sim s(\theta)^{-n} \sim \theta^{-n}$ have the scaling $M_{\text{KK}} \sim \exp(-n\lambda\Theta)$ with respect to the proper field distance. This is precisely the behavior stated in the swampland distance conjecture after identifying

$$\alpha \sim \lambda . \quad (8.1.7)$$

Thus, it seems that the original version of the swampland conjecture can be extended to axion directions upon taking into account backreaction effects. It is this generalization that we consider in this thesis. Notice that this formulation of the conjecture not only implies a constraint on the field metrics but also on the shape of the scalar potentials coming from string theory, since the backreaction on the saxions is crucial to obtain such a logarithmic behavior at large-field.

The essential question now is about the value of λ . The original swampland distance conjecture leaves this open³. The set of examples studied in [45] led the authors to define the so-called *refined swampland distance conjecture* (RSDC), that in addition to the contents of the swampland distance conjecture above states $\alpha = O(1)$. We will see that those examples are only particular cases and that in general one can have

$$\Theta_c \sim \frac{1}{\lambda} \sim \left(\frac{M_{\text{heavy}}}{M_{\Theta}} \right)^p \quad (8.1.9)$$

where $p = 0, 1$ depending on the model under consideration. In particular, the models in [45] satisfy $p = 0$, while $p = 1$ corresponds to the loopholes in [57, 58]. For the latter class of models, if one can manage to dynamically freeze the moduli such that $\lambda < O(1/10)$, then one has control over the effective theory for the required $N_e = 60$ e-foldings. However we will see that for $\lambda \ll 1$ there are other reasons beyond the exponential drop-off, why the effective theory fails.

³For an axion, the WGC implies $f S_{\text{inst}} \leq 1$ which can be rewritten in the presence of supersymmetry in terms of the saxionic partner φ as $\sqrt{G_{\varphi\varphi}} \varphi \leq 1$ [45]. After integration one gets

$$\int \sqrt{G_{\varphi\varphi}} d\varphi \leq \int \frac{1}{\varphi} d\varphi \iff \phi \leq \log \varphi , \quad (8.1.8)$$

i.e. the proper field distance grows at best logarithmically as $\phi_c \log \varphi$ with $\phi_c = O(1)$.

8.2 Closed String Model

In this section, we revisit a simple prototype model [32, 64] of closed string moduli stabilization, analyze its relation to the swampland distance conjecture and how this restricts the potential to provide a controllable string (inspired) model of F-term axion monodromy inflation.

In [64] it was found that the considered single field inflationary models with a parametrically light axion fail to also preserve the required hierarchy of mass scales, thus spoiling parametric control over the employed effective action. This perfectly matches with the results found in [45, 57] for their IIA counterparts. Within the closed string sector of IIA flux compactifications with RR and NS fluxes, it is not possible to get the mass hierarchy required to suppress backreaction, implying that one always gets a flux-independent $\lambda \sim \mathcal{O}(1)$. Therefore, we do not expect these closed string IIB models to work either. However, they are a perfect playground to exemplify the backreaction problems and the relation to the swampland distance conjecture. Therefore, instead of analyzing an exhaustive list of elaborated models, we will choose the simplest one and discuss the problems arising when trying to drive inflation in the regime $\Theta > \Theta_c$.

Let us now consider the most simple model of tree-level flux induced moduli stabilization, i.e. a flux-scaling scenario as introduced in section 4.3.3. More precisely, we take only the two always present moduli into account, the axio-dilaton $S = s + ic$ and the overall volume modulus $T = \tau + i\rho$ in accordance with table 2.3. This exactly solvable example already reveals the main problem with achieving large-field inflation for F-term axion monodromy. It can be thought of as an isotropic T^6 with frozen complex structure modulus. Note that we will later refer to this model as C1 for closed string model one.

Moduli stabilization, masses and backreaction

At large values of the saxions (s, τ) , the Kähler potential at leading order is given by

$$K = -\log(S + \bar{S}) - 3\log(T + \bar{T}), \quad (8.2.1)$$

and the flux-induced superpotential (4.1.15) is chosen to be

$$W = -if_0 + ihS + iqT. \quad (8.2.2)$$

The resulting scalar potential (4.1.16) reads

$$V = \frac{(hs + f_0)^2}{16s\tau^3} - \frac{6hqs - 2qf_0}{16s\tau^2} - \frac{5q^2}{48s\tau} + \frac{\theta^2}{16s\tau^3} \quad (8.2.3)$$

with the linear combination $\theta = hc + q\rho$. This field will be our inflaton candidate. There exists a non-supersymmetric, tachyon-free AdS minimum (cf. section 4.3.3)

$$\tau_0 = \frac{6f_0}{5q}, \quad s_0 = \frac{f_0}{h}, \quad \theta_0 = 0. \quad (8.2.4)$$

The masses for the canonically normalized fields are

$$M_{\text{mod},i}^2 = \nu_i \frac{h q^3}{f_0^2}, \quad (8.2.5)$$

with $\nu \in \{0, 0.43, 0.21, 0.78\}$. The cosmological constant in the minimum is $V_0 = -\frac{25}{216} \frac{h q^3}{f_0^2}$.

Thus, the mass of the axion θ is parametrically of the same order as the masses of the two saxions. Comparing to section 8.1, this means that $\lambda = O(1)$ and the backreaction should set in right at the Planck-scale. Indeed, for field excursions in the direction θ , the backreaction on the saxions can be exactly solved and gives

$$\begin{aligned} \tau_0(\theta) &= \frac{3}{20q} \left(4f_0 + \sqrt{10\theta^2 + 16f_0^2} \right), \\ s_0(\theta) &= \frac{1}{4h} \sqrt{10\theta^2 + 16f_0^2}. \end{aligned} \quad (8.2.6)$$

Looking at the discriminant, it is clear that beyond the critical field-value $\theta_c = \sqrt{\frac{8}{5}} f_0$ the backreaction becomes substantial. The kinetic term for θ is

$$\mathcal{L}_{\text{kin}}^{\text{ax}} = \frac{3}{4(3h^2 s^2 + q^2 \tau^2)} \partial_\mu \theta \partial^\mu \theta, \quad (8.2.7)$$

implying that for $\theta < \theta_c$ the canonically normalized axion is $\Theta = \frac{5}{\sqrt{74}} \frac{\theta}{f_0}$. The critical proper field distance is flux independent $\Theta_c = \sqrt{\frac{20}{37}} \approx 0.73$, i.e. for the canonically normalized axion the backreaction becomes substantial right at the Planck-scale. The backreacted potential as a function of the proper field distance is shown in figure 8.1. Note that we added a constant uplift.

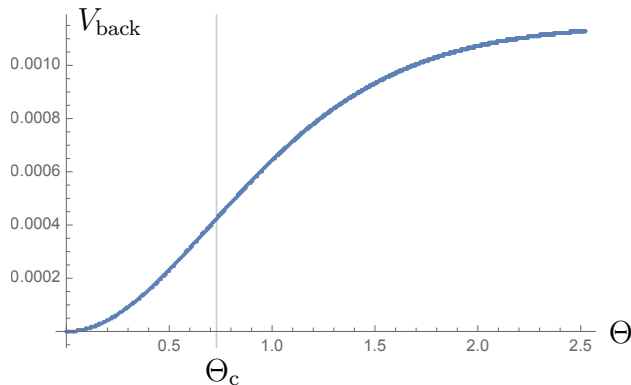


Figure 8.1: The backreacted potential $V_{\text{back}}(\Theta)$ (after adding a constant uplift) depending on the proper field distance.

It is evident that beyond Θ_c the potential is not any more of quadratic form and therefore one cannot realize large-field inflation. Indeed, in the trans-Planckian regime one finds

$$\mathcal{L}_{\text{kin}}^{\text{ax}} = \frac{2}{\gamma^2} \left(\frac{\partial \theta}{\theta} \right)^2, \quad (8.2.8)$$

with $\gamma = 2\sqrt{\frac{7}{5}}$. The canonically normalized field can be defined as

$$\Theta = \frac{2}{\gamma} \log \left(\frac{\theta}{2\theta_c} \right). \quad (8.2.9)$$

This is precisely the logarithmic behavior (8.1.6) satisfying $\lambda \sim \mathcal{O}(1)$ expected from the refined swampland distance conjecture. After assuming a constant uplift by $|V_0|$, the scalar potential reads

$$V_{\text{back}}(\Theta) = |V_0| \left[1 - \left(\frac{2\theta_c}{\theta} \right)^2 \right] = |V_0| \left[1 - e^{-\gamma\Theta} \right]. \quad (8.2.10)$$

Like the Starobinsky model of section 5.2.1, V_{back} is a plateau potential for $\Theta > \Theta_c$.

Therefore, the strong backreaction led to a significant flattening of the potential, the initial quadratic potential of the axion became plateau-like. If $H_{\text{inf}} < M_{\text{mod}} < M_{\text{KK}}$ could be parametrically guaranteed, the potential (8.2.10) by itself could still support inflation with a resulting lower value of the tensor-to-scalar ratio

$$r = \frac{8}{(\gamma N_e)^2} \sim O(10^{-3}). \quad (8.2.11)$$

This looks promising at a first glance, but as we work just at the limit of having control, there are three serious caveats:

- In the trans-Planckian regime, the Kaluza-Klein masses show the expected exponential drop-off

$$M_{\text{KK}} \sim \frac{1}{\tau} \sim \frac{q}{f_0} \exp \left(-\frac{\gamma}{2} \Theta \right), \quad (8.2.12)$$

while the inflationary mass scale $M_{\text{inf}} = |V_0|^{\frac{1}{4}}$ stays constant on the plateau. Using the relation $V_0 = 3M_{\text{Pl}}^2 H_{\text{inf}}^2$, one finds for the ratio

$$\frac{M_{\text{KK}}}{H_{\text{inf}}} \sim \frac{1}{(qh)^{\frac{1}{2}}} \exp \left(-\frac{\gamma}{2} \Theta_* \right). \quad (8.2.13)$$

Thus we parametrically get $H_{\text{inf}} \gtrsim_p M_{\text{KK}}$ so that we are outside the regime of controlling the effective action.

- We were assuming here a constant uplift potential, which is however not realistic, as in string theory all known potentials drop-off at infinity. The task then is to identify a realistic uplift term that still admits the plateau up to the pivot scale before it drops-off towards larger values for the inflaton. This issue will be addressed below in section 8.2.

- Since the mass of the inflaton candidate is of the same scale as the mass of the other moduli, the latter cannot really be integrated out and one has to treat the model in the framework of multifield inflation. This will affect the trajectory and the scalar potential along it.

Thus, this example confirms in an analytically deducible way the statement of the *refined swampland distance conjecture* even for the case of axionic fields with a shift symmetry. It is the backreaction onto the saxionic fields that limits the parametrically controllable field range to be smaller than the Planck-scale. We have also identified a tower of Kaluza-Klein modes that become exponentially light in the trans-Planckian regime. Hence, even Starobinsky-like inflation on a sufficiently broad plateau is not under parametric control.

As we will explain next, to get such a plateau is also challenged from another perspective, namely by considering more realistic (non-constant) uplift terms. This latter point has also been observed in [184] for a class of models including instanton contributions, like for KKLT or the Large Volume Scenario.

A semi-realistic uplift

So far we were just assuming a constant uplift. Due to the backreaction this implied to a constant plateau for $\Theta \rightarrow \infty$. For models with a realistic uplift potential, like $\overline{D3}$ branes in a warped throat, such a behavior will not happen. Instead there will be another critical value Θ_{up} beyond which the uplift term dominates the backreaction.

For the simple closed string model from section 8.2, it is found that an uplift potential via $\overline{D3}$ branes in a warped throat

$$V_{\overline{D3}} = \frac{\epsilon}{\tau^2} \tag{8.2.14}$$

does not work as the full potential $V_F + V_{\overline{D3}}$ does not admit tachyon-free Minkowski-minima (after fine-tuning of the warp factor ϵ). In principle, an assumed uplift potential

$$V_{\text{up}} = \frac{\epsilon}{s} \tag{8.2.15}$$

works much better⁴. Here, the full potential provides a tachyon-free Minkowski-minimum for the values

$$\tau_0 = \frac{3\mathfrak{f}_0}{2q}, \quad s_0 = \frac{7\mathfrak{f}_0}{2h}, \quad \theta_0 = 0, \quad \epsilon = \frac{2q^3}{9\mathfrak{f}_0}. \tag{8.2.16}$$

Note that in the perturbative regime ϵ becomes small. The masses for the canonically normalized fields scale in the same way as in the non-supersymmetric AdS minimum

$$M_{\text{mod},i}^2 = \nu_i \frac{hq^3}{\mathfrak{f}_0^2}, \tag{8.2.17}$$

⁴We do not know which string theoretic, supersymmetry breaking object can lead to this functional form of an uplift potential.

with $\nu \in \{0, 0.55, 0.10, 0.87\}$.

When computing the backreaction of a large-field excursion of θ onto the saxions, one finds that the scaling (8.2.6) only holds up to a threshold scale

$$\theta_{\text{up}} \approx 2 f_0, \quad (8.2.18)$$

above which the uplift term becomes dominant. The consequence of this behavior is that for values $\theta > \theta_{\text{up}}$, the local minimum for the saxions is not present any more, i.e. the valley one is following up comes to an end at θ_{up} . This is shown for a concrete choice of fluxes in figure 8.2. In this example, the critical scale θ_{up} is between θ_c (the convex-concave turning

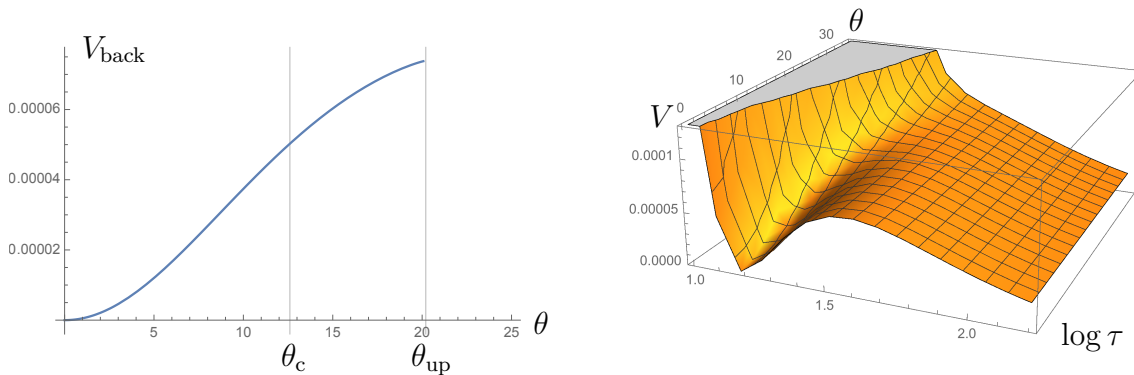


Figure 8.2: We plotted on the left the backreacted potential $V_{\text{back}}(\theta)$ including the uplift and on the right a slice of the potential $V(\theta, s_0(\tau), \tau)$. Both pictures show the destabilization of the inflationary valley.

scale of the potential) and the scale where one reaches the top of the plateau. Therefore, for this more realistic non-constant uplift potential, including the backreaction, one can never reach the top of the plateau. Of course, this is just a simple model but, together with the observations made in [184], we think that it exemplifies another generic obstacle to realize plateau-like large-field inflation in string theory. We will come back to this point when we discuss large-field inflation in KKLT and large volume scenario in section 8.3.4.

Therefore, it seems clear that one cannot drive inflation in the regime $\Theta > \Theta_c$. After having familiarized ourselves with the relevant issues that appear when one wants to realize large-field inflation in a controlled manner, let us now challenge the *refined swampland distance conjecture* by trying to follow a recent idea on how one could achieve a trans-Planckian critical field value $\Theta_c \gg 1$ by introducing open string fields. Notice that we also found a closed string model showing this feature when incorporating an axionic odd G modulus. As it turned out, this model suffers, however, from the same issues which we will describe in the next section about open string moduli.

8.3 Open String Models

The example in the previous section featured $\Theta_c = \mathcal{O}(1)$, providing support for the refined swampland distance conjecture. In this example, Θ_c was flux independent and we had no chance to tune it larger. The aim of this central section is to provide examples involving brane deformation moduli that admit an in principle tunable flux dependent Θ_c .

8.3.1 Superpotential for Brane Deformations

It was argued in [61, 62] that D7-brane position moduli give rise to a superpotential of the form

$$W \supset \mu \Phi^2. \quad (8.3.1)$$

Its microscopical origin can be deduced from reducing the DBI and Chern-Simons actions of the D7-brane or from the T-dual type IIA description with D6-branes [58, 159]. Additional motivation of this superpotential arises from F-theory where complex structure and D7 position moduli are put on an equal footing. For our examples it is crucial that the factor μ is quantized. Hence, let us elucidate the form of the superpotential in more detail.

Recall that the D7-brane is wrapping a homological 4-cycle C_4 in a Calabi-Yau three-fold ambient space \mathcal{M} and is embedded via a map $\iota : C_4 \rightarrow \mathcal{M}$. In the perturbative type IIB superstring theory the relevant F-term potential is (see e.g. [185])

$$W_o = \int_{\Gamma_5} \Omega_3 \wedge (\iota^* B_2 + F) + \Delta W_o \quad (8.3.2)$$

where Γ denotes the 5-chain swept out by pulling the D7-brane off the orientifold $O7$ -plane. Moreover, $\iota^* B_2$ denotes the pull-back of the ambient NS-NS 2-form B_2 onto the world-volume of the D7-brane. The gauge field strength F on the brane can be expanded into a basis of $H^2(C_4, \mathbb{Z})$ and splits into 2-cocycles that are pull-backs from 2-cocycles on \mathcal{M} and those whose push-forward to \mathcal{M} is trivial, i.e. $F = F^{\mathcal{M}} + \tilde{F}$.

Clearly, Γ_5 depends on the deformation moduli⁵ [76] $\Phi \in H^0(C_4, N_{C_4}) = H^{2,0}(C_4, \mathbb{Z})$ and the induced obstruction appears when by pulling off the brane from the $O7$ -plane a $(0, 2)$ -component of $\mathcal{F} = (\iota^* B_2 + F)$ is generated. Since the Calabi-Yau ambient space itself generically does not have any closed $(0, 2)$ -form, this can only happen if $dB_2 = H \neq 0$ or for the flux components \tilde{F} that are cohomologically trivial on \mathcal{M} . In a toroidal set-up, the generation of such an obstruction via a non-trivial H -flux was demonstrated explicitly in [186]. The discussion of the \tilde{F} fluxes appeared in [83] and for toroidal configurations does not provide a contribution to W_o .

⁵Note that there are no $(1, 1)$ -forms in the massless spectrum of a $D7$ -brane.

Note that in type IIB the co-chain ι^*B_2 (for $H = dB_2$) is not necessarily quantized as an integer. It was argued in [61] that by taking the weak coupling limit of F-theory, an additional term

$$\Delta W_o = \frac{i}{2\pi} \int_{\mathcal{M}} H \wedge \log \left(\frac{P_{D7}}{P_{O7}} \right) \Omega_3 \quad (8.3.3)$$

appears. Here P_{D7} and P_{O7} are polynomials in the coordinates on the base that vanish at the location of the D7-branes and O7-planes, respectively. In particular, they depend on the complex structure and brane moduli. They arise due to the fact that in F-theory the axio-dilaton is not constant but

$$\tau = \tau_0 + \frac{i}{2\pi} \log \left(\frac{P_{D7}}{P_{O7}} \right) \quad (8.3.4)$$

in the orientifold limit. In F-theory all fluxes reside in $G_4 \in H^4(Y, \mathbb{Z})$ and are quantized. Therefore, the extra term ΔW_o in the type IIB superpotential can be considered to be necessary for compensating the non-quantization of the term involving ι^*B_2 .

Thus, the naive type IIB superpotential (that treats the brane as a probe, thus ignoring backreaction effects) presumably admits non-quantized open string fluxes, whereas in the full F-theory treatment the quantization of all open and closed string fluxes is manifest.

Since the Kähler potential that we use is motivated by a single D7-brane wrapping the isotropic T^6 , let us lay out what the form of the superpotential could be.

Superpotential for a D7-brane on a six-torus

Consider a $T^6 = (T^2)^3$ and on each T^2 we introduce a complex structure $z_a = x_a + iU_a y_a$ with $a = 1, 2, 3$ according to (2.1.1). Moreover, we introduce a D7-brane wrapping the first two T^2 factors. Since this brane does not contain any 2-cycles that are trivial in the bulk T^6 , the only source for a brane superpotential is a non-vanishing H -flux. Such a flux will however generate both a bulk and a brane superpotential.

Using the conventions and techniques from [186], let us see what type of terms can in principle be generated. Turning on the general H_3 form flux

$$\begin{aligned} H = & h_0 dy_1 \wedge dy_2 \wedge dy_3 + \\ & h_1 dx_1 \wedge dy_2 \wedge dy_3 + h_2 dy_1 \wedge dx_2 \wedge dy_3 + h_3 dy_1 \wedge dy_2 \wedge dx_3 + \\ & \tilde{h}_1 dy_1 \wedge dx_2 \wedge dx_3 + \tilde{h}_2 dx_1 \wedge dy_2 \wedge dx_3 + \tilde{h}_3 dx_1 \wedge dx_2 \wedge dy_3 + \\ & \tilde{h}_0 dx_1 \wedge dx_2 \wedge dx_3, \end{aligned} \quad (8.3.5)$$

introduces a bulk superpotential

$$\begin{aligned} W_b = & \left(h_0 - ih_1 U_1 - ih_2 U_2 - ih_3 U_3 - \tilde{h}_1 U_2 U_3 \right. \\ & \left. - \tilde{h}_2 U_1 U_3 - \tilde{h}_3 U_1 U_2 + i\tilde{h}_0 U_1 U_2 U_3 \right) iS. \end{aligned} \quad (8.3.6)$$

Here all fluxes are integers and, since the H -fluxes do have one leg on each T^2 factor, the Freed-Witten anomaly cancellation condition $\int_{D7} H = 0$ is satisfied. In order to find the open string superpotential, we restrict the 3-form onto the brane-worldvolume

$$B_{D7} = h_0 y_3 dy_1 \wedge dy_2 + \dots + \tilde{h}_0 x_3 dx_1 \wedge dx_2. \quad (8.3.7)$$

Now, we have to check whether this contains a $(0, 2)$ component. Indeed, we find

$$B_{D7}^{(0,2)} = \omega^{(0,2)} \left[\frac{\partial_S W_b}{2\text{Re}(U_3)} (\Phi - \bar{\Phi}) + \left(-h_3 + i\tilde{h}_1 U_2 + i\tilde{h}_2 U_1 + \tilde{h}_0 U_1 U_2 \right) \Phi \right] \quad (8.3.8)$$

where $\Phi = z_3$ and

$$\omega^{(0,2)} = \frac{d\bar{z}_1 d\bar{z}_2}{4 \text{Re}(U_1) \text{Re}(U_2)} \quad (8.3.9)$$

denotes the $(0, 2)$ -form on the worldvolume of the D7-brane. On the supersymmetric locus $\partial_S W = 0$ the $(0, 2)$ component of B_2 depends holomorphically on the brane position as

$$B_{D7}^{(0,2)} = \left(-h_3 + i\tilde{h}_1 U_2 + i\tilde{h}_2 U_1 + \tilde{h}_0 U_1 U_2 \right) \Phi \omega^{(0,2)}. \quad (8.3.10)$$

Therefore, the brane position is frozen at $\Phi = 0$. In the full F-theory picture, where the brane is not treated as a probe in a supersymmetric bulk, the bulk/brane superpotential is expected⁶ to read

$$W_{\text{tot}} = ih_0 S + h_1 U_1 S + h_2 U_2 S + h_3 (U_3 S - \Phi^2) - i\tilde{h}_1 U_2 (U_3 S - \Phi^2) - i\tilde{h}_2 U_1 (U_3 S - \Phi^2) - \tilde{h}_3 U_1 U_2 S - \tilde{h}_0 U_1 U_2 (U_3 S - \Phi^2). \quad (8.3.11)$$

As we want to deal with the most simple model, we restrict this to the isotropic torus. We do this in two steps. First we set all complex structures to be equal, $U_1 = U_2 = U_3 \equiv U$. Then (8.3.11) becomes

$$W_{\text{tot}} = ih_0 S + (h_1 + h_2 + h_3) U S - h_3 \Phi^2 - i(\tilde{h}_1 + \tilde{h}_2 + \tilde{h}_3) U^2 S + i(\tilde{h}_1 + \tilde{h}_2) U \Phi^2 - \tilde{h}_0 (U^3 S - U^2 \Phi^2). \quad (8.3.12)$$

Still treating the various fluxes as independent parameters, the coefficients of e.g. the US -term and the C^2 -term could be disentangled. In the following, we will call this the *weakly isotropic* torus. In section 8.3.2, we will present an exactly solvable toy model of this type. Since it has the advantage of being exactly solvable, many of the issues about large-field excursions can be seen very explicitly.

⁶The quadratic form is motivated by the supersymmetry condition $D_\Phi W_{\text{tot}}|_{\Phi=0} = \partial_\Phi W_{\text{tot}}|_{\Phi=0} = 0$.

However, thinking of the isotropic torus as proper Calabi-Yau with only one complex structure modulus, one would not expect to have more components of the H -flux available than the number of three cycles, that would be $b_3 = 4$. This is the reason why for the *strongly isotropic* torus, we also restrict the fluxes to be symmetric, i.e. $h_1 = h_2 = h_3 \equiv \mu_1$, $\tilde{h}_1 = \tilde{h}_2 = \tilde{h}_3 \equiv \mu_2$ and $\tilde{h}_0 \equiv \mu_3$. In this case the superpotential (8.3.11) becomes

$$W_{\text{tot}} = ih_0 S + \mu_1(3US - \Phi^2) - i\mu_2(3U^2S - 2U\Phi^2) - \mu_3(U^3S - U^2\Phi^2) \quad (8.3.13)$$

and a $U^n\Phi^2$ term is always accompanied by a corresponding $U^{n+1}S$ term. We will also discuss examples of this more realistic type in section 8.3.3.

Criteria for models with tunable Θ_c

The purpose of introducing open string fields relies on extending our analysis to models with a tunable flux-dependent critical value Θ_c . Then, one might be able to delay the backreaction and the consequent exponential drop-off of the massive states to a trans-Planckian value for the inflaton $\Theta_c > 1$. As first remarked in [57], this requires the minimum of the potential to satisfy the following condition:

Θ_c will be tunable if one can set the inflaton mass to zero without destabilizing the other scalars.

In other words, one needs to engineer a flat direction which is stabilized by an additional subleading flux μ in a second step. The new minimum will correspond then to the old minimum (without the inflaton) corrected by a term proportional to μ . This is precisely the approach that was also followed in [33] and for the *flux scaling models* considered in [32]. It turns out that the backreacted minima for the saxions - once we move the inflaton away from its minimum - take the following schematic form,

$$s = s_0 + \delta s(\theta), \quad \delta s(\phi) \simeq \lambda \theta \quad (8.3.14)$$

with λ depending on the mass hierarchy as $\lambda \sim (M_\Theta/M_{\text{heavy}})^p$. In the closed string models of section 8.2 and those first analyzed in [45], the above condition is not satisfied since the value of s_0 blows up in the limit $\mu \rightarrow 0$. In those models, the critical canonical field distance before the logarithmic behavior dominates is inevitably fixed at $\Theta_c = \lambda^{-1} = \mathcal{O}(1)$ in Planck units (or equivalently $p = 0$). The inclusion of open string fields allows us to engineer models with $p = 1$ that satisfy the previous condition.

Let us consider the flux superpotential (8.3.13) of the effective theory of a D7-brane living in a strongly isotropic torus derived in the previous section. Every term Φ^2 is accompanied by a bulk term SU . This implies that the only superpotential term for the dilaton which is independent of Φ is the linear term ih_0S . Therefore, we need to have $h_0 \neq 0$ in order to stabilize the dilaton while keeping $\theta = \text{Im}(\Phi)$ massless. We also assume that there are some RR fluxes stabilizing the complex structure modulus U and a non-geometric flux stabilizing T via a superpotential term iqT . We are left then with two possibilities:

- $\mu_1 \neq 0$ and/or $\mu_3 \neq 0$:

As a consequence the superpotential mixes real and imaginary parts of the moduli differently (i.e. even and odd powers of the fields), e.g.

$$W = ihS + \mu_1(3US - \Phi^2) + \dots \quad (8.3.15)$$

The new minimum cannot be understood as a deformation of the old minimum proportional to μ_1 . In particular, the orthogonal direction to the axionic combination $\sigma_0 = hc_0 + q\rho_0$ remains unfixed in the old minimum and gets a vacuum expectation value in the new minimum proportional to μ_1^{-1} . This modifies the vevs of the saxions leading to the same parametric dependence on μ_1^{-1} , so that we do not recover the old minima when setting $\mu_1 = 0$. The strong backreaction then implies $\lambda \sim \mathcal{O}(1)$ independently of the flux choice. A solution comes from adding a term $q_1 UT$ with the non-geometric flux satisfying $q_1 = q\mu_1/h$, which vanishes when μ_1 goes to zero. In this way, the problematic axionic direction remains unfixed and the new minimum is simply a deformation of the old minimum, giving rise to a good candidate for having a flux-tunable λ .

- $\mu_1 = \mu_3 = 0$:

The only possibility to stabilize the open string modulus is now to turn on μ_2 , hence

$$W = ihS + i\mu_2 U(3US - 2\Phi^2) + \dots \quad (8.3.16)$$

This model enters within the class of *flux-scaling models* analyzed in [32]. The new minimum can be understood as a deformation of the old minimum which goes to zero when μ is vanishing. This model is thus a good candidate to obtain a λ depending on the flux-tunable mass hierarchy.

For later convenience, we dub the first model with $\mu_1, q_1 \neq 0$ as O2 and analyze it further in section 8.3.3. Let us remark, though, that we get the same conclusions from analyzing the model with $\mu_2 \neq 0$ and we do not include the explicit analysis simply to avoid cluttering and repetition of results. We will also analyze an extension of O2 by having both μ_1 and μ_3 non-vanishing. This allows us to discuss an example in which the μ -parameter entering on λ is not a flux integer but an effective parameter depending also on field vacuum expectation values. Notice that the other possibility, having both μ_1 and μ_2 non-vanishing, does not really lead to an effective parameter. This is due to the relative factor of $i = \sqrt{-1}$ in the superpotential.

In addition, one can also consider the weakly isotropic torus (8.3.12) which allows us to drop the condition of having the same flux parameter for the SU and Φ^2 terms. In this manner we can stabilize the dilaton independently of the inflaton, without the need of a linear term ihS . The new minimum will be a deformation of the old minimum, yielding a good candidate for having again a tunable flux-dependent λ . Due to its computational

simplicity, we will first analyze this model, dubbed as $O1$, in section 8.3.2, and leave the model $O2$ for section 8.3.3.

Our analysis will show that, in spite of having in principle a tunable flux dependent λ , the flux choice required to delay backreaction cannot be done without losing parametric control of the effective theory. In particular, by requiring a mass hierarchy leading to $\lambda < 1$, the moduli masses become heavier than the Kaluza-Klein scale.

8.3.2 Toy Model O1

Consider now the so-called STU -model extended by a complex open string modulus Φ that parametrizes the transversal deformation of the D7-brane. Here the four complex moduli are

$$S = s + ic, \quad T = \tau + i\rho, \quad U = u + iv, \quad \Phi = \varphi + i\theta \quad (8.3.17)$$

where the imaginary parts are axion-like scalars. At large values of the saxions (s, τ, u) , the Kähler potential at leading order is given as

$$K = -3 \log(T + \bar{T}) - 2 \log(U + \bar{U}) - \log \left[(S + \bar{S})(U + \bar{U}) - \frac{1}{2}(\Phi + \bar{\Phi})^2 \right]. \quad (8.3.18)$$

As we have seen, the model could be realized as a D7-brane wrapping a 4-cycle T^4 on an isotropic $T^6 = (T^2)^3$. Now we turn on fluxes to generate the superpotential

$$W = f_0 + 3f_2 U^2 - h S U - q T U - \mu \Phi^2. \quad (8.3.19)$$

Note that for the *strongly isotropic* torus, the fluxes h and μ would not be independent. Thus, this model only makes sense for the *weakly isotropic* torus and could therefore still be in the swampland. Nevertheless, as we will see, it reveals many interesting features and hence is a very good toy model to sharpen our tools. Furthermore, in a more complicated Calabi-Yau, one could aim to disentangle the h and μ fluxes via additional bilinear couplings of the dilaton to other complex structure moduli that contribute to the first but not to the second one. Therefore, it is a good candidate to exemplify the problems arising even if one manages to get $h \neq \mu$. Let us mention that this model is related via mirror-symmetry to a type IIA model with only geometric fluxes ⁷.

⁷Applying three T-dualities in the three x -directions (of $(T^2)^3$), one gets a type IIA flux model, where the $D7$ becomes a $D6$ -brane and the complex structure moduli get exchanged with the Kähler moduli. The Kähler potential reads

$$K = -3 \log(U + \bar{U}) - 2 \log(T + \bar{T}) - \log \left[(S + \bar{S})(T + \bar{T}) - \frac{1}{2}(\Phi + \bar{\Phi})^2 \right]. \quad (8.3.20)$$

Moduli stabilization and masses

This model admits an analytically solvable non-supersymmetric tachyon-free AdS minimum at

$$\begin{aligned} s_0 &= \frac{2^{\frac{7}{4}} \cdot 3^{\frac{1}{2}} (\mathfrak{f}_0 \mathfrak{f}_2)^{\frac{1}{2}}}{5^{\frac{1}{4}} h}, & \tau_0 &= \frac{5^{\frac{3}{4}} \cdot 3^{\frac{1}{2}} (\mathfrak{f}_0 \mathfrak{f}_2)^{\frac{1}{2}}}{2^{\frac{1}{4}} q} \\ u_0 &= \frac{1}{10^{\frac{1}{4}} \cdot 3^{\frac{1}{2}}} \left(\frac{\mathfrak{f}_0}{\mathfrak{f}_2} \right)^{\frac{1}{2}}, & \varphi_0 &= 0 \end{aligned} \quad (8.3.22)$$

$$v_0 = hc_0 + q\rho_0 = \theta_0 = 0,$$

leaving one axionic direction unconstrained. The value of the scalar potential in the AdS minimum is

$$V_0 = -\frac{1}{120 \cdot 3^{\frac{1}{2}} \cdot 10^{\frac{1}{4}} \mathfrak{f}_0^{\frac{3}{2}} \mathfrak{f}_2^{\frac{1}{2}}} \frac{h q^3}{\mathfrak{f}_0^{\frac{3}{2}} \mathfrak{f}_2^{\frac{1}{2}}}. \quad (8.3.23)$$

For the canonically normalized mass-matrix we obtain

$$M_{\text{closed}}^2 = \nu_i \frac{h q^3}{\mathfrak{f}_0^{\frac{3}{2}} \mathfrak{f}_2^{\frac{1}{2}}} \quad (8.3.24)$$

with $\nu \in \{0, 0.0001, 0.0019, 0.0029, 0.0117, 0.0162\}$ and

$$\begin{aligned} M_\phi^2 &= 0.0022 \left[1 + 14 \frac{\mu}{h} + 24 \left(\frac{\mu}{h} \right)^2 \right] \frac{h q^3}{\mathfrak{f}_0^{\frac{3}{2}} \mathfrak{f}_2^{\frac{1}{2}}} \simeq 0.0022 \frac{h q^3}{\mathfrak{f}_0^{\frac{3}{2}} \mathfrak{f}_2^{\frac{1}{2}}} \\ M_\theta^2 &= 0.0065 \mu \frac{(3.1623 + 8 \frac{\mu}{h}) q^3}{\mathfrak{f}_0^{\frac{3}{2}} \mathfrak{f}_2^{\frac{1}{2}}} \simeq 0.0205 \frac{\mu q^3}{\mathfrak{f}_0^{\frac{3}{2}} \mathfrak{f}_2^{\frac{1}{2}}} \end{aligned} \quad (8.3.25)$$

where on the right hand side we assumed $\mu/h \ll 1$. Therefore, in this regime the open string axion θ is *parametrically* lighter than all the other massive moduli, indeed

$$\frac{M_{\text{heavy}}}{M_\Theta} \sim \sqrt{\frac{h}{\mu}} = \lambda^{-1}. \quad (8.3.26)$$

Comparing this to the relation (8.1.9) from the general discussion of the swampland distance conjecture, one expects that $\lambda = \sqrt{\mu/h}$ is the now flux dependent parameter that controls the backreaction of the inflaton onto the other moduli.

and the superpotential

$$W = \mathfrak{f}_6 + 3\mathfrak{f}_2 T^2 - f_0 ST - f_1 UT - \mu \Phi^2. \quad (8.3.21)$$

Here \mathfrak{f}_6 denotes a R-R 6-form flux, \mathfrak{f}_2 a R-R 2-form flux and f_i geometric fluxes.

Backreaction

Since this model features a parametrically light axion mass, we expect that the backreaction in the slow-roll regime is also under control. Let us analyze this in more detail under the assumption $\lambda \ll 1$. Up to subleading corrections of order $\mathcal{O}(\lambda^2)$, the conditions for the backreacted minima can be solved

$$\begin{aligned} s_0(\theta) &\sim \frac{2^{\frac{7}{4}} 3^{\frac{1}{2}} (f_0 + \mu\theta^2)^{\frac{1}{2}} f_2^{\frac{1}{2}}}{5^{\frac{1}{4}} h}, & \tau_0(\theta) &\sim \frac{5^{\frac{3}{4}} 3^{\frac{1}{2}} (f_0 + \mu\theta^2)^{\frac{1}{2}} f_2^{\frac{1}{2}}}{2^{\frac{1}{4}} q} \\ u_0(\theta) &\sim \frac{1}{10^{\frac{1}{4}} 3^{\frac{1}{2}}} \left(\frac{f_0 + \mu\theta^2}{f_2} \right)^{\frac{1}{2}} \end{aligned} \quad (8.3.27)$$

with all other fields sitting in their minimum at zero. Thus, the critical value of θ where the backreaction becomes significant is

$$\theta_c = \sqrt{\frac{f_0}{\mu}}. \quad (8.3.28)$$

The kinetic term for the inflaton becomes

$$\mathcal{L}_{\text{kin}}^{\text{ax}} = K_{\Phi\bar{\Phi}} \partial_\mu \theta \partial^\mu \theta = \frac{1}{8} \sqrt{\frac{5}{2}} \frac{h}{f_0 + \mu\theta^2} (\partial\theta)^2 \quad (8.3.29)$$

so that the critical value for the canonically normalized inflaton field Θ is

$$\Theta_c = \gamma \sqrt{\frac{h}{f_0}} \theta_c = \gamma \sqrt{\frac{h}{\mu}} = \gamma \lambda^{-1} \quad (8.3.30)$$

with $\gamma = \frac{1}{2} \left(\frac{5}{2}\right)^{\frac{1}{4}} = 0.63$. Therefore, from this perspective, for $\lambda \ll 1$ and $\Theta \ll \Theta_c$ the backreaction can be neglected and one gets the effective potential for the inflaton (after adding a constant uplift)

$$V_{\text{eff}} \simeq \frac{\mu h q^3}{f_0^{\frac{7}{2}} f_2^{\frac{1}{2}}} (2f_0\theta^2 + \mu\theta^4) \simeq \frac{\mu h q^3}{f_0^{\frac{5}{2}} f_2^{\frac{1}{2}}} \theta^2 \simeq \frac{\mu q^3}{f_0^{\frac{3}{2}} f_2^{\frac{1}{2}}} \Theta^2. \quad (8.3.31)$$

Note that the quartic term is parametrically suppressed by a factor θ^2/θ_c^2 relative to the quadratic one. Thus, it seems that by parametrically choosing $\Theta_c \sim \lambda^{-1} > 10$ one can achieve a stringy model featuring large-field inflation with a quadratic potential. This is consistent with the observation already made in [58] for a more complicated, only numerically treatable open string model (without non-geometric fluxes).

Beyond the critical value, the kinetic term for the inflaton takes the form

$$\mathcal{L}_{\text{kin}}^{\text{ax}} = \frac{1}{8} \sqrt{\frac{5}{2}} \frac{h}{\mu} \left(\frac{\partial\theta}{\theta} \right)^2 \quad (8.3.32)$$

so that the canonically normalized inflaton shows the logarithmic behavior

$$\Theta = \Theta_c \log \left(\frac{\theta}{\theta_c} \right) \simeq \frac{1}{\lambda} \log \theta \simeq \frac{M_{\text{heavy}}}{M_\Theta} \log \theta. \quad (8.3.33)$$

Let us mention that, in this regime, the backreacted scalar potential (after constant uplift) becomes

$$V_{\text{back}} \simeq |V_0| \left[1 - \left(\frac{\theta_c}{\theta} \right)^3 \right] = |V_0| \left[1 - \exp \left(-3 \frac{\Theta}{\Theta_c} \right) \right]. \quad (8.3.34)$$

Thus, in this large-field regime $\Theta \gg \Theta_c$ the backreacted potential is not polynomial but of Starobinsky-like type.

Mass scales and the swampland distance conjecture

From the previous section, the model seems promising to realize large-field inflation with an effective quadratic potential once we are able to choose the fluxes such that $\Theta_c \sim \lambda^{-1} \gg 1$ and $\Theta < \Theta_c$. Thus we need $h/\mu = \mathcal{O}(10^2)$. This could easily be achieved, if the flux μ could be tuned much smaller than one. However, the origin of this flux in F-theory suggests that also this open string flux is a quantized integer (see section 8.3.1). In this case, one can only introduce a large flux $h > \mathcal{O}(10^2)$.

The question is whether such large fluxes are consistent with the use of the low-energy effective field theory that we employed for our analysis. To see what happens let us consider the various mass scales, like string scale, Kaluza-Klein scales, heavy moduli masses and the inflaton mass. As mentioned in the beginning of this section, we will not be concerned with model dependent numerical prefactors, but will focus on desired mass hierarchies that are guaranteed or spoiled parametrically.

Thus, up to numerical coefficients, the relevant masses scale in the following way with the fluxes (recall that we set $M_{\text{Pl}} = 1$): The string scale (4.1.33) is

$$M_s^2 \sim \frac{1}{\tau^{\frac{3}{2}} s^{\frac{1}{2}}} \sim \frac{h^{\frac{1}{2}} q^{\frac{3}{2}}}{f_0 f_2}. \quad (8.3.35)$$

Moreover, considering our model as being realized on the isotropic T^6 , we now have *two* Kaluza-Klein scales

$$M_{\text{KK}}^2 \sim \frac{1}{\tau^2} u^{\pm 1}, \quad (8.3.36)$$

for $u > 1$, yielding a *heavy* and a *light* Kaluza-Klein mass

$$M_{\text{KK,h}}^2 \sim \frac{q^2}{f_0^{\frac{1}{2}} f_2^{\frac{3}{2}}}, \quad M_{\text{KK,l}}^2 \sim \frac{q^2}{f_0^{\frac{3}{2}} f_2^{\frac{1}{2}}}. \quad (8.3.37)$$

132 8. Axion Monodromy Inflation and the Swampland Distance Conjecture

Recall that the mass of the heavy moduli and the inflaton scaled as

$$M_{\text{mod}}^2 \sim \frac{h q^3}{f_0^{\frac{3}{2}} f_2^{\frac{1}{2}}}, \quad M_{\Theta}^2 \sim \frac{\mu q^3}{f_0^{\frac{3}{2}} f_2^{\frac{1}{2}}}. \quad (8.3.38)$$

Therefore, one gets

$$\frac{M_s^2}{M_{\text{KK},h}^2} \sim \left(\frac{h f_2}{q f_0} \right)^{\frac{1}{2}}. \quad (8.3.39)$$

Thus, by choosing the fluxes $\{f_0, f_2, h, q\}$ all of the same size, parametrically one can still keep all moduli at the boundary of the perturbative regime and have the *heavy* Kaluza-Klein scale parametrically not bigger than the string scale, i.e. $M_s \stackrel{\sim}{\simeq}_p M_{\text{KK},h}$.

To relate the mass structure of this model to the swampland distance conjecture, reviewed in chapter 6, we can also evaluate the various mass-scales in the large-field regime. Due to (8.3.27), this means that we just have to change

$$f_0 \rightarrow \mu \theta^2 \rightarrow f_0 \left(\frac{\theta}{\theta_c} \right)^2 \rightarrow f_0 \exp \left(2 \frac{\Theta}{\Theta_c} \right) \quad (8.3.40)$$

so that the string scale becomes

$$M_s^2 = M_s^2|_0 \exp \left(-2 \frac{\Theta}{\Theta_c} \right). \quad (8.3.41)$$

Similarly, the Kaluza-Klein scales in the large-field regime are

$$M_{\text{KK},h}^2 = M_{\text{KK},h}^2|_0 \exp \left(-\frac{\Theta}{\Theta_c} \right), \quad M_{\text{KK},l}^2 = M_{\text{KK},l}^2|_0 \exp \left(-3 \frac{\Theta}{\Theta_c} \right) \quad (8.3.42)$$

and for the heavy moduli masses we obtain

$$M_{\text{mod}}^2 = M_{\text{mod}}^2|_0 \exp \left(-3 \frac{\Theta}{\Theta_c} \right). \quad (8.3.43)$$

Therefore, all these mass scales show the expected exponential drop off (8.1.5) at large values in the field space. Thus, for very large values of Θ/Θ_c we have many exponentially light states that invalidate the use of the low-energy effective action. For still moderate values of Θ/Θ_c , one might argue that this by itself would not be disastrous, as long as the order is preserved. However, we also get

$$\frac{M_s^2}{M_{\text{KK},h}^2} = \frac{M_s^2}{M_{\text{KK},h}^2} \Big|_0 \exp \left(-\frac{\Theta}{\Theta_c} \right) \quad (8.3.44)$$

which means that for field excursions $\Theta/\Theta_c > 1$ all *heavy* Kaluza-Klein states are heavier than the string scale, i.e. $M_{\text{KK},h} \gtrsim M_s$. This invalidates the usage of the low-energy effective supergravity action.

This is all consistent with the swampland distance conjecture. The question now is whether we also get constraints for the critical value $\Theta_c \sim \lambda^{-1}$. Can it really be tuned by fluxes to be larger than M_{Pl} or do we find support for the *refined swampland distance conjecture* that says Θ_c is close to M_{Pl} ?

For this purpose, let us consider the quotient of the *light* KK-mass and the heavy moduli mass

$$\frac{M_{\text{KK},l}^2}{M_{\text{mod}}^2} \sim \frac{1}{h q}. \quad (8.3.45)$$

This ratio is independent of f_0 and therefore of Θ in the large-field regime. Now, we can distinguish two cases:

1. In the case that we could tune λ small by choosing the open string flux μ small, there is no problem with the mass hierarchies. As discussed in section 8.3.1, this would be in principle possible if one just considers the naive type IIB form of the open string superpotential.
2. However, in the backreacted F-theory picture μ is quantized. It is obvious that for large H -flux h (i.e. $\lambda \ll 1$) the ratio (8.3.45) is parametrically smaller than one and the moduli masses are heavier than the Kaluza-Klein mass. This spoils the usage of an effective four-dimensional effective action for studying the stabilization of the former massless moduli⁸.

For case 2. one has $\lambda = \mathcal{O}(1)$ and consequently $\Theta_c = \mathcal{O}(1)$. Thus, we found evidence that the distance in proper field space Θ , where the logarithmic behavior sets in, is around the Planck-scale and cannot be much increased without invalidating the effective theory. In addition, this means that the inflaton cannot be kept parametrically lighter than the other moduli. Therefore, integrating out the latter first is not a self-consistent approach. We emphasize that this is precisely what the *refined swampland distance conjecture* states.

With $\Theta_c = \mathcal{O}(1)$ for trans-Planckian field excursions one gets the plateau-like potential (8.3.34). Analogous to the former closed string example, for the ratio of the Kaluza-Klein scale to the Hubble scale one finds

$$\frac{M_{\text{KK},l}}{H_{\text{inf}}} \sim \frac{1}{(q h)^{\frac{1}{2}}} \exp\left(-\frac{3\Theta_*}{2\Theta_c}\right). \quad (8.3.46)$$

We again find the parametric relation $H_{\text{inf}} \gtrsim M_{\text{KK},l}$. Having Kaluza-Klein modes lighter

⁸Recall that for the strongly isotropic torus, one has $\mu = h$ and therefore $\Theta_c = \mathcal{O}(1)$ from the very beginning.

than the Hubble scale, spoils the possibility of realizing large-field plateau-like inflation in a controlled way.

8.3.3 Model O2 on the Strongly Isotropic Torus

Let us now consider a model on the strongly isotropic torus. Unfortunately, it is not exactly solvable, but the intuition we gained from the previous examples, allows us to extract the value of λ at least in a perturbative approach. Here we follow the procedure described in section 8.3.1 and laid out in [32, 33], i.e. in a first step we freeze all moduli except the axionic inflaton candidate. Then we scale these fluxes up and introduce an additional order one flux to freeze the inflaton. As long as the initial values of the moduli are shifted only slightly, we can integrate them out and determine an effective potential for the inflaton. This allows us to read off the ratio of the heavy moduli masses and the inflaton masses. From the former analysis, we expect that this ratio is directly related to $\Theta_c = \lambda^{-1}$, the scale which determine the backreaction.

Moduli stabilization and masses

The model is defined by the same Kähler potential (8.3.18) and the superpotential

$$W = \Lambda \left(i\mathfrak{f}_1 U + i\tilde{\mathfrak{f}}_0 U^3 + ihS + iqT \right) - \mu_1 (3US - \Phi^2) - q_1 3UT, \quad (8.3.47)$$

where Λ is a large scaling factor of the four fluxes that, in the first step, will fix all four saxions and two axionic directions. It turns out that the effective approach is only justified if one choose $hq_1 - q\mu_1 = 0$, i.e. that only the axionic combination $hc + q\rho$ appears in the superpotential. Thus, the orthogonal combination will remain massless. Otherwise, we would not recover the old minimum when setting $\mu_1 = 0$ and the strong backreaction would imply $\Theta_c \sim \mathcal{O}(1)$ from the very beginning.

In the first step, we set $\mu_1 = q_1 = 0$ and find that there exist a tachyon-free non-supersymmetric minimum at

$$\begin{aligned} s_0 &= \frac{2^{\frac{5}{4}} \cdot 5^{\frac{1}{2}}}{3^{\frac{9}{4}}} \frac{\mathfrak{f}_1^{\frac{3}{2}}}{h \tilde{\mathfrak{f}}_0^{\frac{1}{2}}}, & \tau_0 &= \frac{5^{\frac{1}{2}}}{2^{\frac{3}{4}} \cdot 3^{\frac{5}{4}}} \frac{\mathfrak{f}_1^{\frac{3}{2}}}{q \tilde{\mathfrak{f}}_0^{\frac{1}{2}}} \\ u_0 &= \frac{5^{\frac{1}{2}}}{2^{\frac{1}{4}} \cdot 3^{\frac{3}{4}}} \left(\frac{\mathfrak{f}_1}{\tilde{\mathfrak{f}}_0} \right)^{\frac{1}{2}}, & \varphi_0 &= 0 \end{aligned} \quad (8.3.48)$$

$$v_0 = hc_0 + q\rho_0 = 0,$$

leaving one axionic direction unconstrained. The masses of the massive moduli are all of the same scale

$$M_{\text{heavy}}^2 \sim \frac{\Lambda^2 h q^3 \tilde{f}_0^{\frac{5}{2}}}{f_1^{\frac{9}{2}}}. \quad (8.3.49)$$

In the second step we now scale Λ up and turn on the small fluxes μ_1 and q_1 . Since the axion $\theta = \text{Im}(\Phi)$ only appears in these extra term in W , we expect that it receives a small mass. In order to estimate it, we integrate out the former stabilized heavy moduli and compute an effective scalar potential for θ . In this regime, the canonically normalized mass of the axion Θ is

$$M_{\Theta}^2 \sim \frac{\mu_1^2 q^3 \tilde{f}_0^{\frac{3}{2}}}{h f_1^{\frac{7}{2}}}. \quad (8.3.50)$$

so that, for the scale where the backreaction is expected to become substantial, we obtain

$$\Theta_c \sim \frac{M_{\text{heavy}}}{M_{\Theta}} \sim \frac{\Lambda h \tilde{f}_0^{\frac{1}{2}}}{\mu_1 f_1^{\frac{1}{2}}} \gg 1. \quad (8.3.51)$$

This is large for a sufficiently large flux-scaling factor Λ . Note that at this stage, Θ_c is flux dependent and by appropriate choices can be tuned large.

As in the previous example O1, let us compute the various mass scales. We obtain for the string scale, the heavy and light Kaluza-Klein scales in the minimum

$$M_s^2 \sim \frac{h^{\frac{1}{2}} q^{\frac{3}{2}} \tilde{f}_0}{f_1^3}, \quad M_{\text{KK,h}}^2 \sim \frac{q^2 \tilde{f}_0^{\frac{1}{2}}}{f_1^{\frac{5}{2}}}, \quad M_{\text{KK,l}}^2 \sim \frac{q^2 \tilde{f}_0^{\frac{3}{2}}}{f_1^{\frac{7}{2}}}. \quad (8.3.52)$$

For the ratio of the string and the heavy Kaluza-Klein scale one finds

$$\frac{M_s^2}{M_{\text{KK,h}}^2} \sim \left(\frac{h \tilde{f}_0}{q f_1} \right)^{\frac{1}{2}} \gg 1, \quad (8.3.53)$$

that we require to be parametrically larger than one. However, the ratio of the light Kaluza-Klein scale and the heavy moduli mass is given by

$$\frac{M_{\text{KK,l}}^2}{M_{\text{heavy}}^2} \sim \frac{1}{\Lambda^2 q^2} \left(\frac{q f_1}{h \tilde{f}_0} \right)^{\frac{1}{p}} \lesssim 1 \quad (8.3.54)$$

which becomes parametrically small for large Λ . Therefore, even to get all the high scales in the correct order, we can at best work at the boundary of parametric control, where all fluxes are of order $\mathcal{O}(1)$. However, in this case also the critical field distance becomes of order one $\Theta_c = \mathcal{O}(1)$ for quantized flux μ_1 .

The only possible loop-hole could be that μ_1 is not quantized and can be significantly smaller than one. This will be analyzed next.

A comment on tuning in the landscape

From the discussed examples it is clear that a possible loop-hole is the assumption about the quantization of the fluxes. Of course, all the fluxes in the initial superpotential are quantized but, following the idea of the landscape, one could imagine that it is a linear combination of terms that leads to an effective flux μ_{eff} that eventually appears in Θ_c . This effective flux could depend, not only on flux integers but, also on vacuum expectation values of other fields. Here we present a model which exemplifies the above idea and discuss the difficulties to get a substantial tuning.

In the framework of the isotropic torus, we can extend the model O2 by additional flux induced terms⁹

$$W = \Lambda \left(i\mathfrak{f}_1 U + i\tilde{\mathfrak{f}}_0 U^3 + ihS + iqT \right) - \mu_1 (3US - \Phi^2) - q_1 3UT + \mu_3 U^2 (US - \Phi^2) + q_3 U^3 T. \quad (8.3.55)$$

Again, to control the minimum of the potential we choose the fluxes such that only the combination $hc + q\theta$ appears in W , i.e. $hq_1 - q\mu_1 = hq_3 - q\mu_3 = 0$. This guarantees that all Bianchi identities are satisfied, as well. Integrating out the heavy moduli, the mass of the inflaton takes the same form as in (8.3.50)

$$M_{\Theta}^2 \sim \frac{\mu_{\text{eff}}^2 q^3 \tilde{\mathfrak{f}}_0^{\frac{3}{2}}}{h \mathfrak{f}_1^{\frac{7}{2}}}, \quad (8.3.56)$$

but with an effective flux parameter

$$\mu_{\text{eff}}^2 = \mu_1^2 - \frac{5}{12\sqrt{6}} \left(\frac{\mathfrak{f}_1}{\tilde{\mathfrak{f}}_0} \right) \mu_1 \mu_3 + \frac{25}{54} \left(\frac{\mathfrak{f}_1}{\tilde{\mathfrak{f}}_0} \right)^2 \mu_3^2. \quad (8.3.57)$$

As mentioned above, this effective parameter is also moduli dependent and therefore is certainly not an integer. The question is whether in the perturbative regime $\mathfrak{f}_1 > \tilde{\mathfrak{f}}_0$ (so $s_0, \tau_0 > 1$), the effective flux can be non-zero and significantly smaller than one. First, for $\mu_1 \neq 0$, the effective flux μ_{eff} can be expressed as

$$\mu_{\text{eff}}^2 = \frac{63}{64} \mu_1^2 + \frac{25}{54} \left(\frac{\mathfrak{f}_1}{\tilde{\mathfrak{f}}_0} \right)^2 \left(\mu_3 - \frac{3\sqrt{3}}{20\sqrt{2}} \left(\frac{\tilde{\mathfrak{f}}_0}{\mathfrak{f}_1} \right) \mu_1 \right)^2 \geq \frac{63}{64} \mu_1^2 \quad (8.3.58)$$

showing that μ_{eff} is larger than $63/64 \approx 1$. For $\mu_1 = 0$, it is also clear that $\mu_{\text{eff}} > 25/54$ giving us the total lower bound for the effective flux. Thus, we conclude that in this model one cannot substantially tune the effective flux in the landscape. As a consequence, the critical field distance is still of order one.

⁹Applying a T-duality in the three x -directions, the fluxes μ_3 and q_3 become non-geometric R-fluxes in type IIA.

Up to now, we have analyzed all possible models arising from the brane superpotential (8.3.13) corresponding to a single D7-brane living on an isotropic torus T^6 , although the results also apply to the case of a Calabi-Yau with a single complex structure modulus. The natural forthcoming step would be to generalize the previous idea of tuning in the landscape to more elaborated models including more than one complex structure modulus, with the hope of getting a more intricate effective flux parameter μ_{eff} that can be tuned small.

However, the inclusion of more fields makes it necessary to extend the backreaction analysis to also these new fields and the corresponding Kaluza-Klein scales. Of course, this issue cannot so easily be addressed in full generality, but we would like to emphasize a universal obstacle which seems difficult to overcome even if appealing to landscape arguments. This universal obstacle is the backreaction coming from the dilaton field. The best thing one can intend, is to stabilize the dilaton by inducing mixing terms between the latter and other complex structure moduli that do not couple to the open string modulus. In this way, one can hope to decouple the scale of S and Φ and delay the backreaction. As pointed out in [34], this tuning is in principle possible in the context of F-theory, where the D7 position moduli and the dilaton become part of the complex structure moduli of the Calabi-Yau four-fold. Let us remark, though, that this is precisely the mechanism underlying the model O1, in which in principle one can get a tunable flux-dependent λ . However, as we have seen, even in this case the model fails from realizing large-field inflation. The required mass hierarchy cannot be achieved without getting into trouble with the Kaluza-Klein scale. Therefore, we suspect similar results might hold for more generic models with more than one complex structure modulus. A more thorough analysis of Calabi-Yau geometries is surely interesting and deserves more investigation, so we leave it for future work.

8.3.4 Models with Instanton Corrections

Let us consider now the case of open string models within the framework of KKLT [63] and large volume scenario (LVS) [15]. Recall the review section 4.3. The inflaton is still a D7-brane position modulus. The Kähler moduli are not stabilized by non-geometric fluxes, though, but by non-perturbative effects. These non-perturbative corrections can arise, for instance, from Euclidean D3-branes or gaugino condensation of a stack of distant D7-branes. As in the previous examples, the complex structure and axio-dilaton moduli will be stabilized by R-R and NS-NS fluxes.

The backreaction of a field excursion of the inflaton onto the complex structure and axio-dilaton moduli proceeds analogously to the previous section and leads to a logarithmic scaling of the proper field distance at large field. The critical value at which this happens is given by the mass ratio M_u/M_θ . In contrast to the previous models, now this value can in principle be tuned large, because the Kaluza-Klein scale entering (8.3.45) depends on the Kähler modulus whose stabilization is now disentangled from the stabilization of the complex structure and axio-dilaton moduli. In fact, in the analysis of the KKLT and LVS

scenarios we will assume a hierarchy of scales

$$M_u > M_\tau > M_\theta, \quad (8.3.59)$$

and analyze the effective models after integrating out the complex structure and the axio-dilaton moduli. The question is whether this effective field theory also shows the typical control issues that we found for the previously studied models. As opposed to the previous flux examples, here the backreaction can only be determined up to next-to-leading order. The relevant parameter controlling when the backreaction of the inflaton field onto the Kähler modulus becomes substantial is $\theta_c \sim (M_\tau/M_\theta)^p$. Notice that the saxions that determine the kinetic term for the inflaton have already been integrated out. Therefore, one does not see the logarithmic behavior from the swampland distance conjecture for very large-field excursions. However, as before, we find a potential problem that can invalidate the possibility of large-field inflation.

As already observed in [184, 187], in the presence of a dynamical uplifting term, the backreaction on the Kähler moduli can destabilize the vacuum. If the relative displacement of the Kähler moduli during inflation is of order one, the minimum and the maximum of the KKLT potential merge into a saddle point so that the minimum disappears and the theory decompactifies. This is the same effect that we also found in section 8.2 for an uplift for the closed string model. Thus, the trajectory does not extend into the regime $\theta > \theta_c$. The question is, then, whether one can parametrically obtain $\theta_c > 1$, i.e. the mass hierarchy between the inflaton and the Kähler modulus. This is an obvious challenge for KKLT and LVS as the open string modulus is stabilized at tree-level, whereas Kähler moduli are fixed by non-perturbative corrections.

We also believe that a full treatment of the backreaction, i.e. including the complex structure and axio-dilaton moduli, would also reveal behavior from the swampland distance conjecture.

KKLT scenario

Let us start analyzing the case of KKLT extended by an open string modulus Φ . The effective theory, once the dilaton and complex structure moduli are integrated out, is given by the Kähler potential

$$K = -3 \log(T + \bar{T}) + \frac{(\Phi + \bar{\Phi})^2}{2}, \quad (8.3.60)$$

and the superpotential

$$W = W_0 + \mu \Phi^2 + A e^{-aT}. \quad (8.3.61)$$

For simplicity we have set $4su = 1$ (in eq. (2.3.26)), as one can show that otherwise the constraints discussed below become even stronger. Moreover, we have approximated the

Kähler potential by assuming a small real part of the open string modulus $\text{Re}(\Phi) = \phi$, which will in fact be stabilized at zero. W_0 and the Pfaffian A are determined in terms of fluxes and the stabilized values of the complex structure moduli. In the following we make the assumptions of KKLT, namely $A = \mathcal{O}(1)$ and $W_0 \ll 1$. Moreover, we have in mind that μ is quantized so that we will work in the regime $W_0 \ll \mu$.

The interplay between large-field inflation and KKLT moduli stabilization was already analyzed in [184] and further examined in [58]. Here we just borrow some of the relations derived there. The supersymmetric AdS minimum of the scalar potential is at $\Phi = 0$ and for a τ_0 satisfying the transcendental relation

$$W_0 = -Ae^{-a\tau_0} \left(1 + \frac{2a\tau_0}{3}\right). \quad (8.3.62)$$

The masses of the Kähler modulus and the inflaton $\theta = \text{Im}(\Phi)$ are given by

$$M_\tau^2 = \frac{(aW_0)^2}{2\tau_0}, \quad M_\theta^2 = \frac{1}{2\tau_0^3} \left(\mu^2 + \frac{3}{2}\mu W_0\right) \quad (8.3.63)$$

where the latter is the sum of a supersymmetric mass and a soft mass. If the inflaton is displaced away from its minimum, the minimization condition for the Kähler modulus changes in such a way that the minimum for τ becomes θ -dependent with

$$\tau = \tau_0 \left[1 + \frac{1}{2} \left(\frac{\theta}{\theta_c}\right)^2 + \dots\right], \quad \theta_c^2 = \frac{a\tau_0 W_0}{\mu}. \quad (8.3.64)$$

The backreaction becomes substantial beyond the critical field distance θ_c . In the regime of interest $W_0 \ll \mu$, the supersymmetric mass term for M_θ is dominant so that one gets the relation

$$\theta_c = \sqrt{\frac{M_\tau}{M_\theta}}, \quad (8.3.65)$$

i.e., as for the previous examples, large-field inflation is possible once we parametrically control the mass ratio $\frac{M_\tau}{M_\theta} > 1$. Let us now analyze the two possible obstructions mentioned above:

- **Controlling θ_c**

From (8.3.64) it is already clear that one cannot get $\theta_c > 1$ for μ quantized and $W_0 \ll 1$ (as required in KKLT). Employing the condition (8.3.62), we obtain an upper bound for the critical field distance¹⁰

$$\theta_c^2 = \frac{|A|}{\mu} (a\tau_0) e^{-a\tau_0} \left(1 + \frac{2a\tau_0}{3}\right) = \frac{|A|}{\mu} F(a\tau_0) \lesssim \frac{|A|}{\mu}. \quad (8.3.66)$$

¹⁰Here we used the fact that the function $F(x) = x e^{-x} \left(1 + \frac{2x}{3}\right)$ is bounded from above by $F_{\max} = 3 \exp\left(-\frac{3}{2}\right) \sim 0.67$.

Thus, for $A = \mathcal{O}(1)$ one can get $\theta_c > 1$ only for a parametrically small value of μ . This was already noticed in [58]. Therefore, the situation is very similar to the cases studied before, where the Kähler moduli were stabilized via fluxes. This supports the conjecture that one cannot achieve single large-field inflation in a parametrically controlled effective theory.

- **Destabilization due to dynamical uplift**

As shown in [58, 184, 187], in the presence of an uplift term (which goes to zero in the decompactification limit) the relative displacement of the Kähler modulus $\delta\tau/\tau_0$ cannot be made larger than one since otherwise the AdS minimum and the maximum of the potential merge into a saddle point, destabilizing the Kähler modulus. Thus, around the critical value θ_c the inflationary trajectory stops before reaching the top of the backreacted potential.

Let us remark that, unlike in the previous models, there is no problem related to Kaluza-Klein states becoming light. Indeed, the Kaluza-Klein scale stays heavier than the rest of the scales as long as $W_0 \ll 1/(a\sqrt{\tau_0})$, which is satisfied for large volume.

Large volume scenario

One could think that the above problems can be avoided by considering a scheme in which W_0 is not necessarily small. This is indeed one of the ideas proposed in [58] to avoid the above control problems. As an example, we now consider the LVS scenario [15] extended by a D7-brane position modulus $\Phi = \phi + i\theta$. The important feature of LVS is that there exists a non-supersymmetric AdS minimum in which the leading order α' -correction to the Kähler potential is balanced against a non-perturbative correction to the superpotential. This leads to an exponentially large overall volume \mathcal{V} that parametrically controls the vacuum against higher order corrections.

After integrating out the complex structure and axio-dilaton moduli, we get an effective model for a typical swiss-cheese manifold with large and small Kähler moduli T_b and T_s , respectively,

$$\begin{aligned} W &= W_0 + Ae^{-aT_s} + \mu\Phi^2, \\ K &= -2\log\left[(T_b + \bar{T}_b)^{\frac{3}{2}} - (T_s + \bar{T}_s)^{\frac{3}{2}} + \xi\right] + \frac{(\Phi + \bar{\Phi})^2}{2}. \end{aligned} \tag{8.3.67}$$

Here, ξ denotes the usual α' -correction term and W_0 and A are treated as effective parameters of order one. In particular, denoting the overall volume by $\mathcal{V} \approx \tau_b^{3/2}$ and the small 4-cycle volume as $\tau = \text{Re}(T_s)$, in the minimum one gets for their values

$$\mathcal{V}_0 = \frac{3W_0\sqrt{\tau_0}}{\sqrt{2}aA} e^{a\tau_0} \left(1 - \frac{3}{4a\tau_0}\right). \tag{8.3.68}$$

The relevant mass scales for this model are given by

$$M_{\mathcal{V}} \sim \frac{W_0}{\mathcal{V}_0^{\frac{3}{2}}}, \quad M_{\tau} \sim \frac{W_0}{\mathcal{V}_0}, \quad M_{\text{KK}} \sim \frac{1}{\mathcal{V}_0^{\frac{2}{3}}}, \quad (8.3.69)$$

where, compared to \mathcal{V}_0 , we have treated the value of τ_0 as a number of order one. The requirement of having the small 4-cycle Kähler modulus lighter than the Kaluza-Klein scale already imposes an upper bound for W_0 ,

$$W_0 < \mathcal{V}_0^{1/3}. \quad (8.3.70)$$

The mass of the open string inflaton was derived in [184] and at leading order in $1/\mathcal{V}$ it takes the simple form

$$M_{\theta}^2 \sim \frac{4\mu^2}{\mathcal{V}_0^2}. \quad (8.3.71)$$

The backreaction of an inflaton excursion onto the Kähler moduli has also been examined in [184](eq. (5.21)). At leading order in $1/\mathcal{V}$, it can be expressed as

$$\begin{aligned} \mathcal{V} &= \mathcal{V}_0 \left[1 + O(1) \frac{\mu^2 \mathcal{V}_0}{W_0^2} \theta^2 + \dots \right] \\ \tau &= \tau_0 \left[1 + O(1) \frac{\mu^2 \mathcal{V}_0}{W_0^2} \theta^2 + \dots \right], \end{aligned} \quad (8.3.72)$$

where the order one prefactors include powers of τ_0 and a . Thus, the critical field distance can be read off as

$$\theta_c \sim \frac{W_0}{\mu \mathcal{V}_0^{\frac{1}{2}}} \sim \frac{M_{\mathcal{V}}}{M_{\theta}}. \quad (8.3.73)$$

and, as usual, is related to the quotient of the masses. Finally, we are ready to consider the issues we have already encountered for KKLT:

- **Controlling θ_c**

Employing the condition (8.3.70), we immediately arrive at the constraint

$$\theta_c < \frac{1}{\mu \mathcal{V}_0^{\frac{1}{6}}}, \quad (8.3.74)$$

which for quantized μ and large volume is parametrically smaller than one. Only for very small values of μ with $\mu < \mathcal{V}_0^{-\frac{1}{6}}$ it could exceed the Planck-scale. Clearly, this problem just reflects the naive expectation that it is hard to control an inverted mass hierarchies, i.e. that a non-perturbative mass term should be larger than a tree-level mass.

- **Destabilization due to dynamical uplift**

As for the KKLT example, it was found in [184] that in the presence of a dynamical uplift, the overall volume gets destabilized and the theory decompactifies if the energy during inflation is bigger than the potential barrier. This occurs when the displacement of the overall volume field becomes comparable to the value at the minimum, i.e. at θ_c . Therefore, the trajectory does not extend in the regime $\theta > \theta_c$.

Hence, LVS does not provide a better framework than KKLT in this regard. We can conclude that for a quantized open string flux $\mu \geq 1$, the effective KKLT and LVS scenarios for Kähler moduli stabilization feature the similar control issues that we already saw for the previous example of tree-level Kähler moduli stabilization.

The loophole again comes from considering an effective μ -parameter depending on other scalars such that it could be tuned small in the landscape. Whether this tuning is indeed possible is still an open question and deserves more investigation. Notice that the difficulties outlined in section 8.3.3 also apply to these models. Let us also mention that here we are assuming that W_0, A can be disentangled from the mass scale of the complex structure moduli. But it could very well be that in a full fledged global compactification the two parameters controlling the backreaction of complex structure and Kähler moduli are related, which could reveal the behavior from the swampland distance conjecture at a lower scale than naively expected. Unfortunately, the global 10d action of these scenarios is not known, so we cannot address this issue in more detail for the moment (see though [188] for an effective analysis of the effect of field-dependent Pfaffians A).

CHAPTER 9

Challenging the Refined Swampland Distance Conjecture

Before we dwell into the formal analysis, let us point out that the motivation for this chapter follows naturally from the analysis of the last two chapters 7 and 8.

Axion monodromy represents a promising way towards large-field inflation in string theory as discussed earlier. However, the refined swampland distance conjecture (RSDC) puts very strong constraints on such models. In order to apply RSDC to axion monodromy models it was necessary to take backreaction effects during moduli stabilization into account, which is an important extension of the original formulation. To justify the powerful impacts of the conjecture, a convincing prove of the RSDC seems indispensable. This would probably require a much better understanding of quantum gravity and is therefore not conceivable at the moment. Instead the aim of this chapter confines to highly non-trivial tests of the RSDC in Calabi-Yau moduli spaces. The models of the last chapter 8 are build at region in the moduli space of large volume and large complex structure. But, in chapter 7 interesting phenomena arose at the conifold, i.e. special regions of the moduli space show very distinct features. Hence, in this chapter we will challenge the RSDC in widely different regimes of the moduli space.

To explain the qualitative difference of phases in moduli spaces and how we are going to test the RSDC, we begin with an overview section. Then there will be a short section about the one-parameter (mirror) quintic to illustrate our approach in simple(r) terms. The main application are then the two-parameter models in section 9.3. Note that the calculation of all required periods of the moduli spaces has already been carried out in chapter 3 and appendix A. The methods and results of this chapter in particular the two-parameter section 9.3 are largely taken from our publication [65]. Ultimately, note that all distances here are in units of the Planck mass M_{Pl} , even though we might drop the unit

occasionally.

9.1 Setup and Objective

Let us remind the reader of some basic facts of type II compactifications on Calabi-Yau manifolds as introduced in chapters 2 and 3. Consider the compactification of type IIA superstring theory on a Calabi-Yau manifold \mathcal{M} with Hodge numbers $(h^{2,1}, h^{1,1})$. The four-dimensional effective theory has $\mathcal{N} = 2$ space-time supersymmetry. The dimension of complex structure moduli space gives rise to $h^{2,1}$ hypermultiplets and the dimension of the Kähler moduli space to $h^{1,1}$ vector multiplets. Such a compactification is dual to type IIB compactified on the mirror Calabi-Yau manifold \mathcal{W} with Hodge numbers $h^{2,1}(\mathcal{W}) = h^{1,1}(\mathcal{M})$ and $h^{1,1}(\mathcal{W}) = h^{2,1}(\mathcal{M})$, which gives the same massless spectrum.

Since the two descriptions have to agree, we are free to use for our models either the language of the complex structure or the Kähler moduli space. Throughout this chapter, we will focus on the Kähler moduli space, i.e. we will speak of large and small radius regime. When we say conifold locus (that is actually defined in the complex structure moduli space), we mean the mirror dual of it. The advantage is that Kähler moduli more directly set the mass scale of the Kaluza-Klein modes.

In chapter 2 the Kähler moduli were defined in a type IIB setup. For type IIA compactifications the complexified Kähler moduli are composed of the anti-symmetric 2-form B_2 as well as the Kähler (1, 1)-form J

$$t_i = \int_{\Sigma_i} B_2 + i \int_{\Sigma_i} J, \quad i = 1, \dots, h^{1,1}, \quad (9.1.1)$$

where the 2-cycles Σ_i are a basis of $H_2(\mathcal{M})$. Due to this definition the imaginary parts of our Kähler moduli govern the size of cycles and the overall volume of the Calabi-Yau. Therefore, they also determine the Kaluza-Klein scales. Of course, the precise mass formula for Kaluza-Klein states of general compactifications may be complicated and for instance also depend on complex structure moduli (cf. [181]). Hence, we are going to use in the following the estimate¹

$$M_{\text{KK}} \sim \frac{M_s}{\sqrt{\text{Im}(t)}} \sim \frac{M_{\text{Pl}}}{[\text{Im}(t)]^2}. \quad (9.1.2)$$

These states will be the ones (i.e. $\Theta \simeq \text{Im}(t)$) satisfying the swampland distance conjecture [43, 44]

$$M \sim M_0 e^{-\lambda \Theta}. \quad (9.1.3)$$

¹Note that this estimate is expected to be between heavier and lighter Kaluza-Klein masses. Imagine for instance a torus T^2 with one large and one small cycle. According to [181] the cycle with large radius will lead to a Kaluza-Klein mode lighter than our average estimation and hence improve our argument.

To say it once more, an infinite tower of states becomes exponentially light as the geodesic distance diverges $\Theta \rightarrow \infty$. See chapter 6 for details. Note that the geodesic distance is measured with the metric on the moduli space.

In the initial version of the conjecture, λ is still an undetermined parameter that specifies when the exponential drop-off becomes significant. Let us show that one finds quite generically $\lambda^{-1} \sim \mathcal{O}(1)$ for trajectories in the large volume regime of Calabi-Yau compactifications.

In the large volume regime the Kähler potential for the Kähler moduli of \mathcal{M} is given in terms of the triple intersection numbers as

$$K = -\log \left(-\frac{i}{6} \kappa^{ijk} (t_i - \bar{t}_i)(t_j - \bar{t}_j)(t_k - \bar{t}_k) \right) \quad (9.1.4)$$

where the t_i , with $i = 1, \dots, h^{1,1}$, denote the complexified Kähler moduli. Following a generic trajectory inside the Kähler cone $\text{Im}(t_i) \sim \alpha_i r$, $\alpha_i \in \mathbb{R}$, for very large r the effective Kähler potential behaves as $K = -3 \log r$. Hence, the Kähler metric along the trajectory becomes

$$G(r) = \frac{3}{4r^2}. \quad (9.1.5)$$

There might exist special trajectories for which the numerator is smaller than three but it will never be larger. The proper field distance Θ along a trajectory $x^\alpha(\tau)$ is defined as

$$\Theta = \int_{\tau_0}^{\tau_*} d\tau \sqrt{G_{\alpha\bar{\beta}} \frac{dx^\alpha}{d\tau} \frac{d\bar{x}^{\bar{\beta}}}{d\tau}}, \quad (9.1.6)$$

which in this case becomes

$$\Theta = \int_{r_0}^{r_*} dr \sqrt{G(r)} = \frac{1}{\lambda} \log \left(\frac{r_*}{r_0} \right) \quad (9.1.7)$$

with $\lambda = \frac{2}{\sqrt{3}} \approx 1.15$. This logarithmic scaling has a dramatic consequence for the validity of the effective field theory for which the Kaluza-Klein modes are assumed to be integrated out. The generic Kaluza-Klein mass-scale (9.1.2) can be estimated as

$$M_{\text{KK}} \sim \frac{M_{\text{Pl}}}{r^2} \sim M_{\text{KK},0} \exp(-2\lambda\Theta) \quad (9.1.8)$$

which implies that for trans-Planckian field excursions $\Theta > \lambda^{-1} \approx 0.87$ an infinite tower of Kaluza-Klein states becomes light. In the following we define $\Theta_\lambda \equiv \lambda^{-1}$ to stay in accordance with [65].

Infinitely many states becoming exponentially light in field space indicates that the effective quantum gravity theory has only a finite range of validity in the scalar moduli space. For general compactifications and arbitrary geodesics it is, however, difficult to determine

the *exact* value of the displacement where the effective theory breaks down. One would need to take all relevant mass scales into account. Therefore, the exact upper bound on the displacement is highly model-dependent, but it is sure that in the presence of the exponential drop-off, any physics that we might derive for larger values $\Theta > \Theta_\lambda$ cannot be trusted.

A priori it is not clear at which finite value of the distance Θ_0 along a geodesic this exponential drop-off commences in the first place. Note that the scale Θ_λ was derived already in the large radius regime without any reference to the point where the geodesic started. In [45, 181], by analyzing a couple of string theory models, evidence was provided that Θ_0 is equal to the natural mass scale in quantum gravity, namely² M_{Pl} . In fact, for these simple examples all scales turned out to be related, i.e. $\Theta_0 \simeq \Theta_\lambda$. Let us point out that these papers focused on stabilized moduli in contrast to the original work of [43]. In the case of unstabilized moduli, general arguments were given in [44] in favor of the *refined swampland distance conjecture* which states that $\Theta_\lambda \lesssim \mathcal{O}(1)$ as well as $\Theta_0 \lesssim \mathcal{O}(1)$ (in Planck units). In other words, for any starting point of a geodesic, one cannot follow it for a longer distance than M_{Pl} before the validity of the effective theory breaks down.

The objective of this chapter is to test this highly non-trivial conjecture in the Kähler moduli space of type IIA string compactifications on Calabi-Yau manifolds. For that purpose we head out to compute the critical values Θ_0 and Θ_λ for a plenitude of different trajectories/geodesics in various Calabi-Yau manifolds. Even more evidence was collected in the reference [65] where one can in particular find an extensive analysis of one-parameter models, i.e. Calabi-Yau with $h^{1,1} = 1$, as well as the full 101-parameter quintic.

Testing the RSDC in Calabi-Yau moduli spaces

The intuition for the swampland distance conjecture originates from the form of the Kähler potential in the large radius regime. It is known that the Kähler moduli space of a Calabi-Yau manifold also contains non-geometric regions where α' corrections become important. Recall from chapter 3, the Kähler moduli space of the quintic is of the form shown in figure 9.1.

As indicated, there are three distinguished special points: the large volume point, the conifold and the Landau-Ginzburg (LG) point. The LG or Gepner point is the one of minimal radius. To cover the whole moduli space, one needs at least two charts, whose radii of convergence are shown by the dashed arc in figure 9.1.

Figure 9.1 naturally leads to the question whether the RSDC still holds for geodesics starting in the small volume regime. We will see that the conifold and LG points are at *finite* distance in the moduli space so that the only region featuring infinite distances is the

²There, the displaced field was actually an axion, hence the consequences of the SDC were only visible through backreaction effects induced by moduli stabilization.

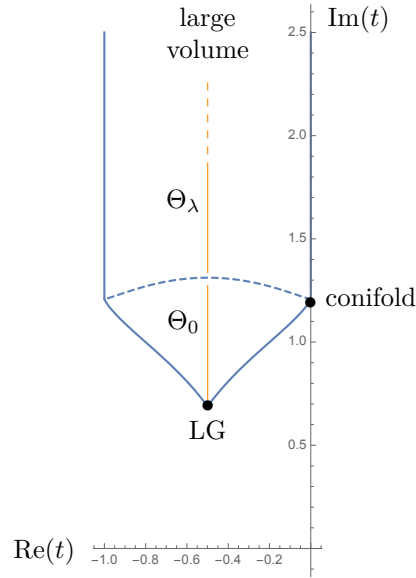


Figure 9.1: Sketch of the Kähler moduli space of the quintic. We are particularly interested in geodesics (e.g. orange curve) crossing different phases. Θ_0 is determined in the LG phase where the logarithmic behavior is still absent. In the large volume phase the geodesic may traverse another distance Θ_λ , before the effective theory finally breaks down.

large volume regime. Following a geodesic from the LG point to the large volume regime, one expects that the proper field distance depends on $\text{Im}(t)$ like shown in figure 9.2.

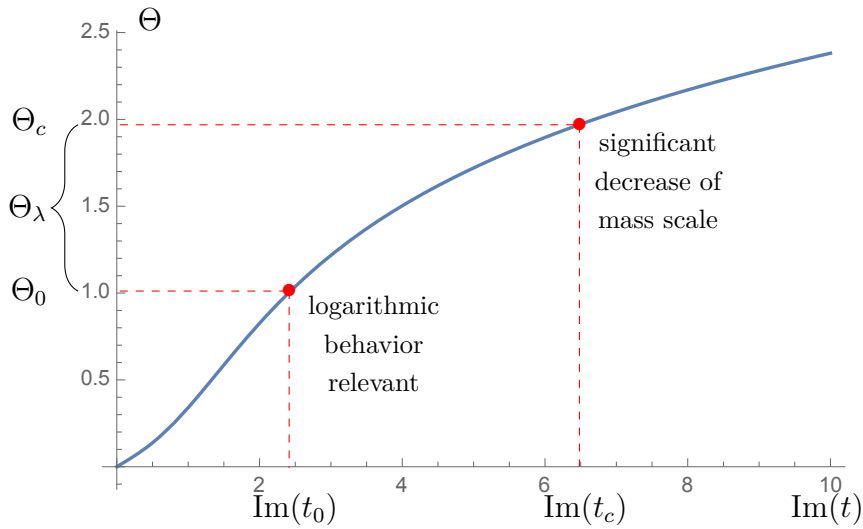


Figure 9.2: Expected relation between proper field distance Θ and $\text{Im } t$.

As long as one stays in the small volume regime the proper field distance scales polynomially

with $\text{Im}(t)$ and at some point $(\text{Im}(t_0), \Theta_0)$ the logarithmic scaling becomes dominant. As a consequence, we define the critical field distance as the sum

$$\Theta_c = \Theta_0 + \Theta_\lambda, \quad (9.1.9)$$

which includes the distance Θ_0 . This makes sense as we would like to know how much distance can one travel along a geodesic before the effective field theory breaks down. For the quintic example, displacing the Kähler modulus from the LG point towards the large volume phase, Θ_0 would be at least the proper distance to the edge of the convergence region of the LG phase, which is approximately the same as the distance between the LG and conifold point. Figure 9.1 also underlines the difference between Θ_0 and Θ_λ .

Clearly, if Θ_0 determined in this way was already larger than the Planck-scale, the RSDC would be falsified. Said the other way around, if the RSDC is correct, the proper field distance that can be traveled in the small volume regime must be smaller than M_{Pl} . Therefore, the (proper) radius of convergence for any chart that does not contain a region of infinite distance should be sub-Planckian.

It was motivated in section 2.3 of [65] that the identification of Θ_0 with the radius of convergence is indeed a sensible approximation. There it was shown that the logarithm describes the behavior of the proper distance over the whole large volume phase and only breaks down at the boundary to non-geometric regions. Thus, the only relevant contribution to Θ_0 comes from inside the non-geometric phases and the behavior predicted by the SDC sets in immediately after crossing the phase boundary. Here, we will not justify this further since we are mostly interested in two-parameter models where the computation of a large geodesic crossing several phases was not possible. Let us postpone details to section 9.3.

To summarize, the goal of this chapter is to check two very concrete predictions of the RSDC, namely that both Θ_λ and Θ_0 should be bounded by $\mathcal{O}(1)$ in Planck units.

9.2 RSDC for the Mirror Quintic

This section attends to compute the critical distances Θ_0 and Θ_λ for an explicit model, that is, the mirror quintic. In particular we will analysis both of its phases separately and thereby emphasis their different behavior with respect to the refined swampland distance conjecture. Note that here we only summarize the most important concepts of the mirror quintic and sketch the calculations in order to show the analogy with the more complicated two-parameter models in section 9.3. We highly recommend to consult [65] for details about the quintic.

According to chapter 3, the quintic $\mathbb{P}^4_{11111}[5]$ has one Kähler modulus and hence its mirror dual continues simply a single complex structure modulus ψ . The Kähler moduli space

obeys the schematic form pictured in figure 9.1. Now we work on the mirror dual, i.e. in the moduli space of the complex structure modulus ψ , which is depicted in the figure (a) of 9.3. The plot separates the Landau-Ginzburg (LG) and the large volume phases and also indicates the conifold singularity at $\psi = 1$. Recall the \mathbb{Z}_5 symmetry on the ψ -space, i.e. $\psi \rightarrow \exp\left(\frac{2\pi i}{5}\right) \psi$.

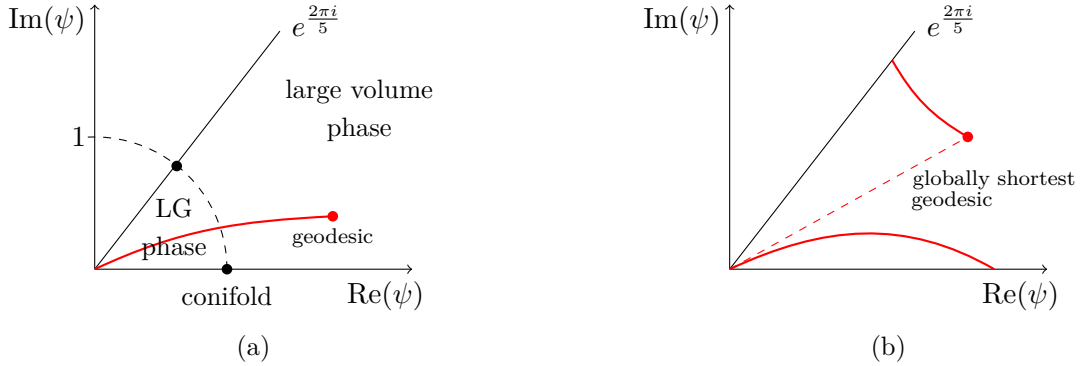


Figure 9.3: Plot (a) shows the complex structure moduli space of the mirror quintic with the two different phases and a example geodesic (red line). We are interested in the geodesic distance as emphasized in plot (b).

In the following we are interested in the geodesic distance between two points in the moduli space. This is for instance indicated by the line in plot (a) of figure 9.3. Trajectories like the solid line in plot (b) of the figure might be geodesics, but they are not the geodesic distance represented by the dashed line. In other words, let us point out that the RSDC does not have to hold for arbitrary geodesics, but certainly for the geodesic distance between two points in the moduli space. Therefore, we stop integrating the length of a geodesic as soon as it hits the axis at $\text{Arg}(\psi) = 0$ or $\text{Arg}(\psi) = \frac{2\pi i}{5}$.

Landau-Ginzburg phase

At first, we compute distances in the stringy quantum regime of small volume in the LG phase $|\psi| < 1$ with $\psi = 1$ being the conifold point. The point deepest in this non-geometric region is the LG point at $\psi = 0$. We split the complex structure modulus $\psi = r \exp(i\theta)$, such that the LG phase is bounded by $0 \leq r < 1$ and $0 \leq \theta \leq \frac{2\pi i}{5}$. The Kähler potential in this phase is given by (3.2.19)

$$K_{\text{LG}} = -\log\left(19.217617 r^2 - 3.694710 r^4 + 0.429576 r^6 + \mathcal{O}(r^7)\right). \tag{9.2.1}$$

Higher order terms $\mathcal{O}(r^7)$ contain also a periodic θ dependence. Thus, these terms spoil a continuous phase shift symmetry and reduce it to a discrete one $\theta \rightarrow \theta + 2\pi n/5, n \in \mathbb{N}$. See chapter 3 for more explanations.

For small ψ the Kähler metric may be approximated by the first three shift symmetric terms in (9.2.1)

$$G_{\psi\bar{\psi}}^{\text{LG}} = 0.192256 - 0.0154879 r^2 + \mathcal{O}(r^4). \quad (9.2.2)$$

A geodesic is then just a ray of constant θ . The proper distance between LG point and conifold is therefore given by

$$\Delta\Theta = \int_0^1 dr \sqrt{G_{\psi\bar{\psi}}^{\text{LG}}(r)} \sim \sqrt{0.192256} \sim 0.43. \quad (9.2.3)$$

With the periods computed up to order $\mathcal{O}(100)$ we have also numerically evaluated the integral. For the proper field distance we find for instance the numerical results

$$\Delta\Theta(\theta = 0) = 0.45, \quad \Delta\Theta(\theta = \frac{2\pi}{10}) = 0.42. \quad (9.2.4)$$

In fact, there are no geodesic distances longer than 0.45 in the LG phase. The metric in figure 3.3 underpins this conclusion. So in contrast to the large volume point, the LG point is at finite proper field distance. Moreover, the distance does not exhibit a logarithmic behavior as necessary for the swampland distance conjecture. Geodesic distances in the LG phases contribute therefore to Θ_0 defined in the last section. Here, we find $\Theta_0 \lesssim 0.45$, which is sub-Planckian and hence in agreement with the refined version of the SDC.

Large volume phase

It has been already mentioned in the previous section that the large volume region asymptotically obeys a logarithmic scaling of the proper distance with ψ . From this behavior one is able to read-off the parameter Θ_λ defined in (9.1.7) ($\Theta_\lambda = \lambda^{-1}$). For that purpose we solve the geodesic equations

$$\frac{d^2 x^\mu}{d\tau^2} + \Gamma_{\alpha\beta}^\mu \frac{dx^\alpha}{d\tau} \frac{dx^\beta}{d\tau} = 0, \quad (9.2.5)$$

where τ is an affine parameter, for trajectories that start at the LG point and have initial velocity in radial direction. These geodesics, each with a different initial angle θ , are plotted in figure 9.4. Note that the geodesics are symmetric around the central one (solid red line) due to the symmetric form of the metric, see figure 3.3.

We will skip the details of this numerical analysis here and refer to [65] instead. In order to determine Θ_λ , there we have computed the proper distance of each geodesic in terms of the mirror map (see (3.2.22)) and fitted the ansatz (α_0 and α_1 are fit parameters)

$$\Theta(t) \simeq \Theta_\lambda \log(t) + \alpha_0 + \frac{\alpha_1}{t^3}. \quad (9.2.6)$$

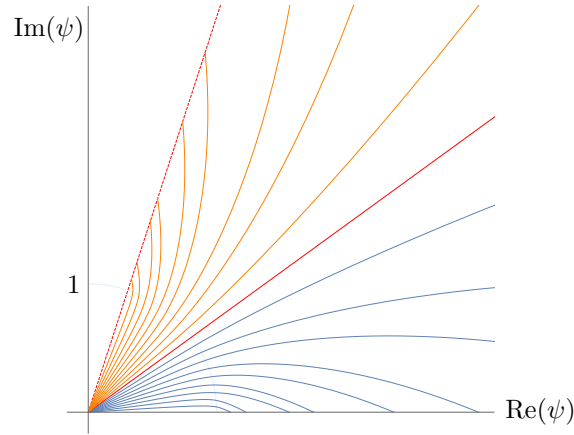


Figure 9.4: Geodesics for the initial data $(r, \dot{r}, \theta, \dot{\theta}) = (0, 1, i \cdot \pi/50, 0)$, for $i = 1, \dots, 10$. The orange geodesics are the \mathbb{Z}_2 images.

Sampling over all geodesics, we obtain for the value of the Kähler modulus at the phase transition an average value of $\text{Im}(t_0) \simeq 1.31$. The average for Θ_λ turned out to be in perfect agreement with the refined swampland distance conjecture [65]:

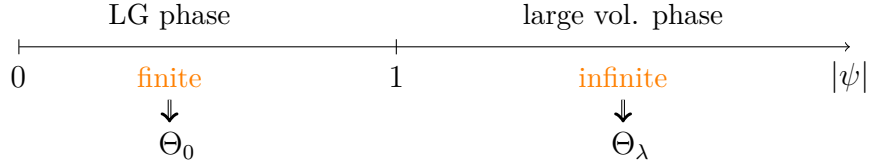
$$\Theta_\lambda \simeq 0.9343, \quad \text{i.e. sub-Planckian.} \quad (9.2.7)$$

As a cross-check of our method, for the central geodesic with $\theta = \pi/5$ we can compare the numerical result for Θ_λ with the analytic result (9.1.7). The numerical value for $\Theta_\lambda \simeq 0.866$ agrees indeed perfectly with the analytically expected value $\sqrt{3/4}$.

An interesting observation is also that the geodesics passing closer to the conifold and thus deviate the most from being straight lines in the ψ -plane have the largest Θ_λ . This is because of the fact that while both the real and imaginary part of the complexified Kähler modulus contribute to the proper distance, only the imaginary part controls a mass scale. The imaginary part of the Kähler modulus is (asymptotically) mapped to the absolute value $|\psi|$ through the mirror map, while the real part is mapped to $\text{Arg}(\psi)$. Curving into the “axionic” direction in moduli space thus decreases the rate of the exponential mass fall-off. The fact that we still find $\Theta_\lambda < M_{\text{pl}}$ for all geodesics is a non-trivial test of the RSDC. It seems to be not unrelated to the statement that periodic directions of the moduli space should have a sub-Planckian periodicity.

Finite versus infinite distances in the moduli space

Before finally moving to the two-parameter models, let us stress the different implications of the refined swampland distance conjecture for the two characteristically distinct phases. At the bottom line one phase is finite whereas the other one infinite in moduli field space:



The logarithmic scaling of the proper distance appears only in the large volume phase and is induced by Kähler metric and mirror map. This shall be briefly illustrated in the following.

Consider the large volume phase where the metric is asymptotically given by (9.1.5) (for $\psi = r \exp(i\theta)$)

$$G_{\psi\bar{\psi}}^{\text{LV}}(r) \simeq \frac{3}{4(r \log r)^2}. \quad (9.2.8)$$

The proper distance along the central geodesic (solid red line) of figure 9.4 grows therefore with a double logarithm

$$\Theta(r) \simeq \frac{\sqrt{3}}{2} \log(\log(r)). \quad (9.2.9)$$

Recall the mirror map from (3.2.23) which obeys a logarithmic growth as well

$$t_{\text{LV}}(\psi) = \frac{5}{2\pi} \log(5) + \frac{5}{2\pi} i \log \psi + \dots \quad \text{for } |\psi| > 1. \quad (9.2.10)$$

Combining the expressions for $\Theta(r)$ and $t_{\text{LV}}(\psi)$, one can immediately extract the desired (single) logarithm of the proper distance in terms of the Kähler modulus t as well as the exponential decrease of the Kaluza-Klein masses

$$\Theta \simeq \frac{\sqrt{3}}{2} \log(\text{Im}(t_{\text{LV}})) \quad \Rightarrow \quad M_{\text{KK}} \simeq \frac{1}{[\text{Im}(t_{\text{LV}})]^2} \simeq e^{-\frac{4}{\sqrt{3}} \Theta}. \quad (9.2.11)$$

Hence, the special form of metric and mirror map lead exactly to the predicted logarithmic scaling of the swampland distance conjecture. The refined version requires in addition $\Theta_\lambda < 1$.

This changes for the finite LG phase. On the one hand, the metric (9.2.2) does not give a double logarithm in the proper distance. On the other hand, the mirror map (3.2.22)

$$t_{\text{LG}}(\psi) = -\frac{1}{2} + 0.688 i + (0.279 + 0.384 i) \psi + \dots \quad |\psi| < 1, \quad (9.2.12)$$

is not equipped with a logarithm at all. As a consequence, the finite LG phase exhibits no fall-off of Kaluza-Klein states and cannot be constrained by the Swampland Distance Conjecture. The refined version of the conjecture does, however, make a prediction, i.e. all possible finite distances Θ_0 have to be sub-Planckian.

Phase	Log-Behavior/SDC	Refined SDC
finite	×	check $\Theta_0 < 1$
infinite	✓	check $\Theta_\lambda < 1$

Table 9.1: The (refined) swampland distance conjecture for finite as well as infinite phases of moduli spaces.

The different behavior of mirror map and metric for finite and infinite phases will appear analogously for two-parameter models in section 9.3. There it is useful to speak of directions as one phase may have a finite as well as infinite direction (see hybrid phases below). In table 9.1 we wrapped-up for which directions the swampland distance conjecture applies and where we calculate Θ_0 , Θ_λ .

9.3 RSDC for Calabi-Yau Manifolds with $h^{1,1} = 2$

In this section we will extend our analysis to Calabi-Yau three-folds with two Kähler moduli. As a consequence, in addition to the LG and large volume phase (LV) we obtain two *hybrid* regimes. As a new feature, these hybrid phases have solely one complex parameter ψ or ϕ bounded, whereas the other one is able to reach infinite distances. Our goals are to determine the precise proper length of finite directions in the different phases of the moduli space, extract the logarithmic behavior of proper distances along infinite directions and last but not least analytically compute the critical distance Θ_λ for certain accessible regimes.

More precisely, if we consider an infinite direction, we will always encounter a log-structure in the mirror map. Thus the corresponding Kähler modulus may grow only logarithmically past some critical distance, which is expected to cause a Kaluza-Klein state becoming exponentially light. Therefore, the appearance of the logarithm is in agreement with the swampland distance conjecture [43], where the state in question is given by this Kaluza-Klein mode.

Recall that the RSDC makes a stronger statement by predicting the invalidity of the effective theory after having traversed at most $\mathcal{O}(1) M_{\text{Pl}}$ in moduli space. Hence, the log-term behavior in the proper distance has to occur roughly at proper distance one and finite directions in the moduli space have to have proper length less than one. In this section, we will explicitly confirm the latter and asymptotically approach the log-scaling.

We shall discuss one example, that is \mathbb{P}^4_{11222} [8], quite extensively and briefly list the results for other two parameter Calabi-Yau three-folds. Let us point out again, that this section is taken from the reference [65].

9.3.1 An Illustrative Example: $\mathbb{P}_{11222}^4[8]$

Let us at first focus on the weighted projective space $\mathbb{P}_{11222}^4[8]$ which was studied in great detail in the literature, see for instance [90, 97, 100]. Recall the construction of the Kähler metric on the mirror dual in section 3.3. In terms of the homogeneous coordinates $[x_1, x_2, x_3, x_4, x_5]$, consider the Calabi-Yau hypersurface

$$P = x_1^8 + x_2^8 + x_3^4 + x_4^4 + x_5^4 - 8\psi x_1 x_2 x_3 x_4 x_5 - 2\phi x_1^4 x_2^4, \quad (9.3.1)$$

with two complex parameters (ψ, ϕ) corresponding to complex structure moduli. The smooth family of three-folds given by the quotient $\{P = 0\}/(\mathbb{Z}_4)^3$ identifies the mirror of $\mathbb{P}_{11222}^4[8]$. Following [100] it is convenient to mod the hypersurfaces $\{P = 0\}$ by an even larger group, which requires to mod the parameter space $\{(\psi, \phi)\}$ by a \mathbb{Z}_8 . Its generators act according to (with α being the 8th root of unity)

$$(\psi, \phi) \mapsto (\alpha\psi, -\phi) \quad (9.3.2)$$

The special points of the moduli space appear when the hypersurface constraint (9.3.1) becomes singular, that is, for nontrivial solutions to $P = 0$ and $\partial P/\partial x_i = 0$ for all x_i . One finds a conifold singularity at

$$(\phi + 8\psi^4)^2 = 1 \quad (9.3.3)$$

as well as another singularity for³

$$\phi^2 = 1. \quad (9.3.4)$$

The two singularities above split the moduli space into four phases: a smooth Calabi-Yau, a Landau-Ginzburg (orbifold) and two hybrid regimes, which we call hybrid \mathbb{P}^1 and hybrid orbifold.

9.3.1.1 The phase structure of the Kähler moduli space

Let us explain the origin and connection of these four-phases. We start in the LG phase. In this phase both complex structures are bounded and all homogeneous coordinates x_i are classically vanishing, such that the target space is simply a point. However, there are massless quantum fluctuations around their vacuum expectation values or in other words, there exists a residual \mathbb{Z}_8 symmetry on the coordinates x_i . Hence effectively we have a Landau-Ginzburg (orbifold) theory living on $\mathbb{C}^5/\mathbb{Z}_8$.

The singularity of $\mathbb{C}^5/\mathbb{Z}_8$ can be “blown-up” by replacing the singularity with an exceptional divisor. Here, it turns out that this divisor has two irreducible components [97]: $\mathbb{C}^3 \times \mathbb{P}^1$ and

³The singular three-folds at the locus $\phi = 1$ are birationally equivalent to the mirror of the one-parameter space $\mathbb{P}_{11111}^5[2, 4]$ (see [90]).

\mathbb{P}^4 . The four different phases are obtained by separately blowing up to these components of the divisor. For instance, consider blowing-up to the component $\mathbb{C}^3 \times \mathbb{P}^1$. This leads to a one dimensional target space given by a Landau-Ginzburg (orbifold) bundle over a \mathbb{P}^1 space. That is why we denote this regime as hybrid \mathbb{P}^1 phase. Again, some of the x_i were only fixed classically, such that one still faces a residual \mathbb{Z}_4 symmetry at every point of \mathbb{P}^1 .

In a second step, also blowing-up along the second component \mathbb{P}^4 of the exceptional divisor resolves the \mathbb{Z}_4 singularities in each fiber. Satisfying in addition a hypersurface constraint gives a $K3$ surface fibered over the \mathbb{P}^1 base. Thus, one arrives at a smooth Calabi-Yau manifold. The full procedure can be summarized as follows

phase	LG theory on $\mathbb{C}^5/\mathbb{Z}_8$	$\xrightarrow[\mathbb{C}^3 \times \mathbb{P}^1]{\text{resolved by}}$	hybrid theory on $\mathbb{C}^4/\mathbb{Z}_4$	$\xrightarrow[\mathbb{P}^4]{\text{resolved by}}$	smooth Calabi-Yau
target space	point		\mathbb{P}^1		$K3$ fibration over \mathbb{P}^1 base

Alternatively, one may first blow-up the \mathbb{P}^4 component. In this case one ends up in a hybrid orbifold phase. This regime is an orbifold because its target space is still equipped with \mathbb{Z}_2 quotient singularities.

Following [97] let us introduce the coordinates

$$\rho_1 = \frac{1}{2\pi} \log |4\phi^2|, \quad \rho_2 = \frac{1}{2\pi} \log \left| \frac{2^{11} \psi^4}{\phi} \right|. \tag{9.3.5}$$

The separation of the four phases of the complex structure moduli space can be nicely depicted in these coordinates, see figure 9.5. Moreover, the $\rho_{1,2}$ coordinates make the spatial extension of the conifold singularity $(\phi + 8\psi^4)^2 = 1$ apparent, which is marked by the shaded area in the plot.

An obvious question is whether one can circumvent the singular area in plot 9.5 or in other words, transit between any of the four phase of the moduli space. In principle this is indeed possible by computing the periods in charts covering the whole moduli space. However, our periods derived in section 3.3 do not converge for the entire moduli space. Instead they cannot be trusted arbitrarily close to the conifold singularity. Let us explain this point in more detail for the case of \mathbb{P}^4_{11222} [8].

The singular loci are fixed by $(\phi + 8\psi^4)^2 = 1$ as well as $\phi^2 = 1$, hence one can clearly circumvent the singularities simply by giving ψ or ϕ a non-zero imaginary part. So, there are in fact trajectories starting and ending in different phases. However, in practice the

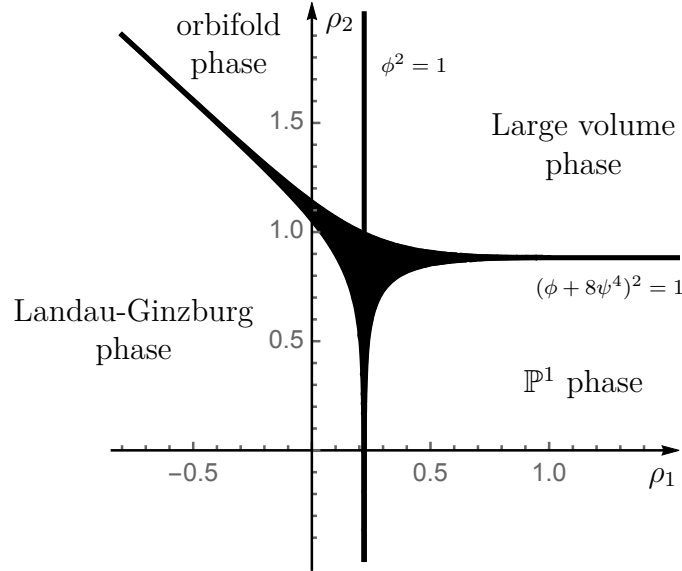


Figure 9.5: The singular loci divide the Kähler moduli space of $\mathbb{P}^4_{11222}[8]$ in four regimes [97]. Note that one is in principle able to transit between the phases if the moduli are equipped with a non-zero imaginary part.

period computation of section 3.3 converges for $|8\psi^4| \leq |\phi \pm 1|$, which agrees with the conifold constraint only for real moduli. Obviously, rotating ψ by some phase shift does not affect the convergence relation, but adding a phase to ϕ does. Figure 9.6 shows three

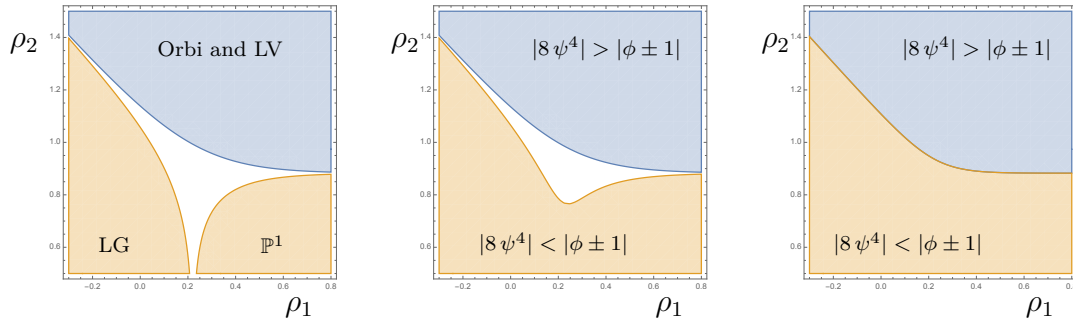


Figure 9.6: These plots depict the convergence regions of the periods for $\mathbb{P}^4_{11222}[8]$, where the blue regions covers $|8\psi^4| > |\phi \pm 1|$ and yellow $|8\psi^4| < |\phi \pm 1|$. Shown are three different phases of ϕ . In the left graph we have chosen $\phi = |\phi|$, hence the convergence area agrees with the phase picture from the conifold constraint $(\phi + 8\psi^4)^2 = 1$. In the middle graph we have $\phi = |\phi| e^{\frac{1}{2}i}$, i.e. the periods derived in section 3.3 cannot describe transitions between blue and yellow phases. As shown in the right graph, the non-convergence area vanishes precisely for choosing $\phi = |\phi| e^{\frac{\pi}{2}i}$. In all plots ψ is real.

plots of the convergence regions of the periods differing by the phase of ϕ . As one can see, a small phase for ϕ opens the border between Landau-Ginzburg and hybrid \mathbb{P}^1 phase. Only

if the phase is precisely $\text{Arg}(\phi) = \frac{\pi}{2}$, the convergence relations reduce to a single condition $|8\psi^4| \leq |\phi|^2 + 1$, such that one is able to traverse between any of the four phases. This is only possible due to the \mathbb{Z}_2 symmetry of ϕ determining the convergence relation.

The same statement holds true for \mathbb{P}_{11226}^4 [12], but not for \mathbb{P}_{11169}^4 [18] as one can observe later. In the case of \mathbb{P}_{11169}^4 [18], ϕ has a \mathbb{Z}_3 symmetry and thus the convergence relations cannot reduce to a single one (see equation 9.3.54 for details). As a consequence, it is impossible to cover the entire moduli space with the charts derived in section 3.3.

9.3.1.2 Tests of the RSDC: computing Θ_0 and log-behavior

As shown in figure 9.7, schematically the different phases of the moduli space can also be depicted in the coordinates (ψ, ϕ) . Here we are assuming to have real fields, i.e. setting $\text{Im}(\psi) = \text{Im}(\phi) = 0$ for simplicity.

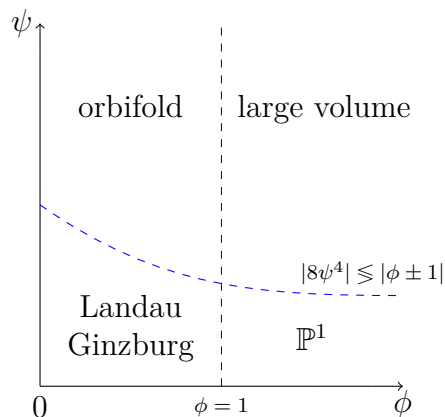


Figure 9.7: A schematic plot of the four phases of \mathbb{P}_{11222}^4 [8] in real (ϕ, ψ) coordinates. The singular locus $|8\psi^4| \sim |\phi \pm 1|$ is actually a two dimensional surface due to the \pm indicating a logical “and”. Directions bounded in field space do not necessarily have to be bounded in their proper distance.

Before starting the discussion about the lengths of curves in the moduli space, let us stress that we are distinguishing three different types of curves: we call any arbitrary path a *trajectory*. If the trajectory is additionally satisfying the geodesic equation it is called *geodesic*. The length of the globally shortest geodesic is denoted as the *distance* or *proper length*. The reason for making such a clear separation between different types of curves will become apparent in the following.

Figure 9.7 might be misleading in the sense that finite sized directions in the fields ψ and ϕ do not necessarily have to be finite in their proper length. In the case of \mathbb{P}_{11222}^4 [8], it will eventually turn out that all these seemingly finite directions in ψ, ϕ are in fact bounded in

their proper lengths. To compare with the prediction of RSDC, in the following we shall calculate the proper length of such finite directions.

Secondly, in this section we will be concerned with trajectories along infinite directions. Both in the large volume and in the hybrid phases the swampland distance conjecture implies that they show a log behavior in their distances. One has to be cautious here, as actually, this has to hold for the globally shortest geodesics between two arbitrary points in the moduli space. Hence, one would have to solve the geodesic differential equations for certain start and end points and minimize the set of solutions regarding their proper lengths. Due to the huge variety of possible trajectories in the four real dimensional moduli space of \mathbb{P}_{11222}^4 [8], this is obviously very elaborate and exceeds our computational capabilities. Therefore, we proceed by doing the analysis in asymptotic regimes of the moduli space where we are able to determine the shortest geodesics.

To see the exponentially light Kaluza-Klein modes it is important to express the final result in terms for the Kähler coordinates t_i that can be determined via the mirror map. As discussed, the mirror map can be found by analyzing the monodromy properties of the periods. For the case at hand this has been done by [65, 100] and the mirror map in all phases is given by

$$\begin{aligned} t_1 &= -\frac{1}{4} + \frac{2\omega_2 + \omega_4}{4\omega_0}, \\ t_2 &= \frac{1}{4} - \frac{2\omega_2 + \omega_4}{4\omega_0} + \frac{3\omega_1 + 2\omega_3 + \omega_5}{4\omega_0}, \end{aligned} \tag{9.3.6}$$

where the periods ω_i have been computed in section 3.3. Later, we will find it useful to state the asymptotic behavior of the Kähler coordinates at special points in moduli space.

Landau-Ginzburg phase

The Landau-Ginzburg regime is similar to the example of the quintic 9.2 in the sense that the algebraic parameters $|\phi|$ and $|\psi|$ are both bounded

$$0 \leq \phi < 1, \quad 0 \leq \psi < \psi_c. \tag{9.3.7}$$

The upper bound ψ_c is determined as a solution of the convergence condition $|8\psi^4| < |\phi \pm 1|$ for fixed ϕ .

As already pointed out, whether all geodesics in the LG phases stay finite is a priori not obvious. If they are finite, it is important to compute their proper lengths. For that purpose let us investigate three trajectories as depicted in figure 9.8. All of these trajectories start close to the smallest possible values of the algebraic moduli $\psi = \phi = 0$. Then, we consider one trajectory only in direction of ψ or ϕ , respectively. Additionally, there will be one moving directly towards the conifold singularity. The labeling of the curves follows figure 9.8. Using the metric computed in section 3.3, we obtain the following lengths for these

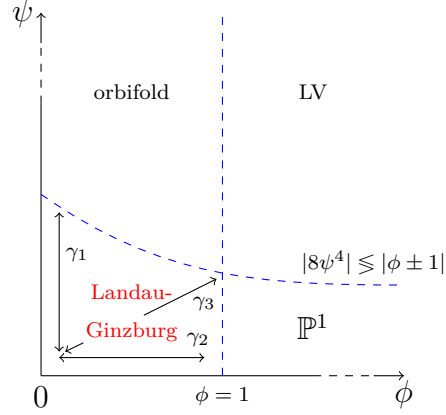


Figure 9.8: The Landau-Ginzburg phase has finite length in every direction. To show this we compute the lengths of the following three paths in (ϕ, ψ) : $\gamma_1 : (0, 0) \rightarrow (0, 0.59)$, $\gamma_2 : (0, 0) \rightarrow (1, 0)$, $\gamma_3 : (0, 0) \rightarrow (0.5, 0.5)$.

trajectories

$$\begin{aligned}
 \Delta\Theta_1 &= \int_{\gamma_1} d\psi \sqrt{G_{\psi\bar{\psi}}(\psi)} = 0.40, \\
 \Delta\Theta_2 &= \int_{\gamma_2} d\phi \sqrt{G_{\phi\bar{\phi}}(\phi)} = 0.24, \\
 \Delta\Theta_3 &= \int_{\gamma_3} d\tau \sqrt{G_{\mu\bar{\nu}}(\psi(\tau), \phi(\tau)) \frac{dx^\mu}{d\tau} \frac{d\bar{x}^{\bar{\nu}}}{d\tau}} = 0.36,
 \end{aligned} \tag{9.3.8}$$

where we have denoted $x^\mu = \{\psi, \phi\}$. All these directions are finite and smaller than one, as expected from the RSDC.

For the sake of completeness, let us point out that the mirror map coordinates in the Landau-Ginzburg regime approach the finite values $t_1 = \frac{1}{2}(-1 + i)$ and $t_2 \simeq 0.5 + 0.21i$ for $\phi, \psi \rightarrow 0$.

Hybrid phase - \mathbb{P}^1

The conceptually new regimes of this moduli space are clearly the hybrid phases \mathbb{P}^1 and orbifold. We begin with the hybrid \mathbb{P}^1 phase, where the two complex structure parameters are limited by the regime

$$1 < \phi < \infty, \quad 0 \leq \psi < \psi_c. \tag{9.3.9}$$

Again, the upper bound ψ_c is determined as solution of the convergence condition $|8\psi^4| < |\phi \pm 1|$ for fixed ϕ .

The phase diagram of figure 9.5 leads naturally to the following questions: First, does really only one Kähler modulus t_i exhibit a logarithmic behavior for large distances in field space? That is to be expected for trajectories parallel to the ϕ axis, but not for the ones parallel to the Landau-Ginzburg regime. Second, does there exist a geodesic moving towards $|\rho_1| \rightarrow \infty$ or is the attractive effect of the conifold singularity strong enough to bend any geodesic into the singularity? Finally, will the RSDC hold true even for geodesic passing the Landau-Ginzburg and a hybrid phase before entering the large volume regime? It seems to be challenging for arbitrary geodesics to collect less than $\mathcal{O}(1) M_{\text{Pl}}$ in the proper distance after crossing two regimes. In order to answer the latter two questions one has to consider actual geodesics. Thus we will comment on these questions later and focus now on the first one by analyzing the trajectories shown in figure 9.9. Note that we assume again for simplicity ψ, ϕ to be real-valued.

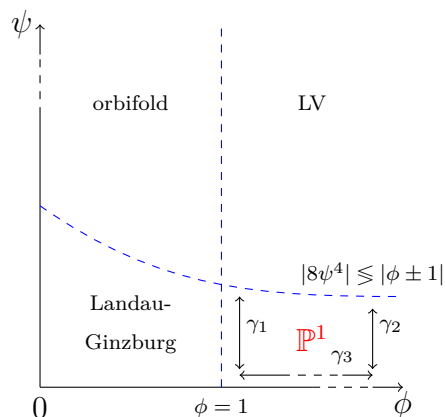


Figure 9.9: The hybrid \mathbb{P}^1 fibration regime has one finite as well as one infinite direction. The dashed arrow and coordinate axes symbolize their extension to infinity. For the calculation we used $\gamma_1 : (1.1, 0) \rightarrow (1.1, 0.33)$.

The curve γ_1 starts near $\psi = 0, \phi = 1$ and moves only in ψ direction, hence along the Landau-Ginzburg regime towards the singularity. Via integration we find its length

$$\Delta\Theta_1 = \int_{\gamma_1} d\psi \sqrt{G_{\psi\bar{\psi}}(\psi)} = 0.24. \quad (9.3.10)$$

This result is consistent with the RSDC and with our expectations, as it is close to to the Landau-Ginzburg phase. Besides, we can estimate the asymptotic distance for large ϕ as depicted by curve γ_2 in figure 9.9. According to section 3.3, in the \mathbb{P}^1 phase the asymptotic behavior of the metric for $(\phi \rightarrow 0, \psi \rightarrow \infty)$ is

$$G_{\mathbb{P}^1}^{\text{asympt}} \simeq \begin{pmatrix} G_{\phi\bar{\phi}}^{\text{asympt}} & 0 \\ 0 & G_{\psi\bar{\psi}}^{\text{asympt}} \end{pmatrix} \simeq \begin{pmatrix} \frac{0.25}{|\phi|^2 (\log|\phi|)^2} & 0 \\ 0 & \frac{0.5905}{\sqrt{|\phi|}} \end{pmatrix}. \quad (9.3.11)$$

Integrating this asymptotic metric for large ϕ leads to a finite and non-zero value

$$\Delta\Theta_2 = \int_{\gamma_2} d\psi \sqrt{G_{\mathbb{P}^1, \psi\bar{\psi}}^{\text{asympt}}(\phi)} \simeq \sqrt{\frac{0.5905}{\sqrt{|\phi|}}} \cdot \sqrt[4]{\frac{|\phi|}{8}} = 0.46. \quad (9.3.12)$$

Finally, we want to point out that the trajectory γ_3 “parallel” to the large volume phase has infinite length. To see that, we would have to integrate the Kähler metric of \mathbb{P}^1 in the ϕ direction towards ∞ . But asymptotically this integral is given by

$$\Theta \sim \int d\phi \sqrt{G_{\mathbb{P}^1, \phi\bar{\phi}}^{\text{asympt}}(\phi)} \sim \log(\log \phi). \quad (9.3.13)$$

As a consequence, the direction ϕ in \mathbb{P}^1 is infinite, in contrast to the ψ direction.

As we have seen, it is the Kähler coordinates $\text{Im}(t_i)$ (following from the mirror map) that control the exponential drop-off of the Kaluza-Klein modes. Using eq. (9.3.6), deep inside the \mathbb{P}^1 phase ($\psi \rightarrow 0, \phi \rightarrow \infty$), we find

$$\begin{aligned} t_1 &\simeq \frac{1}{2}(-1 + i) + \dots, \\ t_2 &\simeq \left(1 - \frac{i}{2}\right) + \frac{8i \log(2)}{2\pi} + \frac{i}{\pi} \log(\phi) + \dots \end{aligned} \quad (9.3.14)$$

This is just right, as the logarithmic scaling behavior with respect to t_2 becomes

$$\Theta \sim \log(\log \phi) \sim \log(\text{Im } t_2). \quad (9.3.15)$$

Hybrid phase - orbifold

As one might guess from figure 9.7, the hybrid orbifold phase is qualitatively quite similar to the \mathbb{P}^1 hybrid phase. Now the algebraic coordinates may vary in the interval

$$0 \leq \phi < 1, \quad \psi_c < \psi < \infty, \quad (9.3.16)$$

with ψ_c as in the other phases. Again, we focus on three trajectories: a finite one γ_1 along the Landau-Ginzburg regime, its asymptotic equivalent γ_2 for large ψ and an infinite direction γ_3 along the large volume regime. Figure 9.10 summarizes these curves schematically.

We begin by computing the distance from $\phi = 0$ to the conifold singularity. Keeping ψ fixed, the integral leads to the length

$$\Delta\Theta_1 = \int_{\gamma_1} d\phi \sqrt{G_{\phi\bar{\phi}}(\phi)} = 0.21, \quad (9.3.17)$$

which is very close to our result (9.3.8) in the Landau-Ginzburg phase.

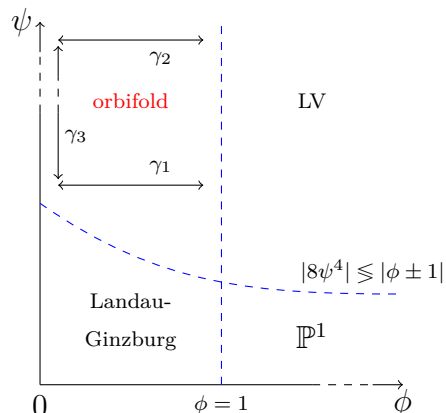


Figure 9.10: In the hybrid orbifold phase we find again an infinite direction γ_3 plus a finite one $\gamma_1 : (0, 0.59) \rightarrow (1, 0.59)$. The distance in the ϕ direction asymptotically (indicated by dashed arrow) to a finite γ_2 , more precisely the distance will be zero.

Let us now check whether this asymptotically approaches a finite distance γ_2 as in the \mathbb{P}^1 fibration regime. The asymptotic metric for real moduli near $\phi \simeq 0$ (see section 3.3 for details) reads

$$G_{\text{orbi}}^{\text{asympt}} \simeq \begin{pmatrix} \frac{0.09}{|\log(\psi)|^2} & 0 \\ 0 & \frac{0.75}{|\psi|^2 (\log|\psi|)^2} \end{pmatrix}. \quad (9.3.18)$$

Consequently, the asymptotic distance γ_2 is indeed finite

$$\Delta\Theta_2 = \int_{\gamma_2} d\phi \sqrt{G_{\text{orbi}, \phi\phi}^{\text{asympt}}(\psi)} \sim \frac{\sqrt{0.09}}{|\log \psi|} \int_0^1 d\phi \xrightarrow{\psi \rightarrow \infty} 0. \quad (9.3.19)$$

This is interesting since the distance to the large volume phase vanishes. In other words, for large ψ we end up at the $\phi = 1$ singularity and hence on the one-parameter subspace \mathbb{P}_{11111}^5 [24].

From the metric one can see that the pure ψ direction γ_3 of the hybrid orbifold phase is infinite. The metric in the ψ direction leads again to a $\Theta \sim \log(\log \psi)$ growth of the distance. The asymptotic form of the mirror map confirms exactly our observation. For $(\psi \rightarrow \infty, \phi \rightarrow 0)$, we find

$$\begin{aligned} t_1 &\simeq \frac{i}{2\pi} \log(8\psi)^4 + \dots, \\ t_2 &\simeq \frac{1}{2} + \dots \end{aligned} \quad (9.3.20)$$

Thus, the distance is in agreement with the Swampland Distance Conjecture as now $\Theta \sim \log(\log \psi) \sim \log(\text{Im } t_1)$.

Only t_1 grows logarithmically for large values of ψ , whereas t_2 approaches a constant. Note that this was exchanged in the \mathbb{P}^1 regime. In addition, the imaginary part $\text{Im}(t_2) = \int_{\Sigma_2} J$

asymptotes to zero⁴. This means that one has a vanishing 2-cycle Σ_2 , validating the interpretation of being located at the one-parameter subspace $\mathbb{P}_{11111}^5[2\ 4]$.

Large volume phase

In the remaining phase of the moduli space under investigation, the algebraic parameters may take values in

$$1 < \phi < \infty, \quad \psi_c < \psi < \infty. \quad (9.3.21)$$

and ψ_c again as in the other phases. By definition it is clear that both directions, ϕ and ψ , are infinite. Therefore we expect the $\Theta \sim \log \log(-)$ -behavior, demanded by the swampland distance conjecture, in any of these directions.

The mirror map confirms this expectation. Around the large volume point, according to [100] they are given by

$$\begin{aligned} t_1 &\simeq \frac{1}{2} + \frac{i}{2\pi} \log \left(\frac{(8\psi)^4}{2\phi} \right) + \dots, \\ t_2 &\simeq \frac{i}{\pi} \log(2\phi) + \dots, \end{aligned} \quad (9.3.22)$$

where the dots denote polynomial corrections. So, whenever one of the algebraic coordinates becomes large, the corresponding Kähler coordinate will grow logarithmically.

9.3.1.3 Tests of the RSDC: computing Θ_λ

So far, we have only motivated the logarithmic behavior of proper distances by analyzing the mirror maps of each phase in the moduli space. Let us now turn towards the critical distance Θ_λ where the logarithm is significant, i.e. challenge the RSDC. For that purpose, two different approaches are presented: calculating Kähler potentials and geodesics in asymptotic regions of the moduli space. Both methods will turn out to give the same results for Θ_λ .

Asymptotic Kähler potentials

Before commenting on geodesics in two-parameter models, recall that the value for Θ_λ deep inside the large volume regime (LV) can be derived from the generic form (9.1.4) of

⁴The (at a first glance surprising) possibility for zero minimum distances in string target spaces was already observed in [189]. In fact, there it was argued that for “sufficiently complicated” topologies a vanishing exceptional divisor demands some other part of the target space to become infinitely large. This is in line with the $\log(\psi)$ term in t_1 .

the asymptotic Kähler potential. It is interesting to compare this Kähler potential in the large volume region to the asymptotic ones in the two hybrid phases.

For the mirror of \mathbb{P}_{11222}^4 [8] the prepotential depending on the Kähler coordinates t_i is asymptotically given by [100]

$$\mathcal{F} = -\frac{4}{3}(t_1)^3 + 2(t_1)^2 t_2 + \dots, \quad (9.3.23)$$

where the dots denote subleading corrections. Employing the standard formula for the periods $\Pi(t_1, t_2) = (1, t_1, t_2, 2\mathcal{F} - \partial_{t_1}\mathcal{F} - \partial_{t_2}\mathcal{F}, \partial_{t_1}\mathcal{F}, \partial_{t_2}\mathcal{F})$ (in inhomogeneous coordinates), we obtain the Kähler potential

$$K_{LV}^{\text{asympt}} \simeq -\log \left[\frac{4i}{3}(t_1 - \bar{t}_1)^3 + 2i(t_1 - \bar{t}_1)^2(t_2 - \bar{t}_2) \right]. \quad (9.3.24)$$

In the hybrid phases we are able to compute an asymptotic expression for the Kähler potential as well:

Hybrid \mathbb{P}^1 phase Expanding the Kähler potential $K_{\mathbb{P}^1}$ of this regime around $\psi \approx 0$ and $\phi \rightarrow \infty$, we find asymptotically

$$\begin{aligned} \exp(-K_{\mathbb{P}^1}^{\text{asympt}}) \simeq 6.99i \frac{\psi\bar{\psi}}{(\phi\bar{\phi})^{\frac{1}{4}}} & \left[5.54 - 2.46 \frac{\psi\bar{\psi}}{(\phi\bar{\phi})^{\frac{1}{4}}} \right. \\ & \left. + \left(1 - 0.59 \frac{\psi\bar{\psi}}{(\phi\bar{\phi})^{\frac{1}{4}}} \right) \log(\phi\bar{\phi}) \right] \end{aligned} \quad (9.3.25)$$

which is consistent with the metric (9.3.11). Taking the mirror map (9.3.14) into account, in leading-order leads to the simple result

$$K_{\mathbb{P}^1}^{\text{asympt}} \simeq -\log(t_2 - \bar{t}_2). \quad (9.3.26)$$

Obviously, the large volume Kähler potential (9.3.24) reduces to the \mathbb{P}^1 expression for small t_1 and very large t_2 . It also confirms the target space geometry since the Kähler modulus t_2 measures the size of the \mathbb{P}^1 space.

Moreover, even without calculating geodesics one can derive a value for Θ_λ in this asymptotic region. That is, using the induced metric

$$G_{t_2\bar{t}_2} = \frac{1}{4(\text{Im } t_2)^2} \quad (9.3.27)$$

and carrying out an analogous calculation as in section 9.1, we obtain a critical proper distance $\Theta_\lambda = \sqrt{0.25} \simeq 0.5$. As $\Theta_\lambda < O(1)$, this is in agreement with the RSDC.

Hybrid orbifold phase Similarly, we approximate the Kähler potential K_{orbi} in the hybrid orbifold phase around $\phi \approx 0$ and $\psi \rightarrow \infty$ by

$$\begin{aligned} \exp(-K_{\text{orbi}}^{\text{asympt}}) &\simeq 26.32i - 0.45i \phi \bar{\phi} + 0.13i \phi \bar{\phi} \log(\psi \bar{\psi}) \\ &+ 17.85i \log(\psi \bar{\psi}) + 4.29i [\log(\psi \bar{\psi})]^2 + 0.34i [\log(\psi \bar{\psi})]^3 \end{aligned} \quad (9.3.28)$$

which is again in line with the asymptotic metric (9.3.18). By plugging in the mirror map (9.3.20), we get the leading-order result

$$K_{\text{orbi}}^{\text{asympt}} \simeq -3 \log(t_1 - \bar{t}_1), \quad (9.3.29)$$

which is as expected from the large volume expression (9.3.24) for t_1 much larger than t_2 . From the target space point of view, t_1 corresponds to the overall volume of the orbifold. The critical proper distance is the same as already computed in section 9.1, $\Theta_\lambda = \sqrt{0.75} \simeq 0.87$.

Next, we challenge the refined conjecture from the perspective of geodesics.

9.3.1.4 Tests of the RSDC: asymptotic geodesics

In order to investigate the refined version of the swampland distance conjecture one has to check whether the proper lengths of *geodesics* grow at best logarithmically after having traversed $\Theta_\lambda \sim \mathcal{O}(1)M_{\text{Pl}}$ distances. This behavior is expected to occur for trajectories moving sufficiently far along one of the infinite directions pointed out above. Obviously, in the two-parameter model the most interesting geodesics cross various phases. It is crucial to note that not every geodesic is automatically the globally shortest path between two points.

Basically the reason boils down to the attractive effect of the singularities in the moduli space at hand. However, the RSDC holds only for the shortest geodesic, which leads to technical difficulties. In fact, it is quite delicate to find the solution to the geodesic equation with minimal proper length for given start and end points. In particular so, as we are now working in real four dimensional space. One could only determine rough upper bounds for Θ_λ from several typical trajectories.

Here we will instead pursue a different approach, where the goal is to compute geodesics in asymptotic regions of the moduli space, where we have already derived a simple analytic expression for the Kähler metric on the moduli space.

Hybrid \mathbb{P}^1 phase At first consider the hybrid \mathbb{P}^1 phase and in particular the regime $\psi \approx 0$ and $\phi \rightarrow \infty$. In this regime a trajectory purely in the ϕ direction will be a geodesic and moreover it will be the shortest one. We show in the following that such a trajectory solves the geodesic equation and compute the critical distance Θ_λ . Note that if it is a geodesic, it is automatically the shortest one due to the symmetric influence of the singularities.

Taking into account that we want to keep $\psi \approx 0$, we assume the initial values $\psi_i = d\psi_i/d\tau = 0$ with an affine proper time parameter τ . As a consequence the two interesting geodesic equations simplify to

$$\frac{d^2\phi}{d\tau^2} + \Gamma_{\phi\phi}^\phi \left(\frac{d\phi}{d\tau} \right)^2 = 0 \quad (9.3.30)$$

$$\frac{d^2\psi}{d\tau^2} + \Gamma_{\phi\phi}^\psi \left(\frac{d\phi}{d\tau} \right)^2 = 0. \quad (9.3.31)$$

Recall that the metric in this regime is asymptotically given by eq. (9.3.11)

$$G_{\mathbb{P}^1}^{\text{asympt}} \simeq \begin{pmatrix} \frac{0.25}{|\phi|^2 (\log|\phi|)^2} & 0 \\ 0 & \frac{0.5905}{\sqrt{|\phi|}} \end{pmatrix}. \quad (9.3.32)$$

Due to the simple structure of the metric, the Christoffel symbols are straightforward to compute

$$\Gamma_{\phi\phi}^\phi = -\frac{1}{\phi} \left(1 + \frac{1}{\log\phi} \right), \quad \Gamma_{\phi\phi}^\psi = 0. \quad (9.3.33)$$

Hence the geodesic equation (9.3.31) for ψ shows that there is no movement in the ψ direction, i.e. we stay at $\psi \approx 0$. In other words, a trajectory γ purely in ϕ direction is indeed a geodesic. The geodesic equation (9.3.30) for ϕ can be solved analytically with two integration constants C_1, C_2 . The solution turns out to be a double exponential of the form

$$\phi(\tau) = \exp[\exp(C_1\tau + C_1C_2)]. \quad (9.3.34)$$

If we then evaluate the proper distance Θ for the geodesic γ , we find a direct proportionality to τ . This is clear since Θ and τ are affine parameters. The crucial factor is the $\sqrt{0.25}$ from the numerator of $G_{\mathbb{P}^1, \phi\phi}^{\text{asympt}}$. More precisely we find the following proper distance

$$\Theta = \int_\gamma d\tau \sqrt{G_{\mathbb{P}^1, \phi\phi}^{\text{asympt}} \left(\frac{d\phi}{d\tau} \right)^2} = \frac{1}{2} C_1 \tau. \quad (9.3.35)$$

The SDC predicts an exponential growth of the Kähler coordinate depending on the proper distance. Here, one can observe this directly for the geodesic (9.3.34) and the mirror map t_2 from eq. (9.3.14)

$$\text{Im}(t_2) = -\frac{1}{2} + \frac{8 \log 2}{2\pi} + \frac{1}{\pi} \exp(2\Theta + C_1C_2). \quad (9.3.36)$$

The exponential factor becomes relevant beyond a critical distance $\Theta_\lambda = 0.5$ according to our definition in section 9.1. Since we satisfy $\Theta_\lambda < 1$, we are clearly in agreement with the RSDC.

Hybrid orbifold phase One can perform the same analysis for the hybrid orbifold phase with similar results. There, we consider a trajectory at $\phi \approx 0$ in the limit $\psi \rightarrow \infty$, i.e. moving far from the origin purely in the ψ direction. The asymptotic metric (9.3.18) was again diagonal and included the component $G_{\text{orbi}, \psi\bar{\psi}}^{\text{asympt}} = 0.75/|\psi \log \psi|^2$. Assuming now $d\psi/d\tau \approx 0$, the geodesic equations and its solutions are equivalent to the hybrid \mathbb{P}^1 phase (with two constants C_1, C_2). The proper distance is now given by $\Theta = \sqrt{0.75} C_1 \tau$, such that the mirror map (9.3.20) obeys the following relation

$$\text{Im}(t_1) = \frac{6 \log 2}{\pi} + \frac{2}{\pi} \exp\left(\frac{\Theta}{\sqrt{0.75}} + C_1 C_2\right). \tag{9.3.37}$$

The critical distance is now found to be $\Theta_\lambda = \sqrt{0.75} \sim 0.87 < 1$ and hence satisfies the RSDC, as well. Note that all results from investigating geodesics agree precisely with the one derived from asymptotic Kähler potentials.

To consolidate our results, we consider other two-parameter moduli spaces and perform a similar analysis.

9.3.2 $\mathbb{P}^4_{11226}[12]$

In this section we analyse, by analogy with $\mathbb{P}^4_{11222}[8]$, the moduli space of $\mathbb{P}^4_{11226}[12]$, which was also investigated in [100]. The defining hypersurface polynomial is now given by

$$P = x_1^{12} + x_2^{12} + x_3^6 + x_4^6 + x_5^6 - 12\psi x_1 x_1 x_3 x_4 x_5 - 2\phi x_1^6 x_2^6. \tag{9.3.38}$$

The mirror of $\mathbb{P}^4_{11226}[12]$ can again be identified with the Calabi-Yau three-fold satisfying the constraint $\{P = 0\}/G$, where in this case the group G may be enlarged to include a \mathbb{Z}_{12} symmetry. Its action on the algebraic parameters reads

$$(\psi, \phi) \mapsto (\alpha\psi, -\phi) \tag{9.3.39}$$

with $\alpha = \exp(2\pi i/12)$. As explained in [100], the structure of the moduli space is very similar to the one of $\mathbb{P}^4_{11222}[8]$. In particular, the four different phases appear again: Landau-Ginzburg, large volume, hybrid \mathbb{P}^1 and hybrid orbifold. The singular loci in case of $\mathbb{P}^4_{11226}[12]$ are $\phi^2 = 1$ and the conifold surface $(\phi + 864\psi^6)^2 = 1$. The singular three-folds at $\phi^2 = 1$ are again birationally equivalent to the mirror of a one-parameter model. In this case they correspond to the CICY $\mathbb{P}^5_{111113}[2\ 6]$.

The periods may be calculated with the techniques described in section 3.3. The series expansion of the fundamental period converges for

$$|864\psi^6| \lesssim |\phi \pm 1|, \quad (9.3.40)$$

depending on the regime we want to investigate. Note that the \pm stands again for a logical “and”.

Let us now briefly investigate various distances in the moduli space of the mirror \mathbb{P}_{11226}^4 [12] in analogy with the schematic drawings in figures 9.8, 9.9, 9.10. In particular we want to determine infinite directions and estimate characteristic finite ones. Let us point out that we assume again real moduli ψ, ϕ for simplicity.

Furthermore, we shall calculate the mirror map and analyze its asymptotic behavior for each phase. Eventually, we will encounter the same structure as for the \mathbb{P}_{11222}^4 [8] including the logarithms. The formula for the mirror map follows [100]

$$\begin{aligned} t_1 &= -\frac{1}{2} + \frac{\omega_2 + \omega_4}{2\omega_0}, \\ t_2 &= \frac{1}{2} - \frac{\omega_2 + \omega_4}{2\omega_0} + \frac{\omega_1 + \omega_3 + \omega_5}{2\omega_0}, \end{aligned} \quad (9.3.41)$$

where the periods ω_i have been computed in section 3.3.

Landau-Ginzburg phase The boundaries of this phase are governed by the constraints $0 \leq \phi < 1$ and $0 \leq \psi < \psi_c$, where the maximal value ψ_c is the real solution to $|864\psi_c^6| < |\phi \pm 1|$. Then, we start at $\psi = \phi = 0$ deep in the Landau-Ginzburg regime and consider two trajectories: one purely in direction ϕ keeping ψ fixed and one vice versa. By integration we find the maximal length in these directions

$$\begin{aligned} \Delta\Theta_1 &= \int_0^{\psi_c} d\psi \sqrt{G_{\psi\bar{\psi}}(\psi)} = 0.21, \\ \Delta\Theta_2 &= \int_0^1 d\phi \sqrt{G_{\phi\bar{\phi}}(\phi)} = 0.32. \end{aligned} \quad (9.3.42)$$

Hence, we conclude that the Landau-Ginzburg phase is again of finite size in any direction with distances shorter than $\mathcal{O}(1) M_{\text{Pl}}$. The mirror map (9.3.41) asymptotes to finite values as well. For $\phi, \psi \rightarrow 0$ we end up with $t_1 \simeq -\frac{1}{2} + 0.866i$ and $t_2 \simeq \frac{1}{2} + 0.134i$.

\mathbb{P}^1 hybrid phase The algebraic parameters of \mathbb{P}^1 are constrained by the intervals $1 < \phi < \infty$ and $0 \leq \psi < \psi_c$ with ψ_c as above. We begin with a trajectory along the boundary to the Landau-Ginzburg phase. That is, we start at $\psi = 0, \phi = 1.1$ and integrate in ψ direction up to ψ_c without altering ϕ . The length turns out to be finite and quite small

$$\Delta\Theta_1 = \int_0^{\psi_c} d\psi \sqrt{G_{\psi\bar{\psi}}(\psi)} = 0.1. \quad (9.3.43)$$

According to example \mathbb{P}_{11222}^4 [8], we expect this length to asymptote to a finite value. Therefore, we approximate the asymptotic metric for $(\psi, \phi) \rightarrow (0, \infty)$. At leading order we find

$$G_{\mathbb{P}^1}^{\text{asympt}} \simeq \begin{pmatrix} \frac{0.25}{|\phi|^2 (\log |\phi|)^2} & 0 \\ 0 & \frac{27.23 |\psi|^2}{|\phi|^{\frac{2}{3}}} \end{pmatrix}. \quad (9.3.44)$$

Indeed we arrive at a finite result by integration and using $|\psi_c|^2 \sim |\phi|^{\frac{1}{3}} / (864^{\frac{1}{3}})$

$$\Delta\Theta_2 = \int_0^{\psi_c} d\psi \sqrt{G_{\mathbb{P}^1, \psi\bar{\psi}}^{\text{asympt}}(\psi, \phi)} \simeq \frac{\sqrt{27.23}}{|\phi|^{\frac{1}{3}}} \cdot \int_0^{\psi_c} d\psi \psi^2 = 0.27. \quad (9.3.45)$$

Instead of this approximate analytic approach, one may also evaluate the integral over the full metric numerically, which confirms our result for $\Delta\Theta_2$. In contrast, distances of the hybrid \mathbb{P}^1 phase in ϕ may become infinite. One way to see this, is that the integral

$$\Theta \sim \int d\phi \sqrt{G_{\mathbb{P}^1, \phi\bar{\phi}}^{\text{asympt}}(\phi)} \sim \log(\log \phi) \quad (9.3.46)$$

does obviously not converge to a finite value.

Next, we evaluate the formulae (9.3.41) for the mirror map. For $\phi \rightarrow \infty$ and $\psi \simeq 0$, we obtain asymptotically

$$\begin{aligned} t_1 &\simeq -\frac{1}{2} + 0.866 i + \dots, \\ t_2 &\simeq 1 + 0.10 i + \frac{i}{\pi} \log(2\phi) + \dots \end{aligned} \quad (9.3.47)$$

On the one hand, t_1 is finite as in the Landau-Ginzburg phase. On the other hand, t_2 grows logarithmically in ϕ and hence the proper distance is $\Theta \sim \log t_2$ in agreement with the SDC.

Orbifold hybrid phase In this regime the algebraic parameter may vary within $0 \leq \phi < 1$ and $\psi_c < \psi < \infty$, employing the constraint $|864 \psi_c^6| \geq |\phi \pm 1|$. At first, we compute the trajectory from $\phi = 0$ to $\phi = 1$ keeping ψ constant at a minimal value $\psi \sim 0.32$. Basically we integrate along the border to the Landau-Ginzburg phase. A simple calculation shows:

$$\Delta\Theta_1 = \int_0^1 d\phi \sqrt{G_{\phi\bar{\phi}}(\phi)} = 0.16. \quad (9.3.48)$$

Recall that asymptotically for large ψ this length was decreasing to zero in the example \mathbb{P}_{11222}^4 [8]. In fact, we will observe the same behavior here. The metric near $\phi \simeq 0$ and $\psi \rightarrow \infty$ leads to the expression

$$G_{\text{orbi}}^{\text{asympt}} \simeq \begin{pmatrix} \frac{0.04}{|\log(\psi)|^2} & 0 \\ 0 & \frac{0.75}{|\psi|^2 (\log |\psi|)^2} \end{pmatrix}. \quad (9.3.49)$$

Thus, the asymptotic proper distance in ϕ direction is again vanishing due to its scaling $\int_0^1 d\phi \sqrt{G_{\text{orbi}, \phi\phi}^{\text{asympt}}(\psi)} \sim 1/|\log \psi|$. One then ends up at the $\phi = 1$ locus which is birational equivalent to the complete intersection Calabi-Yau \mathbb{P}_{111113}^5 [2 6]. Note that one may traverse infinite distances in ψ direction as expected. This is easy to see from the metric and in direct analogy with \mathbb{P}_{11222}^4 [8].

This time, for $\psi \rightarrow \infty$ and $\phi \simeq 0$ the mirror map (9.3.41) approaches the values

$$\begin{aligned} t_1 &\simeq -\frac{3}{4} + \frac{i}{2\pi} \log(12\psi)^6 + \dots, \\ t_2 &\simeq \frac{1}{2} + \dots, \end{aligned} \tag{9.3.50}$$

indicating a logarithmic growth of the proper distance depending on the Kähler modulus t_1 . Analogously to \mathbb{P}_{11222}^4 [8], the imaginary part of t_2 vanishes asymptotically, i.e. the 2-cycle Σ_2 shrinks to zero [189]. Again, we arrive then on the $\phi = 1$ locus which corresponds to the one-parameter CICY \mathbb{P}_{111113}^5 [2 6].

Large volume phase Finally, the large volume regime $1 < \phi < \infty$ and $\psi_c < \psi < \infty$ (ψ_c as above) is infinite in both directions ϕ, ψ . As expected, we find a logarithmic growth of the proper distances in any direction, after employing the mirror map [100]

$$\begin{aligned} t_1 &\simeq \frac{1}{2} + \frac{i}{2\pi} \log\left(\frac{(12\psi)^6}{2\phi}\right) + \dots, \\ t_2 &\simeq \frac{i}{\pi} \log(2\phi) + \dots \end{aligned} \tag{9.3.51}$$

The dots indicate polynomial corrections that are sub-leading at infinity.

Summary The different regimes of the moduli space of the mirror \mathbb{P}_{11226}^4 [12] with its finite lengths are schematically depicted in figure 9.11. The results are qualitatively very similar to \mathbb{P}_{11222}^4 [8]. In accordance with the RSDC, all finite characteristic lengths are smaller than $O(1)M_{\text{Pl}}$. Infinite directions show a log-behavior in their corresponding Kähler modulus. This confirms again the predictions from the SDC.

In addition, we were able to determine the critical distance Θ_λ , where the logarithmic behavior becomes essential. The computation is indeed equivalent to the one of section (5.1.4). By using the metrics (9.3.44) and (9.3.49), we find therefore in the hybrid \mathbb{P}^1 phase $\Theta_\lambda = 1/2$ and in the hybrid orbifold phase $\Theta_\lambda = \sqrt{0.75}$.

9.3.3 \mathbb{P}_{11169}^4 [18]

The final example in this section is the moduli space of \mathbb{P}_{11169}^4 [18]. An extensive analysis of this model can be found in [101]. In the literature it was shown that the most general

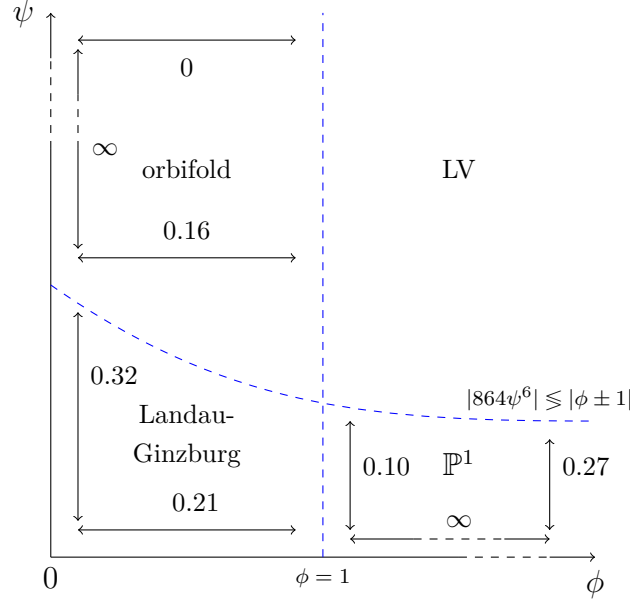


Figure 9.11: Schematic plot of the moduli space of the mirror $\mathbb{P}^4_{11226}[12]$ with finite as well as infinite directions as calculated above.

possible polynomial of degree 18 employed to describe this moduli space may be reduced to

$$P = x_1^{18} + x_2^{18} + x_3^{18} + x_4^3 + x_5^2 - 18\psi x_1 x_2 x_3 x_4 x_5 - 3\phi x_1^6 x_2^6 x_3^6. \quad (9.3.52)$$

The moduli space is again defined by the hypersurface constraint $\{P = 0\}/G$. There exists a scaling symmetry preserving the form of P , which is identified with an enlarged group \hat{G} . This group induces a \mathbb{Z}_{18} action on the algebraic parameters

$$(\psi, \phi) \mapsto (\alpha\psi, \alpha^6\phi) \quad (9.3.53)$$

with the nontrivial 18th root of unity $\alpha = \exp(2\pi i/18)$. In fact, there are additional transformations leaving the hypersurface constraint invariant. For these and further details we simply refer to the literature.

The qualitative structure of the moduli space is similar to the one of $\mathbb{P}^4_{11222}[8]$, in the sense that there are four extended phases: Landau-Ginzburg, orbifold, large volume and an additional hybrid phase. However, now we do not have a hybrid \mathbb{P}^1 phase, but instead the exceptional divisor has a \mathbb{P}^2 component [190] and thus for large ϕ , small ψ we face a \mathbb{P}^2 target space. Moreover, the large volume phase corresponds to a different geometry, that is not a $K3 \times \mathbb{P}^1$ fibration that we ended up with in $\mathbb{P}^4_{11222}[8]$. The singular loci in case of $\mathbb{P}^4_{11169}[18]$ are slightly different as well. Both singularities correspond to conifolds and are located at $\phi^3 = 1$ and $(\phi + 2^2 3^8 \psi^6)^3 = 1$.

For the calculation of the periods we refer to section 3.3. We will restrict our analysis again to the computation of finite distance in the moduli space according to the schematic curves plotted in figures 9.8, 9.9 and 9.10. One can show that the series expansion of the fundamental period converges for

$$|2^2 3^8 \psi^6| \lesssim |\phi - \alpha^{-6\tau}|, \quad (9.3.54)$$

depending on the regime we want to investigate. Now we have three constraints as τ may vary between 0,1,2 with $\alpha = \exp(2\pi i/18)$. Let us point out that we assume again real moduli ψ, ϕ for simplicity.

Infinite directions will show a logarithmic behavior in their proper distances depending on the Kähler moduli. The mirror map for the \mathbb{P}_{11169}^4 [18] model is given by [101]

$$\begin{aligned} t_1 &= \frac{\omega_3 - \omega_0}{\omega_0}, \\ t_2 &= \frac{\omega_4 + \omega_5 - 2\omega_3 + 2\omega_0}{\omega_0}. \end{aligned} \quad (9.3.55)$$

Landau-Ginzburg phase Here, the moduli take values within the intervals $0 \leq \phi < 1$ and $0 \leq \psi < \psi_c$, with ψ_c being the maximal real solution to condition (9.3.54). We compute the following two trajectories: one purely in direction ϕ keeping ψ fixed and one vice versa, starting at $\psi = \phi = 0$. Their lengths are given by

$$\begin{aligned} \Delta\Theta_1 &= \int_0^{\psi_c} d\psi \sqrt{G_{\psi\bar{\psi}}(\psi)} = 0.074, \\ \Delta\Theta_2 &= \int_0^1 d\phi \sqrt{G_{\phi\bar{\phi}}(\phi)} = 0.087. \end{aligned} \quad (9.3.56)$$

Again, both directions are finite and less than $\mathcal{O}(1) M_{\text{Pl}}$. This result is confirmed by the mirror map because they converge to finite values as well. More precisely, for $\phi, \psi \rightarrow 0$ we obtain the asymptotic mirror map (9.3.55) coordinates $t_1 \simeq \omega^{-2} = -\frac{1}{2} + 0.866i$ and $t_2 \simeq 1 + 0.238i$.

\mathbb{P}^2 hybrid phase Considering the parameter space $1 < \phi < \infty$ and $0 \leq \psi < \psi_c$, we compute at first the proper distance of a trajectory along the Landau-Ginzburg phase. Taking $\psi = 0, \phi = 1.1$ as initial values, we integrate along the ψ direction up to ψ_c without altering ϕ

$$\Delta\Theta_1 = \int_0^{\psi_c} d\psi \sqrt{G_{\psi\bar{\psi}}(\psi)} = 0.015. \quad (9.3.57)$$

One can approximate the Kähler metric for $(\psi, \phi) \rightarrow (0, \infty)$

$$G_{\mathbb{P}^2}^{\text{asympt}} \simeq \begin{pmatrix} \frac{0.5}{|\phi|^2 (\log|\phi|)^2} & 0 \\ 0 & \frac{185837.8 |\psi|^6}{|\phi|^{\frac{4}{3}}} \end{pmatrix} \quad (9.3.58)$$

and compute the maximal distance in the ψ direction asymptotically

$$\Delta\Theta_2 = \int_0^{\psi_c} d\psi \sqrt{G_{\mathbb{P}^2, \psi\bar{\psi}}^{\text{asympt}}(\psi, \phi)} \simeq \frac{\sqrt{185837.8}}{|\phi|^{\frac{2}{3}}} \cdot \int_0^{\psi_c} d\psi \psi^3 = 0.12, \tag{9.3.59}$$

with $|\psi_c|^4 \sim |\phi|^{\frac{2}{3}}/(2^2 3^8)^{\frac{2}{3}}$. A numerical evaluation of the integral with the full (not asymptotic) metric gives the same result. Due to the other component of the metric above, distances in the ϕ direction may become infinite.

Computing the mirror maps reveals a logarithmic growth of t_2 in ϕ and hence a logarithmic growth of the proper distance Θ in t_2 as expected due to the swampland distance conjecture. On the other hand, t_1 approaches the finite value which we also found in the Landau-Ginzburg phase. Indeed, in the limit $\phi \rightarrow \infty$ and keeping $\psi \simeq 0$, inserting the periods computed in section 3.3 into (9.3.55) leads to (recall $\omega = \exp(2\pi i/3)$)

$$\begin{aligned} t_1 &\simeq \omega^{-2} + \dots \simeq -\frac{1}{2} + 0.866i + \dots, \\ t_2 &\simeq \frac{3}{2} + \frac{3i}{2\pi} \log(3\phi) + \dots \end{aligned} \tag{9.3.60}$$

Orbifold hybrid phase In this regime the algebraic parameters are fixed by $0 \leq \phi < 1$ and $\psi_c < \psi < \infty$. As before, we begin with computing a trajectory from $\phi = 0$ to $\phi = 1$ keeping ψ constant at a minimal value $\psi \sim 0.32$.

$$\Delta\Theta_1 = \int_0^1 d\phi \sqrt{G_{\phi\bar{\phi}}(\phi)} = 0.065. \tag{9.3.61}$$

In the former examples $\mathbb{P}^4_{11222}[8]$ and $\mathbb{P}^4_{11226}[12]$ this distance was asymptotically vanishing for large ψ . Thus, we approximate the Kähler metric near $\phi \simeq 0$ and $\psi \rightarrow \infty$

$$G_{\text{orbi}}^{\text{asympt}} \simeq \begin{pmatrix} \frac{1}{|\log(\psi)|^6} & 0 \\ 0 & \frac{0.75}{|\psi|^2 (\log|\psi|)^2} \end{pmatrix}. \tag{9.3.62}$$

Thus, also here the distance in ϕ direction is asymptotically zero. However, in ψ direction it is possible to travel infinite distances.

The mirror map coordinates (9.3.55) for $\psi \rightarrow \infty$ and $\phi \simeq 0$ are approximately given by

$$\begin{aligned} t_1 &\simeq -\frac{2}{3} + \frac{i}{2\pi} \log(18\psi)^6 + \dots, \\ t_2 &\simeq 1 + \dots \end{aligned} \tag{9.3.63}$$

Since the proper distance scales like $\Theta \sim \log \log \psi$, we end up once again with a logarithmic growth of Θ in t_1 .

As opposed to the \mathbb{P}^2 hybrid phase, now it is t_1 which may become infinitely large. Again, the imaginary part of t_2 vanishes asymptotically and hence the 2-cycle Σ_2 shrinks to zero [189]. In this limit one finally hits the conifold singularity at $\phi = 1$ as the proper distance to the singularity approaches zero. Recall that in the case of $\mathbb{P}^4_{11222}[8]$ we were running into a non-singular one-parameter subspace instead.

Large volume phase Eventually, the large volume regime $1 < \phi < \infty$ and $\psi_c < \psi < \infty$ (ψ_c as above) is infinite in both directions ϕ, ψ with the mirror map given by [101]

$$\begin{aligned}
 t_1 &\simeq -\frac{1}{2} + \frac{i}{2\pi} \log \left(\frac{(18\psi)^6}{3\phi} \right) + \dots, \\
 t_2 &\simeq \frac{3}{2} + \frac{3i}{2\pi} \log(3\phi) + \dots.
 \end{aligned}
 \tag{9.3.64}$$

Summary Overall, distances of the moduli space of \mathbb{P}^4_{11169} [18] behave similar to the ones of both other two-parameter models, which we discussed above. Figure 9.12 summarized all distances of \mathbb{P}^4_{11169} [18]. The logarithmic dependence of the different mirror maps underline the swampland distance conjecture and the small finite lengths its refined version. Furthermore, we can compute the critical distance Θ_λ in asymptotic regions of the moduli space. Following section 9.3.1 the metrics (9.3.58) and (9.3.62) lead to $\Theta_\lambda = \sqrt{0.5} \approx 0.71$ for the hybrid \mathbb{P}^2 phase and $\Theta_\lambda = \sqrt{0.75}$ for the hybrid orbifold phase. In accordance with the RSDC both distances are less than M_{Pl} .

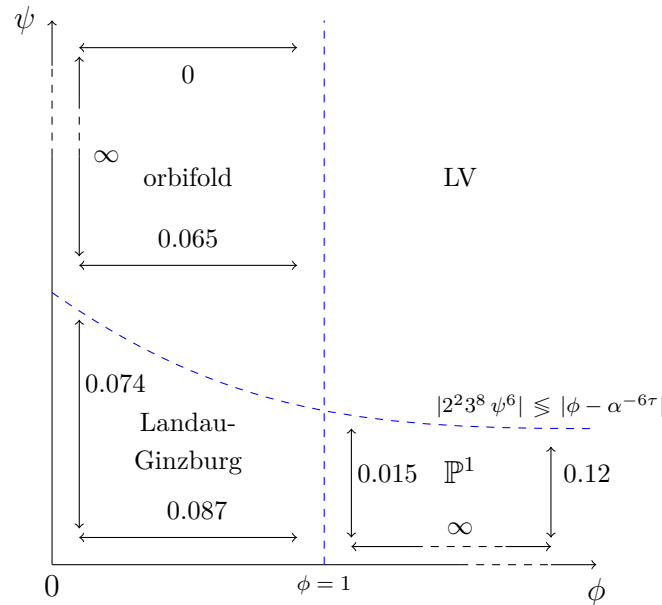


Figure 9.12: Schematic plot of the moduli space of the mirror \mathbb{P}^4_{11169} [18] with finite as well as infinite directions as calculated above. The constraint for one conifold uses $\tau = 0, 1, 2$ and $\alpha = \exp(2\pi i/18)$.

Part IV

Conclusions

CHAPTER 10

Summary and Outlook

Having introduced all necessary concepts, we organized the discussion in part III as follows:

- attempting to realize large-field inflation near a special point in the complex structure moduli space
- general obstacles of axion monodromy inflation due to the (refined) swampland distance conjecture (RSDC)
- tests of the conjecture for moduli spaces of several Calabi-Yau manifolds

Let us briefly sum up our results in the light of the central question (see introduction 1): whether there are underlying string theory or quantum gravity principles constraining/forbidding large-field inflation.

In chapter 7 we considered moduli stabilization and application to large-field inflation in the vicinity of the conifold. The characteristic feature near the conifold is the appearance of a leading logarithmic term in the periods of the complex structure moduli space. The conic modulus Z in the argument of the logarithm was dynamically fixed by turning on fluxes in the spirit of [53]. Actually the vev of Z was exponentially small depending on the value of the axio-dilaton modulus S . Other complex structure moduli and the axio-dilaton S could be stabilized in the perturbative regime [131]. An important consistency condition arose from controlling warping effects:

$$\mathcal{V}|Z|^2 \gg 1, \tag{10.0.1}$$

with the overall compactification volume \mathcal{V} . This constraint guaranteed to be far enough away from the strongly warped region where Kaluza-Klein modes localized in the throat are red-shifted such that they become lighter than certain moduli masses. In other words, one can trust the low-energy effective supergravity description of the moduli fields only

if the constraint (10.0.1) is satisfied. Obviously, the exponentially small conic modulus Z implied then an exponentially large volume \mathcal{V} . The large volume scenario (LVS) was therefore a natural candidate to fix the Kähler moduli. In the end one achieved a mass hierarchy that is consistent, but again only if the constraint (10.0.1) is obeyed. Interestingly, some mass scales exhibited an exponential hierarchy. The main goal of chapter 7 was to analyze whether special points in the moduli space like the conifold can have beneficial consequences for axionic large-field inflation. The conifold seemed particularly attractive due to the exponential mass hierarchies. In fact, integrating out the heavy conic modulus Z induced exponential terms in the superpotential of the form of instanton contributions. Although an interpretation as true instantons on the mirror dual side is unclear, they lead to valuable phenomenological implications. Here we have used these instanton-like terms to realize large-field inflation via axion alignment. The success of our model relied, however, on ignoring the Kähler moduli (an application of the LVS turned out problematic) and very restrictive assumptions about higher-order corrections from the periods. Large-field inflation could at best be saved by a sophisticated choice of several numerical parameters. These control issues support the claim for fundamental principles against string inflation. Note that the mild form of the weak gravity conjecture can be satisfied by the instanton-like terms in the superpotential providing a loop-hole in the sense of [179]. In spite of the promising hierarchical stabilization of moduli, a consistent application of the conifold setup to large-field inflation is ultimately questionable when taking all details and scales into account.

Chapter 8 changed from the conifold to the large complex structure point and from periodic to axion monodromy inflation. However, instead of attempting to engineer an explicit model realizing large-field inflation, we aimed for relating the ubiquitous control issues to the (refined) swampland distance conjecture. Stabilization of closed as well as open string moduli with flux induced superpotentials in the perturbative large volume regime led indeed to further evidence for the conjecture in string theory. More precisely, the backreaction of large-field excursions of the lightest axion θ , i.e. the inflaton, onto the other moduli caused the appearance of exponentially light Kaluza-Klein towers. They were exponentially light because the backreaction implied logarithmic proper field distances $\Theta \sim \log(\theta)$. These backreaction effects nicely interpolated between polynomial and Starobinsky-like inflation with the latter one occurring above $\Theta > \Theta_c$. In the Starobinsky regime large-field inflation was impossible since the light Kaluza-Klein towers invalidated the effective field theory. Figure 10.1 illustrates how backreaction deforms the polynomial inflaton potential to a Starobinsky-like plateau. A crucial point turned out to be the uplift to Minkowski or de Sitter (dS) vacua. The Starobinsky-like scenario was based on a constant uplift which is unrealistic since string theory must decompactify at infinite volume and hence the moduli potential go to zero. In the presence of a dynamical uplift the moduli minimum disappeared and the inflationary trajectory destabilized at a scale close to Θ_c . These are well-known issues from large-field inflaton within KKLT and LVS. Our goal was therefore to postpone the control obstacles by achieving a parametrically large value for the critical scale Θ_c . More concretely, the idea was to make the critical value Θ_c flux-dependent. We were only

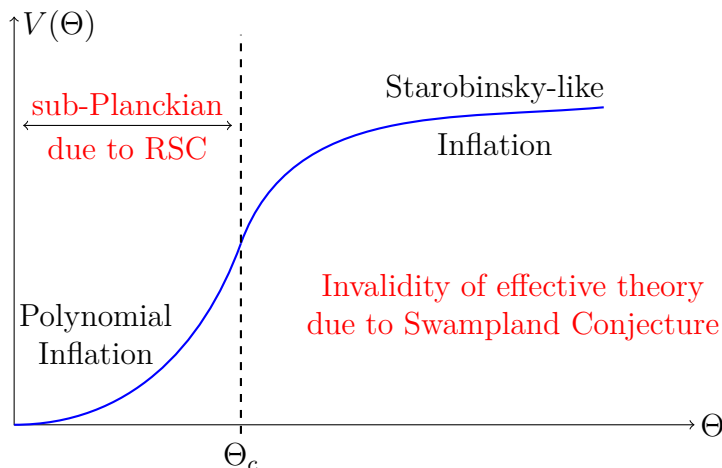


Figure 10.1: The plot (from [65]) depicts schematically a typical potential $V(\Theta)$ for an inflaton Θ achieved via axion monodromy. Above some critical value Θ_c the backreaction of the inflaton onto the other moduli deforms the polynomial potential to a Starobinsky-like plateau. However, in this regime the effective theory breaks down according to the swampland distance conjecture. The refined version of the conjecture (RSDC) sets $\Theta_c \sim 1$, reducing the controllable inflaton field range to sub-Planckian distances.

able to achieve this in models where the inflaton could be stabilized by a sub-leading flux μ , such that the inflaton mass goes to zero for $\mu \rightarrow 0$ without destabilizing the other moduli. Then the critical value Θ_c was proportional to the mass hierarchy between the inflaton mass and the heavy moduli masses. A large mass hierarchy might therefore delay backreaction effects and enable large-field inflation. To be more precise, we have studied tree-level moduli stabilization including non-geometric fluxes in toroidal compactifications of type IIB string theory. The inflaton has been chosen to correspond to an open string modulus to increase its chances to decouple from the other closed string moduli. But whenever we guaranteed a mass hierarchy between inflaton and heavy moduli, we ran into conflicts with separating other mass scales, like heavy moduli and Kaluza-Klein scale. Eventually, parametric control over the effective supergravity theory always demanded a critical scale around the Planck scale, i.e. $\Theta_c \approx 1$. Hence, the four-dimensional effective theory of axion monodromy inflation in string theory was only valid for $\Theta < \Theta_c \approx 1 M_{\text{Pl}}$. This conclusion just reflects the claim of the refined swampland distance conjecture making trans-Planckian moduli displacements generically impossible. Analyzing two scenarios (KKLT and LVS) where the Kähler moduli are not stabilized at tree-level by fluxes but by non-perturbative effects culminated in similar control issues.

In order to justify the powerful statement of the refined swampland distance conjecture (RSDC), we devoted chapter 9 to challenging it in various Calabi-Yau moduli spaces. More precisely, we computed geodesic distances for the quintic with $h^{1,1} = 1$ and three Calabi-Yau manifolds with $h^{1,1} = 2$ defined by hypersurfaces in weighted projective spaces. In

contrast to chapter 8 we have now been focusing on non-periodic scalars (i.e. saxions) just like in the original work [43] about the swampland distance conjecture. The metric on the Kähler moduli space has been found by calculating the metric on the complex structure moduli space of the mirror manifold. As a key feature, these moduli spaces possessed non-geometric phases and for two-parameter models also hybrid phases. In the large volume phases the swampland distance behavior showed up as expected in form of light Kaluza-Klein states. However, for the refined version of the conjecture two further questions needed to be answered: What about distances in the non-geometric and hybrid phases? Is the critical distance in the large volume phase $\Theta_c \leq 1 M_{\text{Pl}}$? The latter can be answered with yes in all examples studied here (and also in [65]). Concerning the non-geometric Landau-Ginzburg phases all distances were finite and smaller than $1 M_{\text{Pl}}$, hence in favor of the RSDC. Discovering a trans-Planckian distance would have falsified the refined conjecture. The hybrid phases of the two-parameter models featured a hybrid behavior regarding their geodesics lengths, meaning there were one finite as well as one infinite direction. Eventually, all distances computed in chapter 9 have been in agreement with the refined swampland distance conjecture. For more Calabi-Yau manifolds with $h^{1,1} = 1$ and stunningly $h^{1,1} = 101$ see [65]. Note that for $h^{1,1} = 2$ we were able to compute only special geodesics in the complex two-dimensional moduli spaces, but qualitative changes for arbitrary geodesics are not expected.

At the bottom line we conclude: guided by all failing attempts in the literature and the models analyzed in this thesis, we think there exists an underlying principle constraining axion inflation, either with periodic potentials or via monodromy, in the framework of string moduli stabilization. Such principles might be the swampland conjectures for which we gathered further non-trivial evidence. If these conjectures are really true, they cause huge implications for phenomenology [65] and answer our central question in the introduction 1 quite drastically:

In string theory (quantum gravity) it is impossible to achieve a parametrically controllable model of large (single) field inflation. The tensor-to-scalar ratio is thus bounded from above by $r \lesssim 10^{-3}$.

Outlook

Such a strong statement requires more evidence for the swampland conjectures as well as additional challenges of their implications. We leave this for future work and only mention some possible loop-holes that might trigger further investigations, although we do not expect they will lead to a fully consistent model of large-field inflation:

- *fine-tuning in the landscape*
Integrating out heavy moduli could lead to an effective parameter in front of a light modulus. This loosens the restrictions of employing only quantized fluxes. A possible

model build on this idea has been analyzed in a toroidal framework in section 8.3.3. However, taking the details seriously we failed to achieve a trans-Planckian field range.

- *more evidence for axionic RSDC*

The swampland distance conjecture affects axions via backreaction effects. In case of strong backreaction or near special points like conifold singularities, extending the conjecture to axionic directions deserves more investigation.

- *numerical fine-tuning*

Our analysis was mainly focusing on parametric control. Suitable numerical prefactors might nevertheless be in favor of generating the right hierarchy of scales. A successful model via numerical coincidences urges a very careful examination of all involved components and did not occur in the examples we have investigated.

- *multi-field inflation*

Does the refined swampland distance conjecture still apply for sophisticated potentials like Dante's inferno [191], where the inflaton travels along specially designed multi-field trajectory?

Leaving these issues for future work, let us at last point out that by now a whole zoo of swampland conjectures exists [43, 161, 167, 192, 193]. They imply additional radical consequences for string phenomenology concerning particle physics as well as cosmology. One provocative publication [161] is known as *swampland de Sitter conjecture* and claims the absence of any extremum of moduli potentials with positive energy or more precisely $|\nabla V|/V \geq \mathcal{O}(1)$. Hence, dS vacua would be impossible in string compactifications and therefore inflation neither. This prohibits a positive cosmological constant and suggests that one can only make sense of the accelerated expansion of our universe via *quintessence models*, where a rolling scalar field (similar to inflation) drives the expansion nowadays. In this case the fate of the universe is uncertain. According to [162] the universe as we know it might come to an end culminating in a new phase, where for instance supersymmetry is restored or the universe contracts. In case the swampland conjectures survive all tests in string theory but disagrees with nature, one could conclude that string theory is still lacking unknown fundamental ingredients or even falsified. Hence, the quest towards quantum gravity remains exciting and we can look forward to future discoveries in experiment and theory.

Part V

Appendices

APPENDIX A

Numerical Evaluation of Periods of Calabi-Yau Manifolds

A conceptual recipe for calculating periods of Calabi-Yau manifolds, that can be constructed as hypersurface constraint in a weighted projective space, was explained rather briefly in chapter 3. In particular, the two-parameter section lacks of details and concrete examples. Therefore, let us at least list here the results for the periods that we have obtained via the standard method á la integration of the holomorphic $(3, 0)$ -form Ω_3 . The solutions are expanded only up to a few orders in the moduli parameters. Note, however, that the analysis in chapter 9 was taking many more orders into account.

A.1 One-Parameter Quintic

Recall that the mirror quintic has one complex structure modulus ψ and obtains a conifold singularity at $u = 5(\psi - 1) = 0$, where a 3-cycle shrinks to zero and the corresponding period vanishes. Let us compute the periods near the conifold, which have been used in chapter 7.

We begin with the fundamental period ω_0 in the Landau-Ginzburg regime $|\psi| < 1$, that was given in (3.2.10). A complete set of periods covering this region of the moduli space can then be calculated via

$$\tilde{\omega}_j(\psi) = \left(\frac{2\pi i}{5}\right)^3 \omega_0(\alpha^j \psi) \tag{A.1.1}$$

with $j = 0, 1, 2, 4$ and $\alpha = \exp(2\pi i/5)$. Note that a factor $(2\pi i/5)^3$ was introduced in order to stay in accordance with [131]. Employing the matrix (B.0.1), the periods are

transformed into a symplectic basis via $\Pi(u) = m\tilde{\omega}$ with $\tilde{\omega} = (\tilde{\omega}_0, \tilde{\omega}_1, \tilde{\omega}_2, \tilde{\omega}_4)$. Up to linear order in u and using the monodromy property (3.2.21), we arrive at

$$\Pi(u) = \begin{pmatrix} F_0 \\ F_1 \\ X^0 \\ X^1 \end{pmatrix} = \begin{pmatrix} (-6.195 + 7.115i) - (1.017 - 0.829i)u \\ \frac{\sqrt{5}}{(2\pi)^2}u \log(u) + 1.071 - (0.419 - 0.178i)u \\ (-12.39 + 12.936i) - (2.033 - 1.508i)u \\ -\frac{\sqrt{5}}{2\pi i}u \end{pmatrix}. \quad (\text{A.1.2})$$

These periods imply a linear term in the log of the Kähler potential in agreement with [85]. The linear term might seem surprising a priori as it dominates over the log-term. However, this contribution is unphysical in the sense that the Kähler metric remains untouched by the linear term. We will choose a different basis which also makes a shift symmetry in the axionic part of the modulus visible. To that purpose consider the $SL(4, \mathbb{Z})$ transformation

$$\begin{pmatrix} -11 & 0 & 6 & 0 \\ 0 & 0 & 0 & -1 \\ 20 & 0 & -11 & 0 \\ 0 & 1 & 0 & 0 \end{pmatrix}. \quad (\text{A.1.3})$$

The periods in the vicinity of the conifold singularity are then of the form¹ [177, 194]

$$\begin{aligned} F_0 &= \tilde{a}_0 + \tilde{b}_0 u + \dots, \\ F_1 &= au + \dots \\ X^0 &= a^0 + b^0 u + \dots, \\ X^1 &= -\frac{1}{2\pi i} F_1 \log u + c + du + \dots \end{aligned} \quad (\text{A.1.4})$$

with the following numerical values of the parameters

$$\begin{aligned} a &= \frac{\sqrt{5}}{2\pi i}, \quad c = 1.07072586843016, \quad d = -0.0247076138044847 \\ a^0 &= 12.3900325542991, \quad b^0 = 2.033209433405164 \\ \tilde{a}_0 &= 6.19501627714957 - 0.64678699225205 i \\ \tilde{b}_0 &= 1.016604716702582 - 0.075383347561773 i. \end{aligned} \quad (\text{A.1.5})$$

Half of the periods can be considered as homogeneous coordinates on the complex structure moduli space. Now we introduce inhomogeneous coordinates by dividing by the period X^0 . Introducing the new complex structure modulus

$$Z = \frac{F_1}{X^0} = \frac{a}{a^0} u + O(u^2), \quad (\text{A.1.6})$$

¹The numerical values have been improved by comparison with [194]. There, one starts with their eq. (3.70) and after using eq. (3.71), transforms with the $SL(4, \mathbb{Z})$ matrix $\begin{pmatrix} 0 & 1 & 0 & 5 \\ 1 & 0 & 0 & 0 \\ 0 & 2 & 0 & 11 \\ 0 & 0 & 1 & 0 \end{pmatrix}$.

which in chapter 7 we also call the “conic” modulus, the period vector $\Pi^T = (F_0, F_1, X^0, X^1)$ can be expressed as

$$\Pi = X^0 \begin{pmatrix} \tilde{A}_0 - \tilde{B}_0 Z + O(Z^2) \\ Z \\ 1 \\ -\frac{1}{2\pi i} Z \log Z + C + DZ + O(Z^2) \end{pmatrix} \quad (\text{A.1.7})$$

with parameters

$$\begin{aligned} \tilde{A}_0 &= \frac{\tilde{a}_0}{a^0} = \frac{1}{2} - 0.05220220281242 i \\ \tilde{B}_0 &= -\frac{a^0 \tilde{b}_0 - b^0 \tilde{a}_0}{a a^0} = 0.08641832567733 \\ C &= \frac{c}{a^0} = 0.08641832567733 = \tilde{B}_0 \\ D &= \frac{1}{a} \left(d - \frac{b^0 c}{a^0} + \frac{a}{2\pi i} \log \left(\frac{a}{a^0} \right) \right) = -\frac{1}{4} + 0.00185911259239 i. \end{aligned} \quad (\text{A.1.8})$$

Note the non-trivial relation $C = \tilde{B}_0$. For these values, the corresponding Kähler potential for the complex structure modulus is given by

$$\begin{aligned} K_{\text{cs}} &= -\log \left[-i \Pi^\dagger \Sigma \Pi \right] \\ &= -\log \left[\frac{1}{2\pi} |Z|^2 \log(|Z|^2) + A + O(|Z|^2) \right] \end{aligned} \quad (\text{A.1.9})$$

with $A = 0.10440$ and the symplectic pairing

$$\Sigma = \begin{pmatrix} 0 & 0 & 1 & 0 \\ 0 & 0 & 0 & 1 \\ -1 & 0 & 0 & 0 \\ 0 & -1 & 0 & 0 \end{pmatrix}. \quad (\text{A.1.10})$$

Note that the linear terms in K_{cs} cancel so that, as advocated in [195], the Kähler potential respects the continuous phase shift symmetry $Z \rightarrow e^{i\theta} Z$.

A.2 Two-Parameter Spaces

Using the formulas for the periods in chapter 3 and [65] let us also list the leading-order behavior for two-parameter moduli spaces. Note that the results of chapters 7 and 9 rely on period expansions up to much higher orders. Nevertheless, let us emphasize their general structure and in particular their logarithmic dependence. We will only state $\vec{\omega} = (\omega_0, \dots, \omega_5)$ which gives $\Pi = m\vec{\omega}$ via the matrices m of appendix B. The moduli space of

\mathbb{P}^4_{11222} [8], \mathbb{P}^4_{11226} [12] and \mathbb{P}^4_{11169} [18] have four phases. As the large complex structure phase has not been part of the analysis in chapter 9, only the periods for the Landau-Ginzburg, \mathbb{P}^1 and orbifold phases are listed here. Besides, note that overall factors (typically of ψ) in the periods may be neglected as they correspond to an irrelevant Kähler transformation. Eventually, the periods are given by:

\mathbb{P}^4_{11222} [8]

- **Landau-Ginzburg regime** $|\phi| < 1$ and $|8\psi^4| < |\phi \pm 1|$

$$\frac{\vec{\omega}_{\text{LG}}}{\psi} = \begin{pmatrix} (3.47 - 1.44i) + (0.25 + 0.61i)\phi \\ (3.47 + 1.44i) + (0.25 - 0.61i)\phi \\ (1.44 + 3.47i) - (0.61 - 0.25i)\phi \\ (-1.44 + 3.47i) + (0.61 + 0.25i)\phi \\ (-3.47 + 1.44i) - (0.25 + 0.61i)\phi \\ (-3.47 - 1.44i) - (0.25 - 0.61i)\phi \end{pmatrix} + \mathcal{O}(\phi^2, \psi^2) \quad (\text{A.2.1})$$

- **\mathbb{P}^1 hybrid regime** $|\phi| > 1$ and $|8\psi^4| < |\phi \pm 1|$

$$\frac{\vec{\omega}_{\mathbb{P}^1}}{\psi} = \begin{pmatrix} (3.31 + 0.00i) \\ (4.58 + 1.27i) + (1.05 + 1.05i) \log \phi \\ (0.00 + 3.31i) \\ (-1.27 + 4.58i) - (1.05 - 1.05i) \log \phi \\ (-3.31 + 0.00i) \\ (-4.58 - 1.27i) - (1.05 + 1.05i) \log \phi \end{pmatrix} \phi^{-1/4} + \mathcal{O}(\phi^{-1/2}) \quad (\text{A.2.2})$$

- **orbifold hybrid regime** $|\phi| < 1$ and $|8\psi^4| > |\phi \pm 1|$

$$\vec{\omega}_{\text{Orbi}} = \begin{pmatrix} 1 \\ (0.00 - 0.34i)(\log \psi)^3 + (0.81 - 2.15i)(\log \psi)^2 \\ (0.81 + 0.00i)(\log \psi)^2 \\ (0. + 1.03i)(\log \psi)^3 - (1.62 - 6.44i)(\log \psi)^2 \\ -(1.62 + 0.00i)(\log \psi)^2 \\ -(0. + 1.03i)(\log \psi)^3 + (0.81 - 6.44i)(\log \psi)^2 \end{pmatrix} + \mathcal{O}(\log \psi, \phi) \quad (\text{A.2.3})$$

\mathbb{P}^4_{11226} [12]

Since chapter 7 examines effects appearing in the vicinity of the conifold, we will also compute the periods near $864\psi^6 + \phi = 1$ and $\phi = 0$. The computation relies on [131] and the resulting Kähler potential motivates the ansatz in section 7.2.

- **Landau-Ginzburg regime** $|\phi| < 1$ and $|864\psi^6| < |\phi \pm 1|$

$$\frac{\vec{\omega}_{\text{LG}}}{\psi} = \begin{pmatrix} (4.66 - 1.25i) + (0.16 + 0.61i)\phi \\ (4.66 + 1.25i) - (0.16 - 0.61i)\phi \\ (3.41 + 3.41i) - (0.45 - 0.45i)\phi \\ (1.25 + 4.66i) - (0.61 - 0.16i)\phi \\ (-1.25 + 4.66i) - (0.61 + 0.16i)\phi \\ (-3.41 + 3.41i) - (0.45 + 0.45i)\phi \end{pmatrix} + \mathcal{O}(\phi^2, \psi^2) \quad (\text{A.2.4})$$

- \mathbb{P}^1 **hybrid regime** $|\phi| > 1$ and $|864\psi^6| < |\phi \pm 1|$

$$\frac{\vec{\omega}_{\mathbb{P}^1}}{\psi} = \begin{pmatrix} (4.39 + 0.00i) \\ (5.61 + 0.70i) + (1.21 + 0.70i) \log \phi \\ (2.20 + 3.80i) \\ (2.20 + 5.21i) + (0.00 + 1.40i) \log \phi \\ (-2.20 + 3.80i) \\ (-3.41 + 4.51i) - (1.21 - 0.70i) \log \phi \end{pmatrix} \phi^{-1/6} + \mathcal{O}(\phi^{-5/6}) \quad (\text{A.2.5})$$

- **orbifold hybrid regime** $|\phi| < 1$ and $|864\psi^6| > |\phi \pm 1|$

$$\vec{\omega}_{\text{Orbi}} = \begin{pmatrix} 1 \\ -(0.00 + 0.58i)(\log \psi)^3 + (0.91 - 4.33i)(\log \psi)^2 \\ (0.00 + 0.91i)(\log \psi)^2 \\ (0.00 + 1.16i)(\log \psi)^3 - (0.91 - 8.66i)(\log \psi)^2 \\ -(0.00 + 0.91i)(\log \psi)^2 \\ -(0.00 + 0.58i)(\log \psi)^3 - (0.00 + 4.33i)(\log \psi)^2 \end{pmatrix} + \mathcal{O}(\log \psi, \phi) \quad (\text{A.2.6})$$

- **conifold regime**

Starting with the periods $\omega_j(\psi, \phi)$ in the Landau-Ginzburg region and multiplying with a factor $(2\pi i)^3/\psi$ to be in line with [131], we transform into the symplectic basis using the matrix m of (B.0.3). Then, we restrict to the region around the point $\psi = \psi_0 = 864^{-\frac{1}{6}}$ and $\phi = 0$ on the conifold locus. Writing $\psi = \psi_0 + \xi$, we numerically evaluate the periods up to quadratic order in (ξ, ϕ) . This has also been done up to linear order in [196], but not to the level of accuracy that we need for our purposes. The numerical computation of the period series up to $n \sim 20000$ gives ²

$$\begin{aligned} F_0 &= 4323.04i - 1548.4i \xi + 107.7i \phi - 3893.22i \xi^2 - 278.46i \xi \phi + 27.78i \phi^2, \\ F_1 &= 3191 \xi + 172.29 \phi + 7583.59 \xi^2 - 533.36 \xi \phi + 65.2 \phi^2, \\ F_2 &= (-492.72 + 1976.76i) + (372.45 - 302.3i)\xi - (258.97 + 58.87i)\phi \\ &\quad - (436.95 - 262.39i)\xi^2 - (6.5 + 14.41i)\xi \phi - (3.09 - 24.14i)\phi^2 \end{aligned} \quad (\text{A.2.7})$$

²For some of these numbers we gained a better precision, which was then also used in the following computations.

and

$$\begin{aligned}
X^0 &= -(994.58 + 184.76i) + (859.48 + 471.9i)\xi + (10.04 - 112.7i)\phi \\
&\quad + (1831.84 + 2209i)\xi^2 - (136.09 - 124.82i)\xi\phi + (3.13 + 10.25i)\phi^2, \\
X^1 &= -\frac{1}{2\pi i} F_1 \log F_1 + 784.36i - 4997.53i\xi - 185.8i\phi + \dots, \\
X^2 &= 369.52i - 943.81i\xi + 225.4i\phi - 4418i\xi^2 - 249.64i\xi\phi - 20.5i\phi^2.
\end{aligned} \tag{A.2.8}$$

Note that the order two terms in X^1 will not be relevant for computing the Kähler potential up to quadratic order. Next, we go to inhomogeneous coordinates where $F_0 = 1$ and substitute

$$\phi \rightarrow -18.52\xi + 25.09iZ - 231.17\xi^2 + 408.85i\xi Z + 222.58Z^2 \tag{A.2.9}$$

followed by a second substitution

$$\xi \rightarrow 1.97Y + 1.13iZ - 62.84Y^2 - 8.7iZY + 4.07Z^2. \tag{A.2.10}$$

Finally, in terms of the fields Z and Y , up to quadratic order, the periods take the form

$$\begin{aligned}
F_0 &= 1, \\
F_1 &= Z, \\
F_2 &= (0.46 + 0.11i) + (1.10 - 2.17i)Y - 0.19Z \\
&\quad - (7.34 - 14.73i)Y^2 + (2.71 + 1.42i)YZ + (0.11 - 1.69i)Z^2
\end{aligned} \tag{A.2.11}$$

and

$$\begin{aligned}
X^0 &= (-0.04 + 0.23i) + (1.10 + 0.06i)Y + 0.17Z \\
&\quad - (7.34 + 1.83i)Y^2 + (0.55 + 1.42i)YZ + (0.11 - 0.17i)Z^2, \\
X^1 &= -\frac{1}{2\pi i} Z \log Z + 0.18 - 0.42Y - 1.43iZ + \dots, \\
X^2 &= 0.09 - 2.19Y + 14.67Y^2 - 2.84iYZ - 0.22Z^2.
\end{aligned} \tag{A.2.12}$$

Here we have set a numerical number to zero, if it vanishes up to the order $O(10^{-4})$. Moreover, the numbers appearing in the periods are not unrelated. Up to order $O(10^{-4})$, we find e.g.

$$\begin{aligned}
2X^0 + X^2 &= 0.46i + 0.13iY + 0.33Z - 3.66iY^2 + 1.11YZ - 0.34iZ^2 \\
F_2 - X^0 &= (0.5 - 0.11i) - 2.24iY - 0.36Z + 16.56iY^2 + 2.16YZ - 1.52iZ^2.
\end{aligned} \tag{A.2.13}$$

Due to these relations, the resulting Kähler potential at linear order simplifies considerably

$$\begin{aligned}
K_{\text{cs}} &= -\log [-i\Pi^\dagger \Sigma \Pi] \\
&= -\log \left[\frac{1}{2\pi} |Z|^2 \log(|Z|^2) + A + \text{Re}Y + B(\text{Re}Y)^2 + C|Z|^2 \dots \right]
\end{aligned} \tag{A.2.14}$$

with $A = 0.44$ and $B = -19.05$ and $C = -2.86$. As for the quintic, the Kähler potential exhibits the shift symmetry $Z \rightarrow e^{i\theta}Z$ and in addition the shift symmetry $\text{Im}(Y) \rightarrow \text{Im}(Y) + \theta$. Therefore, in this regime close to the conifold, $\text{Im}(Y)$ behaves like an axion.

$\mathbb{P}^4_{11169}[18]$

Recall that here $\alpha = \exp(2\pi i/18)$ and $\tau = 0, 1, 2$. Notice the difference to the last two manifolds. We neglect indicating higher order terms in the period expansion.

- **Landau-Ginzburg regime** $|\phi| < 1$ and $|2^2 3^8 \psi^6| < |\phi - \alpha^{-6\tau}|$

$$\frac{\vec{\omega}_{\text{LG}}}{\psi} = \begin{pmatrix} (6.69 - 1.18i) - (0.46 - 1.25i)\phi \\ (6.69 + 1.18i) - (0.46 + 1.25i)\phi \\ (5.88 + 3.40i) + (1.15 + 0.67i)\phi \\ (4.37 + 5.20i) - (1.31 - 0.23i)\phi \\ (2.32 + 6.38i) + (0.86 - 1.02i)\phi \\ (0.00 + 6.79i) + (0.00 + 1.33i)\phi \end{pmatrix} \quad (\text{A.2.15})$$

- \mathbb{P}^1 **hybrid regime** $|\phi| > 1$ and $|2^2 3^8 \psi^6| < |\phi - \alpha^{-6\tau}|$

$$\frac{\vec{\omega}_{\mathbb{P}^1}}{\psi} = \begin{pmatrix} (5.79 + 0.00i) \\ (0.33 - 0.57i)(\log \psi)^2 + (0.93 - 1.62i) \log \psi + (5.92 - 0.22i) \\ -(0.33 - 0.57i)(\log \psi)^2 + (1.46 + 3.00i) \log \psi + (7.60 + 4.68i) \\ (2.90 + 5.02i) \\ (0.66 + 0.00i)(\log \psi)^2 + (1.87 - 0.00i) \log \psi + (3.15 + 5.02i) \\ -(0.66 + 0.00i)(\log \psi)^2 - (1.87 - 2.77i) \log \psi + (-0.25 + 8.92i) \end{pmatrix} \phi^{-1/6} \quad (\text{A.2.16})$$

- **orbifold hybrid regime** $|\phi| < 1$ and $|2^2 3^8 \psi^6| > |\phi - \alpha^{-6\tau}|$

$$\vec{\omega}_{\text{Orbi}} = \begin{pmatrix} 1 \\ -(0.00 + 1.31i)(\log \psi)^3 + (1.37 - 11.33i)(\log \psi)^2 + (7.91 - 28.20i) \log \psi \\ (0.00 + 1.31i)(\log \psi)^3 + (0.00 + 11.33i)(\log \psi)^2 + (0.00 + 29.63i) \log \psi \\ (0.00 + 0.95i) \log \psi \\ (0.00 + 0.95i) \log \psi \\ (0.00 + 0.95i) \log \psi \end{pmatrix} \quad (\text{A.2.17})$$

APPENDIX B

Transformation Matrix m for Periods

The periods $\vec{\omega}$ have to be transformed into a symplectic basis $\Pi = m\vec{\omega}$ according to (3.2.16). The matrices m can be found in the literature¹ [52, 65, 100, 101, 197, 198]. For the Calabi-Yau manifolds investigated in this thesis they are given by

- P_{11111}^4 [5]

$$m = \begin{pmatrix} -\frac{3}{5} & -\frac{1}{5} & \frac{21}{5} & \frac{8}{5} \\ 0 & 0 & -1 & 0 \\ -1 & 0 & 8 & 3 \\ 0 & 1 & -1 & 0 \end{pmatrix} \quad (\text{B.0.1})$$

- P_{11222}^4 [8]

$$m = \begin{pmatrix} -1 & 1 & 0 & 0 & 0 & 0 \\ 1 & 0 & 1 & -1 & 0 & -1 \\ \frac{3}{2} & 0 & 0 & 0 & -\frac{1}{2} & 0 \\ 1 & 0 & 0 & 0 & 0 & 0 \\ -\frac{1}{4} & 0 & \frac{1}{2} & 0 & \frac{1}{4} & 0 \\ \frac{1}{4} & \frac{3}{4} & -\frac{1}{2} & \frac{1}{2} & -\frac{1}{4} & \frac{1}{4} \end{pmatrix} \quad (\text{B.0.2})$$

1

The expression for P_{11226}^4 [12] differs from [65] by a symplectic transformation, which does not affect the Kähler metric.

- $P_{11226}^4[12]$

$$m = \begin{pmatrix} \frac{3}{2} & \frac{3}{2} & \frac{1}{2} & \frac{1}{2} & -\frac{1}{2} & -\frac{1}{2} \\ -1 & 1 & 0 & 0 & 0 & 0 \\ 1 & 0 & 1 & 0 & 0 & 0 \\ -\frac{1}{2} & 0 & \frac{1}{2} & 0 & \frac{1}{2} & 0 \\ 1 & 0 & 0 & 0 & 0 & 0 \\ \frac{1}{2} & \frac{1}{2} & -\frac{1}{2} & \frac{1}{2} & -\frac{1}{2} & \frac{1}{2} \end{pmatrix} \quad (\text{B.0.3})$$

- $P_{11169}^4[18]$

$$m = \begin{pmatrix} -1 & 1 & 0 & 0 & 0 & 0 \\ 1 & 3 & 3 & 2 & 1 & 0 \\ 0 & 1 & 1 & 1 & 0 & 0 \\ 1 & 0 & 0 & 0 & 0 & 0 \\ -1 & 0 & 0 & 1 & 0 & 0 \\ 2 & 0 & 0 & -2 & 1 & 1 \end{pmatrix} \quad (\text{B.0.4})$$

Bibliography

- [1] **ATLAS, CMS** Collaboration, G. Aad *et al.*, “Combined Measurement of the Higgs Boson Mass in pp Collisions at $\sqrt{s} = 7$ and 8 TeV with the ATLAS and CMS Experiments,” *Phys. Rev. Lett.* **114** (2015) 191803, 1503.07589.
- [2] P. Candelas, G. T. Horowitz, A. Strominger, and E. Witten, “Vacuum configurations for superstrings,” *Nuclear Physics B* **258** (1985) 46 – 74.
- [3] V. Braun, Y.-H. He, B. A. Ovrut, and T. Pantev, “The Exact MSSM spectrum from string theory,” *JHEP* **05** (2006) 043, hep-th/0512177.
- [4] B. S. Acharya and E. Witten, “Chiral fermions from manifolds of G(2) holonomy,” hep-th/0109152.
- [5] B. S. Acharya, K. Bobkov, G. L. Kane, J. Shao, and P. Kumar, “The G(2)-MSSM: An M Theory motivated model of Particle Physics,” *Phys. Rev.* **D78** (2008) 065038, 0801.0478.
- [6] R. Donagi and M. Wijnholt, “Model Building with F-Theory,” *Adv. Theor. Math. Phys.* **15** (2011), no. 5, 1237–1317, 0802.2969.
- [7] C. Beasley, J. J. Heckman, and C. Vafa, “GUTs and Exceptional Branes in F-theory - I,” *JHEP* **01** (2009) 058, 0802.3391.
- [8] G. Aldazabal, L. E. Ibanez, F. Quevedo, and A. M. Uranga, “D-branes at singularities: A Bottom up approach to the string embedding of the standard model,” *JHEP* **08** (2000) 002, hep-th/0005067.
- [9] H. Verlinde and M. Wijnholt, “Building the standard model on a D3-brane,” *JHEP* **01** (2007) 106, hep-th/0508089.
- [10] R. Blumenhagen, M. Cvetič, P. Langacker, and G. Shiu, “Toward realistic intersecting D-brane models,” *Ann. Rev. Nucl. Part. Sci.* **55** (2005) 71–139, hep-th/0502005.

- [11] R. Blumenhagen, B. Kors, D. Lust, and T. Ott, “The standard model from stable intersecting brane world orbifolds,” *Nucl. Phys.* **B616** (2001) 3–33, [hep-th/0107138](#).
- [12] G. Aldazabal, S. Franco, L. E. Ibanez, R. Rabadan, and A. M. Uranga, “D = 4 chiral string compactifications from intersecting branes,” *J. Math. Phys.* **42** (2001) 3103–3126, [hep-th/0011073](#).
- [13] G. Aldazabal, S. Franco, L. E. Ibanez, R. Rabadan, and A. M. Uranga, “Intersecting brane worlds,” *JHEP* **02** (2001) 047, [hep-ph/0011132](#).
- [14] C. Amsler, “Astrophysics and Cosmology,”.
- [15] V. Balasubramanian, P. Berglund, J. P. Conlon, and F. Quevedo, “Systematics of moduli stabilisation in Calabi-Yau flux compactifications,” *JHEP* **03** (2005) 007, [hep-th/0502058](#).
- [16] A. A. Penzias and R. W. Wilson, “A Measurement of excess antenna temperature at 4080-Mc/s,” *Astrophys. J.* **142** (1965) 419–421.
- [17] ESA and the Planck Collaboration, “Planck CMB,” 2013.
- [18] D. Baumann, “Inflation,” in *Physics of the large and the small, TASI 09, proceedings of the Theoretical Advanced Study Institute in Elementary Particle Physics, Boulder, Colorado, USA, 1-26 June 2009*, pp. 523–686. 2011. [0907.5424](#).
- [19] **Planck** Collaboration, N. Aghanim *et al.*, “Planck 2018 results. VI. Cosmological parameters,” [1807.06209](#).
- [20] **Keck Array and BICEP2 Collaborations** Collaboration, P. A. R. Ade, Z. Ahmed, R. W. Aikin, K. D. Alexander, D. Barkats, S. J. Benton, C. A. Bischoff, J. J. Bock, R. Bowens-Rubin, J. A. Brevik, I. Buder, E. Bullock, V. Buza, J. Connors, B. P. Crill, L. Duband, C. Dvorkin, J. P. Filippini, S. Fliescher, J. Grayson, M. Halpern, S. Harrison, G. C. Hilton, H. Hui, K. D. Irwin, K. S. Karkare, E. Karpel, J. P. Kaufman, B. G. Keating, S. Kefeli, S. A. Kernasovskiy, J. M. Kovac, C. L. Kuo, E. M. Leitch, M. Lueker, K. G. Megerian, C. B. Netterfield, H. T. Nguyen, R. O’Brient, R. W. Ogburn, A. Orlando, C. Pryke, S. Richter, R. Schwarz, C. D. Sheehy, Z. K. Staniszewski, B. Steinbach, R. V. Sudiwala, G. P. Teply, K. L. Thompson, J. E. Tolan, C. Tucker, A. D. Turner, A. G. Vieregg, A. C. Weber, D. V. Wiebe, J. Willmert, C. L. Wong, W. L. K. Wu, and K. W. Yoon, “Improved Constraints on Cosmology and Foregrounds from BICEP2 and Keck Array Cosmic Microwave Background Data with Inclusion of 95 GHz Band,” *Phys. Rev. Lett.* **116** (Jan, 2016) 031302.
- [21] D. H. Lyth, “What would we learn by detecting a gravitational wave signal in the cosmic microwave background anisotropy?,” *Phys.Rev.Lett.* **78** (1997) 1861–1863, [hep-ph/9606387](#).

- [22] M. Cicoli, C. P. Burgess, and F. Quevedo, “Fibre Inflation: Observable Gravity Waves from IIB String Compactifications,” *JCAP* **0903** (2009) 013, 0808.0691.
- [23] K. Freese, J. A. Frieman, and A. V. Olinto, “Natural inflation with pseudo - Nambu-Goldstone bosons,” *Phys.Rev.Lett.* **65** (1990) 3233–3236.
- [24] D. Baumann and L. McAllister, “Inflation and String Theory,” 1404.2601.
- [25] G. Dvali, “Three-form gauging of axion symmetries and gravity,” hep-th/0507215.
- [26] N. Kaloper and L. Sorbo, “A Natural Framework for Chaotic Inflation,” *Phys.Rev.Lett.* **102** (2009) 121301, 0811.1989.
- [27] E. Silverstein and A. Westphal, “Monodromy in the CMB: Gravity Waves and String Inflation,” *Phys.Rev.* **D78** (2008) 106003, 0803.3085.
- [28] F. Marchesano, G. Shiu, and A. M. Uranga, “F-term Axion Monodromy Inflation,” *JHEP* **09** (2014) 184, 1404.3040.
- [29] T. Banks, M. Dine, P. J. Fox, and E. Gorbatov, “On the possibility of large axion decay constants,” *JCAP* **0306** (2003) 001, hep-th/0303252.
- [30] J. E. Kim, H. P. Nilles, and M. Peloso, “Completing natural inflation,” *JCAP* **0501** (2005) 005, hep-ph/0409138.
- [31] S. Dimopoulos, S. Kachru, J. McGreevy, and J. G. Wacker, “N-flation,” *JCAP* **0808** (2008) 003, hep-th/0507205.
- [32] R. Blumenhagen, A. Font, M. Fuchs, D. Herschmann, E. Plauschinn, Y. Sekiguchi, and F. Wolf, “A Flux-Scaling Scenario for High-Scale Moduli Stabilization in String Theory,” *Nucl. Phys.* **B897** (2015) 500–554, 1503.07634.
- [33] R. Blumenhagen, D. Herschmann, and E. Plauschinn, “The Challenge of Realizing F-term Axion Monodromy Inflation in String Theory,” *JHEP* **01** (2015) 007, 1409.7075.
- [34] A. Hebecker, P. Mangat, F. Rompineve, and L. T. Witkowski, “Tuning and Backreaction in F-term Axion Monodromy Inflation,” *Nucl. Phys.* **B894** (2015) 456–495, 1411.2032.
- [35] J. P. Conlon, “Quantum Gravity Constraints on Inflation,” *JCAP* **1209** (2012) 019, 1203.5476.
- [36] N. Kaloper, M. Kleban, A. Lawrence, and M. S. Sloth, “Large Field Inflation and Gravitational Entropy,” *Phys. Rev.* **D93** (2016), no. 4, 043510, 1511.05119.
- [37] A. Hebecker, P. Henkenjohann, and L. T. Witkowski, “Flat Monodromies and a Moduli Space Size Conjecture,” *JHEP* **12** (2017) 033, 1708.06761.
- [38] C. Vafa, “The String landscape and the swampland,” hep-th/0509212.

- [39] T. Rudelius, “Constraints on Axion Inflation from the Weak Gravity Conjecture,” *JCAP* **1509** (2015), no. 09, 020, 1503.00795.
- [40] T. Rudelius, “On the Possibility of Large Axion Moduli Spaces,” *JCAP* **1504** (2015), no. 04, 049, 1409.5793.
- [41] M. Montero, A. M. Uranga, and I. Valenzuela, “Transplanckian axions!?,” *JHEP* **08** (2015) 032, 1503.03886.
- [42] J. Brown, W. Cottrell, G. Shiu, and P. Soler, “Fencing in the Swampland: Quantum Gravity Constraints on Large Field Inflation,” *JHEP* **10** (2015) 023, 1503.04783.
- [43] H. Ooguri and C. Vafa, “On the Geometry of the String Landscape and the Swampland,” *Nucl. Phys.* **B766** (2007) 21–33, hep-th/0605264.
- [44] D. Klaewer and E. Palti, “Super-Planckian Spatial Field Variations and Quantum Gravity,” *JHEP* **01** (2017) 088, 1610.00010.
- [45] F. Baume and E. Palti, “Backreacted Axion Field Ranges in String Theory,” *JHEP* **08** (2016) 043, 1602.06517.
- [46] T. W. Grimm, E. Palti, and I. Valenzuela, “Infinite Distances in Field Space and Massless Towers of States,” 1802.08264.
- [47] **Planck** Collaboration, P. A. R. Ade *et al.*, “Planck 2015 results. XVII. Constraints on primordial non-Gaussianity,” *Astron. Astrophys.* **594** (2016) A17, 1502.01592.
- [48] R. Blumenhagen, B. Körs, D. Lüst, and S. Stieberger, “Four-dimensional String Compactifications with D-Branes, Orientifolds and Fluxes,” *Phys. Rept.* **445** (2007) 1–193, hep-th/0610327.
- [49] S. Gukov, C. Vafa, and E. Witten, “CFT’s from Calabi-Yau four folds,” *Nucl. Phys.* **B584** (2000) 69–108, hep-th/9906070. [Erratum: Nucl. Phys.B608,477(2001)].
- [50] T. R. Taylor and C. Vafa, “R R flux on Calabi-Yau and partial supersymmetry breaking,” *Phys. Lett.* **B474** (2000) 130–137, hep-th/9912152.
- [51] N. Arkani-Hamed, L. Motl, A. Nicolis, and C. Vafa, “The String landscape, black holes and gravity as the weakest force,” *JHEP* **06** (2007) 060, hep-th/0601001.
- [52] P. Candelas, X. C. D. L. Ossa, P. S. Green, and L. Parkes, “A pair of Calabi-Yau manifolds as an exactly soluble superconformal theory,” *Nuclear Physics B* **359** (1991), no. 1, 21 – 74.
- [53] S. B. Giddings, S. Kachru, and J. Polchinski, “Hierarchies from fluxes in string compactifications,” *Phys. Rev.* **D66** (2002) 106006, hep-th/0105097.
- [54] S. Franco, D. Galloni, A. Retolaza, and A. Uranga, “On axion monodromy inflation in warped throats,” *JHEP* **02** (2015) 086, 1405.7044.

- [55] K. Kooner, S. Parameswaran, and I. Zavala, “Warping the Weak Gravity Conjecture,” 1509.07049.
- [56] A. Hebecker, J. Moritz, A. Westphal, and L. T. Witkowski, “Axion Monodromy Inflation with Warped KK-Modes,” *Phys. Lett.* **B754** (2016) 328–334, 1512.04463.
- [57] I. Valenzuela, “Backreaction Issues in Axion Monodromy and Minkowski 4-forms,” 1611.00394.
- [58] S. Bielleman, L. E. Ibáñez, F. G. Pedro, I. Valenzuela, and C. Wieck, “Higgs-otic Inflation and Moduli Stabilization,” *JHEP* **02** (2017) 073, 1611.07084.
- [59] A. Hebecker, S. C. Kraus, and L. T. Witkowski, “D7-Brane Chaotic Inflation,” *Phys. Lett.* **B737** (2014) 16–22, 1404.3711.
- [60] L. E. Ibáñez and I. Valenzuela, “The inflaton as an MSSM Higgs and open string modulus monodromy inflation,” *Phys. Lett.* **B736** (2014) 226–230, 1404.5235.
- [61] M. Arends, A. Hebecker, K. Heimpel, S. C. Kraus, D. Lüst, C. Mayrhofer, C. Schick, and T. Weigand, “D7-Brane Moduli Space in Axion Monodromy and Fluxbrane Inflation,” *Fortsch. Phys.* **62** (2014) 647–702, 1405.0283.
- [62] L. E. Ibáñez, F. Marchesano, and I. Valenzuela, “Higgs-otic Inflation and String Theory,” *JHEP* **01** (2015) 128, 1411.5380.
- [63] S. Kachru, R. Kallosh, A. D. Linde, and S. P. Trivedi, “De Sitter vacua in string theory,” *Phys. Rev.* **D68** (2003) 046005, hep-th/0301240.
- [64] R. Blumenhagen, A. Font, M. Fuchs, D. Herschmann, and E. Plauschinn, “Towards Axionic Starobinsky-like Inflation in String Theory,” *Phys. Lett.* **B746** (2015) 217–222, 1503.01607.
- [65] R. Blumenhagen, D. Kläwer, L. Schlechter, and F. Wolf, “The Refined Swampland Distance Conjecture in Calabi-Yau Moduli Spaces,” *JHEP* **06** (2018) 052, 1803.04989.
- [66] R. Blumenhagen, D. Lüst, and S. Theisen, *Basic concepts of string theory*. Theoretical and Mathematical Physics. Springer, Heidelberg, Germany, 2013.
- [67] L. E. Ibanez and A. M. Uranga, *String theory and particle physics: An introduction to string phenomenology*. Cambridge University Press, 2012.
- [68] J. Polchinski, “String theory. Vol. 1: An introduction to the bosonic string; String theory. Vol. 2: Superstring theory and beyond.”
- [69] B. R. Greene, “String theory on Calabi-Yau manifolds,” in *Fields, strings and duality. Proceedings, Summer School, Theoretical Advanced Study Institute in Elementary Particle Physics, TASI’96, Boulder, USA, June 2-28, 1996*, pp. 543–726. 1996. hep-th/9702155.

- [70] P. Griffiths and J. Harris, *Principles of Algebraic Geometry*. John Wiley & Sons, 1994.
- [71] T. W. Grimm and J. Louis, “The Effective action of $N = 1$ Calabi-Yau orientifolds,” *Nucl. Phys.* **B699** (2004) 387–426, [hep-th/0403067](#).
- [72] E. Plauschinn, “Type IIB Orientifolds, D-Brane Instantons And The Large Volume Scenario,” *Fortsch. Phys.* **58** (2010) 913–1019.
- [73] I. Brunner and K. Hori, “Orientifolds and mirror symmetry,” *JHEP* **11** (2004) 005, [hep-th/0303135](#).
- [74] E. Plauschinn, “The generalized Green-Schwarz mechanism for type IIB orientifolds with D3- and D7-branes,” *Journal of High Energy Physics* **2009** (2009), no. 05, 062.
- [75] R. Blumenhagen, V. Braun, T. W. Grimm, and T. Weigand, “GUTs in type IIB orientifold compactifications,” *Nuclear Physics B* **815** (2009), no. 1, 1 – 94.
- [76] H. Jockers and J. Louis, “The Effective action of D7-branes in $N = 1$ Calabi-Yau orientifolds,” *Nucl. Phys.* **B705** (2005) 167–211, [hep-th/0409098](#).
- [77] T. W. Grimm, “The Effective action of type II Calabi-Yau orientifolds,” *Fortsch. Phys.* **53** (2005) 1179–1271, [hep-th/0507153](#).
- [78] A. Strominger, “SPECIAL GEOMETRY,” *Commun. Math. Phys.* **133** (1990) 163–180.
- [79] B. Craps, F. Roose, W. Troost, and A. Van Proeyen, “What is special Kahler geometry?,” *Nucl. Phys.* **B503** (1997) 565–613, [hep-th/9703082](#).
- [80] L. Andrianopoli, M. Bertolini, A. Ceresole, R. D’Auria, S. Ferrara, P. Fre, and T. Magri, “ $N=2$ supergravity and $N=2$ superYang-Mills theory on general scalar manifolds: Symplectic covariance, gaugings and the momentum map,” *J. Geom. Phys.* **23** (1997) 111–189, [hep-th/9605032](#).
- [81] H. Jockers, “The Effective Action of D-branes in Calabi-Yau Orientifold Compactifications,” *Fortsch. Phys.* **53** (2005) 1087–1175, [hep-th/0507042](#).
- [82] F. Marchesano, D. Regalado, and G. Zoccarato, “On D-brane moduli stabilisation,” *JHEP* **11** (2014) 097, [1410.0209](#).
- [83] H. Jockers and J. Louis, “D-terms and F-terms from D7-brane fluxes,” *Nucl. Phys.* **B718** (2005) 203–246, [hep-th/0502059](#).
- [84] I. Garcia-Etxebarria, H. Hayashi, R. Savelli, and G. Shiu, “On quantum corrected Kahler potentials in F-theory,” *JHEP* **03** (2013) 005, [1212.4831](#).
- [85] N. C. Bizet, O. Loaiza-Brito, and I. Zavala, “Mirror quintic vacua: hierarchies and inflation,” [1605.03974](#).

- [86] K. Aleshkin and A. Belavin, “A new approach for computing the geometry of the moduli spaces for a Calabi–Yau manifold,” *J. Phys.* **A51** (2018), no. 5, 055403, 1706.05342.
- [87] K. Aleshkin and A. Belavin, “Special geometry on the 101 dimensional moduli space of the quintic threefold,” 1710.11609.
- [88] K. Aleshkin and A. Belavin, “Special geometry on the moduli space for the two-moduli non-Fermat Calabi–Yau,” *Phys. Lett.* **B776** (2018) 139–144, 1708.08362.
- [89] B. R. Greene and M. R. Plesser, “Duality in Calabi-Yau Moduli Space,” *Nucl. Phys.* **B338** (1990) 15–37.
- [90] P. Berglund, P. Candelas, X. De La Ossa, A. Font, T. Hübsch, D. Jancic, and F. Quevedo, “Periods for Calabi-Yau and Landau-Ginzburg vacua,” *Nucl. Phys.* **B419** (1994) 352–403, hep-th/9308005.
- [91] P. Green and T. Hübsch, “Polynomial deformations and cohomology of Calabi-Yau manifolds,” *Comm. Math. Phys.* **113** (1987), no. 3, 505–528.
- [92] P. Berglund and T. Hübsch, “Couplings for compactification,” *Nucl. Phys.* **B411** (1994) 223–256, hep-th/9303158.
- [93] M. F. Atiyah, R. Bott, and L. Gårding, “Lacunae for hyperbolic differential operators with constant coefficients. II,” *Acta Math.* **131** (1973) 145–206.
- [94] P. Candelas, “Yukawa Couplings Between (2,1) Forms,” *Nucl. Phys.* **B298** (1988) 458.
- [95] A. Font, “Periods and duality symmetries in Calabi-Yau compactifications,” *Nucl. Phys.* **B391** (1993) 358–388, hep-th/9203084.
- [96] A. Klemm and S. Theisen, “Considerations of one modulus Calabi-Yau compactifications: Picard-Fuchs equations, Kahler potentials and mirror maps,” *Nucl. Phys.* **B389** (1993) 153–180, hep-th/9205041.
- [97] P. S. Aspinwall, “The Moduli space of N=2 superconformal field theories,” in *Proceedings, Summer School in High-energy physics and cosmology: Trieste, Italy, June 13-July 29, 1994*, pp. 0352–401. 1994. hep-th/9412115.
- [98] P. Candelas, P. S. Green, and T. Hübsch, “Rolling among Calabi-Yau vacua,” *Nuclear Physics B* **330** (1990), no. 1, 49 – 102.
- [99] A. Strominger, “Massless black holes and conifolds in string theory,” *Nucl. Phys.* **B451** (1995) 96–108, hep-th/9504090.
- [100] P. Candelas, X. De La Ossa, A. Font, S. H. Katz, and D. R. Morrison, “Mirror symmetry for two parameter models. 1.,” *Nucl. Phys.* **B416** (1994) 481–538, hep-th/9308083.

- [101] P. Candelas, A. Font, S. H. Katz, and D. R. Morrison, “Mirror symmetry for two parameter models. 2.,” *Nucl. Phys.* **B429** (1994) 626–674, [hep-th/9403187](#).
- [102] S. Hosono, A. Klemm, S. Theisen, and S.-T. Yau, “Mirror symmetry, mirror map and applications to complete intersection Calabi-Yau spaces,” *Nucl. Phys.* **B433** (1995) 501–554, [hep-th/9406055](#). [AMS/IP Stud. Adv. Math.1,545(1996)].
- [103] E. Bergshoeff, R. Kallosh, T. Ortin, D. Roest, and A. Van Proeyen, “New formulations of $D = 10$ supersymmetry and D8 - O8 domain walls,” *Class.Quant.Grav.* **18** (2001) 3359–3382, [hep-th/0103233](#).
- [104] J. P. Conlon, “Moduli Stabilisation and Applications in IIB String Theory,” *Fortsch. Phys.* **55** (2007) 287–422, [hep-th/0611039](#).
- [105] J. P. Conlon, F. Quevedo, and K. Suruliz, “Large-volume flux compactifications: Moduli spectrum and D3/D7 soft supersymmetry breaking,” *JHEP* **0508** (2005) 007, [hep-th/0505076](#).
- [106] J. R. Ellis, A. Lahanas, D. V. Nanopoulos, and K. Tamvakis, “No-Scale Supersymmetric Standard Model,” *Phys.Lett.* **B134** (1984) 429.
- [107] D. Z. Freedman and A. Van Proeyen, “Supergravity,”
- [108] P. Breitenlohner and D. Z. Freedman, “Positive Energy in anti-De Sitter Backgrounds and Gauged Extended Supergravity,” *Phys.Lett.* **B115** (1982) 197.
- [109] K. Choi, J. E. Kim, and H. P. Nilles, “Cosmological constant and soft terms in supergravity,” *Phys.Rev.Lett.* **73** (1994) 1758–1761, [hep-ph/9404311](#).
- [110] A. Brignole, L. E. Ibanez, and C. Munoz, “Towards a theory of soft terms for the supersymmetric Standard Model,” *Nucl.Phys.* **B422** (1994) 125–171, [hep-ph/9308271](#).
- [111] N. Wolchover, “Is nature unnatural?,” *Quanta Magazine* (2013).
- [112] J. P. Conlon, “The QCD axion and moduli stabilisation,” *JHEP* **0605** (2006) 078, [hep-th/0602233](#).
- [113] J. P. Conlon and F. Quevedo, “Astrophysical and cosmological implications of large volume string compactifications,” *JCAP* **0708** (2007) 019, [0705.3460](#).
- [114] T. Ortin, *Gravity and Strings*. Cambridge Monographs on Mathematical Physics. Cambridge University Press, 2015.
- [115] P. Svrcek and E. Witten, “Axions In String Theory,” *JHEP* **0606** (2006) 051, [hep-th/0605206](#).
- [116] A. Sen, “Strong - weak coupling duality in four-dimensional string theory,” *Int. J. Mod. Phys.* **A9** (1994) 3707–3750, [hep-th/9402002](#).

- [117] G. Aldazabal, P. G. Camara, A. Font, and L. Ibanez, “More dual fluxes and moduli fixing,” *JHEP* **0605** (2006) 070, [hep-th/0602089](#).
- [118] D. Lüst and D. Osten, “Generalised fluxes, Yang-Baxter deformations and the $O(d,d)$ structure of non-abelian T-duality,” [1803.03971](#).
- [119] T. Buscher, “A Symmetry of the String Background Field Equations,” *Phys.Lett.* **B194** (1987) 59.
- [120] A. Strominger, S.-T. Yau, and E. Zaslow, “Mirror symmetry is T duality,” *Nucl. Phys.* **B479** (1996) 243–259, [hep-th/9606040](#).
- [121] B. Wecht, “Lectures on Nongeometric Flux Compactifications,” *Class.Quant.Grav.* **24** (2007) S773–S794, [0708.3984](#).
- [122] J. Shelton, W. Taylor, and B. Wecht, “Nongeometric flux compactifications,” *JHEP* **10** (2005) 085, [hep-th/0508133](#).
- [123] M. Grana, J. Louis, and D. Waldram, “ $SU(3) \times SU(3)$ compactification and mirror duals of magnetic fluxes,” *JHEP* **0704** (2007) 101, [hep-th/0612237](#).
- [124] F. Wolf, “Flux-Scaling Scenarios for Moduli Stabilization in String Theory and Axion Monodromy Inflation,” Master’s thesis, Ludwig-Maximilians-Universität, Munich, 2015.
- [125] J. Shelton, W. Taylor, and B. Wecht, “Generalized Flux Vacua,” *JHEP* **0702** (2007) 095, [hep-th/0607015](#).
- [126] P. Bouwknegt, K. Hannabuss, and V. Mathai, “Nonassociative tori and applications to T-duality,” *Commun.Math.Phys.* **264** (2006) 41–69, [hep-th/0412092](#).
- [127] P. Bouwknegt, J. Evslin, and V. Mathai, “T duality: Topology change from H flux,” *Commun.Math.Phys.* **249** (2004) 383–415, [hep-th/0306062](#).
- [128] A. Micu, E. Palti, and G. Tasinato, “Towards Minkowski Vacua in Type II String Compactifications,” *JHEP* **0703** (2007) 104, [hep-th/0701173](#).
- [129] I. Benmachiche and T. W. Grimm, “Generalized $N=1$ orientifold compactifications and the Hitchin functionals,” *Nucl. Phys.* **B748** (2006) 200–252, [hep-th/0602241](#).
- [130] J. Terning, “TASI 2002 lectures: Nonperturbative supersymmetry,” in *Particle physics and cosmology: The quest for physics beyond the standard model(s). Proceedings, Theoretical Advanced Study Institute, TASI 2002, Boulder, USA, June 3-28, 2002*, pp. 343–443. 2003. [hep-th/0306119](#).
- [131] R. Blumenhagen, D. Herschmann, and F. Wolf, “String Moduli Stabilization at the Conifold,” *JHEP* **08** (2016) 110, [1605.06299](#).
- [132] R. Blumenhagen, J. P. Conlon, S. Krippendorf, S. Moster, and F. Quevedo, “SUSY Breaking in Local String/F-Theory Models,” *JHEP* **09** (2009) 007, [0906.3297](#).

- [133] **BICEP2** Collaboration, P. A. R. Ade *et al.*, “Detection of B -Mode Polarization at Degree Angular Scales by BICEP2,” *Phys. Rev. Lett.* **112** (2014), no. 24, 241101, 1403.3985.
- [134] A. H. Guth, “The Inflationary Universe: A Possible Solution to the Horizon and Flatness Problems,” *Phys. Rev.* **D23** (1981) 347–356.
- [135] E. W. Kolb and M. S. Turner, “The Early Universe,” *Front. Phys.* **69** (1990) 1–547.
- [136] A. Starobinsky, “A new type of isotropic cosmological models without singularity,” *Physics Letters B* **91** (1980), no. 1, 99 – 102.
- [137] D. Baumann and L. McAllister, “Advances in Inflation in String Theory,” *Ann. Rev. Nucl. Part. Sci.* **59** (2009) 67–94, 0901.0265.
- [138] R. D. Peccei and H. R. Quinn, “CP Conservation in the Presence of Instantons,” *Phys. Rev. Lett.* **38** (1977) 1440–1443. [,328(1977)].
- [139] R. D. Peccei and H. R. Quinn, “Constraints Imposed by CP Conservation in the Presence of Instantons,” *Phys. Rev.* **D16** (1977) 1791–1797.
- [140] X.-G. Wen and E. Witten, “World-sheet instantons and the Peccei-Quinn symmetry,” *Physics Letters B* **166** (1986), no. 4, 397 – 401.
- [141] M. Dine, N. Seiberg, X.-G. Wen, and E. Witten, “Nonperturbative effects on the string world sheet,” *Nuclear Physics B* **278** (1986), no. 4, 769 – 789.
- [142] K. Freese, J. A. Frieman, and A. V. Olinto, “Natural inflation with pseudo Nambu-Goldstone bosons,” *Phys. Rev. Lett.* **65** (Dec, 1990) 3233–3236.
- [143] F. C. Adams, J. R. Bond, K. Freese, J. A. Frieman, and A. V. Olinto, “Natural inflation: Particle physics models, power law spectra for large scale structure, and constraints from COBE,” *Phys. Rev.* **D47** (1993) 426–455, hep-ph/9207245.
- [144] K. Freese and W. H. Kinney, “On: Natural inflation,” *Phys. Rev.* **D70** (2004) 083512, hep-ph/0404012.
- [145] C. Long, L. McAllister, and P. McGuirk, “Aligned Natural Inflation in String Theory,” *Phys. Rev.* **D90** (2014) 023501, 1404.7852.
- [146] L. McAllister, E. Silverstein, and A. Westphal, “Gravity Waves and Linear Inflation from Axion Monodromy,” *Phys. Rev.* **D82** (2010) 046003, 0808.0706.
- [147] G. Dvali, “A Vacuum accumulation solution to the strong CP problem,” *Phys. Rev.* **D74** (2006) 025019, hep-th/0510053.
- [148] N. Kaloper, A. Lawrence, and L. Sorbo, “An Ignoble Approach to Large Field Inflation,” *JCAP* **1103** (2011) 023, 1101.0026.
- [149] N. Kaloper and A. Lawrence, “Natural chaotic inflation and ultraviolet sensitivity,” *Phys. Rev.* **D90** (2014), no. 2, 023506, 1404.2912.

- [150] N. Kaloper and A. Lawrence, “A Monodromy from London,” 1607.06105.
- [151] S. Bielleman, L. E. Ibáñez, and I. Valenzuela, “Minkowski 3-forms, Flux String Vacua, Axion Stability and Naturalness,” *JHEP* **12** (2015) 119, 1507.06793.
- [152] S. Coleman and F. De Luccia, “Gravitational effects on and of vacuum decay,” *Phys. Rev. D* **21** (Jun, 1980) 3305–3315.
- [153] R. Bousso and J. Polchinski, “Quantization of four form fluxes and dynamical neutralization of the cosmological constant,” *JHEP* **06** (2000) 006, hep-th/0004134.
- [154] J. D. Brown and C. Teitelboim, “Neutralization of the cosmological constant by membrane creation,” *Nuclear Physics B* **297** (Feb., 1988) 787–836.
- [155] J. L. Feng, J. March-Russell, S. Sethi, and F. Wilczek, “Saltatory relaxation of the cosmological constant,” *Nucl. Phys.* **B602** (2001) 307–328, hep-th/0005276.
- [156] L. E. Ibáñez, M. Montero, A. Uranga, and I. Valenzuela, “Relaxion Monodromy and the Weak Gravity Conjecture,” *JHEP* **04** (2016) 020, 1512.00025.
- [157] A. Hebecker, F. Rompineve, and A. Westphal, “Axion Monodromy and the Weak Gravity Conjecture,” *JHEP* **04** (2016) 157, 1512.03768.
- [158] J. Brown, W. Cottrell, G. Shiu, and P. Soler, “Tunneling in Axion Monodromy,” *JHEP* **10** (2016) 025, 1607.00037.
- [159] F. Carta, F. Marchesano, W. Staessens, and G. Zoccarato, “Open string multi-branched and Kähler potentials,” *JHEP* **09** (2016) 062, 1606.00508.
- [160] A. Linde, “Chaotic inflation,” *Physics Letters B* **129** (1983), no. 3, 177 – 181.
- [161] G. Obied, H. Ooguri, L. Spodyneiko, and C. Vafa, “De Sitter Space and the Swampland,” 1806.08362.
- [162] P. Agrawal, G. Obied, P. J. Steinhardt, and C. Vafa, “On the Cosmological Implications of the String Swampland,” 1806.09718.
- [163] F. Denef, M. R. Douglas, and B. Florea, “Building a better racetrack,” *JHEP* **06** (2004) 034, hep-th/0404257.
- [164] F. Denef, “Les Houches Lectures on Constructing String Vacua,” *Les Houches* **87** (2008) 483–610, 0803.1194.
- [165] W. Taylor and Y.-N. Wang, “The F-theory geometry with most flux vacua,” *JHEP* **12** (2015) 164, 1511.03209.
- [166] T. Banks and L. J. Dixon, “Constraints on String Vacua with Space-Time Supersymmetry,” *Nucl. Phys.* **B307** (1988) 93–108.

- [167] T. D. Brennan, F. Carta, and C. Vafa, “The String Landscape, the Swampland, and the Missing Corner,” 1711.00864.
- [168] L. Susskind, “Trouble for remnants,” hep-th/9501106.
- [169] S. Cecotti, *Supersymmetric Field Theories*. Cambridge University Press, 2015.
- [170] A. Nicolis, “On Super-Planckian Fields at Sub-Planckian Energies,” *JHEP* **07** (2008) 023, 0802.3923.
- [171] R. Blumenhagen, D. Herschmann, and F. Wolf, “Challenges for Moduli Stabilization and String Cosmology near the Conifold,” 1704.04140. [PoSCORFU2016,104(2017)].
- [172] P. Candelas and X. C. de la Ossa, “Comments on Conifolds,” *Nucl. Phys.* **B342** (1990) 246–268.
- [173] S. B. Giddings and A. Maharana, “Dynamics of warped compactifications and the shape of the warped landscape,” *Phys. Rev.* **D73** (2006) 126003, hep-th/0507158.
- [174] O. DeWolfe and S. B. Giddings, “Scales and hierarchies in warped compactifications and brane worlds,” *Phys. Rev.* **D67** (2003) 066008, hep-th/0208123.
- [175] S. P. de Alwis, “On Potentials from fluxes,” *Phys. Rev.* **D68** (2003) 126001, hep-th/0307084.
- [176] G. Shiu, G. Torroba, B. Underwood, and M. R. Douglas, “Dynamics of Warped Flux Compactifications,” *JHEP* **06** (2008) 024, 0803.3068.
- [177] G. Curio, A. Klemm, D. Lust, and S. Theisen, “On the vacuum structure of type II string compactifications on Calabi-Yau spaces with H fluxes,” *Nucl. Phys.* **B609** (2001) 3–45, hep-th/0012213.
- [178] G. Curio and V. Spillner, “On the modified KKLT procedure: A Case study for the P(11169) [18] model,” *Int. J. Mod. Phys.* **A22** (2007) 3463–3492, hep-th/0606047.
- [179] A. Hebecker, P. Mangat, F. Rompineve, and L. T. Witkowski, “Winding out of the Swamp: Evading the Weak Gravity Conjecture with F-term Winding Inflation?,” *Phys. Lett.* **B748** (2015) 455–462, 1503.07912.
- [180] X. Dong, B. Horn, E. Silverstein, and A. Westphal, “Simple exercises to flatten your potential,” *Phys. Rev.* **D84** (2011) 026011, 1011.4521.
- [181] R. Blumenhagen, I. Valenzuela, and F. Wolf, “The Swampland Conjecture and F-term Axion Monodromy Inflation,” *JHEP* **07** (2017) 145, 1703.05776.
- [182] W. Buchmuller, C. Wieck, and M. W. Winkler, “Supersymmetric Moduli Stabilization and High-Scale Inflation,” *Phys. Lett.* **B736** (2014) 237–240, 1404.2275.

-
- [183] E. Dudas and C. Wieck, “Moduli backreaction and supersymmetry breaking in string-inspired inflation models,” *JHEP* **10** (2015) 062, 1506.01253.
- [184] W. Buchmüller, E. Dudas, L. Heurtier, A. Westphal, C. Wieck, and M. W. Winkler, “Challenges for Large-Field Inflation and Moduli Stabilization,” *JHEP* **04** (2015) 058, 1501.05812.
- [185] L. Martucci, “D-branes on general N=1 backgrounds: Superpotentials and D-terms,” *JHEP* **06** (2006) 033, hep-th/0602129.
- [186] J. Gomis, F. Marchesano, and D. Mateos, “An Open string landscape,” *JHEP* **11** (2005) 021, hep-th/0506179.
- [187] R. Kallosh and A. D. Linde, “Landscape, the scale of SUSY breaking, and inflation,” *JHEP* **12** (2004) 004, hep-th/0411011.
- [188] F. Ruehle and C. Wieck, “One-loop Pfaffians and large-field inflation in string theory,” 1702.00420.
- [189] P. S. Aspinwall, “Minimum distances in nontrivial string target spaces,” *Nucl. Phys.* **B431** (1994) 78–96, hep-th/9404060.
- [190] S. Hosono, A. Klemm, S. Theisen, and S.-T. Yau, “Mirror symmetry, mirror map and applications to Calabi-Yau hypersurfaces,” *Commun. Math. Phys.* **167** (1995) 301–350, hep-th/9308122.
- [191] M. Berg, E. Pajer, and S. Sjors, “Dante’s Inferno,” *Phys. Rev.* **D81** (2010) 103535, 0912.1341.
- [192] H. Ooguri and C. Vafa, “Non-supersymmetric AdS and the Swampland,” *Adv. Theor. Math. Phys.* **21** (2017) 1787–1801, 1610.01533.
- [193] S. Cecotti and C. Vafa, “Theta-problem and the String Swampland,” 1808.03483.
- [194] M.-x. Huang, A. Klemm, and S. Quackenbush, “Topological string theory on compact Calabi-Yau: Modularity and boundary conditions,” *Lect. Notes Phys.* **757** (2009) 45–102, hep-th/0612125.
- [195] I. García-Etxebarria, T. W. Grimm, and I. Valenzuela, “Special Points of Inflation in Flux Compactifications,” *Nucl. Phys.* **B899** (2015) 414–443, 1412.5537.
- [196] J. P. Conlon and F. Quevedo, “On the explicit construction and statistics of Calabi-Yau flux vacua,” *JHEP* **10** (2004) 039, hep-th/0409215.
- [197] P. Kaste, W. Lerche, C. A. Lutken, and J. Walcher, “D-branes on K3 fibrations,” *Nucl. Phys.* **B582** (2000) 203–215, hep-th/9912147.
- [198] A. Giryavets, S. Kachru, P. K. Tripathy, and S. P. Trivedi, “Flux compactifications on Calabi-Yau threefolds,” *JHEP* **04** (2004) 003, hep-th/0312104.